



GEOCHEMICAL AND MINERALOGICAL STUDIES OF THE TRENCH
TUNGSTEN DEPOSIT, MOUNT MULGINE, WESTERN AUSTRALIA

by

Christopher J.R. Migisha, B.Sc. (Hons.)

Makerere University, Kampala.

Submitted for the degree of M.Sc. through
the Department of Economic Geology
University of Adelaide

October, 1983.

To my dear parents who have set a
good example of "holding on".

TABLE OF CONTENTS (cont'd)

	<u>Page</u>
<u>CHAPTER 4 : MINERALOGY</u>	
4.1	Introduction 41
4.2	Tungsten minerals 44
4.3	Antimony and antimony-bearing minerals 46
4.4	Iron sulphides 47
4.5	Bismuth and bismuth-lead minerals 49
4.6	Silver minerals 51
4.7	Nickel-bearing minerals 52
4.8	Arsenic-bearing minerals 53
4.9	Sphalerite 54
4.10	Iron, titanium and chromium oxides 56
4.11	Copper minerals 59
4.12	Molybdenite 60
4.13	Brannerite(?) 61
4.14	Amphiboles 61
4.15	Epidote 64
4.16	Silica minerals 64
4.17	Carbonates 65
4.18	Feldspars 66
4.19	Micas 66
4.20	Talc, chlorite and serpentine 67
4.21	Pyroxenes 69
4.22	Sphene 70
4.23	Other minerals (apatite, fluorite, stilbite, altered olivine, garnets). 70
<u>CHAPTER 5 : FLUID INCLUSION STUDIES</u>	
5.1	Introduction 74
5.2	Aims of the study 74
5.3	Sample selection 75
5.4	Techniques 77
5.5	The fluid inclusions 78
5.6	Types of inclusions 79
5.7	Freezing experiments 83
5.8	Heating experiments 84
5.9	Fluid inclusion leaching 87
5.10	Melting and homogenization data 90
5.11	Accuracy of the readings 90
5.12	Interpretation of the data 91

List and location of Figures.

<u>Figure</u>	<u>Brief or full title</u>	<u>Before page</u>
1.1	Location map	4
1.2	Regional geology map	6
1.3	Mount Mulgine geology map	7
1.4	Cross-section 10,000N	9
2.1	Titanium vs Na+K in hornblende	
2.2	Histograms of Ti in hornblende	24
2.3	Sodium, Ti vs temperature in hornblende	
2.4	Titanium vs log f_{O_2}	
2.5	Aluminium vs pressure	25
2.6	Rubidium vs K_2O	
3.1	Classification of volcanic rocks	28
3.2	SiO_2 vs Zr/TiO_2 discriminant diagram	
3.3	Zr/TiO_2 vs Nb/Y discriminant diagram	29
3.4	SiO_2 vs Nb/Y discriminant diagram	
3.5	SiO_2 vs FeO/MgO discriminant diagram	
3.6	TiO_2 vs Zr discriminant diagram	
3.7	TiO_2 vs Y/Nb discriminant diagram	
3.8	TiO_2 vs Zr/P_2O_5 discriminant diagram	30
3.9	P_2O_5 vs Zr discriminant diagram	
3.10	Nb/Y vs Zr/P_2O_5 discriminant diagram	
3.11	$TiO_2-K_2O-P_2O_5$ discriminant diagram	33
3.12	TiO_2-Zr-Y discriminant diagram	
3.13	Titanium vs Zr discriminant diagram	34
3.14	TiO_2 vs Zr discriminant diagram	
3.15	Rare earth element patterns	35
3.16	Nickel vs MgO	39
3.17	Chromium vs MgO	
4.1	Generalized paragenetic sequence	45
4.2	Temperature vs As in arsenopyrite	55
4.3	Classification of calcic amphiboles	64
5.1	Depth vs Mo	75
5.2	Depth vs W	
5.3	Molybdenum vs W	77
5.4		
5.5		
5.6	Homogenization and freezing data histograms	91
5.7		
5.8		

List and location of Figures (cont'd)

<u>Figure</u>	<u>Brief or full title</u>	<u>Before page</u>
5.9	Calibration graph	92
5.10	Temperature vs CaCl_2	93
5.11	Stability curves for phengitic micas	} 97
5.12	Pressure-temperature correction curves	
5.13	Pressure vs temperature CO_2 phase diagram	98
6.1	Sulphur isotopic enrichment factors	108
6.2	Stability fields of Fe-S-O minerals and barite	109

List and location of Tables

<u>Table</u>		
2.1	Compositions of Mount Mulgine greenstones	14
2.2	Comparison of meta-rhyodacitic rocks with other rocks	17
2.3	Compositions of granitic rocks from Mount Mulgine	18
2.4	Compositions of Mount Mulgine BIFs	20
3.1	Comparison of Mount Mulgine greenstones with similar rocks	36
4.1	Minerals at Mount Mulgine	42
4.2	Scheelite and huebnerite analyses	45
4.3	Tetrahedrite analyses	47
4.4	Composition of pyrargyrite	52
4.5	Arsenopyrite analyses	53
4.6	Average hornblende analyses	62
4.7	Chlorite and serpentine analyses	68
4.8	Pyroxene analyses	70
4.9	Garnet compositions	73
5.1	Fluid inclusion leach analyses	89
5.2	Si^{+4} content of phengitic muscovites	96
6.1	Sulphur isotope data	107
6.2	Sphalerite geobarometry	113

Location of Plates

<u>Plate(s)</u>		
1.1	(Physiography)	2
2.1-2.3	(Rock textures)	19
4.1-4.9	(Mineral textures)	58
5.1-5.5	(Fluid inclusions)	81

This thesis contains no material which has been accepted for the award of any other degree or diploma in any University, nor to the best of my knowledge and belief, does it contain any material previously published or written by another person, except where due reference is made in the text.

SUMMARY

The Trench deposit is one of two granite-associated W-Mo deposits at Mount Mulgine, Western Australia. Although only 1.5 km apart, the two deposits are of different style - the Trench deposit essentially comprises a mineralized system of quartz veins in a sequence of interlayered ultramafic to felsic greenstones, banded iron formations and extensively greisenised sills, while the other deposit, known as the Hill deposit comprises a mineralized quartz-muscovite greisen at the contact of the Mount Mulgine Granite and the surrounding mafic country rocks.

The two deposits have been actively explored, especially in the last eleven years, but there has been little previous research work. This study has been concerned with the Trench deposit.

The presence of hornblende (and its composition) and of calcic plagioclase indicate that the host rocks attained medium grade (amphibolite facies) metamorphism. The rocks have since suffered retrograde metamorphism as evidenced by abundant epidote after plagioclase, chlorite after biotite and actinolite after pyroxene. Mineralogical and fluid inclusion evidence is consistent with a peak metamorphic temperature of about 500°C. The Si⁺⁴ content of muscovites, the Al content of hornblende and the FeS content of sphalerites, coupled with estimates of the thickness of the volcanic-sedimentary pile and lack of pressure indicator minerals at Mount Mulgine, suggest that the pressure during metamorphism must have been at least 2 kb but less than about 4 kb.

The metamorphic changes and hydrothermal alteration (including K-metasomatism) have modified or destroyed original rock mineralogies and textures, but studies of "immobile" trace elements have shown that the original rocks were tholeiitic basalts. Although these Archaean greenstones resemble present-day island arc tholeiites and mid-oceanic ridge basalts (MORB), they are unlikely to have formed in environments similar to those of their modern equivalents.

Comparing the Mount Mulgine greenstones with similar rocks elsewhere, it is clear that the elements K, Mg, Fe, Si and possibly Mn were added to, while Na, Al, Ca and P were partly subtracted from, the rocks at Mount Mulgine.

The host rocks are chiefly composed of quartz, epidote, actinolite, hornblende, tremolite, biotite, phlogopite, muscovite, plagioclase, K-feldspars, carbonates, sericite, talc, chlorite, diopside and minor apatite, (altered) olivine, spessartine, andradite, and chrysotile. The mineralization (mainly epigenetic minerals) includes scheelite, huebnerite, molybdenite, pyrite, pyrrhotite, magnetite, chromite, tetrahedrite, fluorite, sphalerite, arseno-

pyrite, chalcopyrite, rutile, stibnite, pyrargyrite, native bismuth and antimony and other minor oxides or sulphides of Pb, Bi, U, Fe, Ti, As, Cu, Ni and Sb.

Fluid inclusion studies support the view, derived from quartz-vein relationships and textural evidence, that there were several mineralizing solutions. The spatial relationship between molybdenite and scheelite and the fact that scheelite is Mo-free are believed to be due to deposition of these minerals from different solutions. Different generations of fluids are also believed to be partly responsible for the many types of inclusions observed and the range of the fluid inclusion data obtained.

Some fluid inclusions have abundant daughter minerals. This, plus the very low first and final melting points (e.g., -76°C and -49°C respectively) of some inclusions imply that major amounts of other cations, in addition to Na, are present in the inclusion fluids. This was confirmed by leaching and analysis of the fluids which showed them to be rich in Ca, Na, Mg, K and Fe (in decreasing order of abundance). Although Al and Li were not detected in the fluid inclusion leach analyses, there is evidence that these elements were also present in the mineralizing solutions. The dominant anion is chlorine. Some inclusions are CO_2 -rich, but there is no apparent relationship between mineralization and the CO_2 -rich fluids. Scheelite was apparently deposited from slightly alkaline, moderately saline (average 26 wt.% CaCl_2 equivalent) solutions at temperatures of around 400°C .

$\delta^{34}\text{S}$ values of pyrite and pyrrhotite are close to zero per mil with a mean of 0.4 per mil and a standard deviation of 0.6. This is interpreted to mean that the sulphur had a magmatic source, which is consistent with the mineralization having been derived from the Mount Mulgine Granite. Sulphur isotope fractionation between coexisting pyrite and pyrrhotite indicates that the sulphides formed in the 385°C - 730°C range and this is in fair agreement with the temperature range obtained from fluid inclusion studies viz. 300 - 500°C . The As content of arsenopyrite and the Na and Ti contents of hornblende suggest similar temperatures.

Tungsten mineralization in the Trench deposit is clearly closely associated with quartz veins and no lithological control has been established. The quartz veins mostly formed in fractures which initially acted as channels for the mineralizing solutions. The fractures themselves are believed to have formed mainly during regional folding and/or during the intrusion of the granites. Scheelite precipitation is considered to have been largely controlled by temperature conditions and appears to have occurred during regional metamorphism.

The Trench deposit is not strata-bound although the meta-volcanic sedimentary host rocks are similar to those of the strata- and time-bound (Early Palaeozoic) Felbertal W deposit in Austria. The fluid inclusion and sulphur isotope data are also very similar to those of many W deposits of various types.

In spite of the absence of carbonate rocks at Mount Mulgine, the mineralogy of the Trench deposit is similar to that of typical W skarn deposits (e.g., the scheelite deposits in the Bindal area, northern Norway, and in San Luis, Argentina). The development of the Trench deposit mineral assemblages appears to have been a function of both hydrothermal processes and metamorphism.

Tungsten deposits in the Archaean are rare and, at present, there are no known deposits of this age which are comparable in size to the Trench deposit.

ACKNOWLEDGEMENTS

This thesis would not have been possible without the support (moral or material) and encouragement of many people and to all these people, I am very grateful. I would particularly like to mention the following:

Dr. R.A. Both who suggested and supervised the project. Dr. Both's "duties" often extended beyond those normally expected of a supervisor and I am greatly indebted for his constructive criticisms of drafts of the thesis and his patience and "approachable" manner which made work relatively lighter. Thank you, Ross.

B.W. Hawkins of Union Carbide made the project available and allowed me to use company facilities (camp, transport, food, maps etc.). The same facilities were also extended to me by Minefields Exploration N.L. through their geologist A.D.(Tony) Gibbs with whom I had fruitful discussions about the project. I remained in touch with Tony right up to the end of the project and I appreciated his quick responses to all my queries.

T.W. Middleton of Union Carbide was the geologist on site when I first went to the field and I thank him for introducing me to the rocks at Mount Mulgine. I extend special thanks to the caretaker at the camp, Arthur Moses and his wife, Freda, for feeding me and keeping company in the outback.

Both academic and technical staff of the Departments of Economic Geology and Geology and Mineralogy were most helpful. Professor P. Ypma guided me as far as fluid inclusion work is concerned and kindly read the fluid inclusion chapter(5) and the corresponding Appendix 5. I consulted Dr. J. Foden freely on matters concerning petrology and he read the relevant second and third chapters. His constructive criticisms which resulted in several "last minute" additions and changes are greatly appreciated. I also benefitted from "chats" with Drs. R. Oliver and A. Purvis.

Mr. Evert Bleys showed me fluid inclusions for the first time and did all the photographic work. He also took some of the photos. W. Mussared prepared the rock sections and did the sulphide separations. J. Stanley did the XRF analyses; Dr. K. Turnbull took the sulphur isotope measurements; S. Proferes did all the drafting and P. Mcduie helped with the AA analyses. The Economic Geology Department secretary, H. Malby helped with so many "little things" and the way she handled all these things is my idea of efficiency.

Drs. B. Griffin and K. Bartusek of the Electron Optical Centre, University of Adelaide are thanked for their help with the electron microprobe analyses.

I acknowledge the stimulating discussions I had with fellow post-graduate students, especially F. Ukaigwe, Y. Bone and M. Hochman.

As if I did not have enough to thank her for, Teresa Marciano helped in the preparation of most of the Appendices and she proof "read" them all. I remain indebted to her.

J. Brumby demonstrated her skill and ability to work under pressure by deciphering and typing the whole thesis in time and I thank her.

Lest I forget, this project was financially supported by the Australian Development Assistance Bureau and I am most grateful.

Finally, I would like to thank my brother Sam who spent a lot of money telephoning to give me news which always made me feel at home, away from home.



1.1 General background

The Trench deposit is the larger of the two W-Mo deposits at Mount Mulgine, in the Yalgoo Goldfield, Murchison Province, Western Australia. The extent of the deposit, both laterally and at depth, has not been definitely determined but, with estimated reserves of over 80 million tonnes at 0.14% WO_3 (0.05% WO_3 cut-off) the deposit already ranks among the world's three largest W deposits (excluding the Soviet Union).

The deposit is now owned by Minefields Exploration N.L. Relatively intense diamond drilling of the Trench deposit started in 1977 and since then two shafts have been sunk to obtain bulk metallurgical samples to assess the feasibility of by-product recovery. The feasibility studies take into consideration the recovery of Mo and Ag as well as W.

When all the factors or variables (e.g., age, size, host and associated rocks, mineralogy etc.) are taken into consideration, the Trench deposit is unlike other known W deposits. Tungsten, mainly in the form of scheelite, occurs within or closely associated with quartz veins in a sequence of Archaean ultramafic-mafic to felsic "greenstones" which are interlayered with banded iron formations and greisenised sills and intruded by granitoids.

On one hand, the host rocks and, to a lesser extent, the mineralogy of the Trench deposit are like those of the stratabound Felbertal (near Mittersill) W deposit in the Austrian Alps (Höll et al, 1972) but the present study has shown that these are the only strong similarities between the two deposits and that there are important differences. On the other hand, the Trench deposit is very similar to, and should be regarded as a variety of, skarn deposits. However, it lacks the typical skarn development since there are no recognized carbonate host rocks at Mount Mulgine.

Like most other W deposits the world over, the Trench deposit is associated with a granite - the Mount Mulgine Granite. The nature of this association has required clarification.

Prior to the present investigation there had been no detailed geological research on the Trench deposit. This study has, therefore, been designed to obtain fundamental data required to determine the origin of this unusual W-Mo resource.

Plate 1.1A

A view of Mount Mulgine, taken from the airstrip, facing eastwards.

Plate 1.1B

A view of the southern end of the Trench deposit, taken from the Hill deposit. The airstrip is on the left of the photo. One of the camp buildings can just be seen, as a white spec, at the far end of the grid clearing in the middle of the photo and the water tank can also just be seen as another white spec on the extreme right hand, middle of the photo. Note the flat countryside in the background.

PLATE 1.1



A



B

1.2 Nature of the investigation

This study began with the following broad objectives:

- a) To carry out geochemical studies of the rocks that host W and related mineralization at Mount Mulgine, and hence determine the relationship (if any) between mineralization and lithology. The geochemistry of the host rocks would determine, or at least put constraints on, their original identity and environments of formation.
- b) To document the minerals, mineral textures and assemblages, plus any other features related to mineralization.
- c) To elucidate some of the chemical and physical environments under which mineralization occurred, through fluid inclusion and sulphur isotope studies.
- d) To synthesize information and data from a), b) and c) above, and hence determine the most probable source of the mineralization and why it occurred where it is. This can help in further exploration for similar deposits.

Where appropriate, more specific aims are included at the beginning of the relevant chapters.

1.3 Previous work

There has been little research work done on the Mount Mulgine W-Mo deposits. As far as the writer is aware, the only study specifically devoted to Mount Mulgine was that by Collins (1975). Collins' work was mainly petrographic and focussed on granites from the Hill deposit, with only casual reference to the Trench deposit.

Although Mo is now of secondary importance to W, Mount Mulgine initially attracted attention as a Mo prospect (see below). Some of the earliest reports about the prospect are found in annual reports of the Western Australian Geological Survey, e.g., Maitland (1917), Blatchford (1919) and Matheson (1944). The reports are brief and concluded that there was not enough molybdenite to warrant any large scale mining operation.

Most of the present knowledge about the deposits is contained in reports by company geologists or consultants. Notable among these are A.D. Gibbs of Minefields Exploration N.L. (Gibbs, 1978) and T.W. Middleton of Union Carbide (Middleton, 1979). A.W.G. Whittle has carried out petrographic work for ANZECO (Australia and New Zealand Exploration Company) a former subsidiary of Union Carbide. Most of Whittle's work is contained in his two latest reports (Whittle, 1977, 1978).

All the above workers, especially Gibbs (1978), speculated on how the deposits could have formed. There appears to be general consensus on the following points.

1. The Mount Mulgine Granite played some part in the formation of the deposits.

2. Despite their proximity, the Hill and Trench deposits display different styles of mineralization and are most likely to be of different origin.

3. The Ca for the precipitation of scheelite was most probably derived from the host rocks.

4. Scheelite mineralization at Mount Mulgine is unique and of enormous economic potential.

In view of the last point, it is surprising that Mount Mulgine has not attracted more attention. More will be said about each of the above points later in the text and finally in the discussion on ore genesis.

1.4 Location and access

Mount Mulgine is situated at 29° 12'S and 116° 58'E, in the Yalgoo district, Murchison Province, Western Australia (Figure 1.1). It is 474 kilometres NNE of Perth and 235 kilometres ESE of Geraldton on the west coast of Western Australia. The nearest township is Perenjori, which is 87 kilometres from Mount Mulgine in a WSW direction.

Access by road from Perth is via the Great Northern Highway. A dry weather airstrip, suitable for light aircraft, is a few hundred metres from the camp site.

1.5 Physiography

The only prominent relief feature in the study area is Mount Mulgine which is 515.7 metres above sea level at its peak. The so-called Mount rises only about 100 metres above its immediate surroundings (Plate 1.1A). The view from Mount Mulgine top is one of low-lying hills and very flat alluvial plains (Plate 1.1B). Such subdued relief is a feature of the Yilgarn block as a whole (Gee et al, 1981).

Apart from the granitic rocks which are well exposed on Mount Mulgine, and rubbly outcrops of banded iron formation in the Trench area, no other outcrops were seen. Generally, outcrop exposure is very poor and the geologic map (Figure 1.3) of the area was compiled by Minefields and ANZECO, with the help of information from drill holes.

LOCATION MAP - MT. MULGINE, W.A.

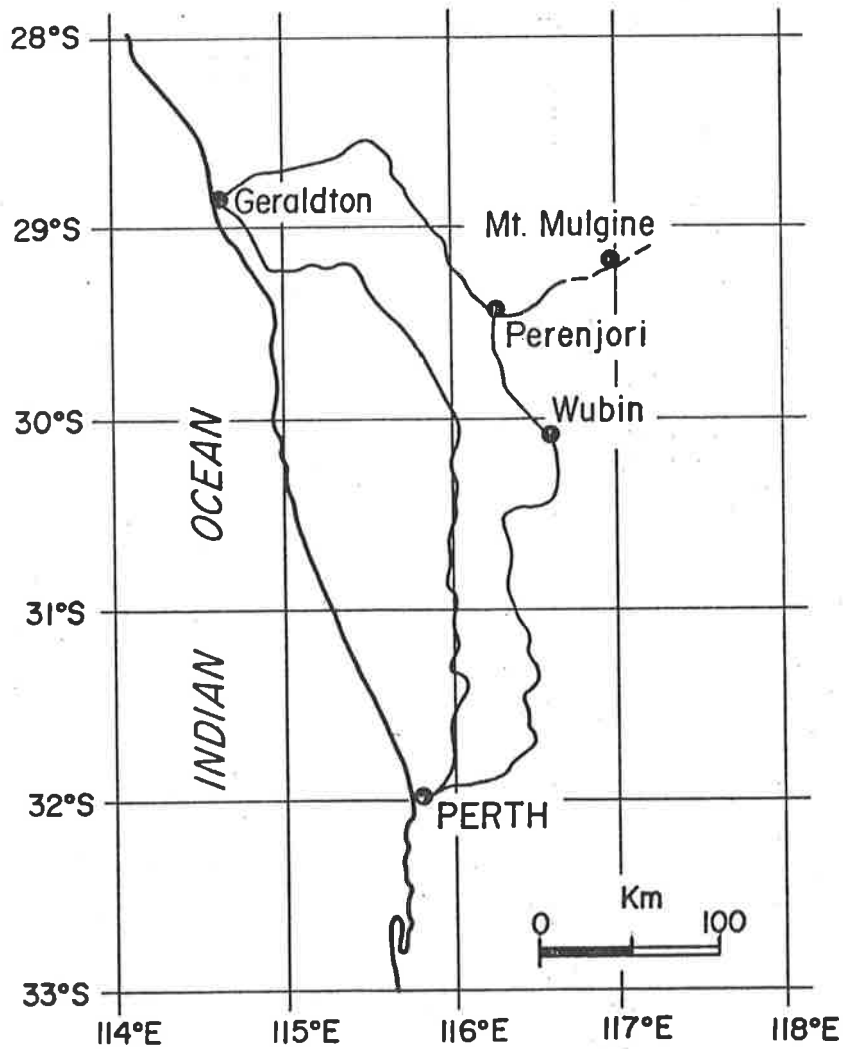
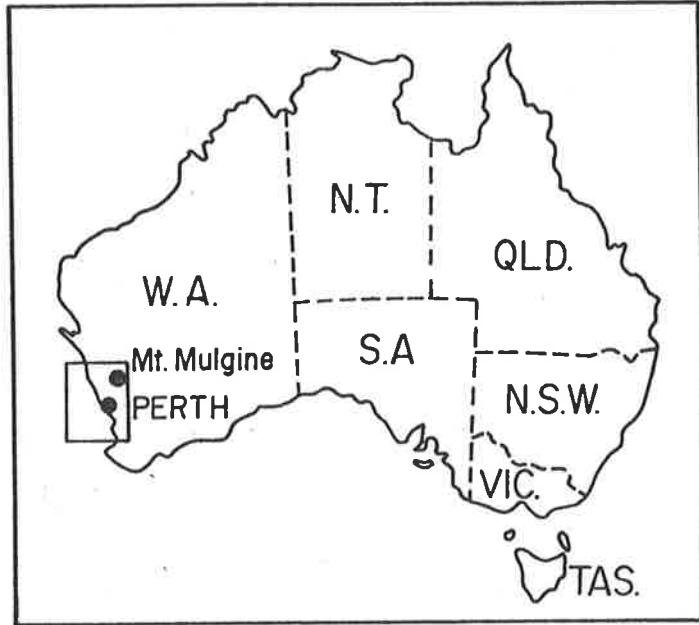


Figure 1.1

The area has mild and sometimes wet winters and very hot dry summers, during which day temperatures are often in the low forties (degrees Celcius).

1.6 History of exploration and mining activities

Prospecting and mining of gold at Mount Mulgine took place at the turn of this century. The occurrence of molybdenite in the Mount Mulgine stock has been known since the early part of the century. Between 1910 and 1920, a 13.7m adit was driven into the granite following high grade molybdenite seams.

Apparently the first company to take interest in the area was Big Bell Mines Ltd. in 1938. In the same year, the company dug 27 trenches and pot holes on the visible molybdenite seams to the south of the hill. Broken Hill Proprietary Co. Ltd. and the Western Australian Government were also interested in the prospect at the beginning of the Second World War.

Later, Westfield Minerals (W.A.) N.L. held claims over the Mount Mulgine stock in 1966-1967 and drilled 47 holes. Results of this operation, like those of earlier operations, are not known.

Matheson (1944a) reported that about 78 tons of molybdenite concentrates were mined during the 1917-1922 period.

In 1967-69, Newmont Pty. Ltd., took over the claims and, encouraged by results of a soil sampling programme, started drilling. Twenty six-inch percussion holes were drilled to depths of 30.5m to 61m and later, the first 16 diamond drill holes were completed. Newmont were primarily after Mo and hoped to find a large "porphyry-type" Mo deposit. It appears Newmont did not analyse for W. They were succeeded by Minefields Exploration N.L. in late 1969 who considered that there had been inadequate exploration for W.

Minefields examined the drill cores from the 16 Newmont diamond drill holes and decided that further exploration, especially for W, was warranted. They drilled 14 more diamond drill holes to depths of around 152m.

Scheelite had been known to occur at Mount Mulgine since the early part of this century, but it was not until late September, 1970, that considerable quantities of the mineral were intersected in diamond drill hole (DDM)29.

Following the discovery of scheelite, the Newmont soil samples were re-analysed for W and Mo by Minefields in 1971. Minefields extended the soil sampling programme and continued drilling. These activities led to the discovery and delineation of both the Hill and Trench deposits. By June 1976, they had increased the number of drill holes to 214 and sunk a sampling shaft in the Hill deposit. By this time, the Hill deposit had been confirmed as being of high grade but low tonnage.

In 1977 Union Carbide, through its subsidiary ANZECO, entered into a joint venture with Minefields. Attention was then focussed on what had been called the Trench area. This is simply an area of W anomalies that had been delineated by the soil geochemical survey programme. The Trench deposit has proved to be a very large but low grade scheelite deposit (see below).

By June 1981 feasibility studies were well advanced and the total number of drill holes had increased to 318, and that of shafts to five (three in the Hill deposit and two in the Trench deposit).

Union Carbide withdrew from the joint venture in October 1982.

1.7 Size and grade of the deposits

The contact metasomatic Hill deposit is of high grade but low tonnage, with ore reserves of just over 1m tonnes of 0.60% WO_3 at a cut-off grade of 0.25% WO_3 . The Trench deposit, in contrast, is of very low grade but high tonnage, with indicated reserves of over 80 million tonnes averaging 0.14% WO_3 at 0.05% WO_3 cut-off. The figure for the Trench deposit includes 36m tonnes of ore averaging 0.077% MoS_2 at 0.05% MoS_2 cut-off.

The average Ag content in the greenstones* analysed is about 6 ppm and that of Cu is 203 ppm. Gold was not analysed for in this study. In a restricted assay confined only to BIF lithologies in DDM 252, the highest gold value obtained was 2.5 ppm Au (Middleton, 1979). From the nearby Highland Chief mine (see Figure 1.3) 26.06 kg of gold were recovered from 2523.87 tonnes of ore between 1917 and 1939 (Baxter and Lipple, 1979).

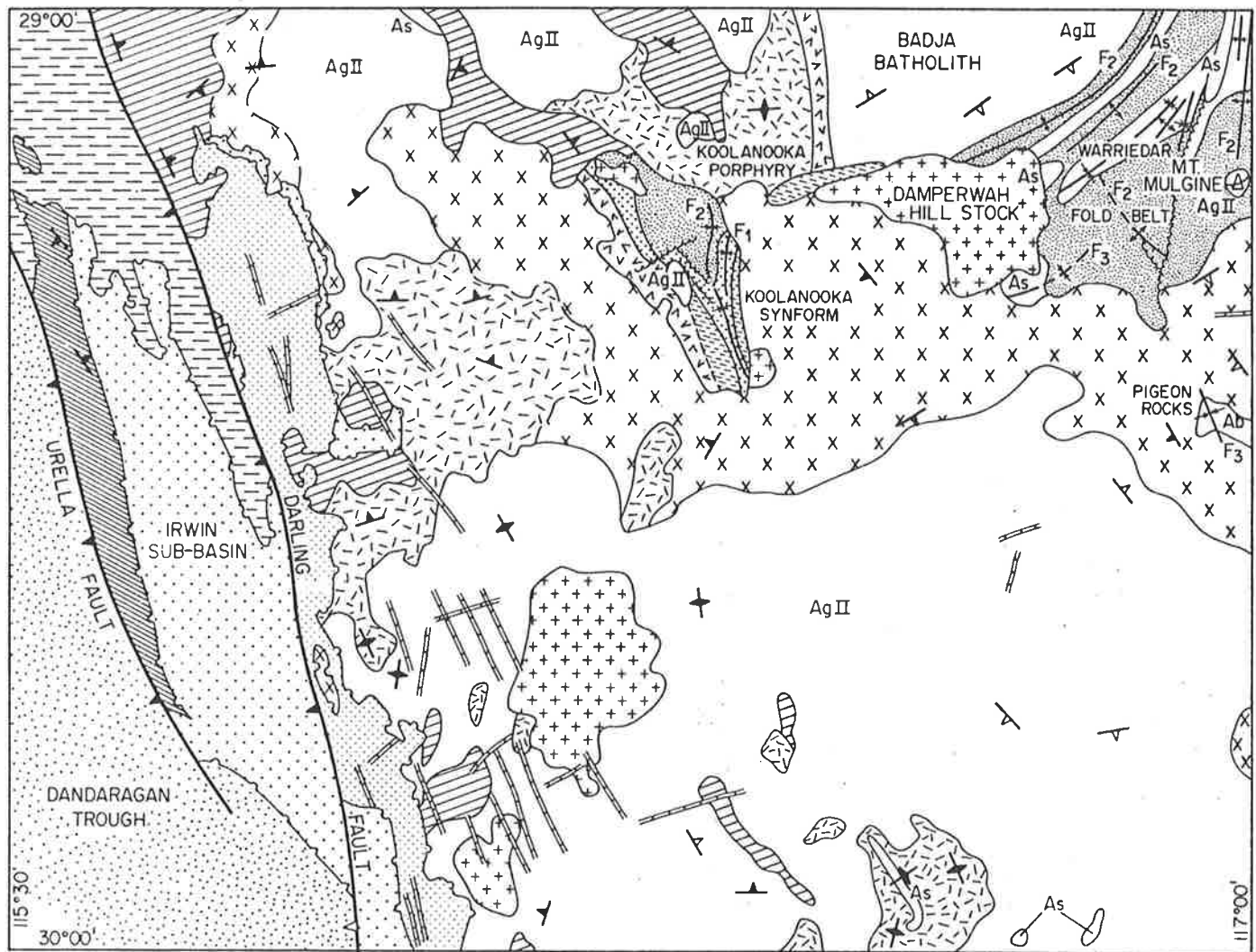
Prospects for increasing the W ore reserves are very good because the Trench deposit is still open both along strike and dip. Also significant quantities of mineralization with less than 0.25% WO_3 exist in the immediate vicinity of the Hill deposit (Baxter and Gibbs, in prep.).

1.8 Geology

Archaean supracrustal rocks in the Yilgarn block are divided into two belts - the Koolanooka Synform and the Warriedar Fold Belt (Baxter and Lipple, 1979). The rocks at Mount Mulgine are part of the Warriedar Fold Belt (Figure 1.2), comprising meta-volcanic and meta-sedimentary sequences which have been intruded by granitoid rocks.

The Mount Mulgine Granite is a small high level stock, intruded near a larger batholith on the eastern side of the Warriedar Fold Belt. It is a

* (see section 1.10 for definitions).



SOLID GEOLOGY INTERPRETATION

REFERENCE SHEET SH505

0 10 20 30 Km

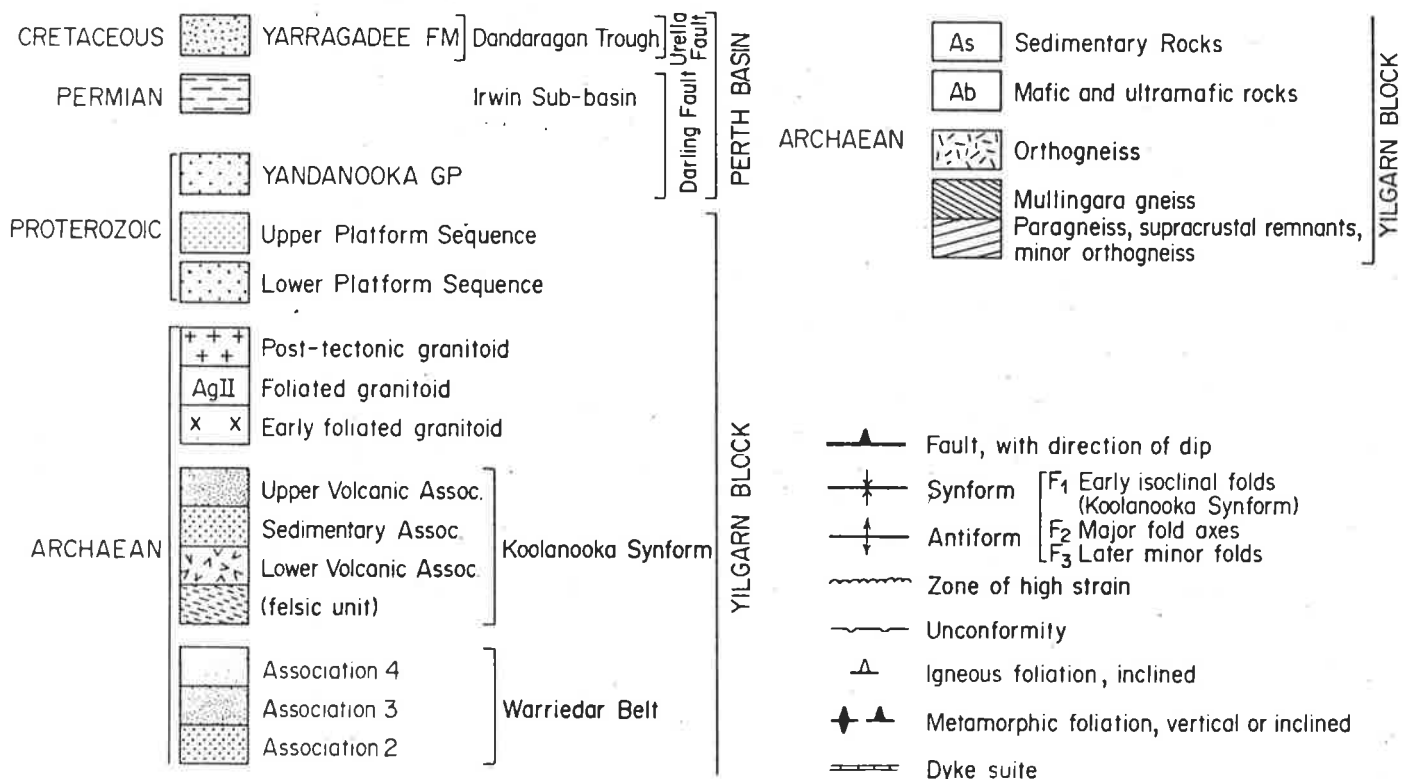


Figure 1.2 (After Baxter and Lipple, 1979).

medium to coarse grained leucogranite which, together with the surrounding country rocks, is cut by dolerite dykes and quartz veins. The meta-volcanic and meta-sedimentary rocks in the vicinity of the granite include meta-basalts (*sensu lato*), banded iron formations (BIF) and minor ultramafics represented by meta-pyroxenites and serpentinites.

The rocks dip at about 35° to 40° to the NW but around the stock the dips are outward in all directions, i.e., *quaquaversal* (Collins, 1975).

Regionally, the rocks belong to Association 3 as described by Baxter and Lipple (1979, pp. 17-18) which is thought to correlate with the Moyagee formation of the Cue area to the north of Mount Mulgine (de la Hunty, 1975). If this correlation is valid, then the supracrustal rocks at Mount Mulgine would have had cover rocks of at least 4 km thickness. At present, the Warriedar Fold Belt supracrustals are in excess of 8 km thick (Baxter and Lipple, 1979). There is evidence that at least some of these rocks were deposited in water (see Chapter 2).

Metamorphism was locally up to medium grade (Winkler, 1979) which is the equivalent of the amphibolite facies, although low grade (greenschist facies) metamorphism was prevalent in the region as a whole. Recrystallization was both static and dynamic. In the former case, original textures are preserved, but in the latter case, the primary rock textures have been obliterated by crystallization which, in places, has resulted in strongly schistose rocks, especially in areas of high strain, close to the intrusions (Collins, 1975; Baxter and Lipple, 1979). The rocks have since suffered retrograde metamorphism as evidenced by abundant epidote, chlorite and actinolite.

At Mount Mulgine, there has been extensive hydrothermal alteration which is believed to be directly associated with mineralization (see Chapter 2). This alteration, superimposed on all the metamorphic effects, makes it difficult to tell the nature of the original rocks. This problem is addressed in Chapter 3.

The Mount Mulgine Granite has intruded the core/axis of the Mulgine anticline. Collins (1975) recognized three granite types which constitute the Mount Mulgine Granite - a porphyritic biotite granite, a muscovite-biotite granite and a muscovite granite. The bulk of the granite is believed to have been intruded during regional metamorphism. Arriens (1971) determined Rb/Sr radiometric ages of 2689 m.y. and 2670 m.y. on muscovites associated with the granite. Several studies of the Yilgarn have indicated that the greenstones and the early granites that intrude them are of about the same age. All these rocks formed over a narrow time span and were related to a major tectono-thermal event between 2800 m.y. and 2600 m.y. ago, the final stages of which led to the cratonization of the Yilgarn block (Gee et al, 1981).

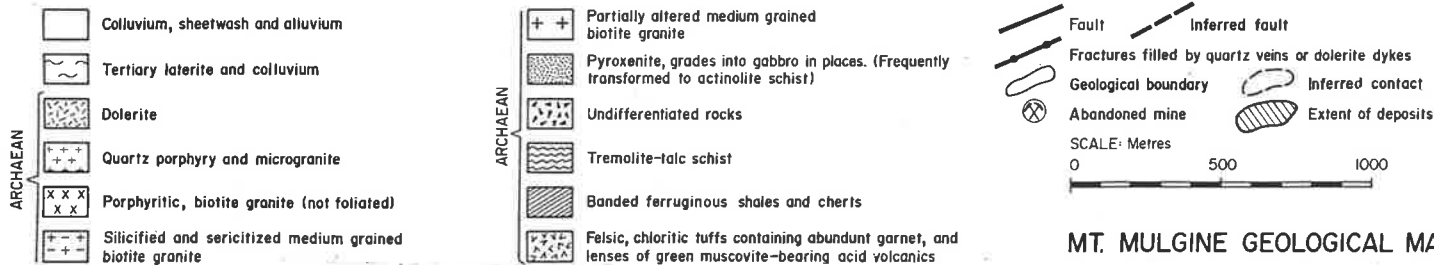
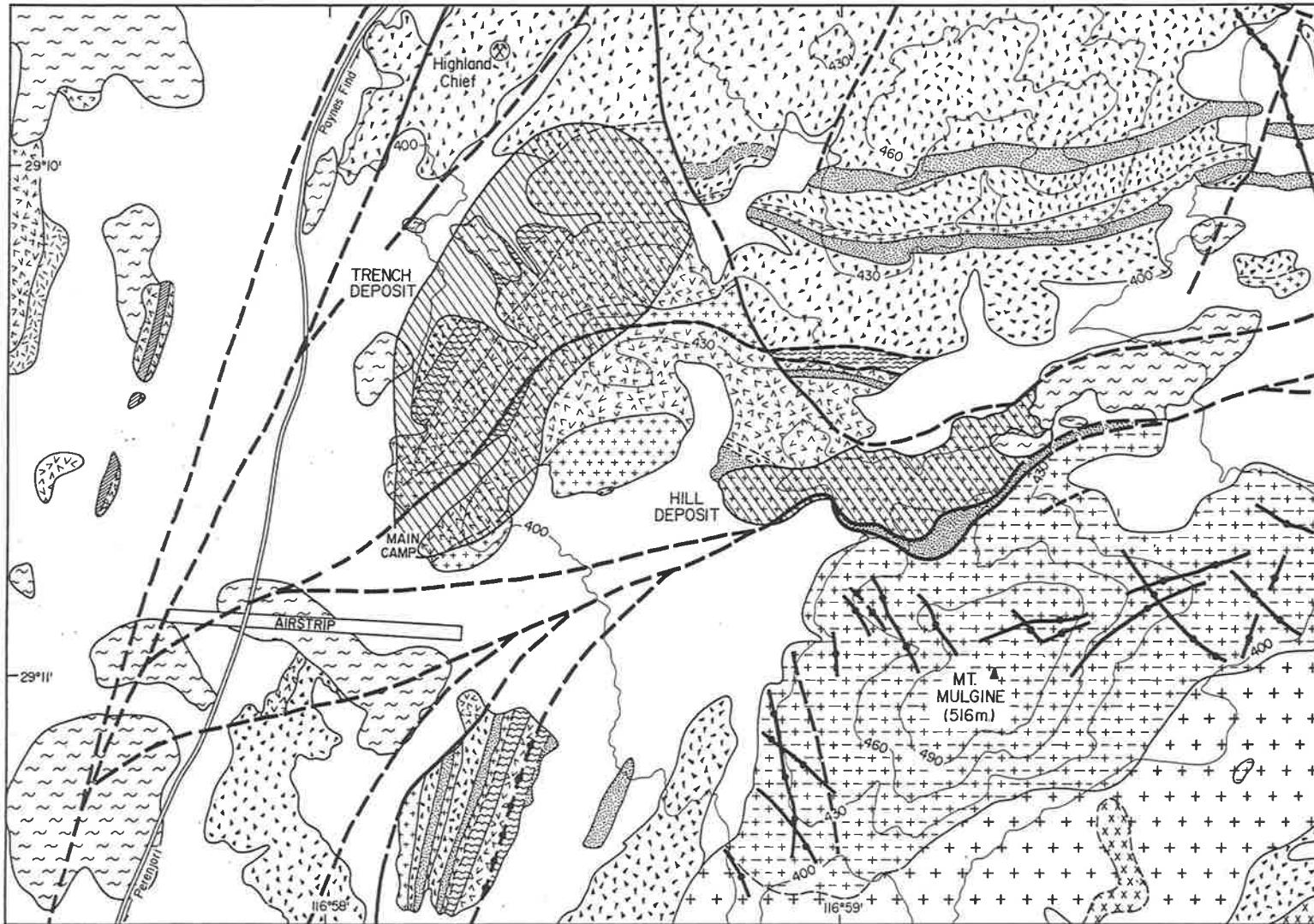


Figure 1.3 (After Minefields and ANZECO).

MT. MULGINE GEOLOGICAL MAP

The Trench deposit is situated on the NW limb of the Mulgine anticline which plunges NNE. The Mulgine anticline is one of a series of folds which are the major structural features in the Warriedar Fold Belt region. The folds are open to closed and have wavelengths varying from 120m to about 7 km (Collins, 1975). Larger fold structures (synclinoria) with wavelengths of up to 15 km have been mapped by Muhling and Low (1973, quoted in Collins, 1975) in the area to the north of Mount Mulgine. Mainly because of size considerations, the larger intrusions, like the Mount Mulgine Granite, are believed to have been intruded in the cores of pre-existing folds. Their intrusion would have accentuated the folds and perhaps created a few more smaller folds. However, most of the smaller folds are thought to have formed much later as a result of buckling caused by the intrusion of later granites. Some mildly deformed granites belong to a second period of granitoid intrusion which appears to extend from about 2600 m.y. to 2200 m.y. (Baxter and Lipple, 1979, p.11).

A number of faults have been inferred in the region around Mount Mulgine (Figure 1.3). The faults are suspected to be present because of inability to trace marker beds (mainly BIF) over any great strike distance and also because of abrupt changes in the direction of strike ridges and topography (Collins, 1975).

The faults are the strike-slip type and are generally oriented NNE to ENE. The latter direction is also the general structural trend of the Murchison province (de la Hunty, 1975). Displacements along these faults appear to be of the order of a few tens of metres.

Major fractures, sometimes continuous with the faults and now largely filled by quartz veins and dolerite dykes, have been mapped in the region.

The fact that most of the above structures are roughly parallel to the NNE trend of the Mulgine anticline implies that they formed or were initiated during early folding. As in the case of folds, the intrusion of the granites would have accentuated these structures or caused some of them. However, there must have been more fracturing, faulting and fracture-filling after the intrusion of the granites because the granites themselves have been affected by and contain these structures. The Mount Mulgine Granite for instance is cut by quartz veins and dolerite dykes all of which are dominantly oriented in a NW through to almost northerly direction (see Figure 1.3). This contrasts with the NNE to ENE trend of similar structures in the surrounding supracrustal rocks. Smaller fractures, and the mineralized quartz-fluorite-carbonate veins that have filled them, are all believed to owe their existence entirely to the granites. The forceful intrusion of the granites created the fractures which were later filled by mineralized late phase differentiates of the granites.

1.9 Summary of mineralization at Mount Mulgine

Tungsten and related mineralization at Mount Mulgine is the core subject of the whole thesis and different aspects of mineralization will be mentioned and discussed in the chapters that follow. At this point, a brief summary of the mineralization of the Trench deposit will suffice.

Although Au and Mo were the first commodities to attract attention at Mount Mulgine, the primary target is now W which occurs almost exclusively as scheelite. Wolframite (huebnerite) has been observed in only three holes (DDM 62, 251 and 259). In some cases it is rimmed and partially replaced by scheelite. In the nearby Hill deposit, scheelite originally at the surface is reported to have been oxidised to tungstite or ferritungstite (Middleton, 1979).

The W mineralization is associated with Mo, Ag, Cu, Sb, As, Bi, Au, Zn, Fe and minor U, Ni and Pb minerals. Tin mineralization, which sometimes occurs associated with W mineralization, does not occur at Mount Mulgine.

Molybdenum occurs as molybdenite; Ag is mainly in pyrargyrite and tetrahedrite; Cu occurs in chalcopyrite; Sb occurs in the native state and also in stibnite, tetrahedrite and ullmannite; Bi occurs as pure bismuth and also in galenobismutite (bismuthinite has also been reported in the Hill deposit by Collins (1975)). Arsenic is in arsenopyrite and in tetrahedrite-tennantite; Zn occurs as sphalerite; Fe occurs as pyrite, magnetite, pyrrhotite plus several other minor phases; Ni occurs in pentlandite and also in some other less common phases (see Table 4.1); Pb occurs as rare galena and in galenobismutite and U occurs in brannerite(?). Gold is known to occur and has been mined at Mount Mulgine. It has been detected in the Trench, but its form of occurrence is not known (Middleton, 1979). Presumably it is locked up in the abundant sulphides, e.g., pyrite.

Metallurgical studies in progress have the aim of recovering Mo and Ag in addition to W. Other elements like Au and Cu might also be recovered.


Figure 1.4 is one of the cross sections and shows the variation of WO_3 (wt.%) with depth. This variation is irregular but, clearly, good WO_3 values may occur in any of the lithologies at Mount Mulgine, as defined by geologists of the exploration companies. Tungsten and Mo values obtained in this study were also plotted against depth (see Figures 5.1 and 5.2). These Figures show that W decreases with increasing depth while Mo increases with increasing depth. However, there is no significant correlation between W and Mo values (see Figure 5.3). Similar plots for Ag, Zn, Cu and Pb suggest that Cu increases with increasing depth while the other elements (Zn, Ag and Pb) decrease with increasing depth, but the correlation coefficients were too low

KEY TO FIGURE 1.4


LITHOLOGIES (After Minefields and ANZECCO).

- R,R/G : META-RHYOLITE : quartz, K spar commonly with banded sulphides viz. pyrite, pyrrhotite \pm chalcopyrite, sphalerite; sometimes garnetiferous. (R/G when sericitised or greisenised). Altered rhyolitic flows or tuffs.
- RD : META-RHYODACITE : as above but with significant epidote and saussurite after plagioclase. Possibly original flows or tuffs.
- D : META-DACITE : plagioclase, usually epidotised, with high mafic content viz. hornblende, biotite, chlorite; usually with fair pyrite, magnetite, leucoxene, sphene content. Field term incorporating meta-quartz trachy-andesite, meta-quartz andesites and possibly meta-tonalites.
- A : META-ANDESITE : quartz-free variant of last, (includes possible microdiorites).
- B,X : META-BASALT : actinolite, hornblende (?), chlorite; more mafic rich than last, from which it is often transitional. X-coarse grained gabbroidal appearance.
- U : META-PYROXENITE, mostly ACTINOLITE-CHLORITE SCHIST : transitional from last with minor plagioclase/epidote content.
- T : META-OLIVINE (?) PYROXENITE, mostly TREMOLITE-TALC SCHIST : variable talc altered, sometimes carbonatised and/or chloritised.
- ,P/U,P/T : PHLOGOPITE SCHIST : pervasively phlogopitised (K,F,Al metasomatisation) variant of U and T.
- I : BANDED IRON FORMATION : mostly thinly banded magnetite quartzite, sometimes with chloritic, biotitic, amphibolitic, sulphidic zones.
- F : Commonly thinly banded sequence of felsic to ultramafic tuffs(?); transitional rocks.
- M,M/G : MICROGRANITE, QUARTZ PORPHYRY : quartz, K spar, sericite, muscovite rock. (M/G when pervasively greisenised by K, F, Al metasomatisation). Occurs as thin dykes or sills usually as M/G.
- G,L : GREISEN : quartz muscovite rock of magmatic or primary pneumatolytic origin (mostly pervasively greisenised leucogranitoid).
L - less greisenised leucogranitoid.
- N : TRANSITIONAL, HYBRID ZONE : hybrid zone between rocks of differing chemical make-up subjected to pervasive alteration e.g. rhyolites - ultramafics.
- Q : Major QUARTZ VEIN.
- K : Intensively kaolinised, leached rocks of indeterminate origin or else qualified by letter code if known.

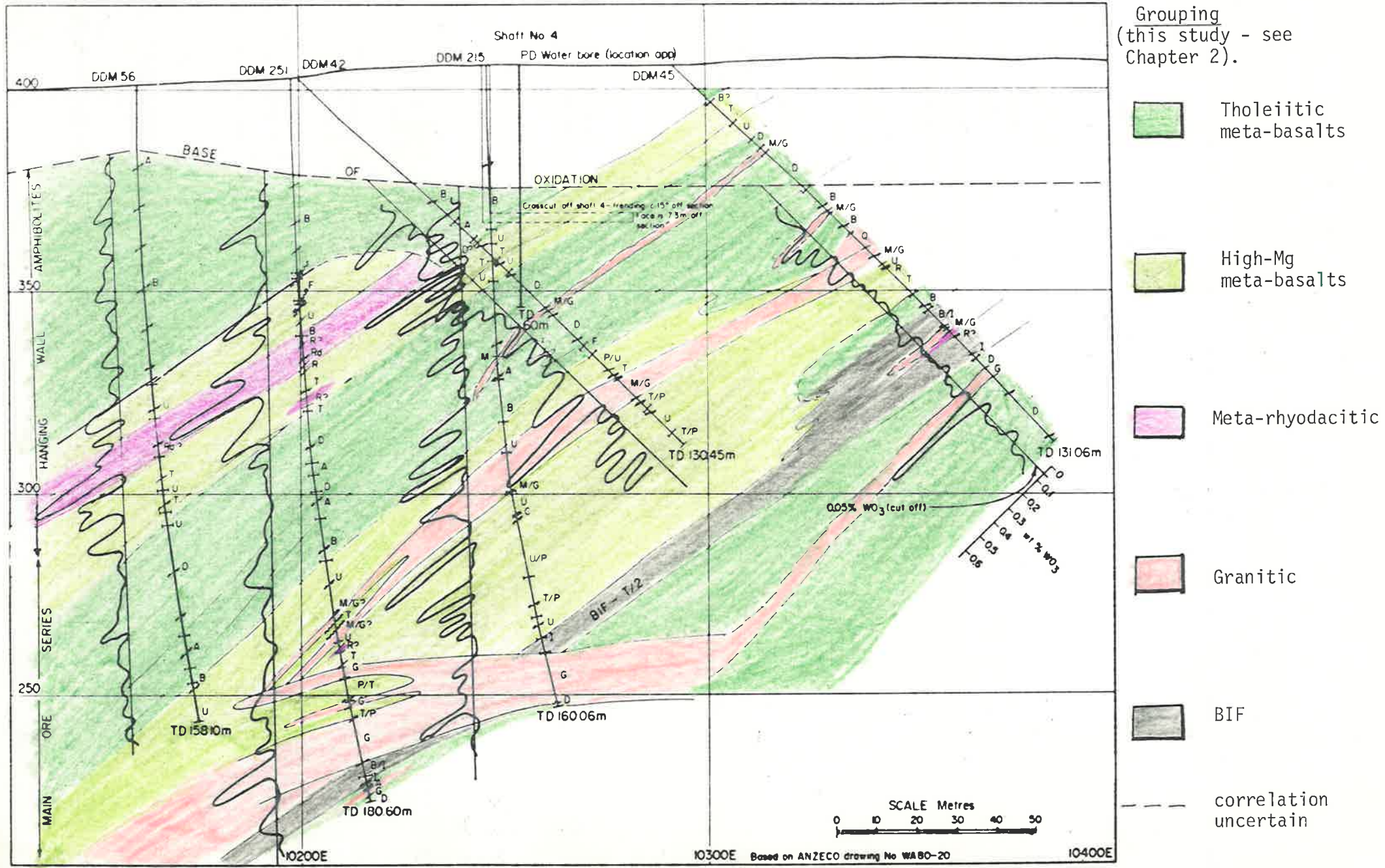
 Contact - clear cut, attitude to core axis shown.

 Contact - irregular.

 Contact - transitional or no clear information.

 Foliation or bedding attitude to core axis.

DRILLING SECTION 10000N GEOLOGY AND WO₃ VARIATION DOWN THE DRILL HOLES



Grouping
(this study - see
Chapter 2).

- Tholeiitic meta-basalts
- High-Mg meta-basalts
- Meta-rhyodacitic
- Granitic
- BIF
- correlation uncertain

Figure 1.4

for these trends to be significant.

Figure 1.4 also shows that there is a slight stratigraphic control on WO_3 values. This is also apparent when WO_3 values are plotted on other cross sections* and it is believed to be mainly due to the fact that most of the mineralized quartz veins are concordant with the host rocks.

The Trench deposit is only about 1-1/2 kilometres NW of the Hill deposit (Figure 1.3). Their proximity makes one suspect that they are very similar - that possibly one is a lateral equivalent or extension of the other. However, all indications so far are that the two deposits are different: in the Hill deposit, scheelite occurs at the contact of a quartz-muscovite greisen sheet and a pyritic phlogopite schist, either as coarse disseminations within the greisen or within numerous quartz and greisen veins in both the schist and the greisen. The contrasting chemical environment at the contact is believed to have initiated precipitation of the scheelite.

In the Trench deposit, mineralization is closely associated with quartz veins. The scheelite is found either within or very close to quartz veins in a succession of greenstones and banded iron formations that have been intruded by aplites, microgranites, quartz porphyry and greisenized sills. These acidic rocks and the quartz veins are thought to be differentiates of a granite at depth (Whittle, 1977; Middleton, 1979).

1.10 Terminology

In this thesis, the following terms are used with the indicated meanings:

1) Mount Mulgine greenstones - refers to all rocks at Mount Mulgine which are neither BIFs nor granitic.

2) Granitic rocks - refers to acidic rocks and/or their altered and metamorphosed equivalents, e.g., greisens, gneisses, rhyolite(?).

3) Mineralization - refers to minerals (mostly opaques) which formed or are believed to have formed as a result of hydrothermal activity. The term is also used to describe the process of deposition of such minerals.

4) Gangue - refers to non-opaque minerals, except scheelite, that occur associated with opaques.

5) Paragenesis - refers to the order of deposition of the minerals (and not to mineral associates, supposedly coexisting in equilibrium as used by Winkler (1979)).

* These cross sections, together with the remnant samples and sample sections are stored in the School of Geology, University of Adelaide, under the reference number 822.

6) Primary mineral - refers to a mineral that formed directly from a melt or solution and whose composition has not significantly changed since formation.

7) Secondary mineral - a mineral that formed from another mineral or other minerals as a result of processes such as metamorphism, weathering or hydrothermal alteration, i.e., a mineral which is not primary as defined above.

CHAPTER 2 : PETROLOGY

2.1 Introduction

The main aim in this chapter, is to briefly describe the mineralogical, structural and textural features of the rocks at Mount Mulgine. The compositions of the rocks are included but discussion of trace element work is avoided as it is the subject of the next chapter. Mineral associations (e.g., replacements and replacement textures) grain size characteristics and paragenetic relationships of the constituent minerals are all covered in Chapter 4. More detailed petrographic descriptions of the rocks have been given by Whittle (1977, 1978) and Collins (1975).

It is stressed that field identification of some of the rocks generally referred to as "greenstones" (see under terminology, page 9/10 can be a problem and it is suggested that this problem might be avoided by using more general names for the rocks. In Chapter 3, it is shown that the Mount Mulgine greenstones are genetically and compositionally similar and so the use of general names is justifiable.

Some of the minerals that compose these rocks are difficult to tell apart even with the optical microscope (the electron microprobe was used to confirm many identifications - see Chapter 4). Their field identifications would be even more uncertain and it is believed that this is part of the reason why lithological correlations between drill holes are not very good, rather than because of facies changes.

The minerals identified in each of the 138 sample sections studied are listed in Appendix 2. The chemical analyses of some of the minerals determined by the electron microprobe, are in Appendix 4.

Fifty seven rock samples (including 5 samples of the Mount Mulgine Granite) were prepared for whole rock and trace element analysis as described in Appendix 3. The whole rock analyses and trace element data are also included in Appendix 3.

The major element analyses were by X-ray fluorescence spectrography (XRF) except for Na which was measured by flame photometry. Some of the trace element data were obtained by XRF and others were obtained using atomic absorption spectrometry (AA). To check on the accuracy of the techniques, the elements Ba, Ni, Rb and Zn were determined by both XRF and AA in the first batch of samples. Also, samples 276/102.05* and 259/84.35 which gave the lowest totals were re-measured. Values obtained from both techniques generally agree

*The sample number shows the diamond drill hole number and the depth in metres (in this example, the sample is from DDM 276; 102.05 metres from the surface.

reasonably and the repeat analyses of the above two samples show that the reproducibility of the XRF data is very good (see Appendix 3).

2.2 Sample selection

With over sixty diamond drill cores averaging well over 100m each, sampling can be a problem. It was decided at the beginning of this study, to take samples systematically from only about 10 drill holes. The drill holes were selected so as to cover as much of the Trench area as possible, in an even manner. The depth reached by the holes, their proximity to the exposed intrusive rocks and the availability of assay and log data at the time of sampling, were the other factors that were taken into consideration in selecting drill cores for detailed sampling. The drill hole location map (Figure A-1) at the beginning of Appendix 1 shows the holes from which most of the samples were collected. In addition, the other drill cores from the Trench area were examined in less detail and any rocks that showed "interesting" mineralization or some other unfamiliar feature(s) were also sampled.

Using the drill hole logs as a guide, samples were selected from the drill cores chosen such that each "different" lithological type from each drill hole was represented. Lithological types were initially defined strictly according to the drill hole log data and a sample was taken from each type, although some "different" types appeared identical to the unaided (and perhaps unfamiliarized?) eye. If rocks, supposed to be the same according to the logs, looked different, a sample of each of the rocks was collected.

Since the interest in the rocks at Mount Mulgine is not just academic, samples were finally selected if they also showed some mineralization. However, since heavily mineralized rocks are not good representatives of the original rocks, samples showing mineralization and rock-type samples were generally separate.

2.3 The rock types

The rocks at Mount Mulgine fall into three distinct groups - greenstones (meta-basalts) acidic rocks (granitoids) and banded iron formations (BIF). According to the drill hole logs and the cross sections constructed from them, all these rocks had been divided into as many as fifteen lithological types. The keys to the cross sections (e.g., Figure 1.4) show the basis that had been used for the recognition of the lithological types during core logging.

It will be noticed that some of the lithologies are weathered or altered equivalents of other rocks while some of the others are minor variations of each other. It appeared to the writer that there was no firm and unequivocal basis for the distinction of many of the lithological types. Further, it seems that dividing the rocks into the fifteen or so lithological

types creates more problems than it solves. For example, the hole to hole rock correlations on the cross sections are, sometimes, not good and this has led to inferences of what appear to be an excessive number of facies changes in such a small area. It is believed that at least part of the reason for the poor correlations is that it is very difficult to consistently distinguish between the very similar lithologies.

Most of the lithological types (as previously denoted on the cross sections) were sampled, analysed and studied in thin section. From the chemical and mineralogical compositions of the rocks (some of which are given below) coupled with conclusions (see page 37) drawn from trace element work presented in the next chapter, it is proposed that for practical purposes, the rocks at Mount Mulgine can be divided into the following six groups with the indicated general names.

- | | | |
|-------------|---|----------------------------|
| Greenstones | { | 1. Tholeiitic meta-basalts |
| | { | 2. High-Mg meta-basalts |
| Acidic | { | 3. Meta-rhyodacitic rocks |
| | { | 4. Granitic rocks. |
| BIF | | 5. Banded iron formations |
| | | 6. Altered rocks. |

The constitution of each of the first five groups will be given below. The last group has been added to accommodate any rock that is so altered (weathered or mineralized) that it cannot be confidently placed in any of the first five groups.

2.3.1 Mount Mulgine greenstones

In this study, the greenstones at Mount Mulgine have been divided into two groups - the tholeiitic meta-basalts and the high-Mg meta-basalts. This division was based on the samples that were analysed which fall into two chemically distinct groups on the basis of their Ti and Mg contents. In Appendix 3, the high-Mg meta-basalts have more than 11 wt.% MgO and less than 0.95 wt.% TiO₂ while the tholeiitic meta-basalts have more than 0.75 wt.% TiO₂ and less than 11 wt.% MgO. Other chemical differences are in Table 2.1 which shows the mean chemical compositions of the Mount Mulgine greenstones and also the compositions of typical rocks in each of the two groups. The more prominent differences are higher Ti, Al, Fe, K, P, Y, Ba, Rb, Sr and Zr in the tholeiitic meta-basalts and higher Mg, Ca, Ni, Co, Pb, Sb, Sc, W, As and Cr in the high-Mg meta-basalts.

It should, perhaps, be reiterated that the names "tholeiitic meta-basalt" and "high-Mg meta-basalt" are being used in a general sense. The

Table 2.1 : Compositions of Mount Mulgine greenstones

	Tholeiitic meta-basalts	High-Mg meta-basalts	Typical tholeiitic meta-basalt	Typical High-Mg meta-basalt
<u>Oxides</u> (wt.%)	(mean)	(mean)	262/135.0	268/131.95
SiO ₂	52.20	51.58	51.42	52.17
TiO ₂	1.21	0.68	1.25	0.87
Al ₂ O ₃	13.74	7.15	14.33	6.53
Fe ₂ O ₃ *	12.62	10.90	13.57	10.04
MnO	0.21	0.24	0.21	0.24
MgO	6.95	14.95	5.69	15.06
CaO	8.22	11.35	9.05	12.72
Na ₂ O	0.75	0.48	0.12	0.32
K ₂ O	3.56	2.25	3.30	1.74
P ₂ O ₅	0.12	0.07	0.12	0.09
Total**	99.51	99.65	99.06	99.77
Loss on ignition	3.53	2.38	2.53	2.33
<u>Elements</u> (ppm)				
Ag	5	6	3	9
As	88	332	240	194
Ba	159	75	244	90
Be	12	13	6	15
Ce	11	7	4	15
Co	36	57	42	52
Cr	304	2100	212	1620
Cu	226	148	165	215
Ga	20	12	20	15
Li	183	217	160	123
Mo	22	9	36	5
Nb	5	3	6	4
Nd	10	10	10	11
Ni	86	286	75	257
Pb	49	33	0	9
Rb	600	490	556	341
Sb	95	147	90	250
Sc	41	54	37	60
Sn	8	8	5	10
Sr	155	74	250	81
V	312	262	348	274
W	112***	162	50	40
Y	21	12	19	15.9
Zn	91	166	105	146
Zr	67	31	66	49

*Total iron as Fe₂O₃

**Total does not include loss on ignition

***A W value of 2190 ppm obtained for sample No. 259/30.90 was omitted in the calculation of the mean. When this sample is included, the value increases from 112 ppm to 202 ppm; which is clearly deceptive.

high-Mg meta-basalts, for example, include rocks which, strictly, may not even be meta-basalts. Another point that needs to be stressed is that the Mount Mulgine greenstones (whether tholeiitic or high-Mg) are all generally meta-basaltic. They thus grade into each other and to emphasize this complete gradation, they are described together. This overlap will be more apparent in the discriminant diagrams in Chapter 3.

The tholeiitic meta-basalts form the largest group of rocks at Mount Mulgine and the high-Mg meta-basalt group is the second largest. All the rocks that have been mapped as "meta-basalts", "meta-andesites", "meta-dacites" and some "meta-pyroxenites (actinolite-chlorite schists)" belong to the tholeiitic meta-basalt group. The rest of the "meta-pyroxenites", the "meta-olivine(?) pyroxenites" and "phlogopite schists" belong to the high-Mg meta-basalt group.

The mineralogical differences between the tholeiitic meta-basalts and high-Mg meta-basalts, like the chemical differences that determined them, are mainly differences in abundance or in proportions of the minerals. The possible exceptions among the following minerals are chlorite and magnetite which were observed in the Al-Fe-rich tholeiitic meta-basalts but usually not in the high-Mg meta-basalts. The main minerals that make up the greenstones studied are quartz, actinolite, hornblende, biotite, chlorite, epidote, plagioclase, K-feldspar, sphene, tremolite, phlogopite, talc, pyroxenes, muscovite, sericite, magnetite, pyrite, chalcopyrite and pyrrhotite. Fluorite and carbonates are often present and may be locally abundant. The minor minerals include apatite, garnets, altered olivine, chrysotile and numerous opaque minerals, generally believed to be part of the mineralization. A more complete list of the minerals that occur at Mount Mulgine is given as Table 4.1.

The high-Mg meta-basalts are mainly composed of tremolite, phlogopite, talc and pyroxenes. The type of pyroxene determined in this study is diopside but other pyroxenes have been reported (see Chapter 4). The tholeiitic meta-basalts are chiefly composed of actinolite or hornblende, epidote, chlorite, biotite and accessory magnetite. Quartz is more common in the tholeiitic meta-basalts than in the high-Mg meta-basalts.

An attempt to list the mineral associations or assemblages in the greenstones led to the conclusion that almost any of the above minerals may occur together. Rather than presenting a long list of combinations of the above minerals, it was decided to list all the minerals that were identified in each of the sample sections that were studied. The mineral lists are the contents of Appendix 2. From this Appendix, it will be noted that some rocks are composed of only a few minerals (some are essentially monomineralic) while others may be composed of as many as a dozen or more minerals. The abundance (volume percent of the rock) of each of the main minerals varies from zero to the

amounts indicated below - all visual estimates.

actinolite and/or hornblende	0-95%
biotite	0-70%
carbonates	0-50%
Chlorite	0-40%
pyroxene	0-50%
epidote	0-60%
magnetite	0-55%
muscovite	0-20%
K-feldspar	0-10%
phlogopite	0-85%
quartz	0-60%
talc	0-40%
tremolite	0-90%
fluorite	0- 5%
sericite	0-50%

The extrusive nature of the Mount Mulgine greenstones is not in doubt because they are generally fine-grained (grain size less than 1 mm). Individual minerals, notably amphiboles, may have medium- or coarse-grained crystals. As their name implies, the rocks are generally green; the type of green depending on the nature and relative abundance of the constituent minerals. The high-Mg meta-basalts are very light green while the tholeiitic meta-basalts may be very dark green or even blue because of the abundance of green-blue amphiboles. The dominant coloured amphiboles are magnesio hornblende (see Chapter 4) and actinolite. Rocks with appreciable amounts of epidote are yellowish and those containing appreciable amounts of biotite may be brownish.

Banding is a strong feature in some of the greenstones, especially the tholeiitic ones. In the majority of cases, banding is believed to be due to original compositional layering. It is so well displayed, in some rocks, that it is taken as evidence that at least some of these rocks were deposited in water (Plate 2.1A). The bands are defined by the presence or absence of certain minerals and not by mineral grain size sorting. More often than not, biotite is involved in the banding; being abundant in some bands and hardly appearing in others.

Some greenstones are strongly schistose. If such rocks are also banded, the schistosity is usually parallel to the banding. The greenstones display a variety of textures. Porphyroblastic texture (Plate 2.1B) is common, especially in the high-Mg meta-basalts in which tremolite and pyrite porphyroblasts are in a groundmass of fine talc and (sometimes) fine quartz. Colloform

texture (Plate 2.1C) was also observed in the high-Mg meta-basalts rocks as well as in the tholeiitic meta-basalts but it is relatively rare. Greenstones that have suffered static-style metamorphism usually display some relict texture, with no mineral alignment (Plate 2.3A) while those, especially the tholeiitic members, from dynamic-style domains have relict flow textures.

2.3.2 Meta-rhyodacitic rocks

There are some rocks at Mount Mulgine which are generally intermediate between the greenstones and the granitic rocks, both in their physical appearance and in some of their chemical parameters. These rocks are here described as meta-rhyodacitic rocks and they comprise a group which includes the rocks that have been mapped as "meta-rhyolites" and "meta-rhyodacites".

Two meta-rhyodacitic rock samples were analysed and their compositions are reproduced in Table 2.2. The Table also contains average compositions of basalts, rhyodacites and granites from the literature for comparison purposes. Comparisons with unaltered rocks have to be done cautiously, because as shown in the next chapter, there has been movement of the major elements in the rocks at Mount Mulgine but even with this in mind, it is clear that the meta-rhyodacitic rocks are unlikely to have been basalts or granites (rhyolites). They are on one hand, too rich in Si and too poor in Ca and Mg to be meta-basalts; while on the other hand, they are too low in Ca and Si, and too rich in Fe and Mg to be granitic.

The present chemical composition of sample 274/154.5 is closest to that of a rhyodacite but the composition of sample 276/128.0 is closer to that of an andesite. In the diagrams in Chapter 3, the latter sample was included among the tholeiitic rocks and the former was grouped with the acidic (granitic) rocks.

The meta-rhyodacitic rocks are essentially composed of quartz (up to 60%) and muscovite (up to 40% of the rock). Biotite, chlorite, fluorite, pyrite and less commonly sphalerite, are usually present and may take up to 30% of the rock volume. Other minerals may occur in minor or trace amounts. The above percentages are all visual estimates.

The rocks are usually very fine-grained and grey in colour when fresh. Clusters of biotite flakes may give them a spotted appearance. Their texture is usually granuloblastic. Apparently, the meta-rhyodacitic rocks "tarnish" relatively rapidly to a yellowish-brown to light green colour. The light green colour is presumably due to altered muscovite which has been called damourite by Whittle (1977, 1978). The porosity of these rocks was/is probably high (some were possibly tuffs originally, according to the cross sections (e.g., Figure 1.4). This would explain why the rocks get altered rapidly when exposed

Table 2.2 : Composition of Mount Mulgine meta-rhyodacitic rocks compared with that of rhyodacites, granites and basalts.

Sample No.	Data from Le Maitre (1976)				
	meta-rhyodacitic		rhyodacite	granite	basalt
	276/128.00	274/154.5			
Oxides (wt.%)					
SiO ₂	62.02	67.30	65.55	71.30	49.20
TiO ₂	1.28	0.37	0.60	0.31	1.84
Al ₂ O ₃	15.86	16.65	15.04	14.32	15.74
Fe ₂ O ₃ *	11.25	5.08	4.16	2.85	10.92
MnO	0.13	0.07	0.09	0.05	0.20
MgO	4.14	2.30	2.09	0.71	6.73
CaO	0.53	0.37	3.62	1.84	9.47
Na ₂ O	0.17	0.18	3.67	3.68	2.91
K ₂ O	4.48	6.70	3.00	4.07	1.10
P ₂ O ₅	0.11	0.20	0.25	0.12	0.35
Total**	99.95	99.22	98.07	99.25	98.46
Loss on ignition	4.02	3.64	1.72	0.82	1.49
Elements (ppm)					
Ag	4	2			
As	8	12			
Ba	107	693			
Be	9	13			
Ce	13	80			
Co	38	8			
Cr	137	85			
Cu	250	250			
Ga	24	23			
Li	195	296			
Mo	7	9			
Nb	3	7			
Nd	11	34			
Ni	88	17			
Pb	9	33			
Rb	658	896			
Sb	20	10			
Sc	42	10			
Sn	10	5			
Sr	14	80			
V	377	92			
W	80	60			
Y	13	7			
Zn	85	68			
Zr	67	130			

*Total iron as Fe₂O₃

**Does not include loss on ignition.

to weathering agents. It would also explain why some of these rocks are sometimes heavily mineralized.

2.3.3 Granitic rocks

This group of rocks comprises all the lithologies that have been mapped as "microgranites", "quartz porphyry" and "greisens". The granitic rocks are very important not only because they are hosts to scheelite mineralization in the Hill deposit but also because they (or their differentiates) must be considered a potential source of W and other anomalously high trace elements in the rocks at Mount Mulgine.

Since this study was mainly concerned with the Trench deposit, the Mount Mulgine Granite itself was just outside the study area; but because of its proximity and postulated importance with regard to the genesis of the deposits, a few samples of the granite were collected for analysis. The geology, geochemistry and genesis of the granite have been described in some detail by Collins (1975).

Analyses of granitic rocks (greisens) from the Trench area and of "granites" from Mount Mulgine itself are given in Table 2.3, more analyses of such rocks are in Appendix 3. There is no significant difference between the analyses and this, plus the fact that the rocks occur close to each other, implies that the Mount Mulgine Granite and the granitic rocks in the Trench area may have the same origin. This supports the general view held by most previous workers that the greisens in the Trench sequence are sills which are off-shoots of a granite at depth that is possibly continuous with the Mount Mulgine Granite. However, there is also a view (A.D. Gibbs, pers. comm.) that the granitic rocks in the Trench may, like the other members of the Trench sequence, be volcanic in origin - that they could have been originally rhyolites. This view, in the light of the fact that the greisens are interlayered with the greenstones and the other rocks in the Trench area, seems reasonable but it overlooks two important facts. Firstly, most evidence points to the fact that the Mount Mulgine Granite, which is clearly intrusive, is related to the greisens (in fact the greisens may be part of the Granite) and secondly, and perhaps more important, it is unusual to find acidic and some basic to ultra-basic rocks repeatedly interlayered with each other with hardly any intermediate members; unless there were several vents tapping different magmatic chambers.

It is, therefore, reasonable to conclude that the granitic rocks are not co-magmatic with the volcanic rocks at Mount Mulgine and further, that they were not volcanics originally. The latter point is clear from the first three discriminant diagrams in Chapter 3. In these diagrams, the granitic rocks generally plot outside the delineated fields for volcanic rocks. Where they do plot in these fields, they do not consistently plot in any one field implying

Table 2.3 : Compositions of Granitic Rocks from Mount Mulgine

Sample No.	Trench deposit			Hill deposit	
	259/135.10	252/138.67	268/106.70	185/~49	10/~120
<u>Oxides(wt.%)</u>					
SiO ₂	72.27	80.76	70.76	74.66	79.00
TiO ₂	0.37	0.03	0.29	0.22	0.14
Al ₂ O ₃	15.23	13.03	15.38	13.34	14.01
Fe ₂ O ₃ *	3.86	1.65	2.75	1.89	1.22
MnO	0.06	0.04	0.05	0.04	0.00
MgO	1.22	0.11	1.18	0.36	0.31
CaO	1.20	0.63	2.16	1.47	0.71
Na ₂ O	0.23	0.56	2.62	4.00	0.19
K ₂ O	5.25	3.17	4.80	3.60	4.42
P ₂ O ₅	0.14	0.01	0.11	0.08	0.02
Total**	99.84	99.99	100.10	99.65	100.02
Loss on ignition	3.70	2.27	2.52	1.22	2.26
<u>Elements(ppm)</u>					
Ag	3	2	9	0.5	1
As	209	25	129	8	5
Ba (XRF)	556	76	1220	875	326
(AA)	580	60	1240	-	-
Be	9	7	9	4	5
Ce	58	11	72	47	15
Co	11	4	7	0	0
Cr	200	240	244	213	179
Cu	85	168	208	14	129
Ga	23	19	24	18	23
Li	490	23	136	33	68
Mo	12	94	8	3	7
Nb	8	28	8	8	17
Nd	24	8	24	14	6
Ni (XRF)	10	22	10	9	4
(AA)	11	23	7	-	-
Pb	4	41	111	46	7
Rb (XRF)	683	254	536	211	435
(AA)	760	290	560	-	-
Sb	25	40	195	<5	55
Sc	6	4	6	3	4
Sn	10	<5	10	<5	<5
Sr	<5	45	203	200	16
V	58	7	53	21	25
W	280	10	120	<10	40
Y	4	11	5	5	6
Zn (XRF)	45	31	65	50	26
(AA)	49	32	72	-	-
Zr	150	50	154	133	86

*Total iron as Fe₂O₃

**Does not include loss on ignition.

that their presence within these fields is only incidental (compare Figures 3.2, 3.3 and 3.4)

The granitic rocks in the Trench area are essentially composed of quartz and muscovite. In sections 264/103.10 and 264/145 only these two minerals were observed. Quartz occupies from 0-90% and muscovite from 10-90% of the granitic rocks. In other samples additional minerals were observed. Plagioclase feldspar may make up to 20% of the rock and K-feldspar, which is more common, may take up to 30% of the rock volume. Biotite or phlogopite is often present as well as fluorite and minor quantities of chlorite and sphene. Garnet and apatite may also be present. In sample 88/64 (from the Hill deposit) apatite occupies about 10% of the rock and the rest is muscovite with trace fluorite. The opaque minerals generally constitute less than 2 volume percent of the granitic rocks, and include pyrite, molybdenite, sphalerite, pyrrhotite, chalcopyrite, chalcocite, tetrahedrite, rutile and ilmenite. Trace scheelite was observed in one or two samples.

The acid rocks are leucocratic and fine- to medium-grained. Some have a schistose appearance ("fluxion structured" according to Whittle, 1977, 1978) due to the alignment of muscovite flakes. The muscovite flakes are sometimes wrapped around quartz megacrysts or quartz pockets. In most cases, the muscovite appears later than quartz. Under the microscope, the texture is granitic (granular) but in some samples it is porphyroblastic with quartz megacrysts in a groundmass of very fine muscovite (sericite) and fine quartz.

The "granite" samples from the Hill deposit have the same mineralogy as the Trench greisens, the only difference being that they have more feldspars at the expense of quartz and muscovite, i.e., they are not as greisenised as the Trench "microgranites". Also, they contain ilmenite which was not observed in the Trench greisens and some of the muscovite has clearly replaced biotite.

The main aim of collecting samples of the Mount Mulgine Granite was to find out what type of granite it is. If the granite classification scheme proposed by Chappell and White (1974) is applicable to altered Archaean granitic rocks, then those at Mount Mulgine would be mainly S-type. Sample 185/~49, however, would be I-type. Since most of the samples analysed are greisens and the greisenization process involves a breakdown of plagioclase and subsequent loss of Na and Ca, the abundances of which are crucial to the classification scheme of Chappell and White (1974), it is likely that all the granitic rocks at Mount Mulgine were originally I-type granites which have since developed an S-type character through alteration. This would agree with Collins' (1975) thesis that the Mount Mulgine Granite formed from "pre-existing granitoid or gneissic rocks" and also with the fact that the granite is associated with W and Mo mineralization. Tin mineralization usually occurs associated with S-type

Plate 2.1A

Strong banding in a quartz-veined phlogopite-epidote-tremolite schist, believed to be due to original compositional layering. Such layering implies deposition in water. The black streaks are iron staining due to solution activity. Note that the grain size (best illustrated by opaques) increases downwards (arrow).

Sample No. 264/67.75, transmitted light.

Plate 2.1B

A tremolite-talc schist showing porphyroblastic texture. The porphyroblasts are euhedral tremolite and pyrite (opaque). The groundmass is mainly talc.

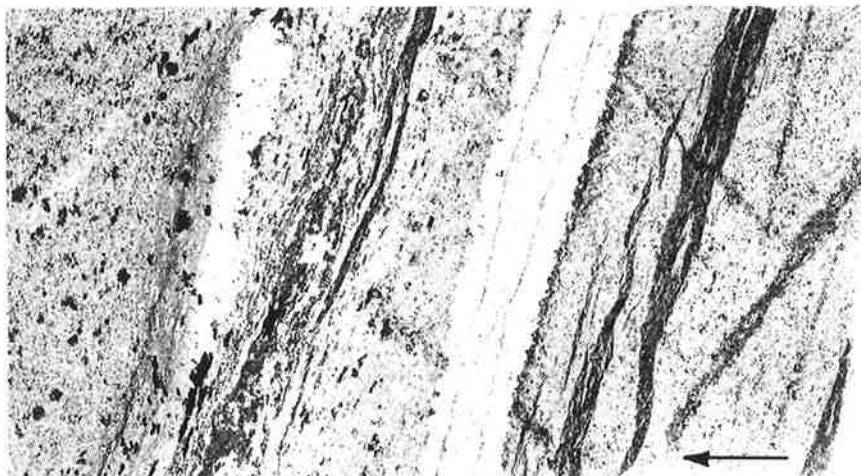
Sample No. 259/123.32, transmitted light.

Plate 2.1C

Colloform texture. The fine laminations are composed of cherty silica. The opaques at the base of the laminations are framboidal pyrite grains. The white mineral on the other side of the opaques is quartz. The white substance in the centre and lower left hand corner is the mounting medium or the microscope glass slide.

Sample No. 268/50.34, transmitted light.

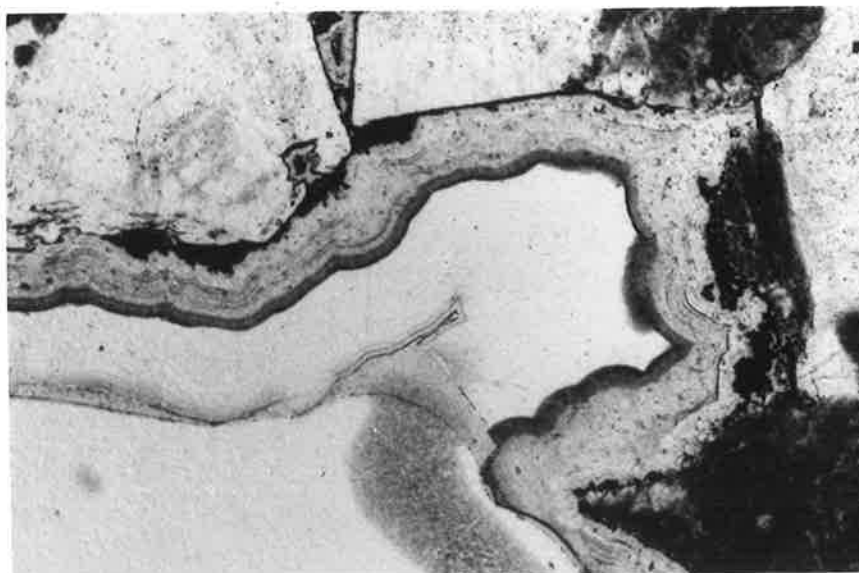
PLATE 2.I



A 10 mm



B 0.5 mm



C 2 mm

Plate 2.2A

Banding in a banded iron formation.

Sample No. 276/88.25, transmitted light.

- MRB = Microband (≤ 1 mm wide)
- LB = Large band (≈ 3 mm wide)
- MSB = Mesoband (≥ 5 mm wide).

Plate 2.2B

Quartz vein illustrating the relative coarseness of minerals found in the vein compared to other minerals in the rock.

Sample No. 276/124.85, transmitted light.

- Ac = actinolite
- Py = pyrite

Plate 2.2C

"Meandering-type" (folded) quartz veins. The veins were fractured during folding and the parallel fractures are generally perpendicular to the main line of stress (arrows). Greenish mica (damourite?) was forced into the fractures.
Sample No. 251/139.4, transmitted light.

PLATE 2.2

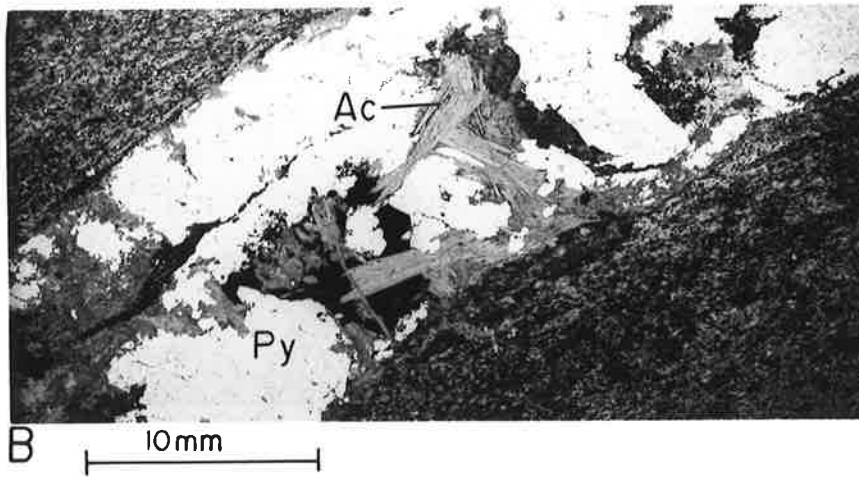
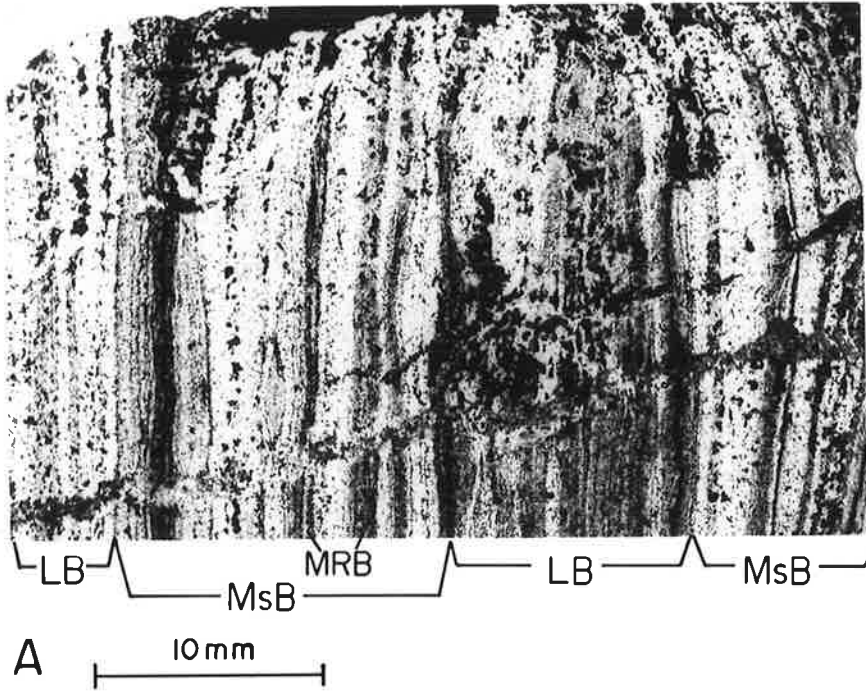


Plate 2.3A

Blastoporphyritic (relict) texture - coarse largely altered amphibole megacrysts can still be seen in a groundmass of fine talc and quartz.

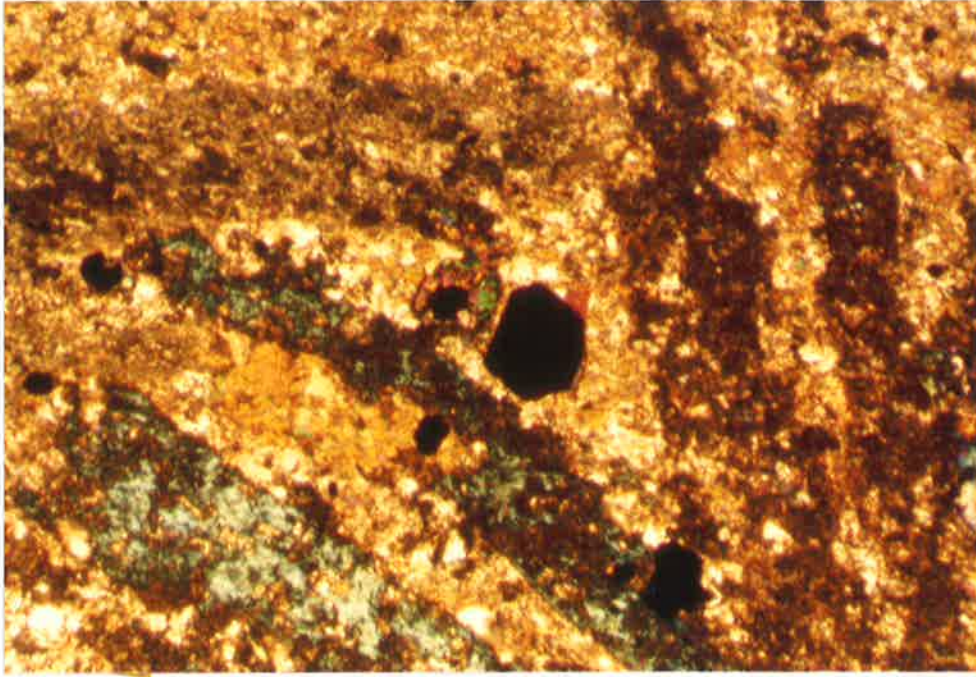
Sample No. 252/50.20. Transmitted light, crossed polars.

Plate 2.3B

Complex veining illustrated by a collection of half-cores from different drill holes.

The half-cores are from DDM 259, 275 and 313.

PLATE 2.3



A 0.5mm



B

granites (Chappell and White, 1974), and there is very little Sn at Mount Mulgine. Collins (1975) also found both S- and I-type granites at Mount Mulgine and inferred that the S-type (a muscovite granite) was also I-type because it appeared to have formed from the residual liquids of the I-type (a muscovite-biotite granite). Perhaps the muscovite granite is just an alteration equivalent of the muscovite-biotite granite.

2.3.4 Banded iron formations (BIFs)

The banded iron formations constitute a relatively small but prominent group of rocks at Mount Mulgine. They form the main stratigraphic marker horizons and, together with the granitic rocks, are the only rocks that were observed exposed in the Trench area. Faults at Mount Mulgine have been inferred from the discontinuity of BIF beds on the surface.

Two BIFs were analysed and their compositions are reproduced in Table 2.4. Mineralogically, they are essentially composed of magnetite and quartz (each of these minerals may constitute up to about 50 volume percent of the rock). Other minerals including amphiboles, sphene, chlorite, biotite, epidote, carbonates, pyrite and chalcopyrite are usually present. Garnets have also been reported (Whittle 1977, 1978).

The BIFs were originally chemical sediments and although they now appear to have been completely recrystallized during metamorphism, they retain initial bedding. The bedding is defined by layers of magnetite or quartz grains giving the BIFs a strongly banded appearance (Plate 2.2A). In those rocks in which banding is well displayed, three types of bands can often be distinguished as labelled in Plate 2.2A. Large bands (LB) would be about 3 mm across and are predominantly composed of either quartz or magnetite (where one mineral dominates, the other is subordinate). Larger bands, here called mesobands (Ms B) also occur and are at least 5 mm across. The mesobands are composite bands of large bands and microbands (MRB) and usually contain bands of other minerals, e.g., biotite. Finally, there are microbands which are less than 1 mm across and are composed of magnetite.

According to Whittle (1977, 1978) the BIFs are of the type which form in a volcanogenic environment by the alternating chemical precipitation of exhalative silica and iron oxides and the accumulation of clastic micaceous detritus. The microcrystalline cherty silica was converted (recrystallized) to fine-grained granuloblastic quartz intergrowths.

2.4 Veining within the rocks

Veining is a very conspicuous feature in all the rocks at Mount Mulgine. By far the vast majority of the veins are quartz veins. In thin section under

Table 2.4 : Compositions of Mount Mulgine BIFs

Sample No.	276/88.25	268/58.54
<u>Oxides(wt.%)</u>		
SiO ₂	40.08	44.97
TiO ₂	0.02	0.10
Al ₂ O ₃	0.26	0.69
Fe ₂ O ₃ *	58.49	48.07
MnO	0.12	0.19
MgO	0.62	2.79
CaO	0.49	2.55
Na ₂ O	0.08	0.17
K ₂ O	0.03	0.25
P ₂ O ₅	0.22	0.13
Total**	100.41	99.91
Loss on ignition	0.63	0.25
<u>Elements(ppm)</u>		
Ag	3	3
As	209	120
Ba (XRF)	2	13
(AA	10	30
Be	2	1
Ce	11	12
Co	29	11
Cr	346	259
Cu	153	90
Ga	5	11
Li	4	30
Mo	2	0
Nb	1	2
Nd	12	4
Ni (XRF)	161	20
(AA	120	10
Pb	0	0
Rb (XRF)	11	54
(AA	30	70
Sb	20	25
Sc	1	9
Sn	5	10
Sr	2	45
V	71	45
W	20	160
Y	8	3
Zn (XRF)	22	276
(AA	31	256
Zr	1	24

*Total iron as Fe₂O₃

**Does not include loss on ignition.

the microscope, it is clear that other minerals also form veins. Carbonate adularia, fluorite, pyrite, chlorite, pyroxene, muscovite, sphene, sphalerite, and sericite veins have all been observed. In each of these veins, the mineral after which the vein is named occurs either alone or with relatively minor quantities of other minerals.

The minerals in the veins or along the vein margins are usually coarser than those in the enclosing rocks and relatively fresh looking (Plate 2.2B). This is believed to be either due to recrystallization or to later crystallization from the siliceous fluids that gave rise to the veins. With the exception of quartz veins, all the other veins are small; the widest among them would be about 0.5 mm across. The quartz veins observed have widths of up to about half a metre. The following remarks, some of which are generally true for all veins, refer specifically to quartz veins.

In well mineralized sections, veining averages about 15-20% of the total rock volume (Middleton, 1979) and the amount of veining is generally proportional to W and Mo mineralization. The smaller veins, which generally occur further away from the intrusive rocks, carry more scheelite while the larger veins, which are often closer to the intrusions, carry more molybdenite. This distribution of scheelite and molybdenite may be due to physico-chemical factors (e.g., the fact that W tends to form oxides while Mo usually forms sulphides, or the availability or activity of elements such as Ca) but in Chapter 5 it is suggested that this zoning may be due to the minerals forming at different times.

As Plate 2.3B attempts to show, the veins can have a wide variety of attitudes and relationships to one another, so the veining is sometimes complex. The majority of the veins are concordant with the schistosity or banding. Others are clearly transgressive and others have pinch and swell (boudinage-type) structures. Pyrite is often concentrated or deposited at the necks of the "boudins". The complexity of the veining in the rocks at Mount Mulgine is believed to be partly due to different generations of veins superimposed on one another as well as being due to folding.

The "meandering" form of some veins may be due to folding; i.e., the "meanders" may, in fact, be miniature folds; results of compression. In sample 251/139.4, there is evidence that this is the case because quartz in the "meandering" veins is fractured and the fractures are generally parallel to each other and roughly perpendicular to what would have been the main direction of stress (Plate 2.2C).

Some of the larger veins have "xenoliths" of the host rocks within them; and this makes it appear as if some of the host rocks were assimilated within

the larger veins.

The relationship of the veins and mineralization has already been mentioned. Not all veins are mineralized, however, and some are clearly barren even when the host rocks are mineralized. This is thought to be due to different generations of veins.

Whittle (1978) observed that in DD70, at a depth of approximately 140m, the epigenetic quartz-pyrite veins contain more rarer element-bearing phases (e.g., fluorite, occasional tourmaline and scheelite) and that below this depth, the veins rapidly merge with the "fluxion-structured" greisens. He concluded that the veins and greisens merge into a hidden cupola below and to the west of DDM70.

2.5 Metamorphism and hydrothermal alteration

2.5.1 Metamorphism

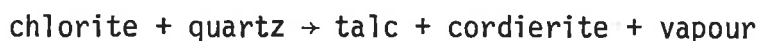
The rocks at Mount Mulgine have suffered dynamothermal metamorphism and they reached medium grade. Although cordierite and staurolite (the positive indicators of medium grade metamorphism, Winkler, 1979) were not observed and have not been reported, the presence of hornblende and calcic plagioclase (An >20, Collins, 1975) indicate that medium grade (the equivalent of amphibolite facies) metamorphism was attained. The absence of cordierite and staurolite is most probably due to inappropriate bulk composition of the rocks (these rocks are not aluminous enough). The presence of clinopyroxene (diopside) and forsterite would also indicate at least medium grade metamorphism (Winkler, 1979, p.82). Diopside and altered forsterite which were observed in some of the more Mg-rich rocks (see Chapter 4) are considered to be original constituents of the rocks and not products of metamorphism. This is because altered forsterite was observed in one sample 22/65.15, which is of an ultramafic (in which forsterite would have been one of the predominant original constituents) and also because metamorphic reactions that result in the formation of diopside (e.g., see Winkler, 1979, p.165-166., Spear, 1981) take place at temperatures much higher than those that appear to have prevailed at Mount Mulgine during metamorphism (see below). Hence the altered forsterite and diopside cannot be used as indicators of metamorphic grade in this case.

The conditions of metamorphism were estimated from mineral assemblages and compositions but they remain tentative because of uncertainty about whether some of the minerals are primary* or secondary* and about the possibility that some of the minerals used, although primary, may have formed after metamorphism. The peak metamorphic temperature is estimated to have been about 500°C (less than 550°C almost certainly) for the following reasons:

*see page 9/10 for "definitions".

a) Chrysotile was observed in some of the rocks. According to Deer et al, (1980), serpentine minerals cannot form above 500°C.

b) The presence of chlorite in contact with quartz and the absence of cordierite indicates the temperature did not exceed 550°C, assuming a 5 kb pressure or 500°C at 2 kb (Fawcett and Yoder, 1966). Otherwise the following reaction would have taken place:



c)* The mean temperature for sulphur isotope fractionation between co-existing pyrite-pyrrhotite pairs is about 505°C (see Chapter 6).

d)* The maximum indicated temperature, from fluid inclusion studies (Chapter 5) assuming a pressure of 2 kb at the time of fluid entrapment is about 500°C.

e) Finally, and perhaps even more important, no single line of evidence was found to suggest that the temperature would have exceeded 550°C.

The estimated peak metamorphic temperature is in contrast with that estimated by Collins (1975). He states (p.108) that the maximum temperature during regional metamorphism "was slightly greater than 650°C, perhaps about 675°C." But at temperatures of about 580°C (depending on the pressure), muscovite would react with quartz, in the presence of plagioclase, to give K-feldspar, vapour and an Al_2SiO_5 mineral (and this would indicate the beginning of high grade metamorphism, Winkler, 1979). If Collins' estimate is correct, then all the muscovite in contact with quartz would have to be secondary. Collins' evidence for his temperature estimate is not clear to the writer. On page 49, he states "The occurrence of epidote and clinozoisite in the meta-dolerite and their absence (emphasis, mine) in the amphibolites suggests that the breakdown of epidote can be used to place limits on the temperature-pressure conditions of the metamorphism. The temperature of the metamorphism is around 700°C and rock pressures of the order of 6 to 8 kilobars are indicated for the breakdown of epidote in similar rocks of the Willyama Complex (Binns, 1964)". Epidote is a very common mineral in the amphibolites at Mount Mulgine (Chapter 4) and its "breakdown" was not recognized in this study.

The pressure of metamorphism was estimated by sphalerite geobarometry (Chapter 6) and the Si^{+4} content of phengitic muscovites (Chapter 5). Although these methods have their limitations, a minimum pressure of 2 kb, indicated by both methods, is considered reasonable. On the other extreme, the pressure is unlikely to have exceeded about 4 kb.

*Mineralization is considered to have been essentially contemporaneous with metamorphism (see "ore genesis" in Chapter 7).

It has long been known that the composition of amphiboles, although primarily dependent on bulk rock chemistry, is also dependent on metamorphic grade (e.g., Leake, 1965., Binns, 1969., Spear, 1981). Since amphiboles may occur in rocks of low, medium or high metamorphic grade, attempts have been made to use amphibole composition as an indicator of the grade of metamorphism.

For proper identification of the type of amphiboles that occur at Mount Mulgine, a few electron microprobe analyses of the amphiboles had been performed (see Chapter 4). It was decided to use the limited data that had thus been obtained to check on the grade and conditions of metamorphism stated above.

Figures 2.1 and 2.2 confirm that the Mount Mulgine rocks reached the amphibolite facies (lower amphibolite facies, according to Figure 2.2). Such diagrams, however, have an inherent uncertainty, mainly due to the fact that it is difficult to distinguish the effects of bulk rock composition from those of metamorphism, on the hornblende composition. This can be done through experimental work similar to that of Spear (1981), who investigated the variability of hornblende composition with temperature (T) pressure (P) and oxygen fugacity (f_{O_2}) in a rock of single bulk composition.

From Spear's (1981) diagrams, the elements in hornblende which show the greatest variation with T, P and f_{O_2} (below about 700°C and 3 kb) are Na, Ti, K and Al. These elements are therefore, the most useful in determining these parameters. Their cation proportions (except K) have been used on Spear's (1981) Figures 3, 4 and 5, parts of which are reproduced here as Figures 2.3, 2.4 and 2.5 respectively. The cation proportions of Al, Na and Ti in the hornblendes analysed (see Appendix 4) vary from 1.13 to 1.48 for Al, from 0.19 to 0.28 for Na and from 0.04 to 0.06 for Ti. When these values are applied to Figures 2.3, 2.4 and 2.5, the conditions under which the hornblende formed are as follows:

Temperature : about 545 - 612°C (using Na values)
and 550 - 610°C (using Ti values)
Pressure : the maximum pressure was 3.9 kb.
Oxygen fugacity : Log f_{O_2} varied from -11.4 to -10.0.

The pressure is within the range previously estimated but the temperatures are slightly on the high side. There are two main reasons why the conditions thus obtained would not be expected to agree closely with those previously estimated. Firstly, there is evidence (see below and Chapter 3) that most elements at Mount Mulgine have been mobile. Secondly, and even more

Figure 2.1

Titanium and Na and K in amphiboles (in formula units).

- I - area of granulite facies.
- II - area of amphibolite facies.
- III - area of regressively altered amphiboles (from the amphibolite facies).

(After Zakrutkin and Grigorenko, 1967).

Figure 2.2

Frequency histograms of Ti content in aluminous hornblendes from meta-basic rocks, grouped according to metamorphic grade.

- A - epidote amphibolite facies
- B - lower amphibolite facies
- C - higher amphibolite facies
- D - granulite facies.

(After Binns, 1969).

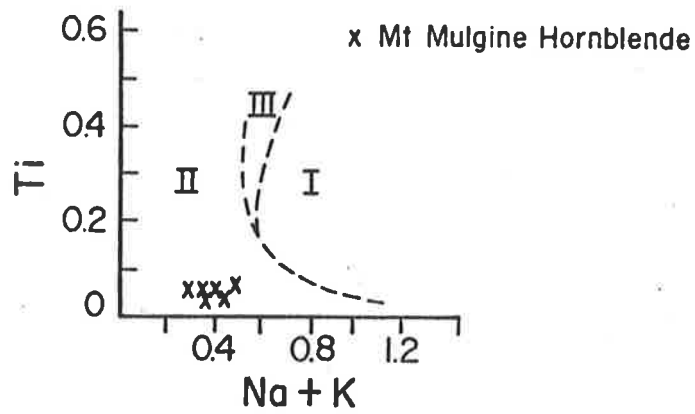


Figure 2.1

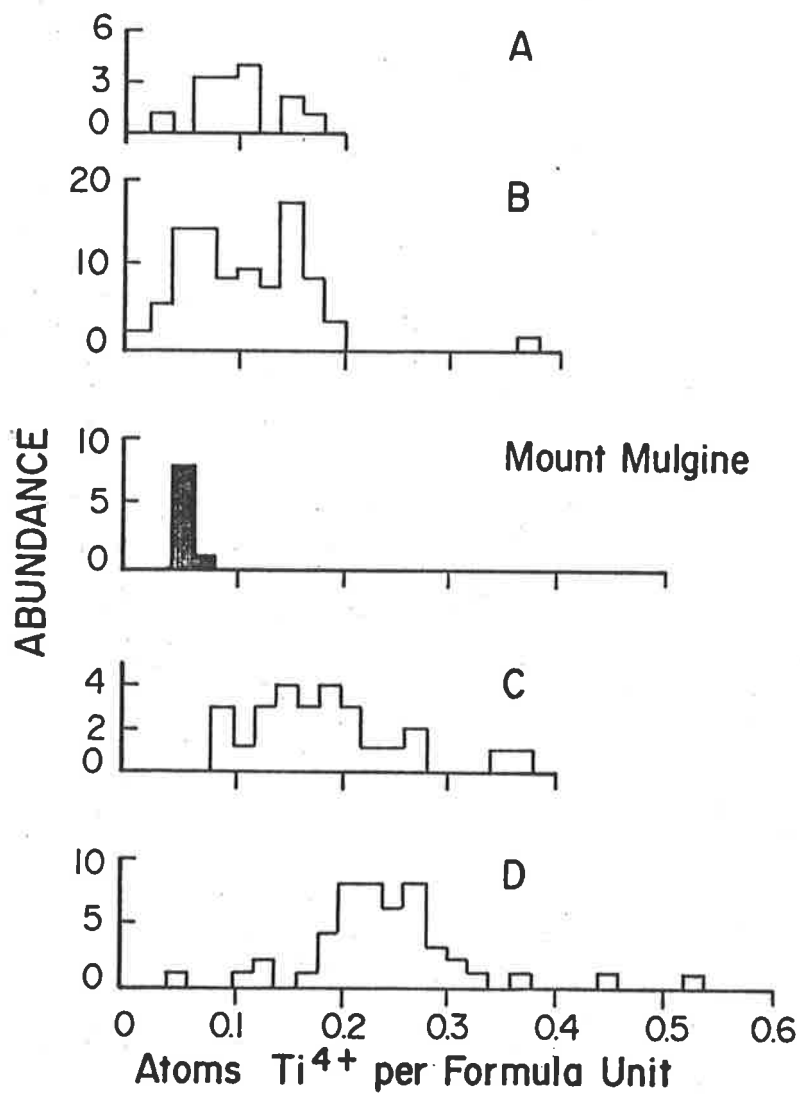


Figure 2.2

Figure 2.3

Sodium and Ti cation proportions of amphibole synthesized directly from basalt, plotted as a function of temperature of experiment.

$P_{\text{fluid}} = 3 \text{ kb}$,

Quartz-fayalite-magnetite (QFM) buffer.

(After Spear, 1981).

Figure 2.4

Titanium cation proportions of amphiboles synthesized directly from basalt plotted against $\log f_{\text{O}_2}$ of formation.

$T = 750^{\circ}\text{C}$

$P_{\text{fluid}} = 3 \text{ kb}$

(After Spear, 1981).

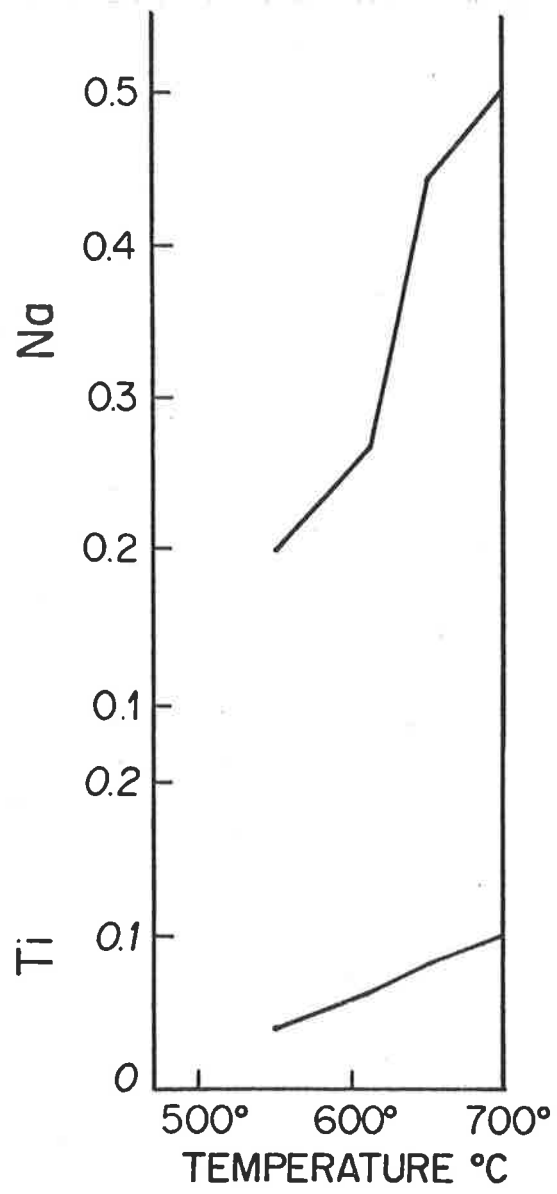


Figure 2.3

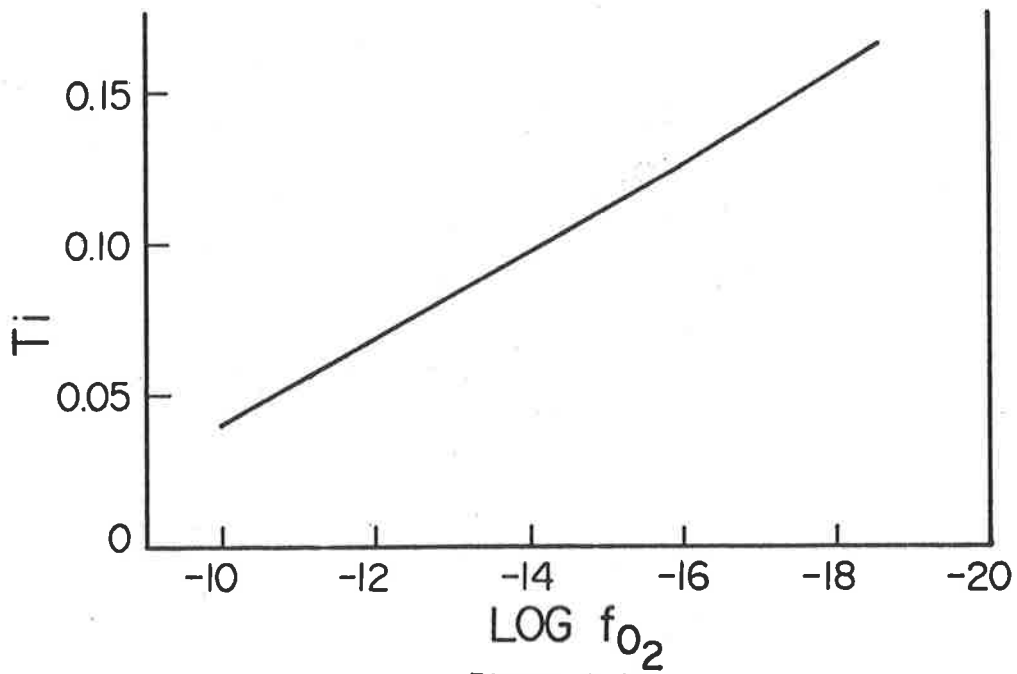


Figure 2.4

important, the bulk rock chemistry and the conditions under which Spear's (1981) experiments were conducted are unlikely to have been naturally duplicated at Mount Mulgine. Differences in these variables plus experimental uncertainty (see Spear, 1981) are enough to explain any such discrepancies. Hence, it can be generally stated that the hornblende composition is consistent with the grade and conditions of metamorphism as previously estimated.

Metamorphism was due to both heat and stress and the latter resulted in some rocks becoming strongly schistose. In areas of low strain, the rocks are more massive and retain relict textures of some presumably primary minerals (see Plate 2.3A).

Retrograde metamorphism has also affected the rocks and this is indicated by the abundant epidote after plagioclase, chlorite after biotite and actinolite and hornblende after pyroxene.

2.5.2 Hydrothermal alteration (K-metasomation)

Superimposed on both the prograde and retrograde metamorphic changes, there has been extensive hydrothermal alteration, the main effects of which were mineralization including carbonitization and K-metasomatism of the rocks.

When the chemical compositions of the Mount Mulgine greenstones are compared with those of similar rocks from other areas (see Table 3.1) the most striking difference is that the Mount Mulgine rocks are extremely rich in K. This is due to K-metasomatism which resulted in intense phlogopitization. The very low Na values have resulted from the same process.

Fluid inclusion leach analyses (see Table 5.1) show that the metasomatizing K-rich fluids were also rich in F, Mg and Fe as well as Ca and Na, and the presence of stilbite in cavities (Chapter 4) implies that Al must have also been present, although it was not detected in the fluid inclusion leaches. The extensive phlogopitization that resulted from the hydrothermal alteration is thus understandable.

Although relatively uncommon, volcanic rocks in which there is an enrichment of K at the expense of Na have been reported. Wilson (1970) found sapphirine-bearing pyroxenites in the Quairading area of W. Australia with considerably more K than Na. Scott (1966) made similar observations in the Tertiary ignimbrite sheets of east-central Nevada. Both authors attributed the high K values and low Na values to K-metasomatism.

The relationship is believed to be due to an alkali ion exchange in which, under the correct conditions, a permeating K-rich aqueous solution causes the exchange of Na for K in the plagioclase lattice, resulting in the

Figure 2.5

Aluminium cation proportions of amphiboles synthesized directly from basalt plotted against P_{fluid} of formation.

$$T = 700^{\circ}\text{C}$$

QFM buffer.

(After Spear, 1981).

Figure 2.6

The Mount Mulgine rocks are very enriched in Rb and K and this is believed to be due to the same metasomatic process (see text).

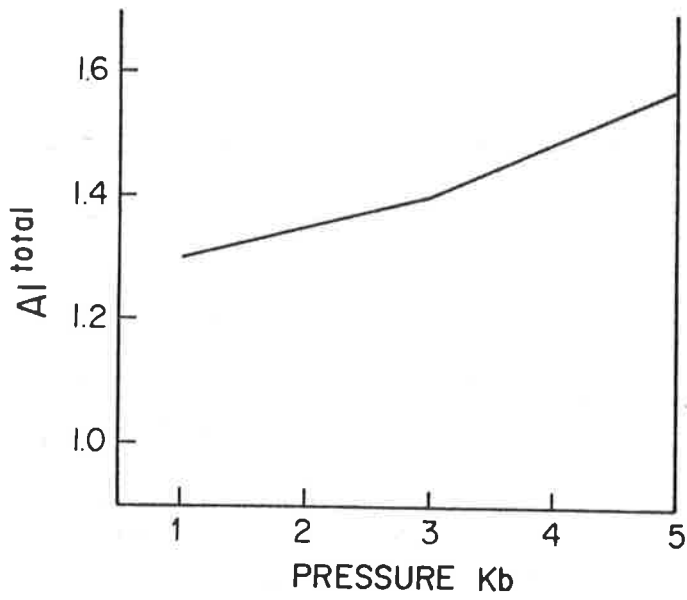


Figure 2.5

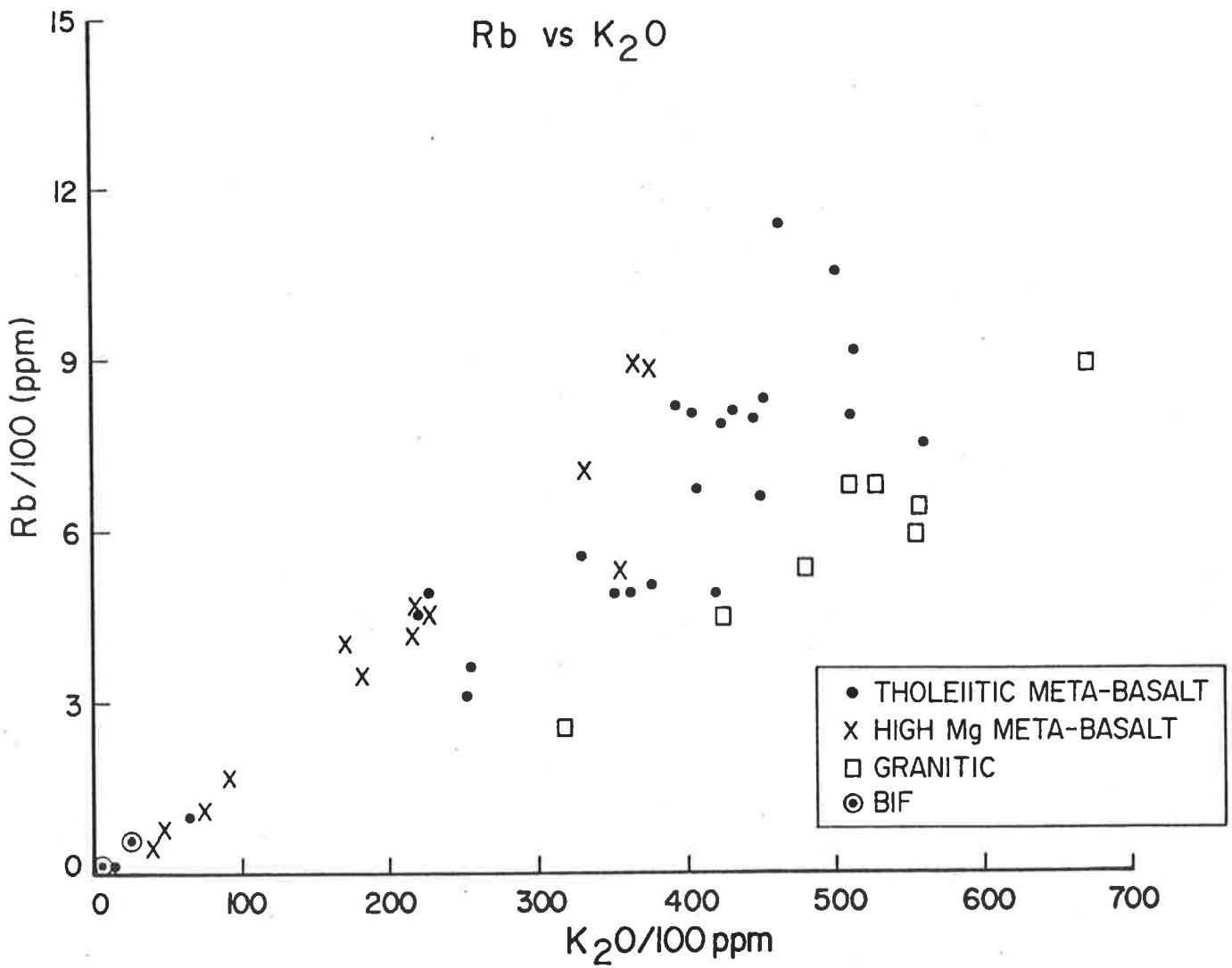


Figure 2.6

expulsion of Na. Orville (1963) demonstrated experimentally that this exchange can take place. However, there is no significant correlation between K and Na values at Mount Mulgine.

Normal weathering may be responsible for the removal of Na and, in the Mount Mulgine case, Ca also. Typical weathering products such as carbonates indicate that weathering has been operative in these rocks.

K-metasomatism may also explain why the rocks at Mount Mulgine are also rich in Rb. The Rb values are at least an order of magnitude higher than would be expected in such rocks. Figure 2.6 is a plot of Rb against K_2O . The correlation coefficient is 0.8274 for the sample points plotted and it can be generally stated that Rb is proportional to K. The two elements are chemically similar and it is believed that the same process was responsible for their enrichment. Potassium and Rb values generally increase with depth and this is consistent with the hydrothermal fluids being associated with or derived from the inferred granite at depth. The increase in K and Rb with depth may also be due to surface leaching and ideally, the variation of these elements with lateral distance from the granite would be more informative about whether the K-Rb-rich solutions were associated with the granite. However, the lateral distance from the granite is difficult to determine when the lateral extent of the granite itself is unknown.

CHAPTER 3: TRACE ELEMENT GEOCHEMISTRY AND THE ORIGINAL NATURE OF THE ROCKS

3.1 Introduction

Prograde and, later, retrograde metamorphism coupled with hydrothermal alteration (see Chapter 2) and mineralization, have modified the original rock compositions at Mount Mulgine; so much so that it is now very difficult to tell the original nature of the rocks. Primary mineralogies and textures have generally been destroyed and there has been movement of the major elements during the above processes. This is apparent when the whole rock analysis data (Appendix 3) are compared with analyses of other similar Archaean rocks in the literature (see Table 3.1). For example, comparing the Mount Mulgine greenstones with other Archaean greenstones from Western Australia (e.g., Hallberg and Williams, 1972) and also with Archaean greenstones from the Canadian shield (e.g., Wilson et al, 1965) it is clear that the following major element movements must have taken place at Mount Mulgine: K, Mg, Fe, Si and possibly Mn were added while Na, Al, Ca and P were removed from the Mount Mulgine greenstones. It is only Ti which seems to have been relatively immobile.

Thus whole rock major element geochemistry alone cannot be confidently used in attempting to determine the former identities of the rocks. With such altered rocks, whole rock trace element work can supply information not only about their original identities, but also about their environment(s) of formation (see below). It was with this in mind that the concentrations of Ba, Ce, Ga, Nb, Nd, Rb, Sc, Sr, Y and Zr were measured and this chapter concerns itself mainly with discussion of the implications of these trace element data. Many other trace elements were analysed in order to determine their abundance and/or variations with depth, rock type etc. These other trace elements are discussed elsewhere in the thesis. In all, 25 trace elements were analysed for in 57 rock samples the analyses are listed in Appendix 3. Average concentrations of the elements in the various groups of rocks are in the Tables in Chapter 2.

3.2 General considerations

Much of the modern understanding of Archaean geology has been through the chemistry of the rocks and most workers dealing with Archaean rocks have adopted the geochemical approach (e.g., Hart et al, 1970; Jahn et al, 1973; Condie, 1976; Sun and Nesbitt, 1977). Consequently there is now a considerable amount of Archaean geochemical data (e.g., see Windley and Naqvi, 1978).

In the last decade the use of minor and trace element geochemistry in the study of volcanic rocks has been well established as a tool for dis-

criminating between parent magma types and also between different tectonic regimes (Pearce and Cann, 1971, 1973; Floyd and Winchester, 1975; Winchester and Floyd, 1977; Pearce, 1980). The elements most commonly used are Ti, Zr, Y, Nb, Ga, Ce and Sc and some major elements (notably Si, K and P). Based on the abundances of these elements in known rocks of certain origin, the above authors constructed discriminant diagrams which have since been used extensively in research involving volcanic rocks. Although most of the diagrams were based on fresh (unaltered) rocks, the same diagrams have been shown to be applicable to variously altered and metamorphosed volcanic suites including Archaean basalts, because most of the elements involved are now known to be "immobile" during post-consolidation processes (e.g., Floyd and Winchester, 1978).

3.3 Classification of the volcanic rocks at Mount Mulgine

Irvine and Baragar (1971) presented a classification system for common volcanic rocks which has been widely accepted. Their classification scheme, reproduced here as Figure 3.1, is based on chemical composition and is therefore applicable to metamorphosed and/or cryptocrystalline rocks for which classification by conventional mineralogical systems is impossible.

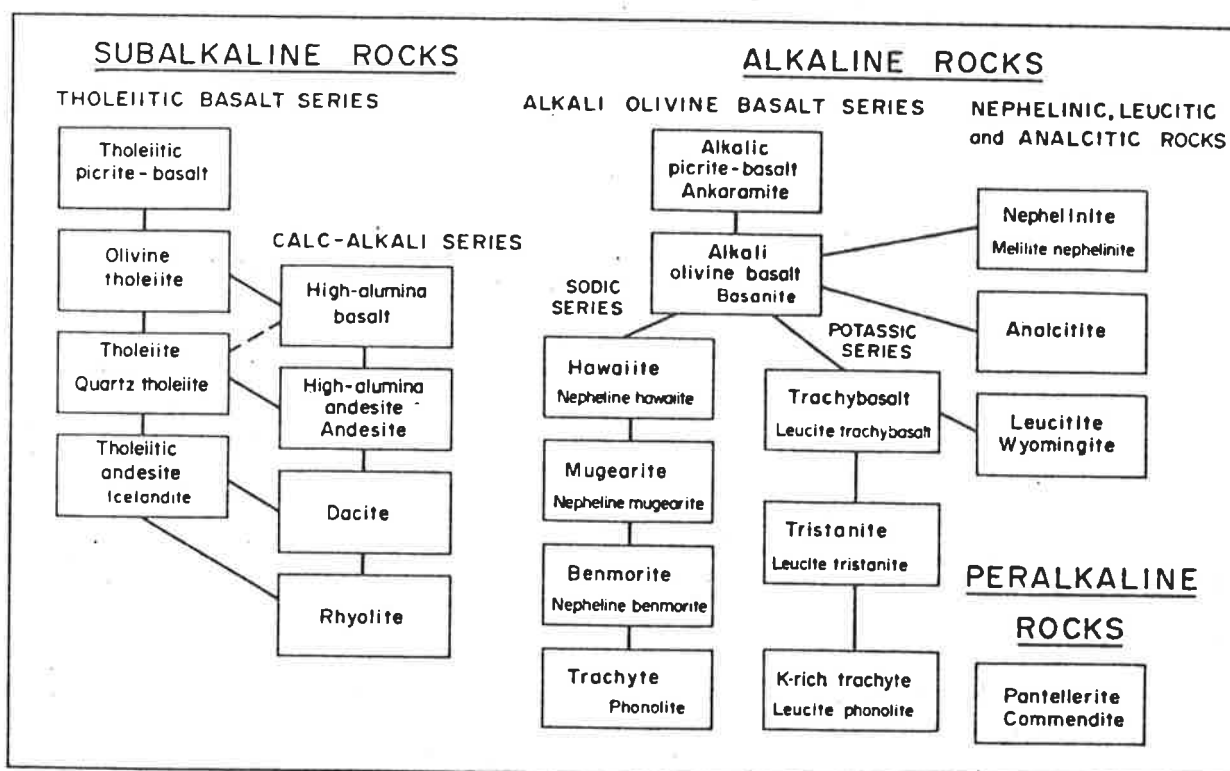


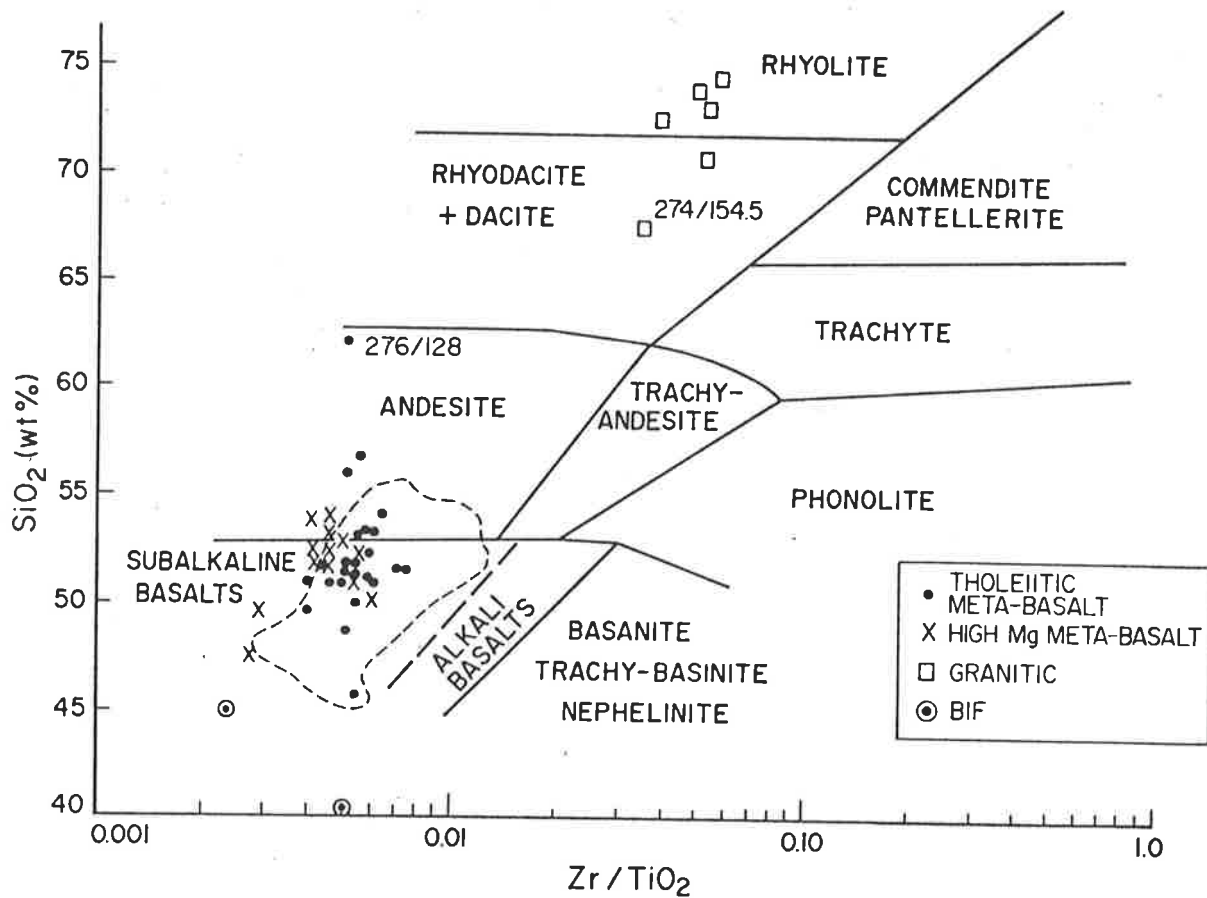
Figure 3.1: General classification scheme for the common volcanic rocks. The lines joining boxes serve to outline common associations. The rocks indicated by small print within the boxes are variants of the main rock. (After Irvine and Baragar, 1970).

Following Figure 3.1, the first major task was to determine to which of the three major divisions the rocks at Mount Mulgine belong. This was done using some of the diagrams of Winchester and Floyd (1977), reproduced here as Figures 3.2-3.4. Figure 3.2 clearly shows that the Mount Mulgine greenstones are sub-alkaline basalts, possibly associated with a few low-silica andesites. Whether the rocks that plot in the andesite field were all originally andesites is difficult to decide at this stage because the rocks at Mount Mulgine are known to have been silicified as evidenced by quartz veins and pockets of quartz grains in the rocks. So, some of the rocks that appear as andesites on the diagram may have been basalts which were silicified, although great care was taken to ensure that the samples analysed did not contain any epigenetic (introduced) quartz.

In Figures 3.3 and 3.4, the vast majority of the Mount Mulgine greenstones again plot in the sub-alkaline basalt/andesite field. A few samples, however, plot in the alkali basalt field. The few samples that appear as alkali basalts on these diagrams clearly do so because of their high Nb/Y ratios. Finlow-Bates and Stumpf (1981) have shown that the "immobile" elements Y, Sc and Nb may be "extremely mobile" during alteration. Since the Mount Mulgine rocks have been metamorphosed and hydrothermally altered (see Chapter 2), and the number of samples (only 4 in Figure 3.3 and 2 in Figure 3.4) is small compared to the total number of volcanic rocks analysed, it is likely that the alkali nature of the few samples may be apparent rather than real.

The fact that the granitic (acidic) rocks do not consistently plot in any one field in Figures 3.2-3.4 was interpreted to mean that the granitic rocks are not, genetically, part of the volcanic suite. If all the rocks in the Trench area at Mount Mulgine were volcanics originally, then, assuming the granitic rocks were rhyolites, one would expect more rocks to plot as andesites, dacites or rhyodacites. Such rocks would be products of the basalt-rhyolite differentiation. But no rocks plot in the dacite or rhyodacite fields in Figures 3.3 and 3.4.

In the previous chapter, samples 276/128.0 and 274/154.5 (the sample points are labelled in Figure 3.2) were considered as meta-rhyodacitic rocks. Such rocks are not common at Mount Mulgine but their occurrence and their inter-layering and gradational relationships with the meta-basalts shows that in some cases, there may have been differentiation among the volcanics from basalts to dacites or possibly rhyodacites. But such differentiation would have been rare as evidenced by the relatively low abundance of the "intermediate" rocks in this type of differentiation. It is possible that the meta-rhyodacitic rocks are crustal melts and not differentiation products (J. Foden, pers. comm.)



Main field of Archaean greenstones from the Eastern Goldfields and Marda, Western Australia. (After Winchester and Floyd, 1977).

Figure 3.2

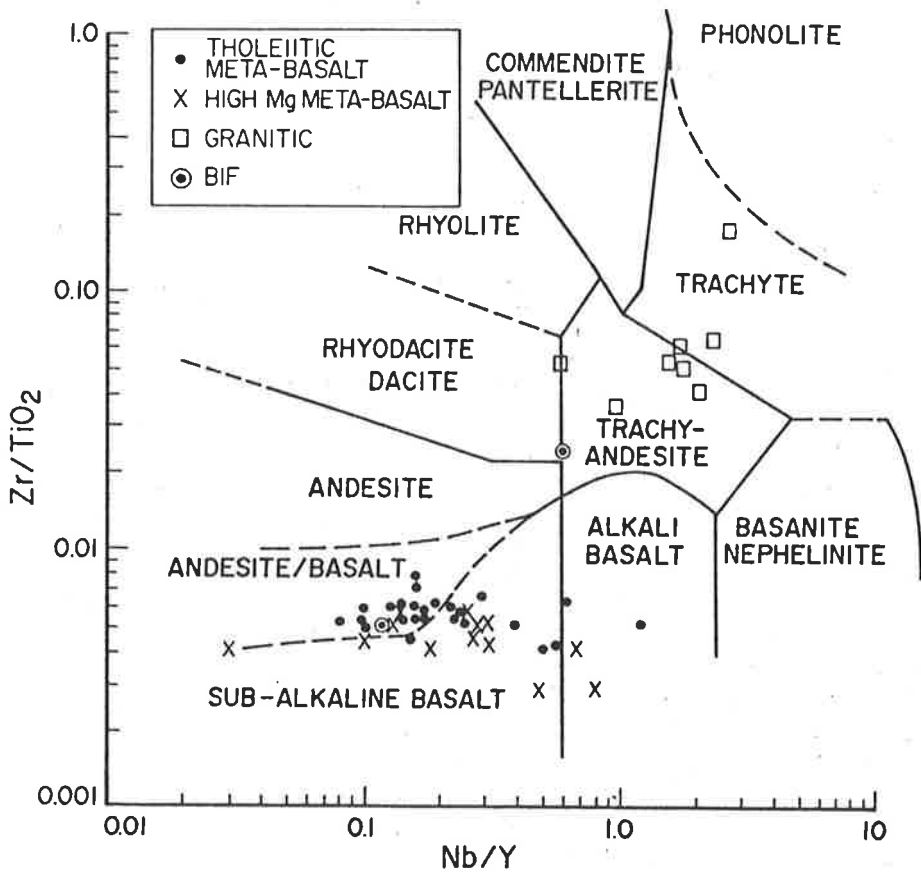


Figure 3.3 (After Winchester and Floyd, 1977).

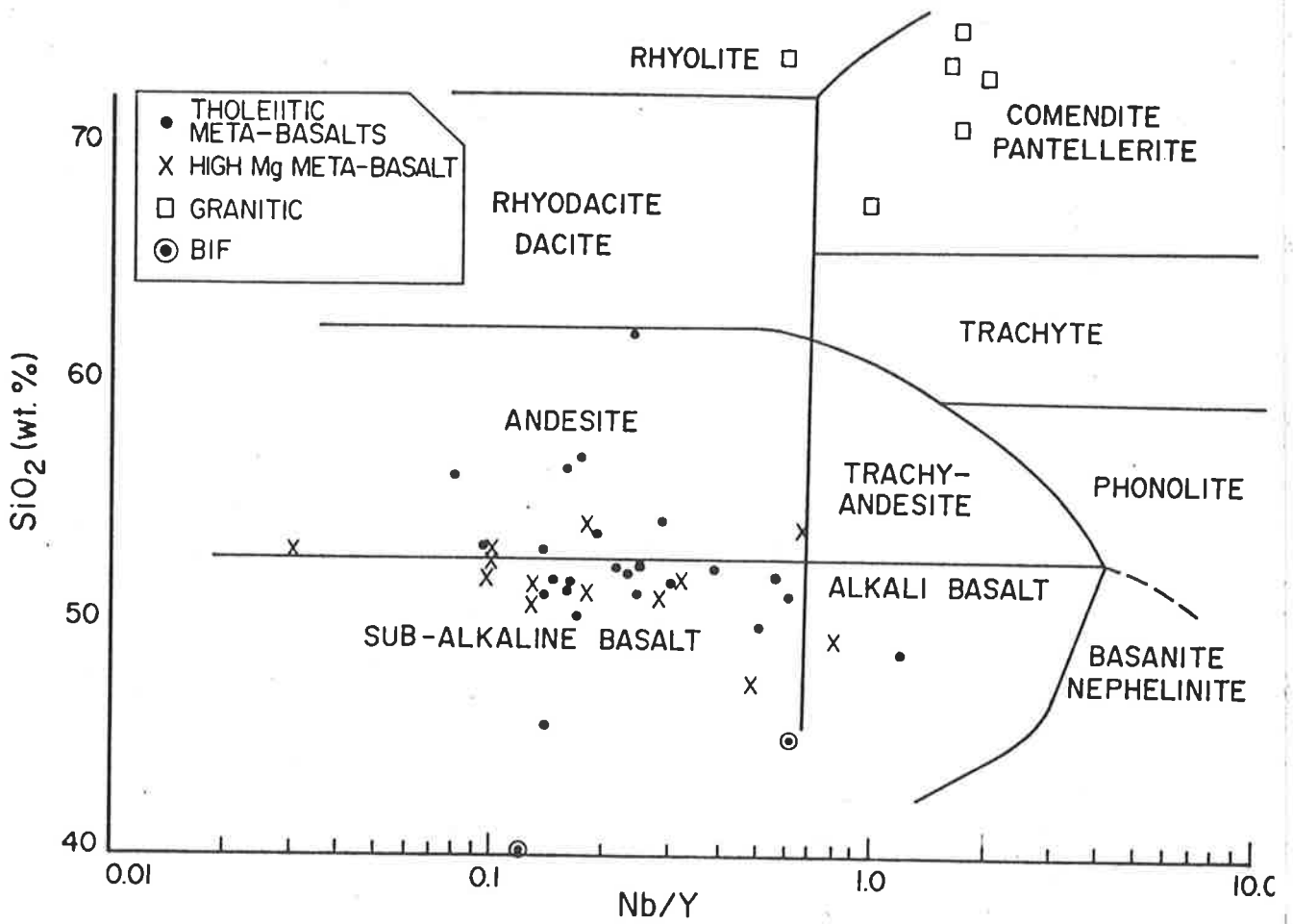


Figure 3.4. (After Winchester and Floyd, 1977).

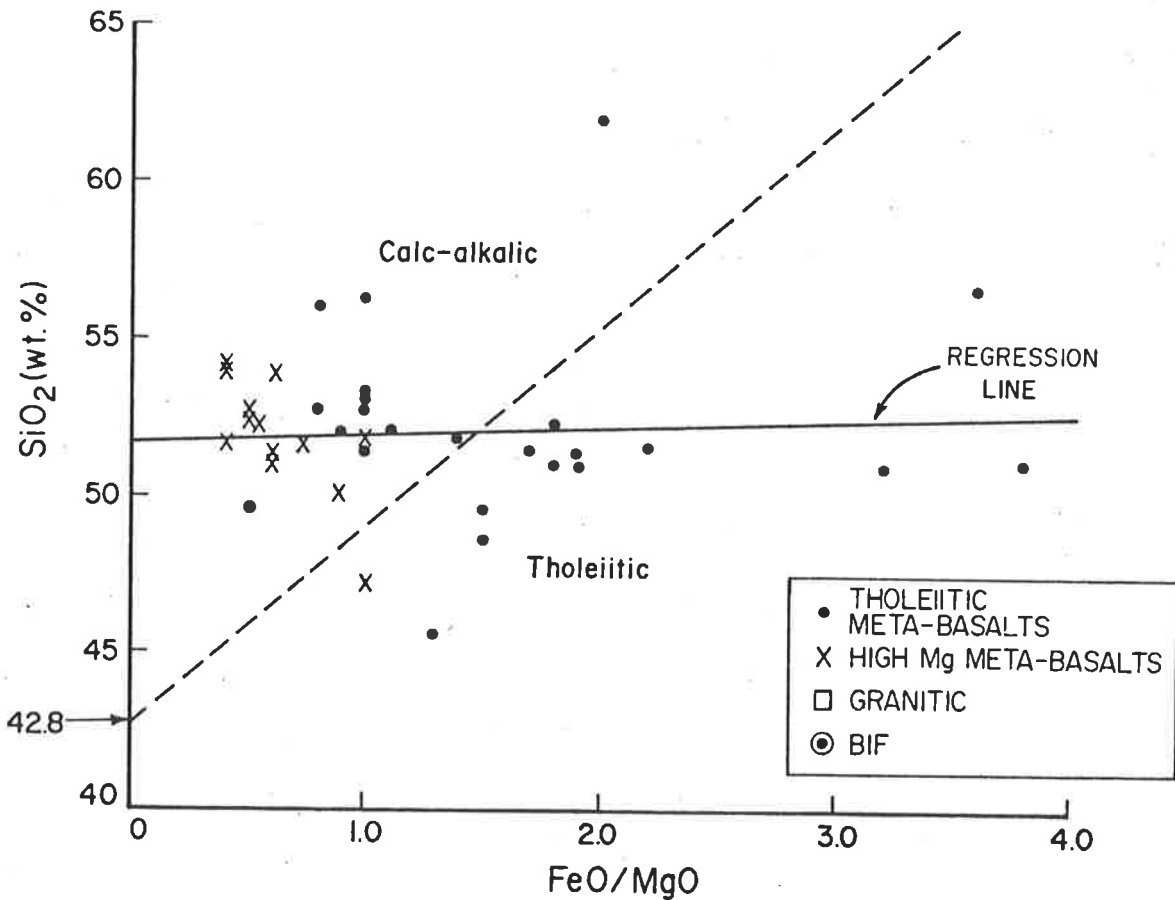


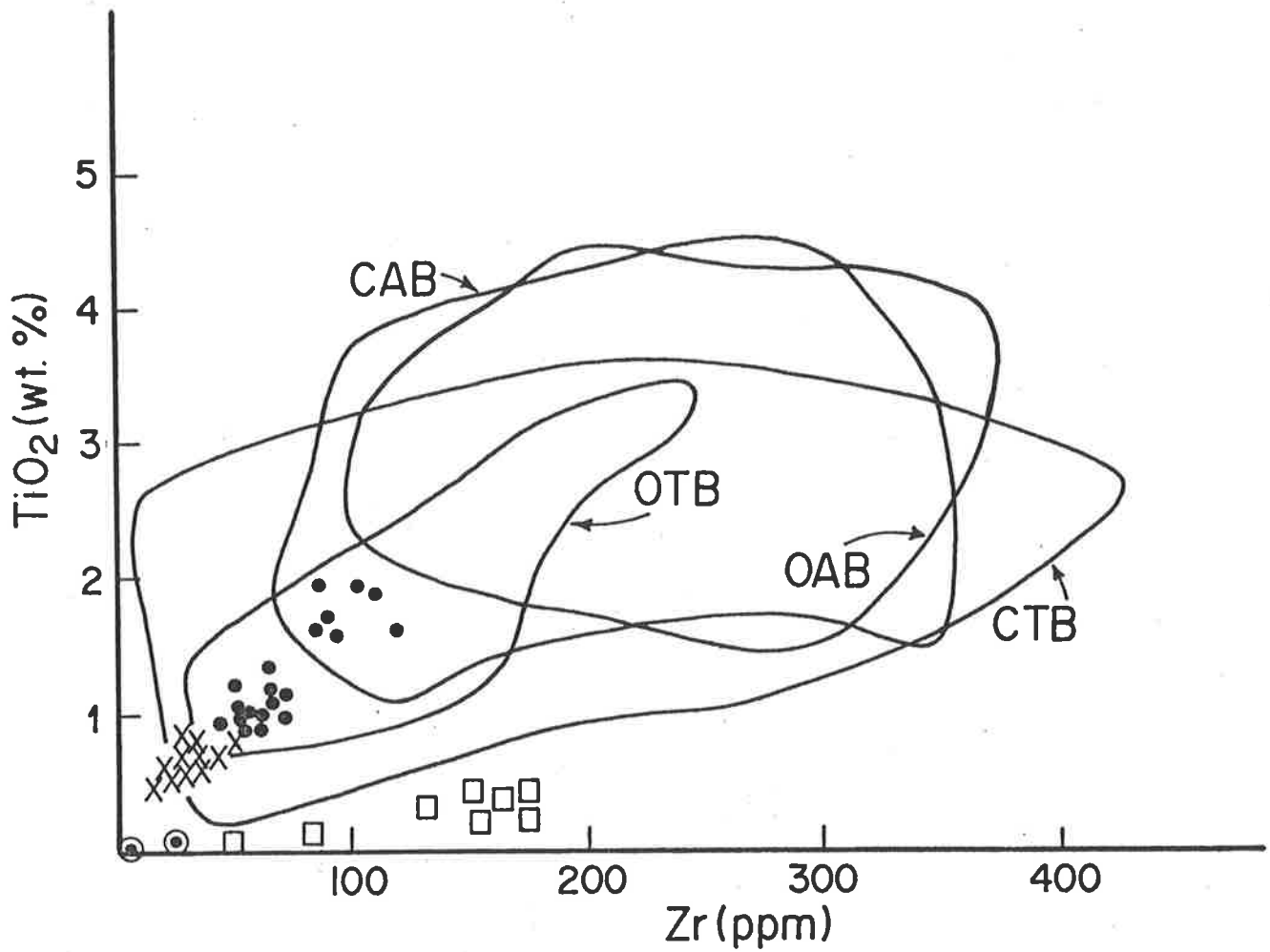
Figure 3.5. (After Miyashiro, 1974).

So far, the following are the apparent facts about the rocks in the Trench area at Mount Mulgine.

- a) The volcanic rocks are mostly sub-alkaline basalts.
- b) The granitic rocks (now largely greisenized) are not volcanic in origin. (This point was also argued in Chapter 2; see page 17).
- c) There may have been differentiation among some of the volcanics leading to the formation of andesites and the rocks described as meta-rhyodacitic (in this study). The paucity of these differentiation products and general lack of other rocks (e.g., dacites) implies that such differentiation was rare.

The next step was to investigate whether the sub-alkaline rocks are tholeiitic or calc-alkalic (see Figure 3.1). Most distinctions between tholeiitic and calc-alkalic rocks (e.g., Irvine and Baragar, 1971) involve major elements (e.g., Na, K, Mg, and Al) which, as already pointed out, were very mobile in the rocks at Mount Mulgine. Such distinctions are therefore generally inapplicable to the rocks at Mount Mulgine. As a first approach the method of Miyashiro (1974) has been used in an attempt to determine whether the rocks under investigation are tholeiitic or calc-alkalic. Although this method also involves major elements (Fe, Mg and Si), it was preferred because all these elements are enriched in the rocks at Mount Mulgine and so their ratios are unlikely to have changed much since the formation of the rocks. The method involves plotting SiO_2 vs FeO/MgO (see Figure 3.5) and then comparing the slope of the trend obtained with the slope of the broken line in Figure 3.5. Calc-alkalic rocks have trends with steeper gradients than that of the broken line whose equation is $\text{SiO}_2 = 6.4 \times \text{FeO/MgO} + 42.8$ (Miyashiro, 1974) while tholeiitic rocks have trends with lower slopes than that of the line. The Mount Mulgine greenstones do not show a clear trend but the regression line in Figure 3.5 can be taken as an approximation of this trend. The rocks have a tholeiitic-type trend. They lack large-scale SiO_2 enrichment which characterizes calc-alkali differentiation. It should be noted that the XRF analyses give only total iron as Fe_2O_3 . An approximation of FeO was obtained from the equation $\text{FeO} = x - \text{Fe}_2\text{O}_3$ where x is the weight percent total iron and $\text{Fe}_2\text{O}_3 = \text{TiO}_2(\text{wt.}\%) + 1.5$ (see Irvine and Baragar, 1971, p.526).

The tholeiitic nature of the rocks shows more clearly on the Floyd and Winchester (1975) diagrams, reproduced here as Figures 3.6-3.10. Some of the more obvious facts expressed diagrammatically in Figures 3.6-3.10 are (Floyd and Winchester, 1975):



- CAB – Continental alkali basalts
- OAB – Oceanic alkali basalts
- OTB – Ocean tholeiitic basalts
- CTB – Continental tholeiitic basalts

- Tholeiitic meta-basalts
- × High Mg meta-basalts
- Granitic
- ⊙ BIF

Figure 3.6. (After Floyd and Winchester, 1975).

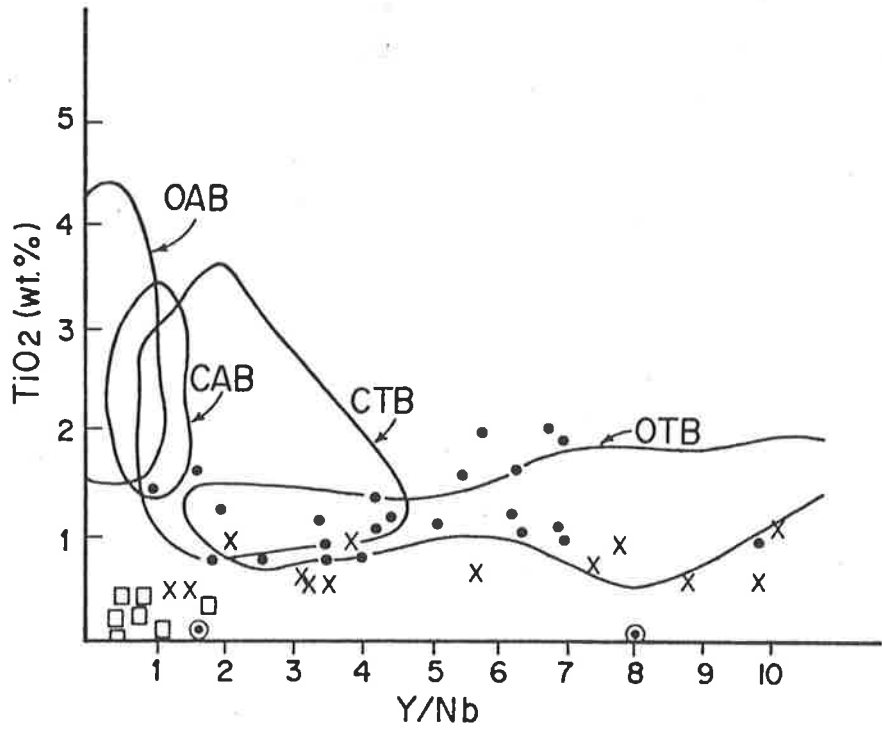


Figure 3.7., for explanation of symbols and abbreviations see Figure 3.6. (After Floyd and Winchester, 1975).

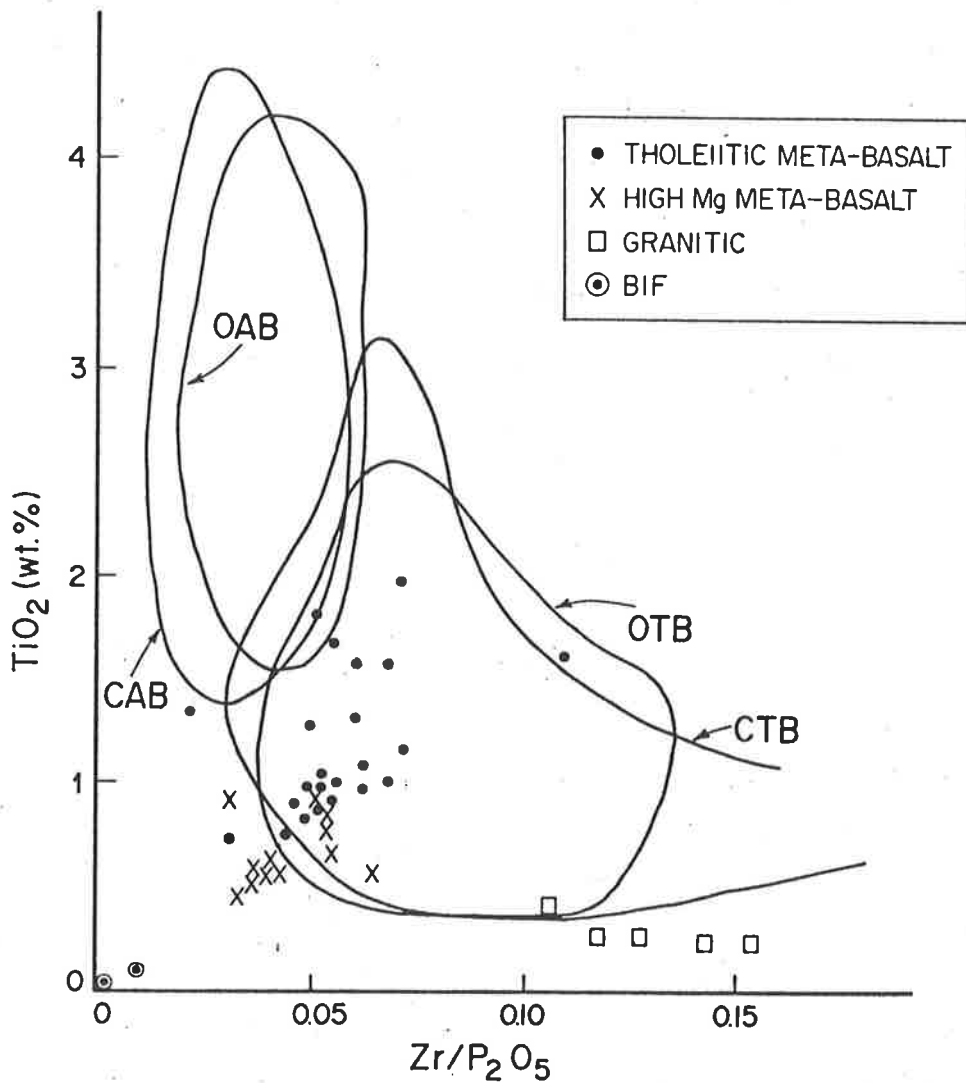


Figure 3.8., for explanation of abbreviations, see Figure 3.6. (After Floyd and Winchester, 1975).

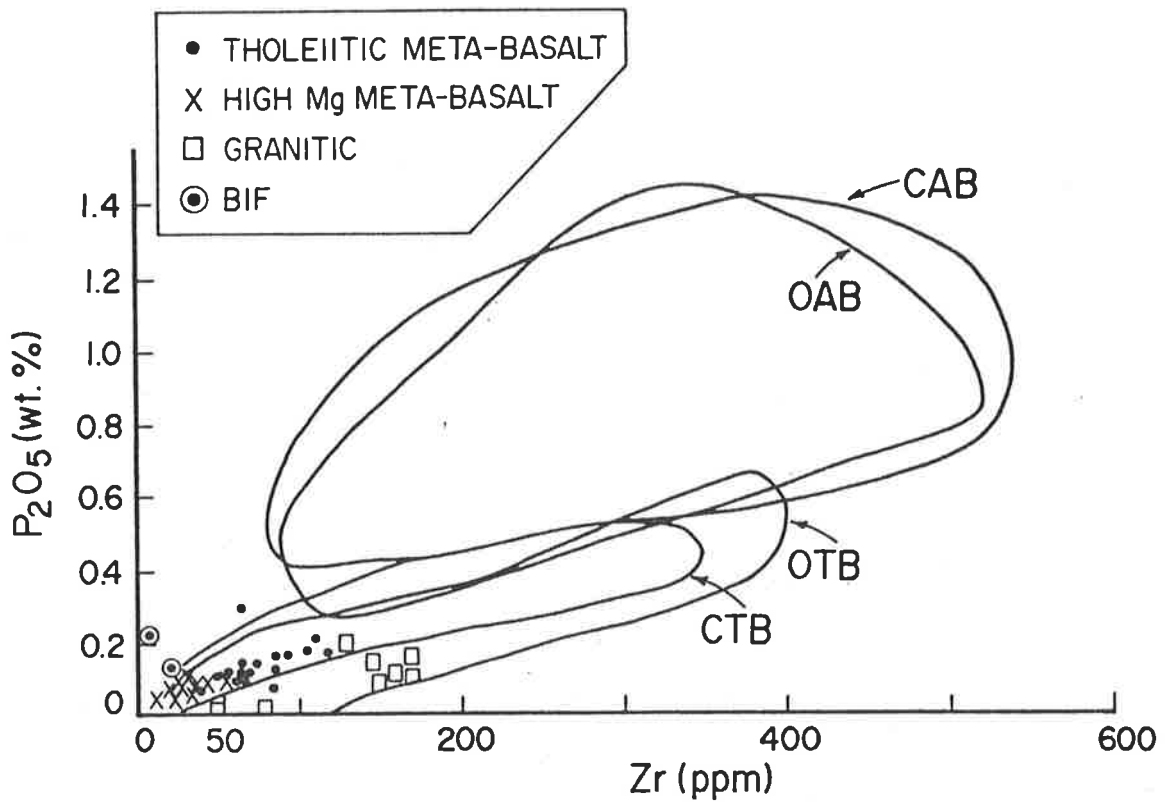


Figure 3.9., for explanation of abbreviations, see Figure 3.6. (After Floyd and Winchester, 1975).

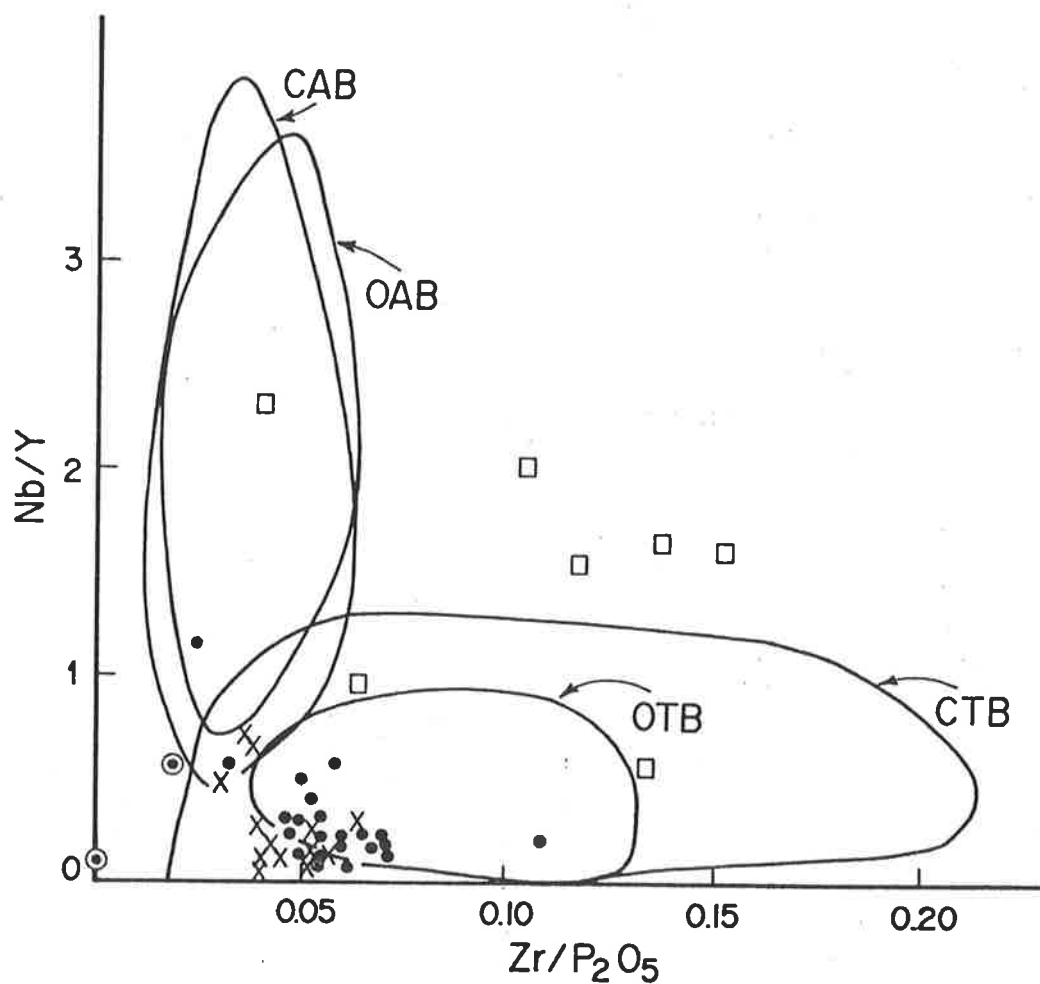


Figure 3.10., for explanation of symbols and abbreviations, see Figure 3.6. (After Floyd and Winchester, 1975).

a) In these diagrams, the rocks are characterised not only by the specific delineated fields (many of which overlap anyway), but also by trends displayed by the rocks as a group. The "proportional" trend (or nearly constant TiO_2/Zr ratio) in obtained Figure 3.6 is characteristic of tholeiitic basalts. (Alkali* basalts would have a "horizontal" trend on this diagram). On the TiO_2 vs Y/Nb diagram (Figure 3.7) the Mount Mulgine rocks show a "horizontal" trend which is what would be expected of tholeiitic rocks. (Alkali rocks would display a "vertical" trend on this diagram).

The TiO_2 vs Zr/P_2O_5 plot is supposed to be generally similar to the TiO_2 vs Y/Nb diagram, its advantage being that the variables Zr and P_2O_5 are nearly always determined in rocks whereas Y and Nb are not always readily available. The two diagrams are supposed to be similar because the Zr/P_2O_5 ratio produces a similar discrimination relationship as the Y/Nb ratio. However, the trends displayed by tholeiitic rocks in both diagrams are not as "similar" as would be anticipated. As just mentioned, the tholeiitic rocks show a "horizontal" trend on the TiO_2 vs Y/Nb plot but in the TiO_2 vs Zr/P_2O_5 diagram, the same rocks show considerable variation resulting in no consistent trend. In the latter diagram, the Mount Mulgine volcanics do not show a well defined trend (see Figure 3.8) and this is consistent with their tholeiitic nature as already indicated by Figures 3.6 and 3.7. (Alkali rocks would display a "vertical" trend, as expected, on the TiO_2 vs Zr/P_2O_5 plot).

One feature worth noting at this stage which Figures 3.7 and 3.8 have in common, but which is generally lacking in the other diagrams in this group, is that in addition to the BIFs and acidic rocks, some greenstones (mostly the high-Mg meta-basalts) plot outside the delineated fields. This is considered to be due to the fact that the elements may have been mobile. Earlier in this chapter it was shown that P is depleted in the Mount Mulgine greenstones and it was also suggested the Y and Nb may have been mobile. In the next chapter some evidence is given which suggests that even Ti may have been mobile, at least locally.

* In these diagrams, the tholeiitic rocks are compared with alkali basalts (and not with calc-alkali basalts) because there was insufficient data on calc-alkali rocks for these rocks to be included in the diagrams (Floyd and Winchester, 1975). Thus the diagrams confirm that the rocks are not alkaline and also that they are not calc-alkalic (by implication).

In the P_2O_5 -Zr diagram (Figure 3.9), like in the TiO_2 -Zr diagram (Figure 3.6), the Mount Mulgine rocks show a "proportional" trend which is what would be expected of tholeiitic rocks. (In this case, alkali rocks would also have a "proportional" trend but the alkali and tholeiitic fields in this diagram are reasonably separate).

Finally, the Nb/Y-Zr/ P_2O_5 diagram (Figure 3.1) which ideally gives the best discrimination between tholeiitic and alkali basalts, should show a "horizontal" trend for tholeiitic rocks. (Alkali rocks would have a "vertical" trend). The "horizontal" trend does not show up well in Figure 3.10, perhaps due to the mobility of the elements mentioned above, but as in Figures 3.6-3.9, the tholeiitic nature of the Mount Mulgine greenstones is clear.

b) The TiO_2 (wt.%) values for the greenstones analysed are all less than 1.8% except for four samples with TiO_2 values of 1.80%, 1.91%, 1.96% and 2.33%. (The majority of alkali rocks would have TiO_2 values greater than 1.8%).

c) The Y/Nb ratios are all much greater than one and there is a wide scatter of points on the TiO_2 -Y/Nb diagram (Figure 3.7) and this is consistent with the tholeiitic nature of the rocks. (The Y/Nb ratio for alkali rocks is less than one and consequently they would not show such a wide scatter of points on the TiO_2 -Y/Nb diagram).

d) All the Mount Mulgine greenstones analysed have much less than 150 ppm Zr and, with the exception of two samples, they all have less than 0.25% P_2O_5 . Again, this is what would be expected in tholeiitic rocks. The majority of alkalic rocks would have more than 0.25 wt.% P_2O_5 and more than 150 ppm Zr).

3.4 Tectonic setting of the rocks

Figures 3.6-3.10 also attempt to distinguish between continental and oceanic basalts but as can be seen and as Floyd and Winchester (1975) clearly pointed out, the diagrams do not effectively discriminate between rocks from the two types of environment because there is considerable (sometimes complete) overlap of the delineated fields in the diagrams. Other diagrams are available which discriminate between rocks from different tectonic settings but before these are introduced, there is a further point about Figure 3.6 worth noting. Among the Floyd and Winchester (1975) diagrams, Figure 3.6 is the only one in which several samples plot as alkali basalts. In fact, seven samples plot in the continental alkali basalt field. Floyd and Winchester (1975) found that ocean island tholeiites were almost entirely responsible for the high Ti and Zr "intrusion" into the oceanic alkali basalt field. In this case, the "intrusion" does not extend as far as the oceanic alkali basalt field, but it is likely that this is the explanation for the seven points that "intrude" the continental alkali basalt field. If this is true, it would imply that there

are some oceanic island-type tholeiites among the rocks at Mount Mulgine.

The $TiO_2-K_2O-P_2O_5$ diagram of Pearce et al (1975) is reputedly very effective in discriminating between oceanic and non-oceanic basalts. Unfortunately, most of the rocks in this study are extremely enriched in K (see Chapter 2 and Appendix 3) and depleted in P which renders this diagram (and any other diagram involving K) virtually useless for most of the rocks at Mount Mulgine. However, a few of the samples analysed do not appear to show K-enrichment. It was decided to use these few samples, hoping that they are more representative of the original unaltered rocks.

Since, for almost all Archaean rocks in the literature, the K_2O value is always much less than 1, it was decided to use those of the Mount Mulgine greenstones which have K_2O values less than 1 wt.% (Appendix 3). As a further constraint, again based on data in the literature, it was decided to plot only those samples in which the Na_2O content is either greater than or about the same ($\pm 20\%^*$) as the K_2O value. After applying the above two constraints only four samples survived. These are 268/22.14, 259/42.9, 256/108 and 269/130.3, and they are plotted on the $TiO_2-K_2O-P_2O_5$ diagram of Pearce et al, (1975), reproduced as Figure 3.11. Two of the samples plot well within the oceanic basalt field, one plots in the continental basalt field, and the fourth sample plots at the boundary between the two fields. According to Pearce et al, (1975), the effect of alteration and metamorphism is to move the samples from the oceanic field into the continental field. The authors emphasize that if an altered sample plots in the oceanic basalt field, then it is unlikely to have a non-oceanic origin. Thus it is possible that both the Mount Mulgine samples that fall outside the oceanic basalt field do so because of metamorphism or alteration. Therefore, according to Figure 3.11, the Mount Mulgine greenstones are probably oceanic in origin.

In the last decade the most frequently used discriminant diagrams, as far as palaeotectonic setting is concerned, have been the Ti-Zr-Y and Ti-Zr diagrams of Pearce and Cann (1973), which are reproduced here as Figures 3.12 and 3.13 respectively. In both figures, the Mount Mulgine greenstones plot in fields A, B and D, implying that they are either ocean floor basalts or low-K tholeiites. Field D in Figure 3.12 is that of within plate basalts, which include continental and ocean island basalts.

*According to Nicholls and Islam (1971) differences of not more than 20% should not be considered significant in comparing whole rock data.

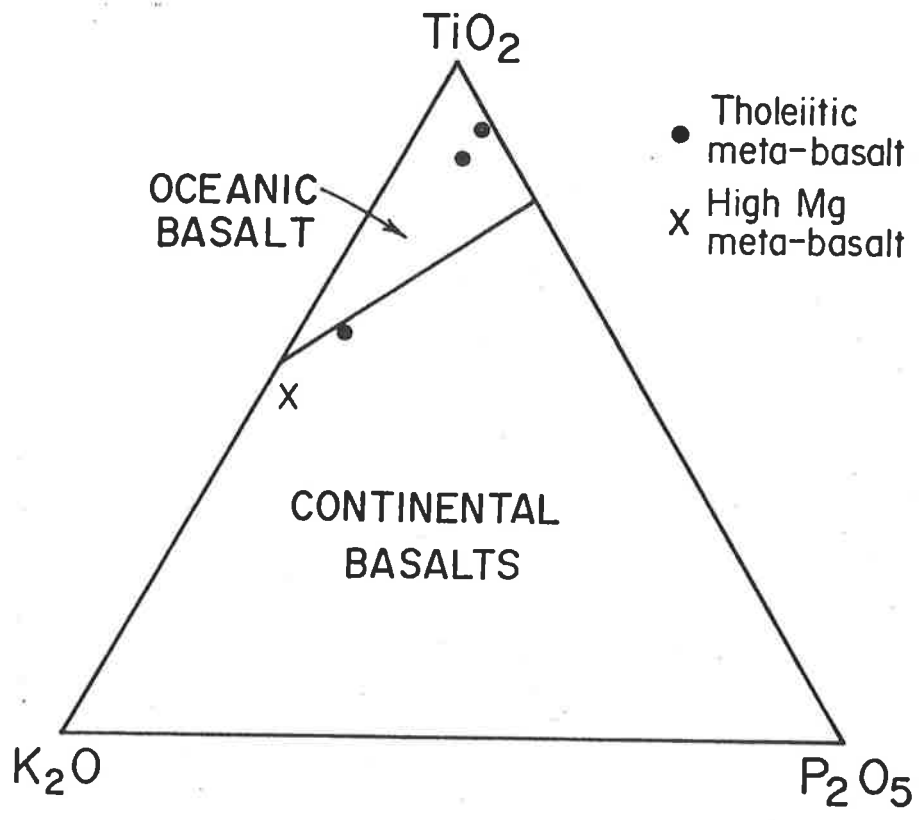


Figure 3.11. (After Pearce et al, 1975).

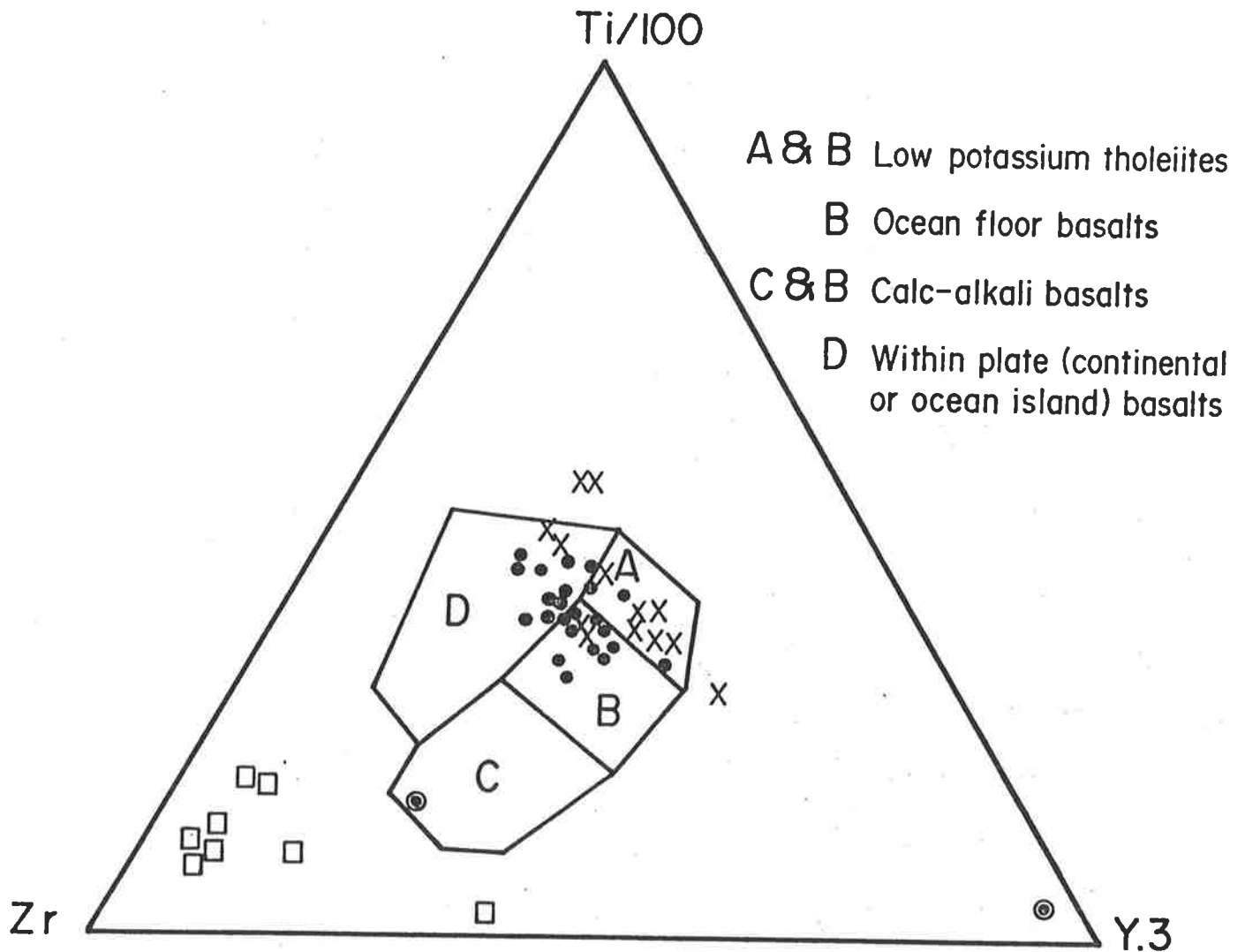


Figure 3.12., for explanation of symbols, see Figure 3.9. (After Pearce and Cann, 1973).

Useful as it may be, several authors have demonstrated that the Ti-Zr-Y diagram has its weaknesses and should, therefore, be used with caution. As early as 1975, Floyd and Winchester (1975) noted that there were cases where clearly continental tholeiites plotted in the ocean-floor field of the diagram, and this led these authors to suggest that the ocean-floor field of the Ti-Zr-Y diagram "represents not only ocean-floor basalts but all tholeiitic basalts formed in a rifting environment (mid-oceanic ridge, continental rifting) from relatively primitive magmas characterised here by low Ti, Zr and Y values". This was confirmed recently by Holm (1982) who concluded that the diagram does not recognise continental tholeiites after demonstrating that about 50% of all truly continental rocks plotted in the ocean-floor basalt field and that none of the rocks plotted in the within-plate field, which is where all continental basalts would be expected to plot.

Wood et al (1979) pointed out that the Ti-Zr-Y diagram does not distinguish between magma types erupted at tectonically anomalous ridge segments (e.g., hot spots) and Prestvik (1982) confirmed this by showing that basalts from anomalous oceanic ridges tend to plot as within-plate basalts.

The main point, from the two preceding paragraphs, is that the Ti-Y-Zr diagram can only be used as an indicator (not as proof) of origin, and that other factors need to be taken into consideration before the tectonic setting can be determined. This is attempted in the brief discussion at the end of this chapter.

Most of the rocks in the high-Mg meta-basalts' group and a number of samples in the tholeiitic meta-basalts' group (see Chapter 2) should, strictly, not have been plotted in Figures 3.12 and 3.13 because they do not fulfil the conditions $20 > \text{CaO} + \text{MgO} > 12\%$, set by Pearce and Cann (1973). They were plotted anyway to emphasize that the rocks in the two groups are not significantly different. For the same reasons, the acidic rocks and BIFs should never have been plotted in Figures 3.12 and 3.13. These were plotted to reiterate the point that they are of a different nature from the greenstones.

The data were also plotted on another Ti-Zr diagram after Pearce (1980), which is shown as Figure 3.14. Most of the Mount Mulgine greenstones plot in the Mid-Oceanic-Ridge-Basalt (MORB) field. Most of the high-Mg meta-basalts plot in the Arc Lavas' field which is consistent with Figures 3.12 and 3.13 since low-potassium tholeiites are the same as tholeiites of island arc series (Jahn et al, 1973).

Summarising, the chemistry of the Mount Mulgine Archaean greenstones suggests that they formed in a MORB-type or island arc-type environment. But

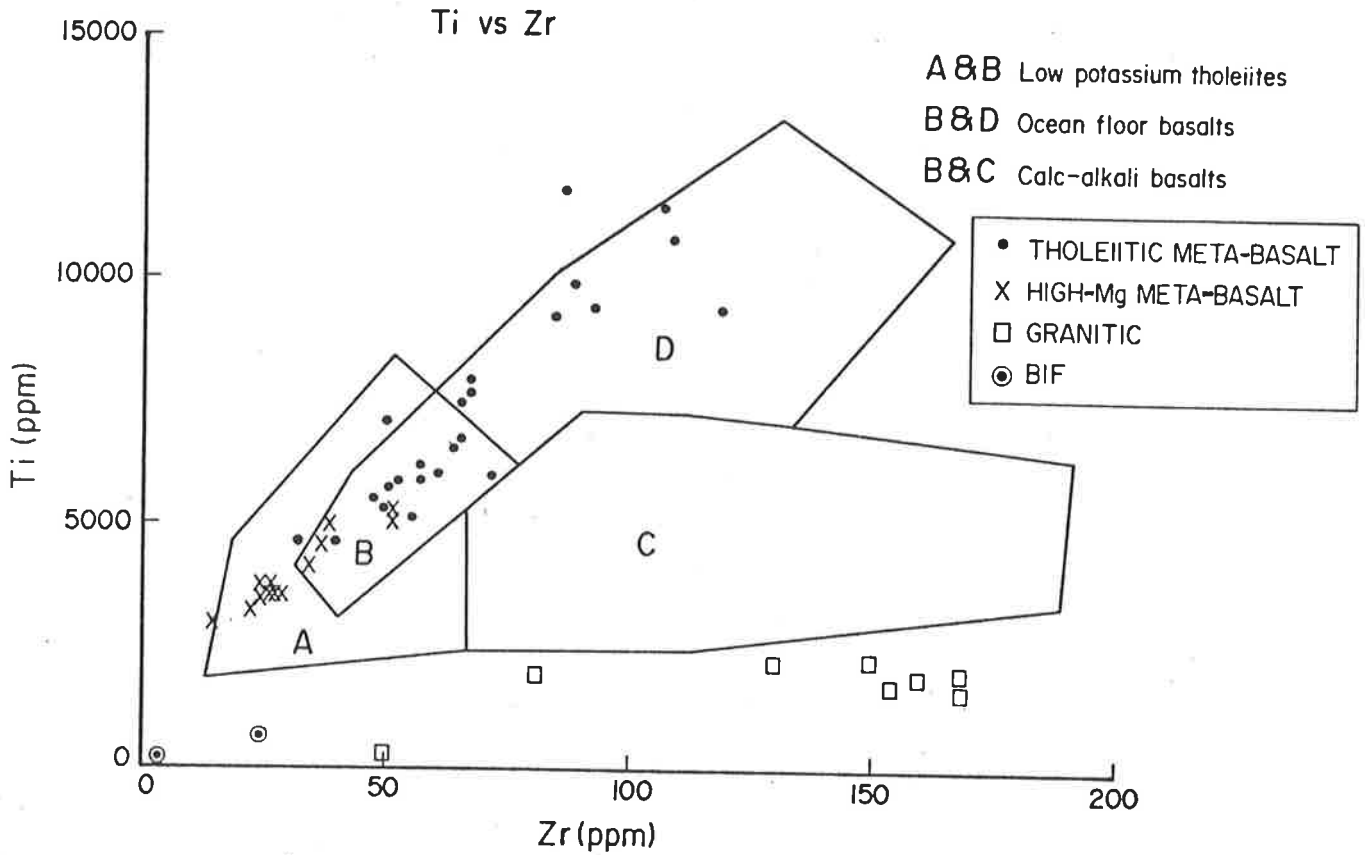


Figure 3.13. (After Pearce and Cann, 1973).

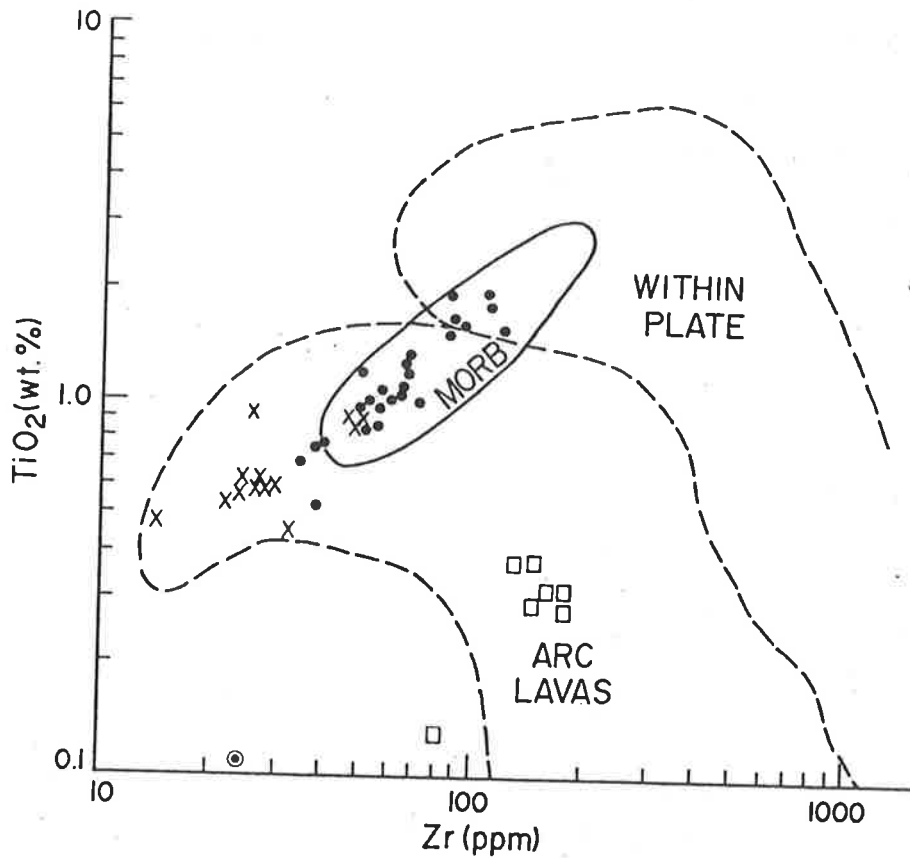


Figure 3.14. MORB = Mid-Oceanic-Ridge Basalts, for explanation of symbols, see Figure 3.13. (After Pearce, 1980).

since a few samples plot in the within-plate fields in Figures 3.12 and 3.14, and since it is known that continental tholeiites do not always plot in the within-plate fields as would be expected, there is a real possibility that the rocks under investigation formed in a continental environment.

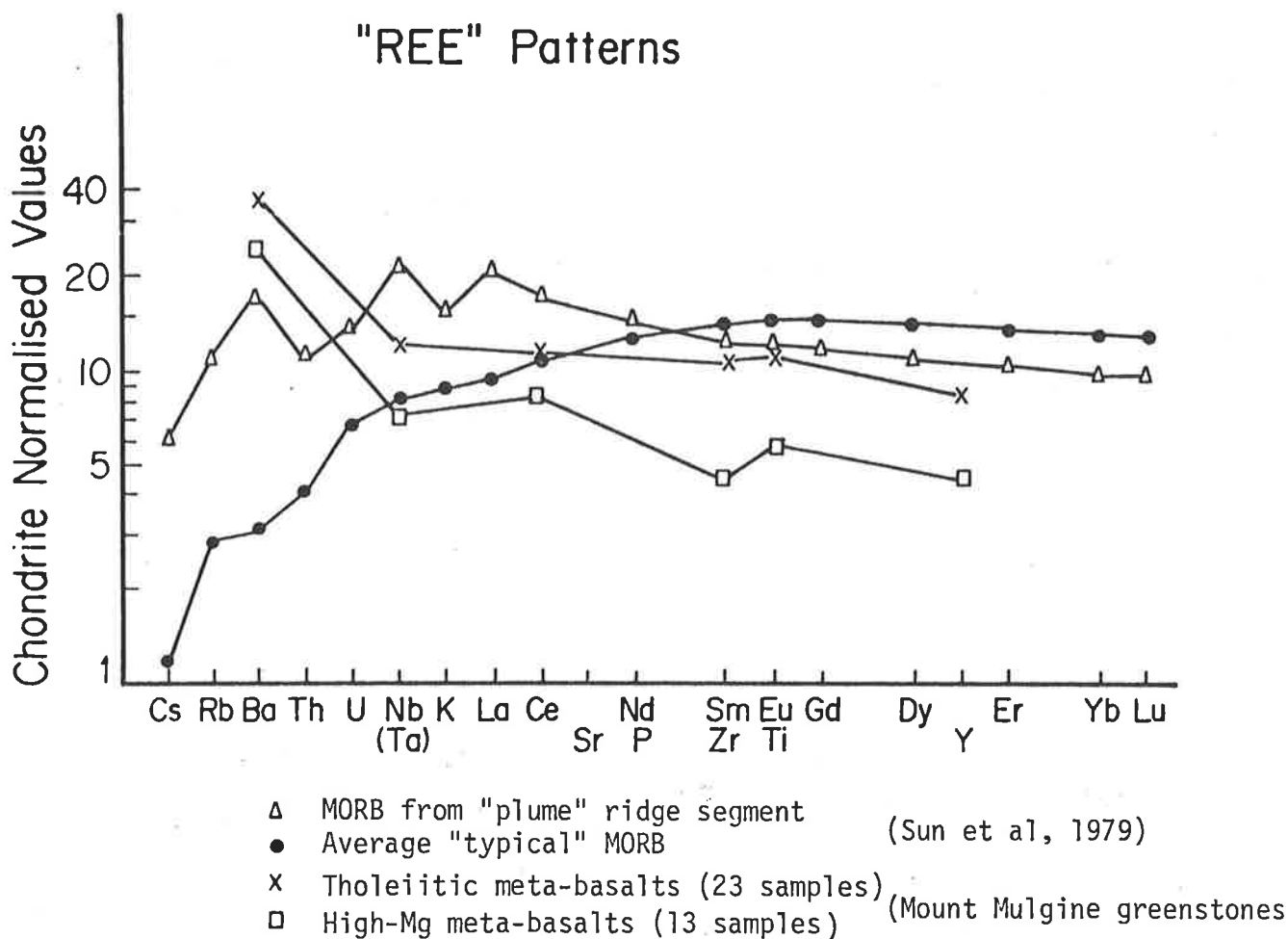


Figure 3.15

3.5 Rare Earth Element (REE) patterns

For a more complete characterization of the rocks, an attempt was made to determine the REE patterns. Since Ce and Nd were the only REE determined, and the Nd values were not considered reliable (see below) it was decided to use the elements Ba, Nb, Zr, Ti and Y to approximate the REE patterns displayed in Figure 3.15. Sun et al (1979) have shown that these elements and others (e.g., Rb, Sr, P and K) can be used to predict the general shape of REE patterns. The latter four elements were not used because they are either depleted (Sr, P) or extremely enriched (Rb, K) in the rocks at Mount Mulgine.

The data for the elements used in approximating the REE patterns was chondrite normalised using the following chondritic abundances, all in parts per million.

K	=	430)	
Rb	=	2.20)	Mason (1971)
Ce	=	0.88)	
Nd	=	0.60)	
Ba	=	3.51)	
Nb	=	0.39)	
Zr	=	5.6)	Sun and Nesbitt (1977)
Y	=	2.2)	
Ti	=	610)	Ahrens (1970)

Figure 3.15 also includes REE patterns for MORB, both the "normal" (depleted) and the "plume" (enriched) types of MORB. Clearly, the Mount Mulgine greenstones have flat chondrite normalised patterns for the middle and heavy REE. Such patterns are typical of MORB (Sun et al, 1979). The difference between "normal" type MORB and "plume" type MORB is in their light rare earth element (LREE) patterns. "Normal" MORB have relatively smooth LREE depleted patterns, while "plume" MORB have relatively irregular LREE enriched patterns (Figure 3.15). Although for many elements there were either no data or the data were unreliable, resulting in lack of detail for the REE patterns of the Mount Mulgine rocks, it is still obvious that these rocks are more like "plume" MORB than the "normal" MORB.

It has been suggested above that the Nd values should be regarded with suspicion. The same is true for Ce values. This is because their values are only slightly above their XRF detection limits. The mean values for Ce and Nd in the greenstones are 10 ppm and 11 ppm respectively. The XRF detection limits for these elements are in the range of 8-15 ppm for Ce and 4-8 ppm for Nd. Also, Nd values often exceed Ce values in the same sample. This might also be due to the imprecision involved in their determination because inspection of data in the literature shows that Nd values are almost always less than Ce values.

3.6 Comparison with other rocks

This study or any other study involving altered rocks of unknown origin, would not be complete without some detailed comparisons with other rocks. This has partly been done already for the major elements and the conclusion reached was that K, Mg, Fe, Si and minor Mn were added to, while Na, Ca, Al and P were subtracted from, the greenstones at Mount Mulgine. This is evident when the Mount Mulgine greenstones are compared with other Archaean greenstones as is done in Table 3.1.

In general, the same major element movements can be seen to have taken place even when the Mount Mulgine rocks are compared with "modern" rocks.

Notes for Table 3.1

- * Total iron as Fe_2O_3
- ** "Total" does not include loss on ignition.
- *** A W value of 2190 ppm (the highest obtained in this study - in sample 259/30.90) was omitted in the calculation of the mean. When the sample is included the mean value increases from 130 ppm to 186 ppm. Such a high mean value would be deceptive.

Column

- 1 Average of 36 Mount Mulgine greenstones (meta-basalts).
- 2 Average of 123 basalts from the Kalgoorlie-Norseman area, W. Australia (Hallberg, 1972).
- 3 Average of 32 depleted Archaean tholeiites (Condie, 1976).
- 4 Average of 53 Archaean basalts and 20 Archaean andesites from the Canadian shield (Wilson et al, 1965).
- 5 Average of tholeiitic basalt from island arcs (Jakes and White, 1971).
- 6 Average of 33 basalt samples dredged from greater than 1 km on the Mid-Atlantic Ridge (Melson and Thomson, 1971).
- 7 Average for oceanic tholeiitic basalt (Engel et al, 1965).

Table 3.1 : Comparison of Mount Mulgine Greenstones with similar Archaean and "modern" rocks.

	Mt. Mulgine Greenstones	Other Archaean Greenstones			"Recent" rocks		
					Island arc	Ocean floor	
	1	2	3	4	5	6	7
<u>Oxides (wt.%)</u>							
SiO ₂	51.98	51.40	51.4	50.8	51.60	49.2	49.3
TiO ₂	1.02	0.90	1.9	1.02	0.80	1.39	1.49
Al ₂ O ₃	11.36	14.80	14.8	14.6	15.90	15.8	17.04
Fe ₂ O ₃ *	12.00	10.60	10.4	11.6	9.78	9.40	8.81
MnO	0.22	0.21		0.19	0.17	0.16	0.17
MgO	9.84	6.70	6.7	6.8	6.73	8.53	7.19
CaO	9.35	10.70	10.7	9.4	11.74	11.14	11.72
Na ₂ O	0.65	2.70	2.7	2.7	2.41	2.71	2.72
K ₂ O	3.09	0.18	0.18	0.26	0.44	0.26	0.16
P ₂ O ₅	0.10	0.13		0.20	0.11	0.15	0.16
Total**	99.61	98.32	97.28	97.57	99.68	98.74	98.76
Loss on ignition	3.11						
<u>Elements (ppm)</u>							
Ag	5						
As	176						
Ba	129		80		75	12	14
Be	12						
Ce	10		10		2.6		
Co	44	59	60				32
Cr	953	395	350		50	296	297
Cu	198	98	110			87	77
Ga	17						
Li	195						9
Mo	17						
Nb	4						<30
Nd	10						
Ni	158	161	225		30	123	97
Pb	43						
Rb	560	9	4		5		<0
Sb	114						
Sc	46						61
Sn	8						
Sr	126	105	100		200	123	130
V	294	320			270	289	292
W	130						
Y	18	22	10			43	43
Zn	118	112	115			122	
Zr	54	60	55		70	100	95

However, when the other Archaean rocks are compared with "modern" rocks, some relationships appear reversed. Thus while K and Mg are enriched in the Mount Mulgine rocks relative to both the other Archaean greenstones and the "modern" rocks, the two elements are generally depleted in the other Archaean greenstones relative to the "modern" rocks. Na and P values in the other Archaean greenstones are about the same as those in "modern" rocks but as said above, they are depleted in the Mount Mulgine greenstones.

The main point here is that the major elements whose concentrations in the Mount Mulgine greenstones differ markedly from their concentrations in comparable rocks are K, Mg, Na and P. These elements would therefore have been the most mobile of the major elements in the volcanic pile at Mount Mulgine. K-metasomatism, resulting from hydrothermal alteration, has already been mentioned as the cause for K enrichment and Na depletion. In fact, it is believed that all element movements (additions, subtractions, redistributions) were largely due to hydrothermal activity. Other processes like weathering would also have aided in element transfer.

Trace element data is generally scanty in the literature as indicated by the gaps in Table 3.1, but assuming the data available are representative, the following interpretations may be made. Zn, Ba, Cu, Cr and Rb are enriched in the Mount Mulgine greenstones relative to both recent and other Archaean rocks. The latter two elements are extremely enriched in the rocks under investigation; the very high Cr values must be partly due to contamination from the chrome-steel grinding vessel that was used in preparing the samples for analysis and, as suggested by evidence given on page 25, Rb, is believed to have been introduced, together with K, during metasomatism. Cobalt and, to a lesser extent, Ni are depleted in the Mount Mulgine greenstones compared with other Archaean greenstones. Compared with "modern" rocks, Co and Ni appear enriched at Mount Mulgine. Vanadium in "modern" rocks is about the same as in the Mount Mulgine greenstones but it appears slightly enriched in the other Archaean greenstones.

The "immobile" elements Ce, Y and Zr have about the same abundance in the Mount Mulgine greenstones as in other Archaean greenstones, but relative to "modern" rocks, Zr and Y are depleted while Ce appears enriched. There is slightly less Sr in other Archaean greenstones but the element has about the same abundance in "modern" (except island arc) rocks, all compared to the Mount Mulgine greenstones. Finally, Li is extremely enriched in the greenstones at Mount Mulgine compared with ocean floor basalts.

The above comparisons are summarised in the following Table 3.2. Note that the Table does not compare other Archaean greenstones with modern rocks (this is done in the text).

TABLE 3.2

	Mount Mulgine Greenstones		
	enriched	depleted	about the same
Other Archaean Greenstones	K, Mg, Fe, Si Mn?, Ba, Cu, Cr?, Rb, Sr	Na, Ca, Al P?, V, Co, Ni	Zn, Ti, Ce, Y Zr
"Modern" rocks	K, Mg, Fe, Si, Mn, Ba, Cu, Cr, Rb, Co, Ni, Ce, Li	Ti, Zr, Y, Al Ca, Na, P	V, Sr, Zn

3.7 Conclusions and discussion

Before attempting a discussion about the points raised in this chapter, the apparent interpretations about the Mount Mulgine rocks in the Trench area are first recapitulated and listed below.

a) The greenstones are mainly tholeiitic meta-basalts. It appears there was minor differentiation in the volcanic pile, leading to the formation of andesitic rocks and, in extreme (rare) cases, rhyodacitic rocks.

b) The granitic rocks (concordant with the greenstones and mostly greisenized) are not part of the volcanic suite i.e., they are not volcanic in origin.

c) Taking into account the effects of hydrothermal alteration, the greenstones are similar to other Archaean greenstones in the Yilgarn block (e.g., see Figure 3.2) and in other parts of the world.

d) The greenstones most resemble present day island arc tholeiites and/or mid-oceanic-ridge-basalts (the "plume" type MORB, according to the approximated REE patterns). REE patterns of ridge basalts and island arc tholeiites are generally quite similar (Jahn et al, 1973).

The above findings are generally consistent with the conclusions of other workers on Archaean greenstones in Western Australia (e.g., Hallberg and Williams, 1972; Hallberg, 1972) and in other parts of the world (e.g., Viljoen and Viljoen, 1969; Naqvi et al, 1981; Sims and Peterman, 1981). The Archaean greenstones in most parts of the earth also contain rocks of calc-alkaline affinity but the majority are tholeiitic.

The Mount Mulgine greenstones that have been described as high-Mg

meta-basalts in this study are, chemically, the equivalents of the high-Mg basalts (ultramafics) described by Hallberg and Williams (1972), although quench-textures were not recognised in the rocks in this study. The same authors also noted a sometimes complete compositional overlap between tholeiitic basalts and the high-Mg basalts and stated (p.195) that the "relationships, if any, between these two groups are not yet fully understood". Despite this, the authors concluded in their abstract "It is believed that the mafic and ultramafic associations represent two distinct magma sources".

Fractional crystallization of olivine and pyroxene could account for the observed differences between the high-Mg meta-basalts and the tholeiitic meta-basalts, without invoking the former presence of "two distinct magma sources". The fact that the rocks are interlayered and grade into each other favours a common source.

Figure 3.16 is a plot of Ni vs MgO and it strongly supports the interpretation that there was fractional crystallization leading to differentiation. Olivine is usually the first phase to crystallize in a cooling basaltic magma and Ni is incorporated in the olivine lattice. Thus when there is fractional crystallization of olivine (forsterite), high Mg values are accompanied by high Ni-values, and this leads to the trend displayed in Figure 3.16 which is a typical trend for this type of differentiation (e.g., Sato, 1977).

There appears to be two trends in Figure 3.16 (see arrows). One is steep and almost vertical and the other flatter. These two trends are also displayed on the Cr vs MgO diagram (Figure 3.17). The almost vertical trend would most probably represent fractional crystallization of olivine and (clino) pyroxene. Sato (1977) has shown that the Ni content of both magma and olivine decreases markedly by 50% after fractional crystallization of 6-12% olivine and this would explain the steep trend. Since the steep trend also shows clearly on the Cr vs MgO diagram, and Cr is usually found in pyroxenes, the initial fractional crystallization must have involved pyroxene or some other Cr-bearing phase e.g., chromite which was observed in this study (Chapter 4). The flatter trend probably represents fractional crystallization of olivine and pyroxene plus some other phase (e.g., plagioclase).

The REE patterns (Figure 3.15) for the two groups of meta-basalts are almost parallel and the tholeiitic meta-basalts have higher REE contents. These two facts are also consistent with fractional crystallization and hence differentiation producing the two groups of rocks.

Since, from the above discussion, it has been fairly well established that there was differentiation at Mount Mulgine, the meta-rhyodacitic rocks have been also interpreted as differentiation products of a largely basaltic magma.

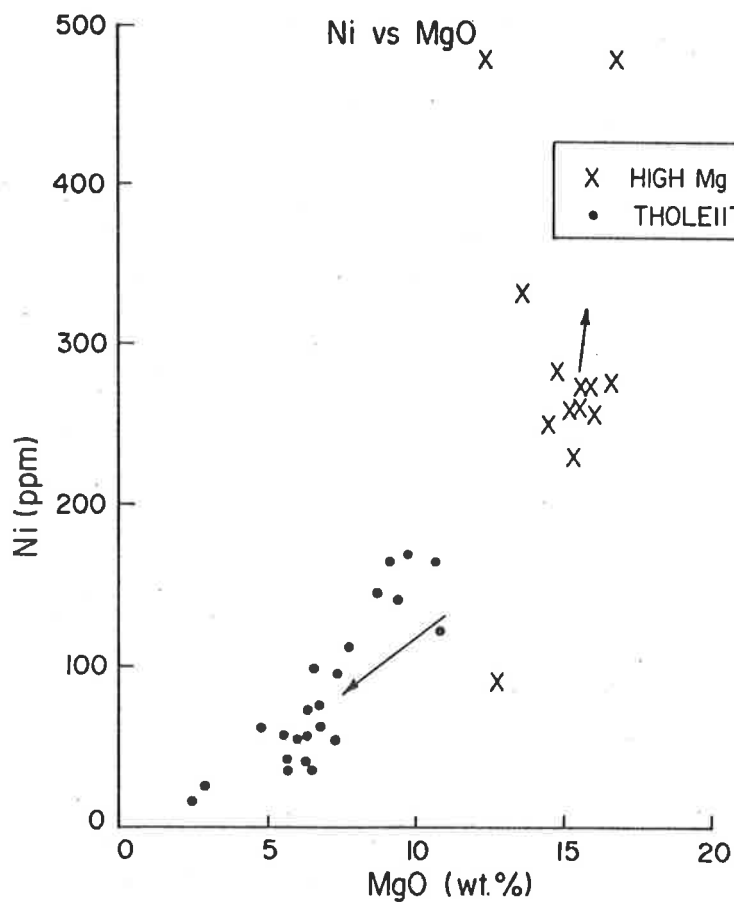


Figure 3.17.

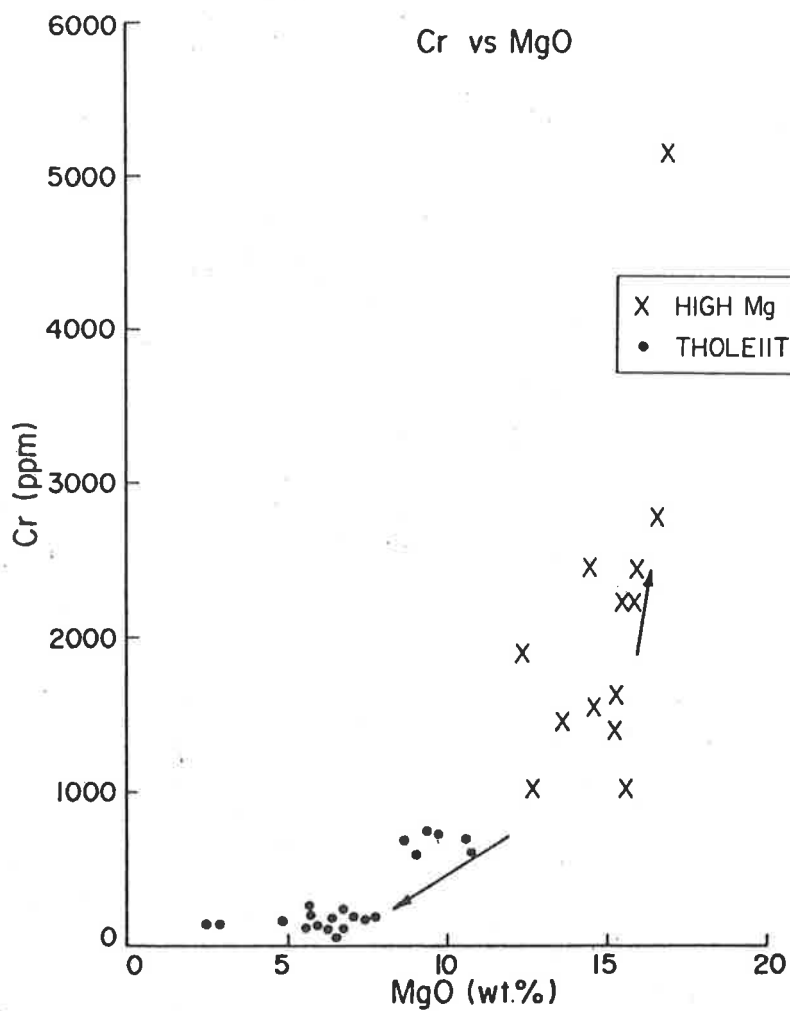


Figure 3.16.

Another possible explanation is that they had a different felsic magma source. But again, the interlayering and gradational relationships with the basaltic rocks does not favour this 'different-magma' hypothesis. The felsic magma would, presumably, have a crustal source while the mafic magma would be mantle derived. As implied earlier, it is difficult to visualize the two magmas being tapped in the same place. Giles and Hallberg (1982) reached similar conclusions for the felsic rocks (rhyodacites, dacites) in the Archaean Welcome Well Volcanic Complex, Western Australia.

As already noted, J. Foden (pers. comm.) suggested that the meta-rhyodacitic rocks may be crustal melts. This means they would have been crustal rocks (rather than magmas) prior to being melted and brought to the surface by the hot ascending basaltic magmas. This is a strong possibility and is considered more plausible than the "different-magma" hypothesis which, as interpreted by the writer, would require a felsic magma to have been present in the "right place at the right time." Both these alternative interpretations are supported by the fact that among the rocks analysed there are virtually none with SiO_2 contents in the 56-67 wt.% range. Such rocks would be expected if the meta-rhyodacitic rocks are differentiation products as suggested.

The close similarity between Archaean greenstones and ocean floor basalts especially island arc volcanics, has been pointed out by many workers (e.g., Wilson et al, 1965; Glickson, 1971; White et al, 1971; Jahn et al, 1973; Condie, 1976) and, applying the well known uniformitarian principle, it has been suggested that Archaean greenstone belts may represent ancient oceanic crust (Hart et al, 1970; White et al, 1971) and an attempt was made to extrapolate modern plate tectonic theory back to the Archaean. The multiple nature of Archaean volcanic belts, for example, was explained in terms of "thin-plate tectonics". The Archaean lithospheric plates are thought to have been thin and incapable of maintaining "large-scale mechanical integrity" (Hart et al, 1970) and so they broke up into many small plates each having a subduction zone for one boundary.

Even in the early seventies, however, some workers were sceptical about direct comparisons of the present with the Archaean, not only because of the time difference, but also because other factors, e.g., BIFs and ultramafic flows, found in the Archaean, have no known modern equivalents (Jahn et al, 1973) and some recent rocks like ophiolites and sheeted dykes are unknown or remain unrecognised in the Archaean (Hallberg and Williams, 1972; McCall, 1981).

Pearce et al (1977) have shown that most Archaean volcanic rocks are unlikely to be exact analogues of modern island arc rocks and support for modern plate tectonic theory as an answer to Archaean problems has declined and rifting

(gravity tectonics) has gained preference (Baer et al, 1978).

The modern majority view summarised by McCall (1981) is that the Archaean globe had shallow seas and small shoal-like emergent land areas. Large oceans with deep subduction at their margins are a feature of not more than the last 1000 m.y. Vertical (rather than horizontal) tectonics are thought to have predominated in the Archaean and resulted in long, narrow and shallow rifts (not unlike modern intracontinental rifts) which became depositories for volcanic and other sediments and are, presently, the greenstone belts. The interpretation that the rifts were shallow is based on lack of evidence for deep water (i.e., pelagic sediments) but they must have subsided (with deposition matching subsidence) to accommodate the very thick sequences recorded in the Archaean. Models in which the Archaean rifts are visualised as back-arc or intracratonic shallow rift basins are the most favoured (Glover and Groves, 1981) and it is still true that there is no single all-embracing model for the Archaean (similar to the plate tectonic theory for the Phanerozoic) which is generally accepted.

CHAPTER 4 : MINERALOGY

4.1 Introduction

In this chapter, more detailed descriptions of the occurrence of the minerals identified are given. These minerals are listed in Table 4.1. While making no claim to completeness, Table 4.1 also contains minerals which have not been identified in this study but which have been reported by previous workers and are known to occur in, or associated with, the Mount Mulgine deposits. This will give a more complete picture of the variety of minerals that occur at Mount Mulgine.

As already mentioned, the electron microprobe was used for the identification of some minerals and for confirmation of the identity of others. There were a few cases when minerals, already positively identified using the optical microscope, were also analysed on the electron microprobe to determine their chemical compositions.

For completeness, all quantitative electron microprobe analyses are included in Appendix 4, although some of the analyses (or their averages) also appear in the text. The measurement conditions of the electron microprobe are also included in Appendix 4.

In most mineral descriptions in the literature, adjectives like "common", "rare" etc. are used freely and sometimes the reader is left wondering how common, "common" is or when it is proper to describe a mineral as "rare", for instance. In this chapter, and only in this chapter, an attempt has been made to qualify these terms. The following arbitrary scheme, which makes the frequency descriptions semi-quantitative, will be followed in this chapter.

Frequency range (percent)	adjective(s)
>70	abundant
45-70	very common
20-45	common
5-20	fairly common
2-5	sparse
<2	rare

What this means for example, is that a mineral will only be described as "abundant" in these rocks only if it was observed in more than 70% of the sections studied. It is important to remember that these terms will only be

Table 4.1 : Minerals at Mount Mulgine (in alphabetical order)

Actinolite	Fluorite	Sphalerite
Adularia	Galena	Sphene
Albite*	Galenobismutite	Spinel**
Andradite	Gersdorffite	Stibnite
Ankerite	Goethite*	Stilbite
Anthophyllite**	Hematite(martite*)	Stilpnomelane*
Antimony	Hornblende	Talc
Apatite	Huebnerite	Tetrahedrite-tennantite
Arsenopyrite	Ilmenite (leucoxene*)	Topaz*
Beryl*	Kobellite-tintinaite	Tourmaline*
Biotite	Lamprobolite(?)*	Tremolite
Bismuth	Magnetite	Ullmannite
Bismuthnite**	Marcasite	Zinnwaldite*
Bowlingite(?)-altered olivine	Microcline	Zircon (Baxter, 1978)
Brannerite(?)	Millerite*	
Calcite	Molybdenite	
Chalcocite	Monazite**	
Chalcopyrite	Muscovite	
Chert	Olivine**	
Chlorite	Orthoclase	
Chromite	Pentlandite	
Chrysocolla (Maitland, 1917)	Phlogopite	
Chrysotile	Pyrargyrite	
Corundum**	Pyrite	
Covellite	Pyrrhotite	
Cummingtonite*	Quartz	
Damourite*	Rutile	
Diopside	Saussurite	
Dolomite	Scapolite*	
Enstatite*	Scheelite	
Epidote(clinozoisite*)	Sericite	
Ferritungstite (Middleton, 1979)	Spessartite	

* Whittle (1977, 1978)
 ** Collins (1975)) Minerals reported but not observed in this study.

used to refer to frequencies of occurrence of the minerals in the samples studied and not to the volumes the minerals occupy in the rocks. The mineral sphene, for example, is very common according to the above scheme but its volume percent in the rocks is very small. Volume percentages of some minerals are given in Chapter 2. It is also worth noting that derivative words such as "abundance", "commonly" etc. have not been qualified and have nothing to do with the above scheme. Statements such as "Huebnerite (rare) is commonly associated with scheelite (which is fairly common)" are not ambiguous and should not be confusing.

In the following mineral descriptions, minerals which may easily be confused (i.e., mistaken for one another) are stressed and an attempt is made to describe how they can be distinguished, if this is possible, without having to use the microprobe. This, hopefully, will save future researchers some time in mineral diagnosis.

A generalised paragenetic sequence of the minerals identified in this study is shown in the following Figure 4.1. The figure is divided into three arbitrary columns labelled "early", "intermediate" and "late". In the left-hand and middle columns, minerals which are considered to be primary are indicated with a line beginning at the left-hand boundary of each column and secondary minerals are indicated with a line starting from about the middle of each column. Broken lines indicate possible but uncertain extent of the minerals.

Generally, "early" minerals are those that were either constituents of the original rocks or were produced during metamorphism (both prograde or early retrograde). The boundary between prograde and retrograde metamorphism is not clear in detail and hence the timing of mineralization in relation to peak metamorphic conditions is uncertain. "Intermediate" primary minerals may have been affected by deformation and metamorphism because hydrothermal deposition of minerals (including hydrothermal alteration) and retrograde metamorphism partly overlapped. The "late" minerals include replacement minerals including supergene alteration products.

Figure 4.1 : Generalised Paragenetic Sequence

	Early	Mineralization	
		Intermediate	Late
Actinolite	-----	-----	
Adularia		-----	-----
Andradite	-----		
Ankerite		-----	-----
Antimony		-----	
Apatite	-----		

Figure 4.1 (cont'd)

	Early	Mineralization	
		Intermediate	Late
Arsenopyrite		—————	
Biotite	—————	- - - - -	
Bismuth			—————
Bowlingite(?)	—————	- - - - -	
Brannerite(?)			—————
Calcite		- - - - -	—————
Chalcocite			- - - - -
Chalcopyrite	—————	—————	—————
Chert		—————	- - - - -
Chlorite	- - - - -	—————	- - - - -
Chromite		—————	
Chrysotile	—————		
Covellite			- - - - -
Diopside	—————	- - - - -	
Dolomite			—————
Epidote	—————	- - - - -	
Fluorite		—————	—————
Galena			—————
Galenobismutite		—————	
Gersdorffite		—————	
Hematite			—————
Hornblende	- - - - -	—————	
Huebnerite		—————	
Ilmenite			—————
Kobellite-tintinaite		—————	
Magnetite	—————	- - - - -	
Marcasite			- - - - -
Microcline	- - - - -	- - - - -	
Molybdenite		- - - - -	- - - - -
Muscovite	- - - - -	- - - - -	
Olivine	—————		
Orthoclase	- - - - -	- - - - -	
Pentlandite		—————	
Phlogopite	—————	—————	- - - - -
Plagioclase feldspar	—————	- - - - -	
Pyrargyrite		—————	
Pyrite	—————	—————	—————
Pyrrhotite	- - - - -	—————	- - - - -

Figure 4.1 (cont'd)

	Early	Mineralization	
		Intermediate	Late
Quartz			
Rutile	-----		-----
Saussurite		-----	
Scheelite			
Sericite	-----	-----	
Spessartite	-----		
Sphalerite			
Sphene		-----	
Stibnite		-----	
Stilbite			-----
Talc	-----	-----	
Tetrahedrite-tennantite		-----	-----
Tremolite	-----	-----	
Ullmannite		-----	

4.2 Tungsten minerals

Scheelite and huebnerite (the manganese member of the wolframite series) are the only W minerals that were identified during this study. Ferri-tungstite has also been reported in the Hill deposit greisens (Middleton, 1979).

Huebnerite has been observed in only three drill cores - DDM 62, 251 and 259 (Middleton, 1979). A sample containing huebnerite was collected from DDM 251. It occurs as relatively coarse grains or aggregates of grains sometimes exceeding 1 cm² in surface area. It is a very dark brown colour and has clearly been partially replaced by scheelite (Plate 4.1A). This replacement is observable even in hand specimen. The huebnerite contains less than 2% FeO (Table 4.2) and is rare.

Scheelite, economically the most important mineral at Mount Mulgine, is fairly common, having been observed in about 17% of the samples studied. It is usually coarse enough to be easily identified in hand specimen, with the largest patches often exceeding 1 cm in their longest dimension. The quickest and easiest way to identify coarse scheelite is to wet the sample. The mineral then "stands out" looking creamy-white against quartz which is transparent to translucent when wet. Where it occurs within the host rocks, it is usually much finer and in this case, it is easier to identify it using a short wave length UV lamp. The scheelite at Mount Mulgine fluoresces a clear whitish-blue colour; an indication that it does not contain any significant Mo which is often found in the scheelite lattice. The scheelite analyses (Table 4.2) show that it is almost pure CaWO₄ and confirm that there is very little or no Mo in it. All the other

Table 4.2 : Scheelite and Huebnerite analyses

(concentrations in wt.%; n.d. means not detected).

Sample No.	SCHEELITE			HUEBNERITE	
	268/35.84	51/108.70	251/64.70	251/64.70	251/64.70
Analysis No.	2	1	5	1	2
P ₂ O ₅	0.14	0.22	0.17	0.16	0.17
SiO ₂	n.d.	n.d.	n.d.	n.d.	n.d.
TiO ₂	n.d.	n.d.	n.d.	n.d.	n.d.
Cr ₂ O ₃	n.d.	0.04	n.d.	n.d.	0.08
FeO	n.d.	n.d.	n.d.	1.63	1.31
MnO	n.d.	n.d.	0.11	21.57	21.80
MgO	n.d.	0.01	n.d.	0.20	0.16
CaO	19.36	18.94	18.95	0.04	0.04
NiO	n.d.	n.d.	n.d.	n.d.	n.d.
Sc ₂ O ₃	n.d.	n.d.	0.03	n.d.	n.d.
WO ₃	83.23	82.41	82.79	79.52	78.49
SnO ₂	n.d.	n.d.	0.10	n.d.	n.d.
MoO ₃	0.24	n.d.	n.d.	n.d.	n.d.
Nb ₂ O ₅	n.d.	n.d.	n.d.	n.d.	n.d.
Ta ₂ O ₅	n.d.	n.d.	n.d.	n.d.	n.d.
UO ₂	n.d.	0.19	n.d.	n.d.	n.d.
Total	102.97	101.81	102.15	103.12	102.05

elements analysed for, together constitute less than 0.65 wt.% of the scheelite (see Appendix 4).

Scheelite may be too fine to be seen or identified in hand specimen in which case a microscope must be used. To a casual observer or someone not familiar with its appearance, scheelite may look very much like epidote or sphene under the microscope in both transmitted and reflected light. In reflected light, it may look like many transparent minerals, e.g., carbonates and fluorite. So, erroneous identifications are possible. Indeed, this is what happened in the early days of this study; the minerals identified as scheelite and wolframite in an interim report on this project, dated February 1982 (Plates 6, 9 and 10 of the report) are sphene and rutile respectively.

Due care must be taken in the identification of scheelite under the microscope because the similar-looking minerals, epidote and sphene are very common in the rocks at Mount Mulgine. What is more, epidote is often found partially replaced by scheelite (Plates 4.1B and 4.2A). In sample 259/84.35, scheelite also grades into and appears to have partially replaced sphene.

In cases where there is a strong possibility of erroneous identification, then factors like grain size, relative abundance and distribution within the rock will be of great help in positive identification short of microprobe analysis. Scheelite grains are usually relatively coarse and few in number (less than 5 grains in most thin sections) and are almost always found within or close to (quartz) veins.

The association of scheelite and quartz veins has already been mentioned. This association is displayed in Plate 4.1C. In one sample (51/89.20) scheelite forms a vein without other minerals and in sample 268/140.55, which does not contain quartz, scheelite was observed in a carbonate vein.

Apart from quartz, epidote and huebnerite, scheelite does not appear to be closely associated with any one mineral or group of minerals. Thus it is not confined to any one rock type although it is noticeably scarce in the acidic members. Scheelite was observed with inclusions of many minerals including pyrite, chalcopyrite, sphalerite, arsenopyrite, tetrahedrite, kobellite-tintinaite and gangue minerals such as quartz, carbonates and phlogopite.

Some scheelite grains show undulose extinction, interpreted to be due to strain*. In some cases, the mineral has responded to stress by fracturing and gangue minerals and molybdenite have been observed in fractures extending into the scheelite. Soft minerals like molybdenite may have moved into the fractures during deformation but it is also possible that they are later than scheelite. More will be said about scheelite later, in the discussion on ore genesis.

*

In a few cases, the undulose extinction seems to be due to replacement.

4.3 Antimony and some antimony-bearing minerals

Native Sb was observed in only one sample and is therefore rare. Initially, it was suspected to be dyscrasite (which it resembles very much in incident light), because of its high reflectance but electron microprobe analysis showed that it is almost 100% Sb with only minor amounts of As and Bi. It is associated with chalcopyrite and tetrahedrite and appears to have partially replaced the latter mineral.

Five Sb-bearing phases were identified. Tetrahedrite and stibnite will be discussed here and the rest (ullmanite, pyrargyrite and kobellite-tintinaite) will be described in other sections to follow.

Tetrahedrite is common in the rocks at Mulgine and is the fourth most frequently observed opaque mineral. It occurs mostly as discrete fine grains, the largest of which would be less than about 0.2 mm. The grains are usually scattered throughout the rock but in a few cases, they were observed grouped together. The minerals most commonly associated with tetrahedrite are arsenopyrite, pyrite and chalcopyrite and all three have been observed partially replaced by the tetrahedrite (Plate 4.3C). Tetrahedrite is generally free of inclusions but in one sample, 264/116.27, it has inclusions of kobellite-tintinaite and appears to have partially replaced them. Tetrahedrite grains were observed in fluorite.

The analysed tetrahedrites (Table 4.3) contain up to 4% Zn, 5% Fe and 13% Ag. One of them had about 9% As and is therefore classified as tetrahedrite-tennantite.

Stibnite, although sparse, is one of the few opaque minerals that sometimes occurs coarse enough to be identified in hand specimen. Its crystals or crystal aggregates sometimes span several centimetres. The occurrence of stibnite crystals means that the temperature of formation must have been less than 556°C its melting point (Vaughan and Craig, 1978). The stibnite is associated with arsenopyrite, chalcopyrite, pyrrhotite and tremolite gangue. Pyrrhotite was found as inclusions in stibnite and also stibnite inclusions were found in pyrrhotite. Two of the four samples in which stibnite was observed do not contain quartz but they contain silica in the form of chert which is involved in colloform texture. Chert is also sparse and its occurrence with stibnite in the same samples makes one wonder whether the two might be genetically associated. It may well be a coincidence.

In sample 318/58.4 stibnite was observed clearly following fractures within quartz. This need not imply that it is later than quartz - it may have been remobilized into the fractures during deformation. Stress may explain the (pressure) twinning which is commonly observed in stibnite

Table 4.3 : Tetrahedrite analyses

(concentrations in wt.%, n.d. means not detected).

	T E T R A H E D R I T E S			Tetrahedrite-Tennantite
Sample No.	264/116.27	259/123.32	301/133.8	259/123.32
Analysis No.	1	1	1	2
Fe	2.27	5.42	2.91	5.43
Cu	28.68	36.28	34.17	31.38
Pb	n.d.	n.d.	n.d.	n.d.
Zn	4.41	1.82	3.94	2.03
Ni	n.d.	n.d.	n.d.	3.59
Sb	23.67	30.58	30.15	26.37
As	3.44	0.33	0.50	9.72
Ag	13.28	1.47	4.37	1.05
S	23.79	24.16	24.38	24.38
Cd	0.37	n.d.	0.64	n.d.
Bi	n.d.	n.d.	n.d.	n.d.
Ti	n.d.	0.05	n.d.	n.d.
Sn	n.d.	n.d.	n.d.	n.d.
Total	99.91	100.11	101.06	103.95

(Plates 4.2B and 4.2D).

4.4 Iron sulphides

Pyrite

Pyrite is the main Fe sulphide and it is abundant at Mount Mulgine. It was observed in 90% of the 138 sample sections studied and its frequency of occurrence is unequalled by that of any other mineral in the study area. Although it was not observed in a few of the sample sections studied, there is no hesitation in stating that it occurs, in varying amounts, in all rock types at Mount Mulgine and may occur together with any of the minerals listed in Table 4.1.

The grain size of pyrite varies from very coarse crystals (>2 cm) suitable for study in hand specimen down to minute grains that can hardly be seen with the optical microscope. The grains are sometimes euhedral to subhedral but, more often than not, they appear anhedral.

From its form, mode of occurrence and association with other minerals, it is quite clear that there are several pyrite generations. It is not easy to say exactly how many but three would be a conservative minimum (Plate 4.2C).

The pyrite is, in places, intergrown with the gangue, not leaving much doubt that it is an original constituent of the host rocks. Fine grained syngenetic pyrite has been observed in layers parallel to schistosity or banding. Such pyrite layers may be transgressively cut by veins of coarser and more massive looking pyrite which may have been remobilized. In other samples, evidence that the pyrite was introduced is impeccable for the pyrite is coarsely crystalline and virtually confined to quartz or fluorite veins. Pyrite veins sometimes occur within quartz veins. Megascopic pyrite veins may look like some cementing or hardened grouting material. It is also found deposited in interstices, fractures and along cleavage planes of micaceous minerals (see Plate 4.5D).

In the few rocks in which colloform texture was observed, framboidal pyrite is found at the base of layers of cherty silica.

Pyrite occurs associated with a wide range of minerals. Inclusions of magnetite, chalcopyrite, pyrrhotite, muscovite and phlogopite are most common in pyrite. The very coarse pyrite grains often have very small inclusions of a pinkish-cream mineral that looks very much like (and may well be) the mineral identified as galenobismutite. Whittle (1977, 1978) reports that most of galena "occurs as binary intergrowths with chalco-

pyrite or as inclusions within the largest of the pyrites". It thus appears that some of the galena identified by Whittle and reported in his 1977, 1978 reports, is what has been identified as galenobismutite in this study (see section 4.5). Inclusions of pyrite were observed in magnetite, tetrahedrite, pyrrhotite, epidote, sphene and fluorite. The association of pyrite and fluorite means that pyrite continued to crystallize right up to the very last stages of mineralization (see Figure 4.1).

In the above-mentioned and other associations of pyrite, it is often not clear whether or not replacement has taken place but the following cases are fairly definite. Pyrite has partially or completely replaced pyrrhotite and has itself been replaced by marcasite and tetrahedrite. Epidote is so often found enclosing pyrite (Plate 4.3A) that it is felt that there must be some genetic connection between the two minerals. The nature of this connection is not understood at present.

Evidence for deformation is provided by some of the coarser pyrite crystals which are often heavily fractured. Pyrrhotite, chalcopyrite, molybdenite and gangue minerals occur in the fractures. Pyrite was analysed and the analyses are in Appendix 4.

Pyrrhotite

The second most important Fe sulphide is pyrrhotite, which is fairly common in the rocks at Mount Mulgine. There seems to be an antipathetic relationship between pyrrhotite and pyrite; where the former mineral occurs in significant quantities, the latter mineral is very minor or absent.

Both hexagonal and monoclinic pyrrhotites occur but the monoclinic variety predominates. Monoclinic pyrrhotite partly or wholly rims hexagonal pyrrhotite, especially where the latter mineral is in contact with gangue or is fractured (Plates 4.3B and 4.3D). This indicates that hexagonal pyrrhotite has been altered to monoclinic pyrrhotite. The alteration of hexagonal to monoclinic pyrrhotite is due to the removal of Fe and/or addition of S or oxygen (Scott et al., 1977). This process can result in the formation of pyrite and marcasite and, in extreme cases, of magnetite or hematite. All these four minerals were observed associated with pyrrhotite in the rocks at Mount Mulgine and this is a further indication that monoclinic pyrrhotite has replaced hexagonal pyrrhotite.

However, unless there were two or more pyrrhotite generations, it is unlikely that the coarser monoclinic pyrrhotite grains were originally hexagonal pyrrhotite which has been completely replaced when similar size or even smaller hexagonal pyrrhotite grains have only been partially replaced.

Thus it is possible that some of the monoclinic pyrrhotite is primary which would indicate low temperatures of deposition (below 254°C, Kissin and Scott, 1982). Alternatively, these observations may simply be due to varying degrees of replacement.

The closest associate of pyrrhotite is chalcopyrite. The two minerals are almost always found close to each other and usually in contact. Pyrrhotite is also associated with pyrite, sphalerite, magnetite and rutile. It has been found, together with chalcopyrite as inclusions in sphalerite (Plate 4.5A).

The identity of hexagonal pyrrhotite was confirmed by microprobe analysis. All the analysed pyrrhotites (Appendix 4) have more than 47.1 atomic % Fe, implying that they are indeed hexagonal as suspected from treatment with a magnetic colloid. Numerous investigations in the Fe-S system have shown that stable monoclinic pyrrhotite has less than 47.1 atomic % Fe. To confidently distinguish the pyrrhotites from each other on the basis of their compositions requires accurate analyses (Scott et al, 1977).

Marcasite

The third of the Fe sulphides recognized in this study is marcasite. It is fairly common and in all cases it was observed in intimate contact with pyrite (Plate 4.4D). This has been interpreted to mean that it has replaced pyrite but this interpretation is questionable in view of the fact that the reaction $\text{marcasite} \xrightarrow{\text{heat}} \text{pyrite}$ is irreversible (Fleet, 1970). This reaction takes place at temperatures as low as 400°C (Fleet, 1970). However, the replacement of pyrite by marcasite seems established in the literature. Ramdohr (1980) suggests that some of the reported cases may represent simultaneous deposition of the two minerals. This is a possibility in this case. The association pyrite + marcasite could be an alteration product of pyrrhotite but this is considered unlikely in this case because of the characteristic appearance of pyrite.

Whatever its mode of formation, the presence of marcasite implies moderate or low temperatures of formation. Primary marcasite forms from acid solutions at temperatures below 450°C (Winchell and Winchell, 1961).

4.5 Bismuth and bismuth-lead minerals

Native Bi, galena, galenobismutite (lillianite?) and kobellite-tintinaite are the Bi and/or Pb minerals that were identified. Each of these minerals is rare at Mount Mulgine.

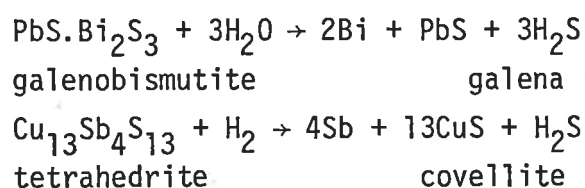
Pure Bi is associated with and appears to have partially replaced a Pb, Bi sulphide that has been called galenobismutite ($\text{PbS.Bi}_2\text{S}_3$) because of

its optical properties and association with Bi, although its composition (Appendix 4) is closer to that of lillianite ($3\text{PbS}\cdot\text{Bi}_2\text{S}_3$). Other minerals associated with Bi are pyrite, chalcopyrite and pyrargyrite (see Plate 4.4B). In the absence of pyrrhotite, the colour of native Bi (pinkish-cream due to tarnishing) can easily be mistaken for that of pyrrhotite. It (Bi) was analysed because of its close association with galenobismutite; otherwise, it would easily have been overlooked as pyrrhotite. The analysis results (Appendix 4) show that it is almost 100% Bi.

The occurrence of the native metals Bi and Sb may be due to reduction of the appropriate sulphides during or after serpentinization, in a manner similar to that suggested by Chamberlain et al, (1965) to explain the occurrence of native metals in the Muskox intrusion, Canada. Hydrogen is produced during serpentinization by the reaction



The hydrogen then reacts with the sulphides liberating the metals. Reactions of the following type may have been involved in the formation of the native metals:



Although neither native Bi associated with galena nor native Sb associated with covellite were observed, the fact that native Bi occurs associated with galenobismutite and that native Sb and tetrahedrite were observed in one sample and tetrahedrite and covellite in another sample, makes it highly likely that the reactions shown above took place at Mount Mulgine.

Only one fine grain of free galena was observed. Its analysis yielded a low total and indicated small quantities of Fe and Sb, but there is not much doubt about its identity. The galena occurs close to but not in contact with pyrite, tetrahedrite and native Sb and so contamination with Fe and Sb is a possibility.

Kobellite-tintinaite was found as very small grains both partly and wholly enclosed by tetrahedrite, within scheelite (Plate 4.4A) in sample 264/116.27. It is assumed that the tetrahedrite has partially replaced the kobellite-tintinaite. Identification was aided by electron microprobe analysis (Appendix 4).

4.6 Silver minerals

Apart from tetrahedrite, which may contain up to 13% Ag, the only other Ag-bearing mineral observed in the samples studied is pyrargyrite ($3\text{Ag}_2\text{S}\cdot\text{Sb}_2\text{S}_3$). Because of its light blue colour, pyrargyrite was almost overlooked as chalcocite, especially since it was in contact with chalcopyrite. But, there was no apparent replacement between the two minerals and besides, there was no trace of covellite (in the samples at Mount Mulgine, it is usually covellite which replaces chalcopyrite while it (covellite) is being replaced by chalcocite). Suspicions about its identity were thus created and were later confirmed when it was analysed and found to be pyrargyrite. The analysis results (Table 4.4) are almost exactly as one would expect from its formula given above.

Table 4.4: Composition of pyrargyrite

Sample No. 51/108.70
concentrations in wt.%, n.d. means not detected.

Element	wt.%
Fe	0.08
Cu	0.09
Pb	n.d.
Zn	n.d.
Ni	n.d.
Sb	23.80
As	0.16
Ag	59.86
S	17.27
Cd	n.d.
Bi	n.d.
Ti	n.d.
Sn	n.d.
Total	101.26

Pyrargyrite was observed in only one sample (51/108.7) and is therefore rare, although it is possible that it was overlooked as chalcocite, or some other copper mineral, in other samples. Only one grain of the mineral was observed and it is less than 0.2 mm long. The one grain is between and in contact with chalcopyrite and pyrite (see Plate 4.4B). The chalcopyrite is also in contact with Bi and the assemblage also includes galenobismu-

tite partially replaced by Bi. Middleton (1979) reports that higher Bi values are invariably accompanied by higher Ag values in the rocks at Mount Mulgine. The above mineral association may explain Middleton's observation.

4.7 Nickel-bearing minerals

The Ni-bearing sulphides pentlandite, ullmannite and gersdorffite were identified in one sample of a phlogopite-chlorite schist. The other opaque minerals in the sample (268/35.84) are molybdenite, pyrite, chalcoppyrite, rutile and minor marcasite. Scheelite also occurs in the same sample.

Ullmannite (NiSbS) and gersdorffite $[(\text{Ni}, \text{Co}, \text{Fe})\text{AsS}]$ are not only strikingly similar in appearance but they also look like pyrite in reflected light (Plate 4.5C). If they had not been in the same field of view with pyrite, they would, almost certainly, have been missed. Since they were observed in only one sample they must be described as rare but as just implied, they may have been mis-identified as pyrite in other samples. In sample 268/35.84, they are relatively abundant with gersdorffite being the second most abundant opaque after pyrite. Each mineral occurs as discrete grains generally less than 0.3 mm long. The grains of each mineral tend to occur in a group. Some of the gersdorffite grains are surrounded by minute grains of another mineral too small to be identified but having a grey colour, in incident light, similar to that of rutile.

The electron microprobe had to be used to distinguish between gersdorffite and ullmannite and to identify them. Their compositions (Appendix 4) and optical properties are as anticipated from published data (e.g., Uytendogaardt and Burke, 1971). Although Co was not analysed for, the analysis results show that there can only be minor amounts of it (if any) in the gersdorffite.

Three pentlandite grains were identified in the same field of view with the ullmannite and gersdorffite. One of them was in close contact with chalcoppyrite and had probably been partially replaced by it, but the others were isolated. The pentlandite grains would have been identified as pyrrhotite but their paucity and very fine size betrayed them. (Pyrrhotite is usually relatively much coarser and abundant wherever it occurs). The electron microprobe results (Appendix 4) confirmed the identity of pentlandite.

With the possible exception of pentlandite (with chalcoppyrite), the Ni phases do not appear to have been involved in any replacement textures.

4.8 Arsenic-bearing minerals

The occurrence of gersdorffite with more than 40 wt.% As has already been mentioned in the previous section. The other phases with appreciable amounts of As are arsenopyrite and tetrahedrite-tennantite. A few other minerals (e.g., ullmannite) contain minor to trace amounts of As.

Arsenopyrite is fairly common at Mount Mulgine. Being one of the most refractory minerals among the common sulphides, arsenopyrite has been used and recommended as a geothermometer (e.g., Kretschmar and Scott, 1976). No serious attempt was made to use it as a geothermometer in this study because of uncertainties about whether or not it crystallized in an aS_2 buffered assemblage. The only sulphide which was observed in contact with arsenopyrite was tetrahedrite and this mineral had partially replaced the arsenopyrite in sample 259/123.32. In this sample, the colours of these minerals in reflected light are not exactly as anticipated from experience with other samples from Mount Mulgine and so, it was decided to analyse the minerals and determine whether the slight differences in colours represent compositional differences. This proved to be so for the tetrahedrite which has about 9% As (see Table 4.3) and has been classified as tetrahedrite-tennantite, but the arsenopyrite is fairly pure as can be seen from the following Table 4.5

Table 4.5: Arsenopyrite analyses

Sample No. 259/123.32

Concentrations in wt.%; n.d. means not detected

Element	Analysis 1	Analysis 2
Fe	35.70	35.40
Cu	0.06	0.19
Pb	n.d.	n.d.
Zn	n.d.	n.d.
Ni	0.17	0.05
Sb	n.d.	n.d.
As	44.67	44.71
Ag	n.d.	n.d.
S	20.79	20.58
Cd	n.d.	n.d.
Bi	n.d.	n.d.
Ti	n.d.	n.d.
Sn	n.d.	n.d.
Total	101.40	100.93

It was decided to take advantage of the few arsenopyrite analyses thus obtained and attempt to estimate its temperature of formation according to the method of Kretschmar and Scott (1976). The arsenopyrite contains less than 0.5 wt.% total impurities and its mean As content is 31.67 atomic %. This indicates a temperature of about 405°C when referred to Figure 4 of Kretschmar and Scott (1976) reproduced here as Figure 4.2. This temperature was obtained using the arsenopyrite + pyrite + pyrrhotite (asp + py + po) line in Figure 4.2. Although these three minerals were not all observed in sample 259/123.32, they were all observed in samples 259/126.87 and 264/126.35.

In determining the above temperature, it was assumed that the arsenopyrite grew in an aS_2 buffered system and that its composition has not changed since its formation (although it is obviously involved in replacement). Even if these assumptions are correct, the fact that only one grain of arsenopyrite was analysed is enough to raise objections to the temperature thus obtained. However, it is interesting to note that this temperature (405°C) is in fair agreement with the mean temperature (396°C) of scheelite formation obtained from fluid inclusion studies (Chapter 5). But this could be fortuitous.

The usual mode of occurrence of arsenopyrite in the rocks at Mount Mulgine is as isolated euhedral crystals or groups of crystals averaging about 0.15 mm across. In sample 276/74.10 arsenopyrite is the most abundant opaque. Apart from tetrahedrite-tennantite mentioned above, arsenopyrite is not associated with any mineral(s) in particular.

Tetrahedrite-tennantite, which is sparse at Mount Mulgine, was positively identified only in sample 259/123.32 but it was observed in other samples, always associated with chalcopyrite. In the above sample, it completely encloses chalcopyrite and may have partially replaced it (Plate 4.3C). Compared to "normal" tetrahedrite, tetrahedrite-tennantite is darker in reflected light with a khaki type of colour.

4.9 Sphalerite

Zinc averaged 103 ppm in all the rocks analysed and its sulphide, sphalerite, is fairly common. In this study, most of the sphalerite identifications were done in transmitted light in which the mineral has a bright red colour. (Huebnerite is also blood red in transmitted light but it is anisotropic). In reflected light, most of the larger sphalerite grains invariably contain inclusions of chalcopyrite and/or pyrite and pyrrhotite. These inclusions may be randomly distributed throughout the mineral or they may be aligned all along its edge, resembling an overgrowth texture (Plate 4.4C) or they may be arranged in irregular veins or veinlets which look like a string of elongated beads (Plate 4.5A).

Such inclusions in sphalerite are common in many ore deposits and have, in the past, generally been interpreted as exsolution bodies. While this interpretation must be at least partly correct, especially in the case of higher temperature ($>400^{\circ}\text{C}$) deposits, some other explanation must be sought for the lower temperature deposits. Recent work by Wiggins and Craig (1980) and Hutchison and Scott (1981) has demonstrated that chalcopyrite will not dissolve in sphalerite in any significant amounts unless the temperature is above 500°C . But abundant inclusions of chalcopyrite in sphalerite have been observed in ores that are known to have formed at much lower temperatures (e.g., Kelly and Rye, 1979; Kim, 1981). They have even been observed in deposits that are known to have formed in the $100\text{-}150^{\circ}$ range (Craig and Vaughan, 1981).

In such cases, exsolution, which is temperature dependent, is not the sole explanation. Such inclusions are now believed to have grown during sphalerite formation or to be due to replacement as Cu- and/or Fe-rich fluids reacted with sphalerite after formation (Craig and Vaughan, 1981). The arrangement of the grains into veins or along sphalerite boundaries may be due to redistribution of the included grains as sphalerite recrystallizes during metamorphism.

The distribution of pyrite inclusions in sphalerite, along the sphalerite-scheelite boundary (Plate 4.4C) is believed to be due to direct deposition of the pyrite as a result of interaction between the sphalerite and later solutions that migrated in the interstices between scheelite and sphalerite. The fact that Fe was found in the fluid inclusions (Chapter 5) is consistent with this interpretation. The quartz grains between the sphalerite and scheelite (see Plate 4.4C) might have formed at about the same time as the pyrite.

Williams (1974) also observed that pyrite and marcasite "tend to occur as inclusions in the grain boundaries of sphalerites" at Zeehan, Tasmania. He essentially suggested the same explanation as above and noted that it was unlikely that the pyrite formed from, and during reequilibration of, sphalerite. It is also considered unlikely that the pyrite formed as a result of a reaction between sphalerite and the adjacent scheelite.

The minerals found as inclusions in sphalerite are its most common associates. Rutile is also commonly associated with sphalerite. Sphalerite grains are generally small but they may be large enough to be seen with the naked eye (by holding the thin section against the light). This is the case in polished thin section 124 (sample 259/115.77) in which sphalerite is found in a vein (see Plate 4.5A).

Sphalerite, in contact with pyrite and pyrrhotite, was analysed in an attempt to use its Fe content to estimate the pressure of formation. Sphalerite geobarometry is dealt with in Chapter 6 and the full analyses are in Appendix 4.

4.10 Iron, titanium and chromium oxides

Five oxides of Fe, Ti and Cr have been identified in the rocks studied. In order of frequency in the rocks, they are rutile (very common) magnetite (common) ilmenite (fairly common) hematite (sparse) and chromite (rare).

Rutile

Rutile is the third most abundant opaque mineral after pyrite and chalcopyrite. It usually occurs in minor or trace amounts but in some samples, for example 276/47.8 and 268/22.14, it predominates over the other opaques. Sample 268/22.14 is one of the rocks that were analysed and it has 0.98 wt.% TiO_2 (see Appendix 3). It can hardly be described as being relatively rich in Ti and the dominance of rutile is, therefore, a little surprising; it is thought to be due to a relative lack of minerals like sphene which take up Ti. Even sample 276/47.8 has only trace sphene in it.

Rutile occurs as fine, roundish and generally discrete grains. The relatively larger grains would average about 0.05 mm across. The grains are sometimes in groups, giving a strong impression that they are, or they represent, an alteration product. The mineral that no longer exists may well have been sphene for presently, rutile grains or groups of grains are often found within sphene (Plate 4.3A). In sample 268/22.14 rutile occurs as needles or rods which look as if they are randomly oriented but they are actually aligned parallel to the cleavage planes of actinolite. (The sample is composed of 80% actinolite). The needle-like habit of rutile (Plate 4.5B) was also observed in section 70/49.90 which is also essentially an actinolite rock (60% actinolite). The rutile needles are extremely thin (less than about 0.01 mm) and their lengths are about 4 to 10 times their widths, on average. Similar needles of rutile have also been reported from Broken Hill (Ramdohr, 1980, p. 1008).

Rutile occurs in almost all Mount Mulgine rocks, associated with many minerals. It is particularly well developed in rocks also containing muscovite, pyrrhotite, chalcopyrite and sphalerite. Grains of the mineral have been observed in pyrrhotite and in some samples ilmenite seems to have partly replaced it. The rutile also appears to have been partially replaced by some U-containing mineral which is suspected to be brannerite (Plate 4.5D).

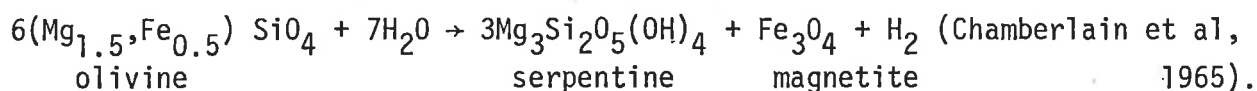
Rutile was occasionally analysed but only qualitatively to make sure it was not ilmenite or magnetite which can be very similar in appearance. The rutile that is associated with brannerite(?) was analysed and found to contain nearly 2 wt.% Nb₂O₅ (see Appendix 4).

Magnetite

Magnetite is very important, especially in BIF in which it may constitute more than 50% of the rock. The occurrence of magnetite seems to have been directly controlled by the availability of Fe in the Mount Mulgine greenstones. With a few exceptions, magnetite is not found in rocks that are chiefly composed of non-Fe-bearing minerals such as phlogopite and tremolite. The greenstone rocks in which magnetite is found are richer in Fe (12.6% Fe₂O₃ on the average compared with an average of 10.9% Fe₂O₃ in non-magnetite-bearing greenstones).

Only in BIF's are magnetite grains greater than 1 mm commonly encountered. The grains are generally anhedral and sometimes have inclusions of chalcopyrite, pyrite or pyrrhotite. Like pyrite, some of the magnetite would be an original accessory component of the host rocks.

Serpentine is invariably associated with magnetite and both these minerals are considered to be a direct result of serpentinization.



In the samples in which the two minerals are found, magnetite partly follows the cleavage of the fibrous serpentine (chrysotile) and so their genetic association is not in much doubt.

The colour of magnetite in reflected light may be almost exactly the same as that of rutile or ilmenite or chromite. Only in those cases when rutile or ilmenite appear isotropic is there a possibility of confusing these minerals with magnetite. Distinguishing between chromite and magnetite (when they occur separately) may be very difficult. Magnetite was observed completely surrounding and apparently having partially replaced ilmenite and chromite. Tetrahedrite was also observed in magnetite but it was not clear if there had been some replacement between the two. Hematite has definitely replaced magnetite; this replacement may be confined to fractures and is considered to be a supergene effect. Like rutile, magnetite is also found as cores in sphene. The two minerals have been observed side by side in the same grain of sphene (Plate 4.6C).

In some samples (e.g., 259/99.2 and 22/33.9), magnetite is not its "normal" brown colour but the colour has a definite purplish or pinkish

Plate 4.1A

Huebnerite (red) partially replaced by scheelite (white).
The gangue is quartz (pinkish cream in the lower right hand
corner).

Sample No. 251/64.70, reflected light.

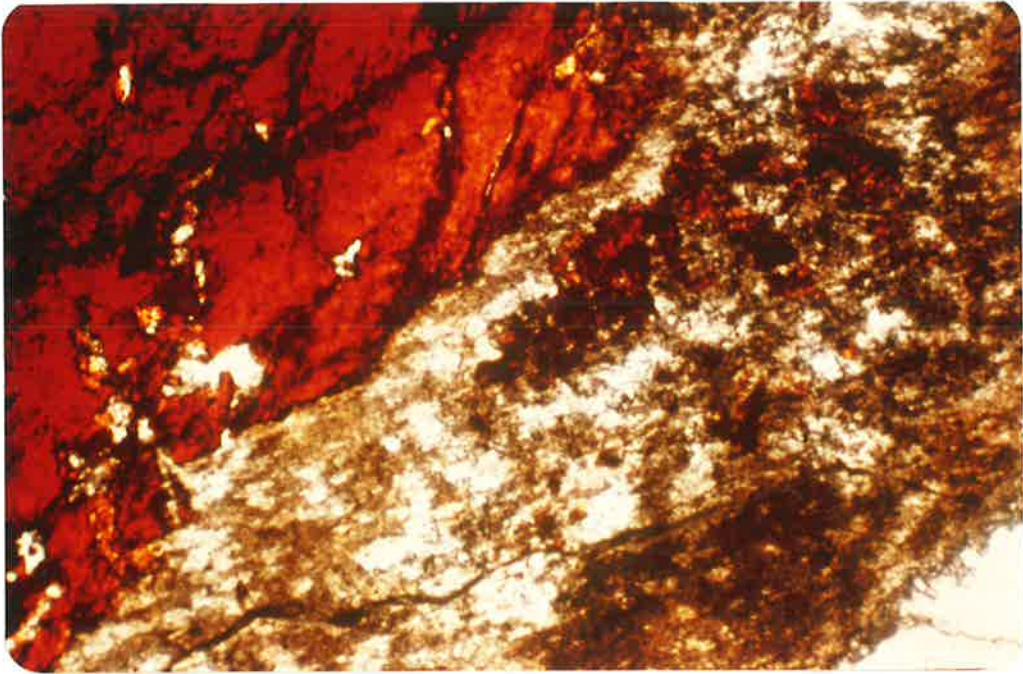
Plate 4.1B

Epidote (multicoloured) partially replaced by scheelite
(brown-grey with a mottled appearance). The other mineral
is quartz. Sample No. 259/30.9. Transmitted light,
crossed polars. See also Plate 4.2A.

Plate 4.1C

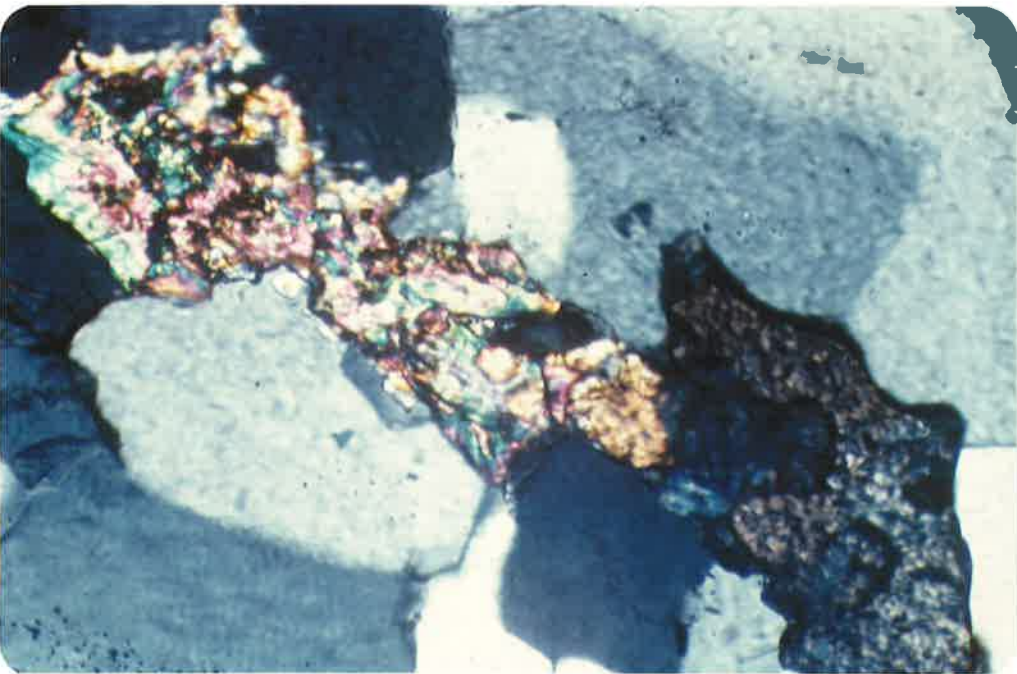
Coarse scheelite fluorescing in short wavelength UV light.
The scheelite is in a quartz vein. Note the smaller scheelite
grains scattered near and along the quartz vein edges. (-----)
Sample No. 93/62.18.

PLATE 4.1



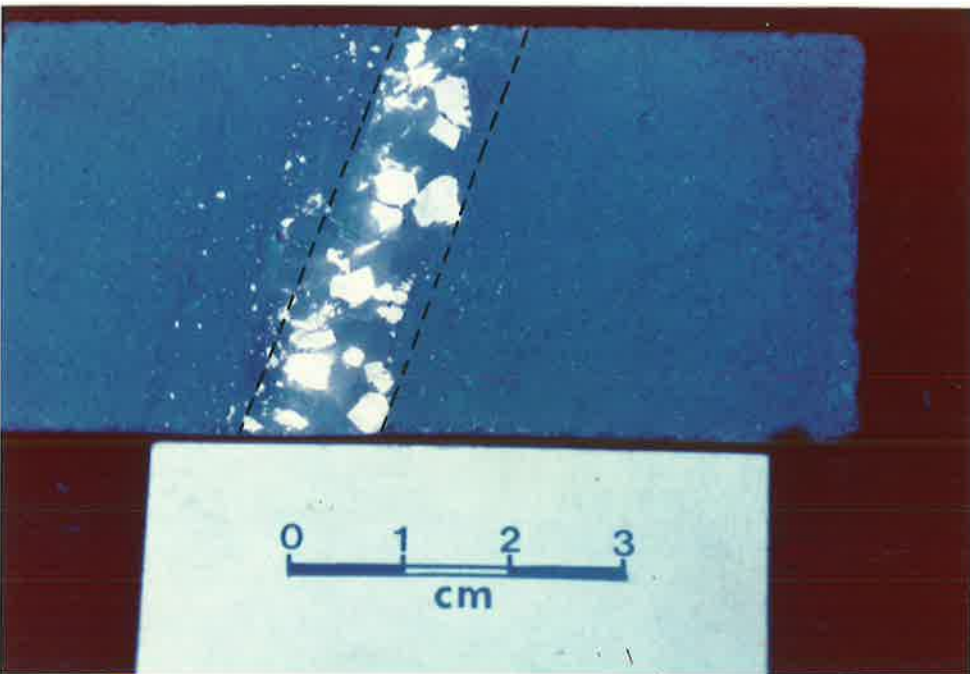
A

0.25 mm



B

0.125 mm



C

0 1 2 3
cm

Plate 4.2A

Same as Plate 4.1B but in reflected light, showing the sometimes striking resemblance between scheelite (Sh) and epidote (Ep) in reflected light.

Plates 4.2B and 4.2D

(B) Pressure twinning in stibnite.

(D) Growth(?) twinning in stibnite.

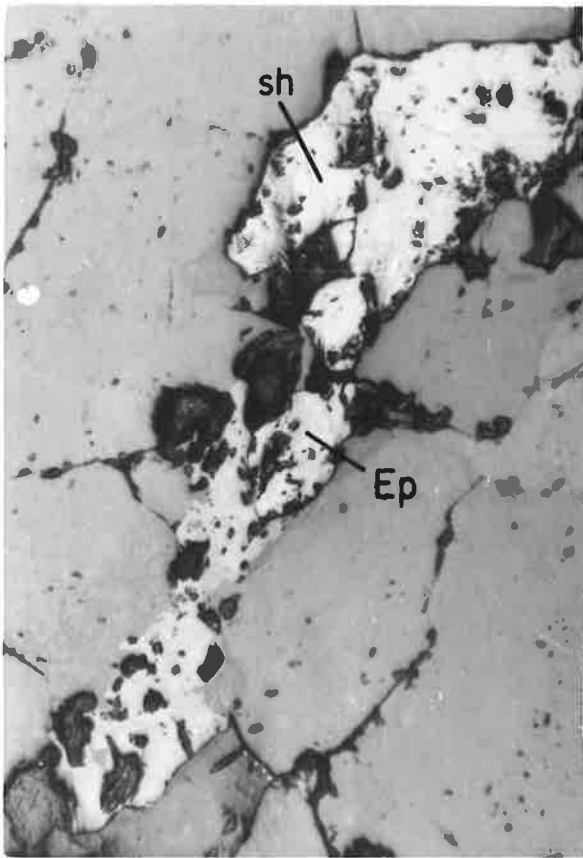
Sample No. 318/54.8. Reflected light, partly crossed polars.

Plate 4.2C

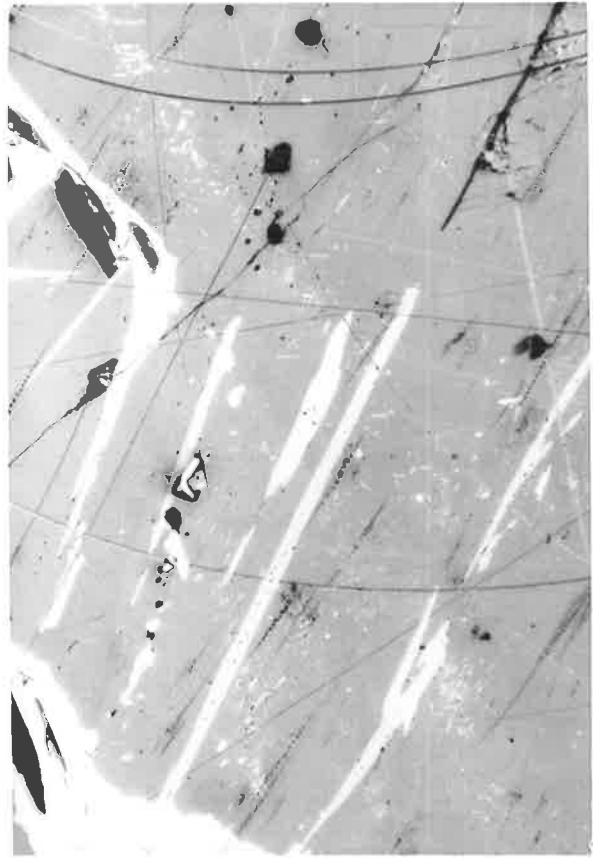
Two, possibly three generations of pyrite: Coarse and sub-hedral, fine and intersititial (vein-like) pyrite. The fine grained and intersititial pyrites may be of the same generation.

Sample No. 51/120.3, reflected light.

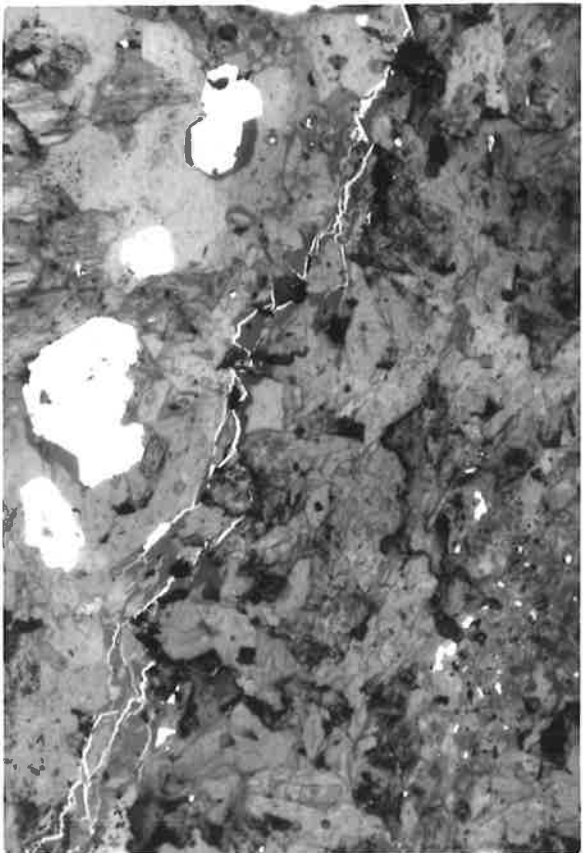
PLATE 4.2



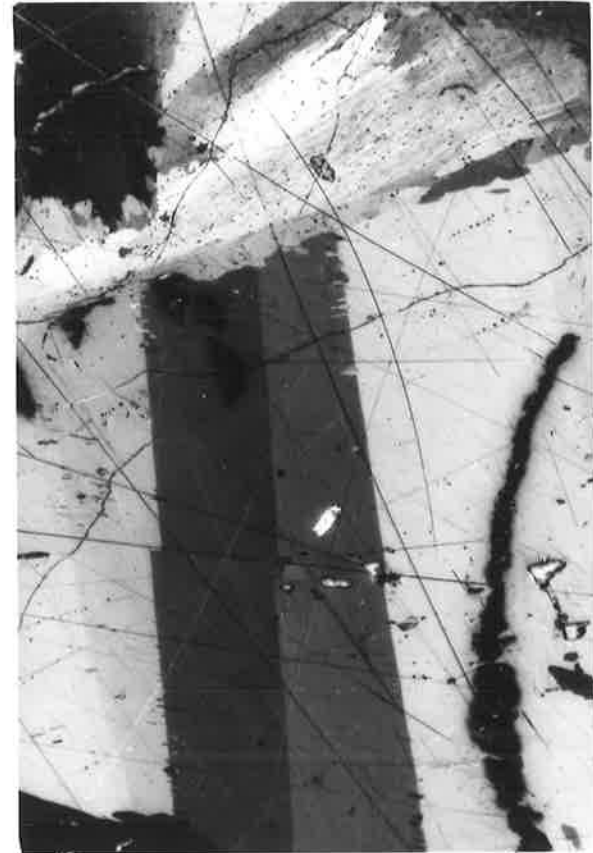
A | 0.125mm



B | 0.25mm



C | 0.25mm



D | 0.25mm

Plate 4.3A

Pyrite (Py) and chalcopyrite (Cpy) in epidote (Ep), and Rutile (R) in sphene (Spe). These are very common associations in the rocks at Mount Mulgine.

Sample No. 259/30.90, reflected light.

Plate 4.3D and 4.3B

(D) Hexagonal pyrrhotite (H Po) partially replaced by monoclinic pyrrhotite (M Po). The alteration is more intense where H Po is in contact with gangue. The M Po is shown by particles from a magnetic colloid. Compare with Plate 4.3B, taken before application of the magnetic colloid.

Sample No. 259/90.70, reflected light.

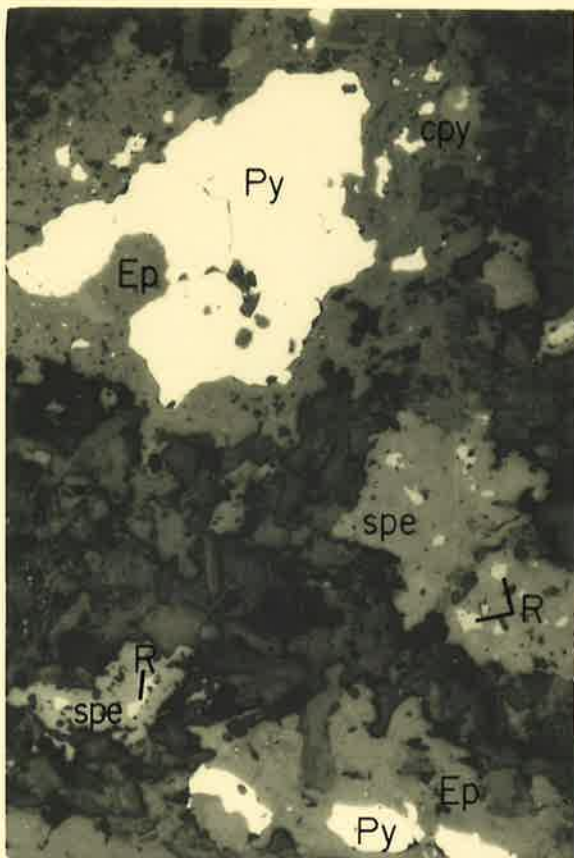
(B) Same as 4.3D before application of the magnetic colloid. The light grey mineral is sphalerite (Sp).

Plate 4.3C

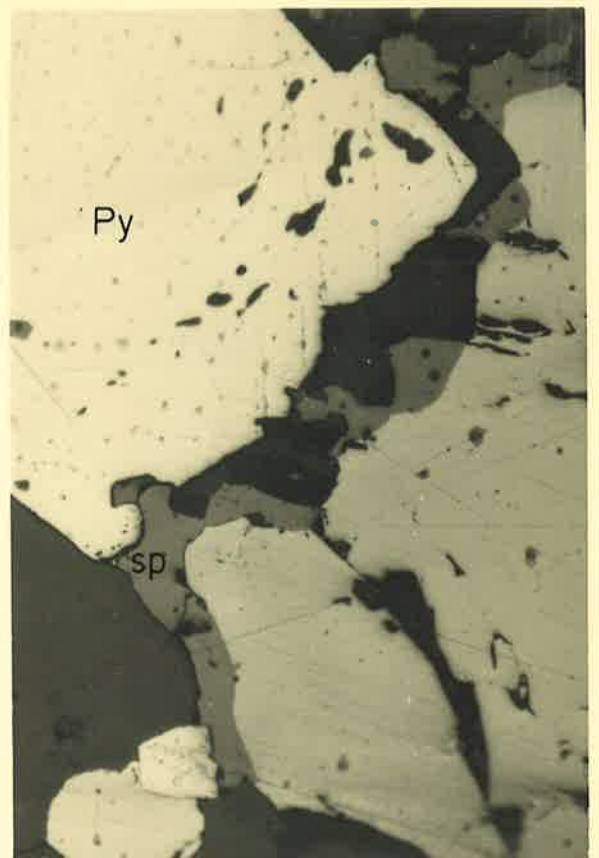
Arsenopyrite (Ars) partially replaced by tetrahedrite (T), and chalcopyrite (Cpy) partially replaced by tetrahedrite-tennantite (T-t).

Sample No. 259/123.32, oil immersion.

PLATE 4.3



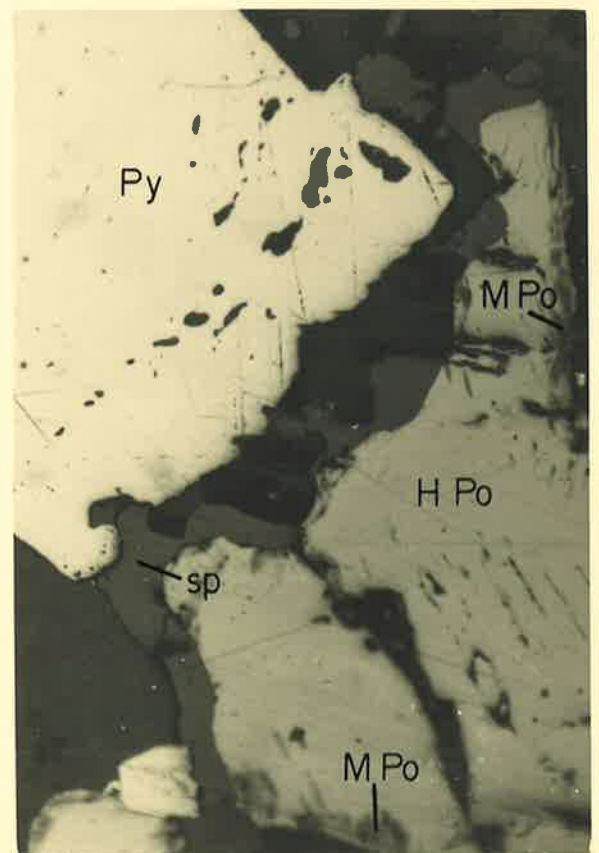
A 0.25mm



B 0.125mm



C 0.1mm



D 0.125mm

Plate 4.4A

Kobellite-tintinaite (K-t) partially replaced by tetrahedrite (T). Both minerals together with pyrite (Py) are within scheelite (Sh). Sample No. 264/116.27, reflected light.

Plate 4.4B

Pyrargyrite (Pr) associated with pyrite (Py) galenobismutite (Gb) and bismuth (Bi). The Bi is assumed to have replaced galenobismutite.

Sample No. 51/108.70, oil immersion.

Plate 4.4C

Overgrowth texture of pyrite (Py) euhedra into sphalerite (Sp) at the contact of the latter and scheelite (Sh). The coarse roundish dark grains are quartz.

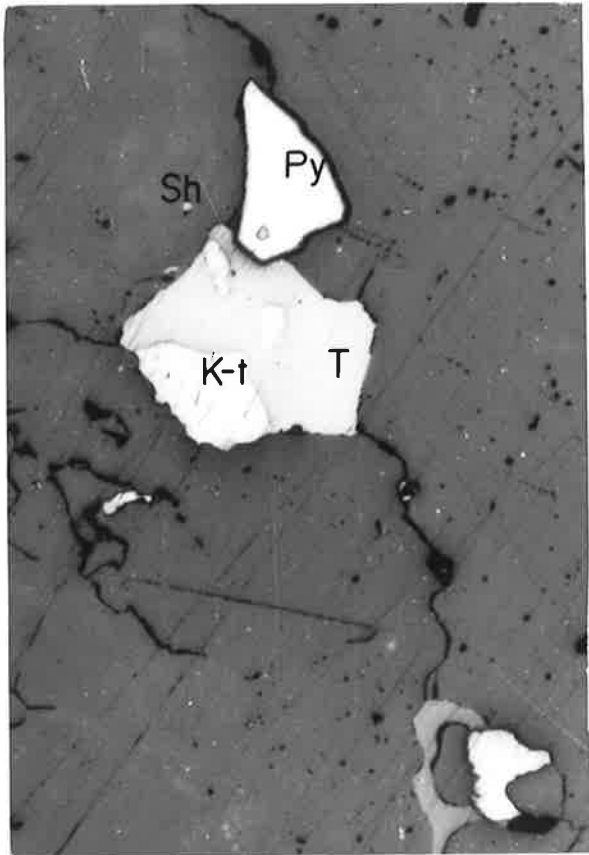
Sample No. 264/116.27, reflected light.

Plate 4.4D

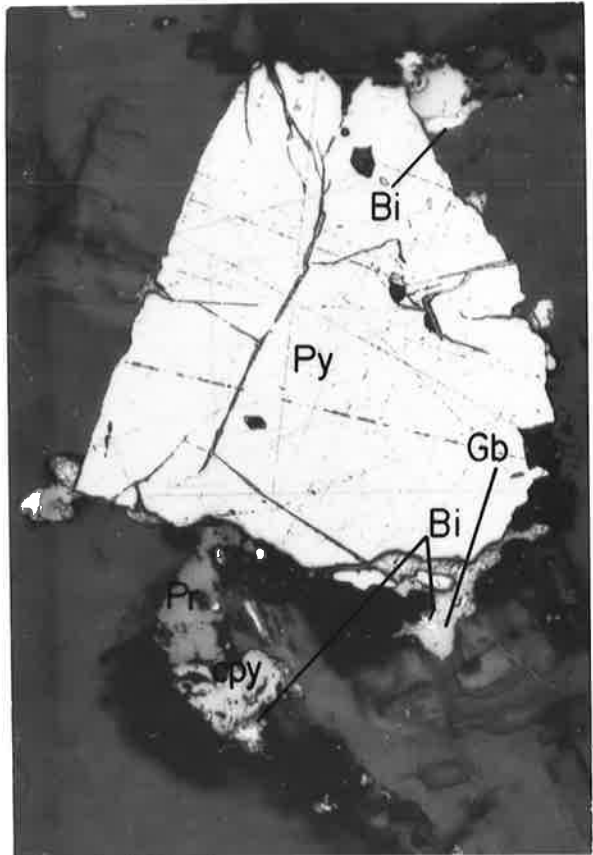
Marcasite (Mc) almost indistinguishable from pyrite (Py) which it is assumed to have replaced. The grey mineral is pyrrhotite (Po). It is also possible that both pyrite and marcasite (and possibly pyrrhotite) crystallized simultaneously.

Sample No. 259/90.70, reflected light.

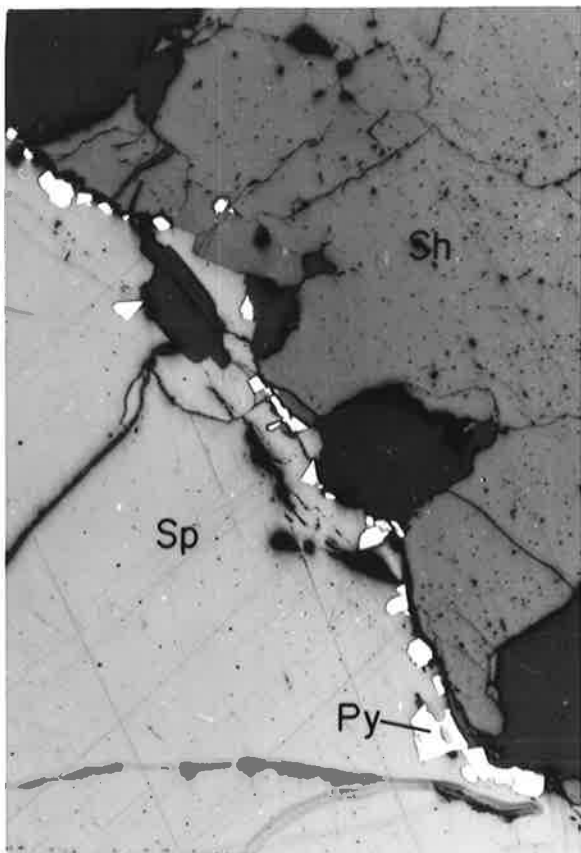
PLATE 4.4



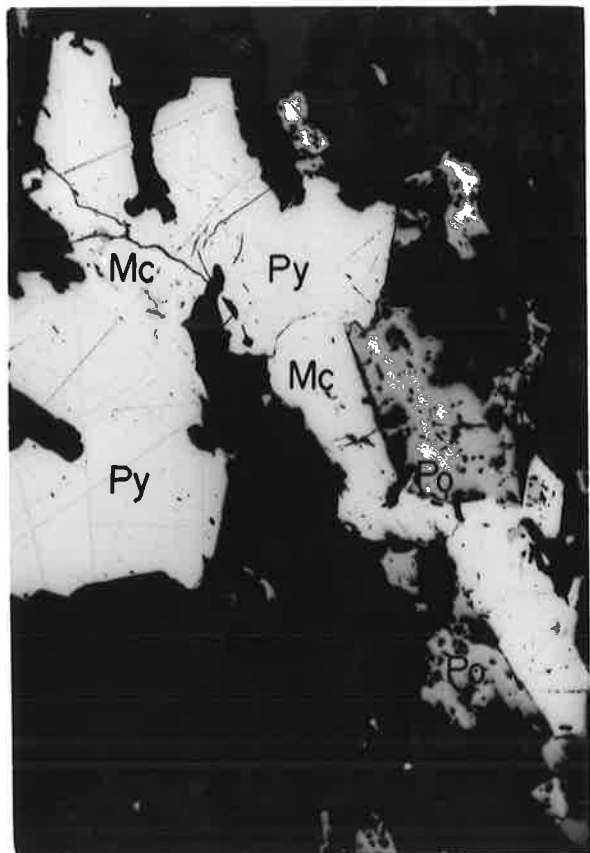
A 0.15mm



B 0.125mm



C 0.5mm



D 0.25mm

Plate 4.5A

A sphalerite (Sp) veinlet with smaller veinlets of chalcopyrite (Cpy) forming patterns. The sphalerite also has a large inclusion of pyrrhotite (Po) which is partly visible in the photomicrograph. The white grains outside the veinlet are also pyrrhotite.

Sample No. 259/115.77, reflected light.

Plate 4.5B

Rutile "needles" in an actinolite schist.

Sample No. 268/22.14, reflected light.

Plate 4.5C

Pyrite (Py) gersdorffite (Ger) and ullmannite (Ul) all looking very much alike in reflected light. Two small grains of each of pentlandite (Pt) and chalcopyrite (Cpy) can also be seen.

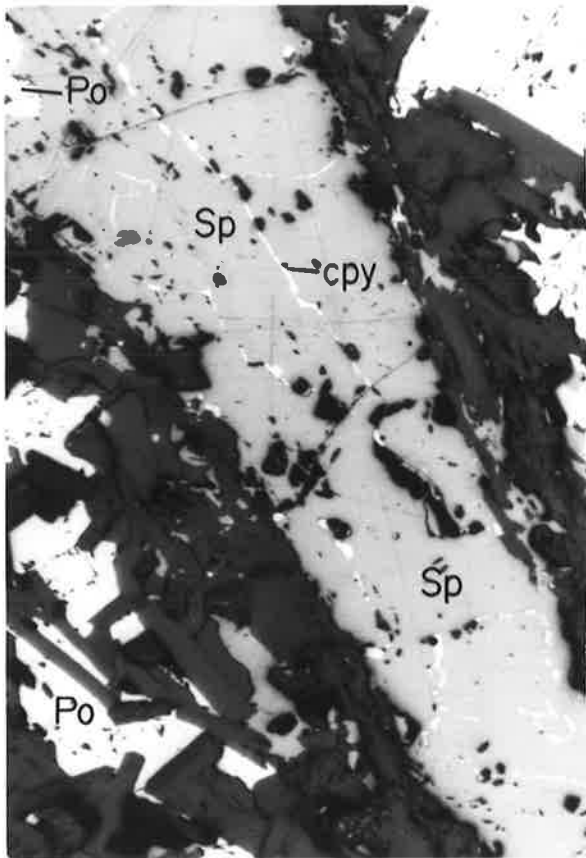
Sample No. 268/35.84, reflected light.

Plate 4.5D

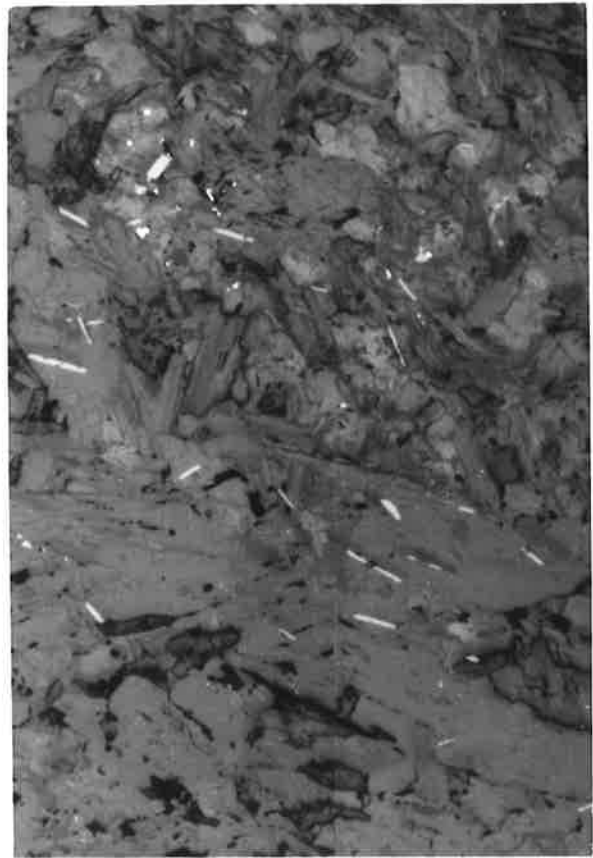
Brannerite?(Brn) associated with rutile (R). Note the round exsolution bodies (anatase?) within the suspected brannerite and also pyrite deposited along cleavage planes of muscovite.

Sample No. 232/~51, reflected light.

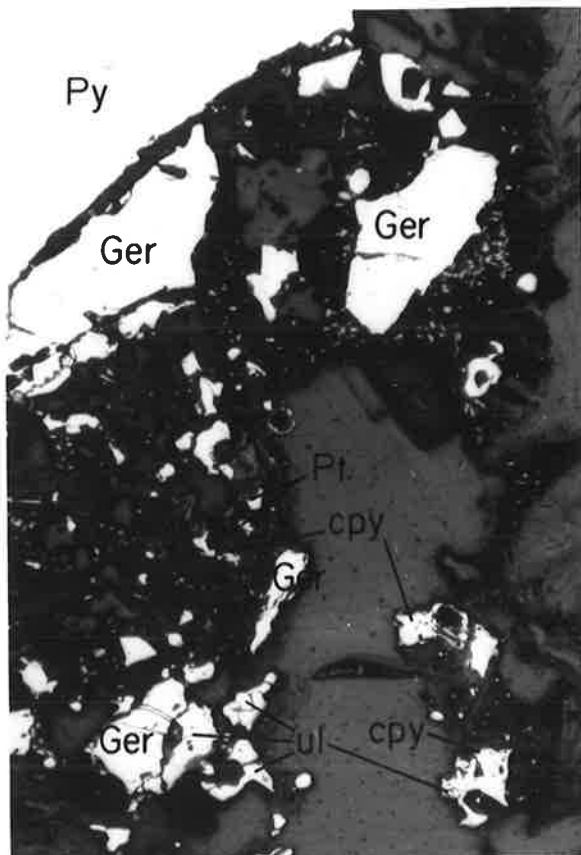
PLATE 4.5



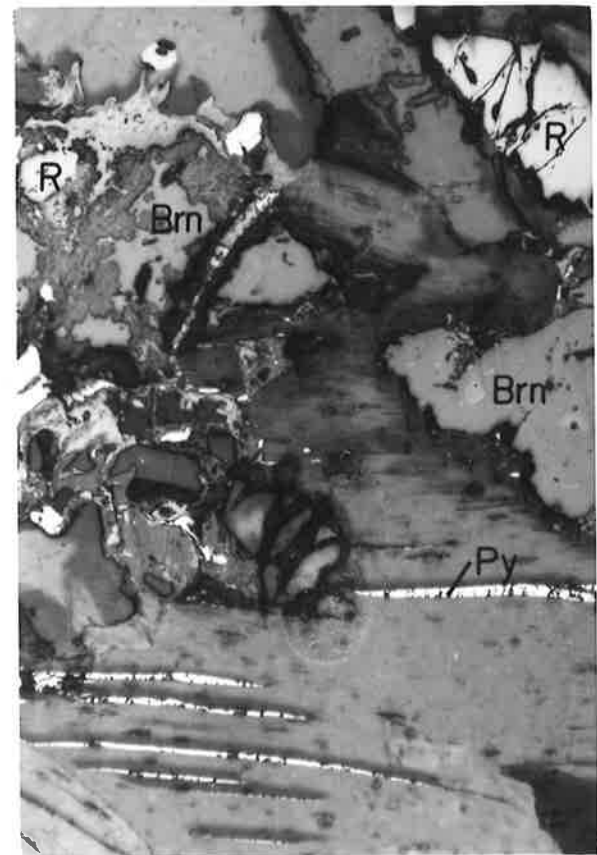
A 0.25mm



B 0.25mm



C 0.25mm



D 0.125mm

Plate 4.6A

Magnetite (Mt) replacing chromite (Chr). Note the dark "halo" looking like a ring between the two minerals. See text for explanation.

Sample No. 268/140.55, reflected light.

Plate 4.6B

Martitization - i.e., hematite (Hm) replacing magnetite (Mt).

Sample No. 259/22.10, oil immersion.

Plate 4.6C

Magnetite (Mt) side by side with rutile (R) which is very similar in appearance, in the same sphene (Spe) grains.

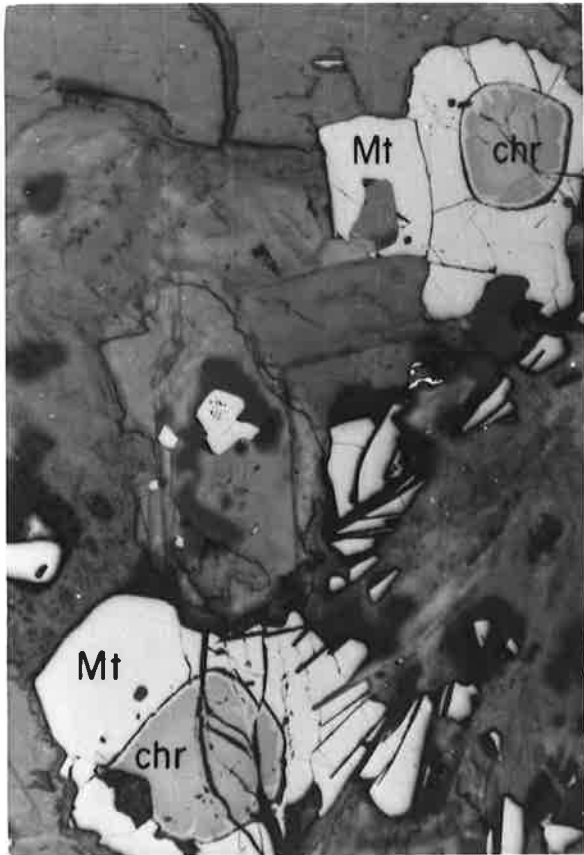
Plate 4.6D

Molybdenite (Mo) occurring along a quartz (Q) vein edge.

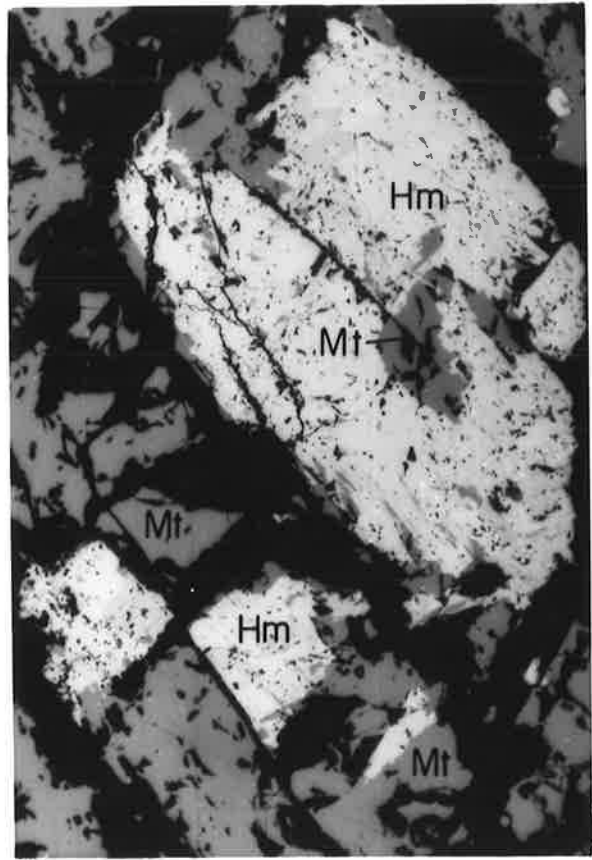
This is its typical form of occurrence.

Sample No. 268/123.66, reflected light.

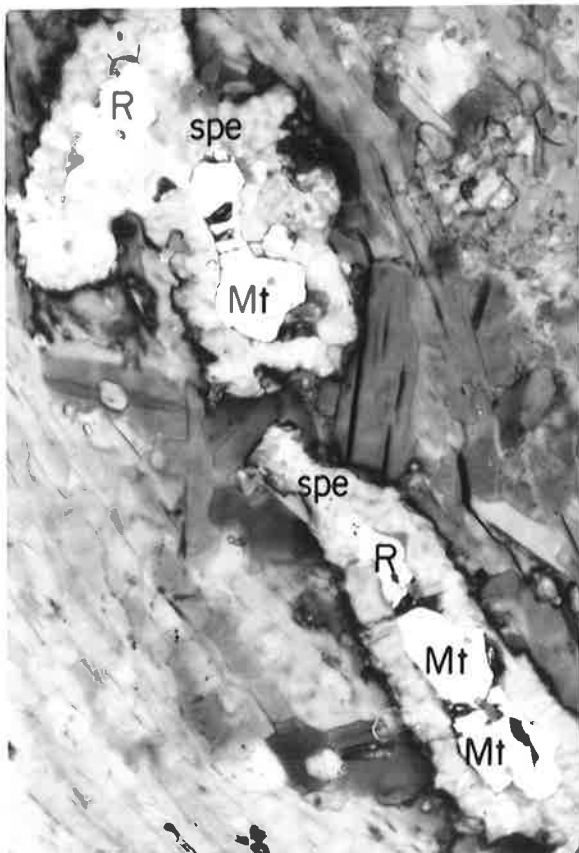
PLATE 4.6



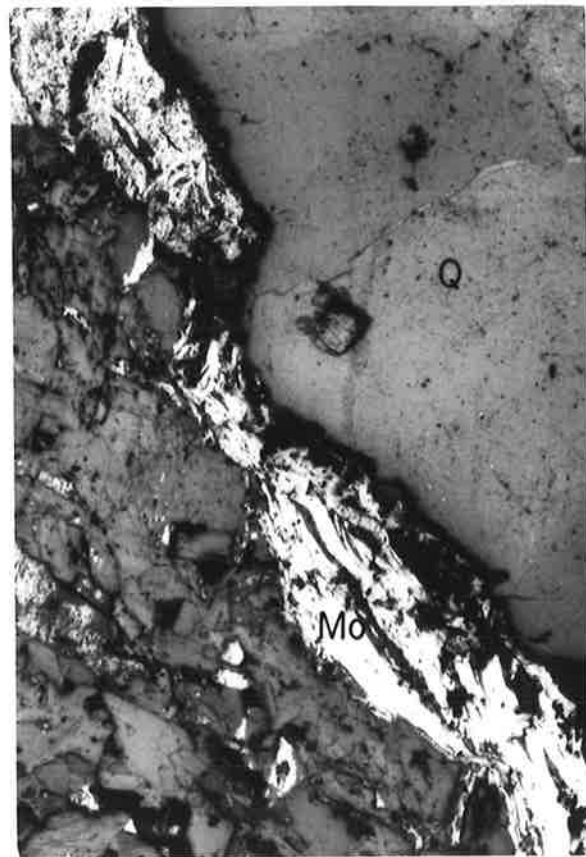
A | 0.5mm



B | 0.125mm



C | 0.125mm



D | 0.5mm

Plate 4.7A

Coarse pyroxene crystal (cream) partially replaced by tremolite (greenish yellow). The opaque is pyrite.
Sample No. 275/88.3, transmitted light.

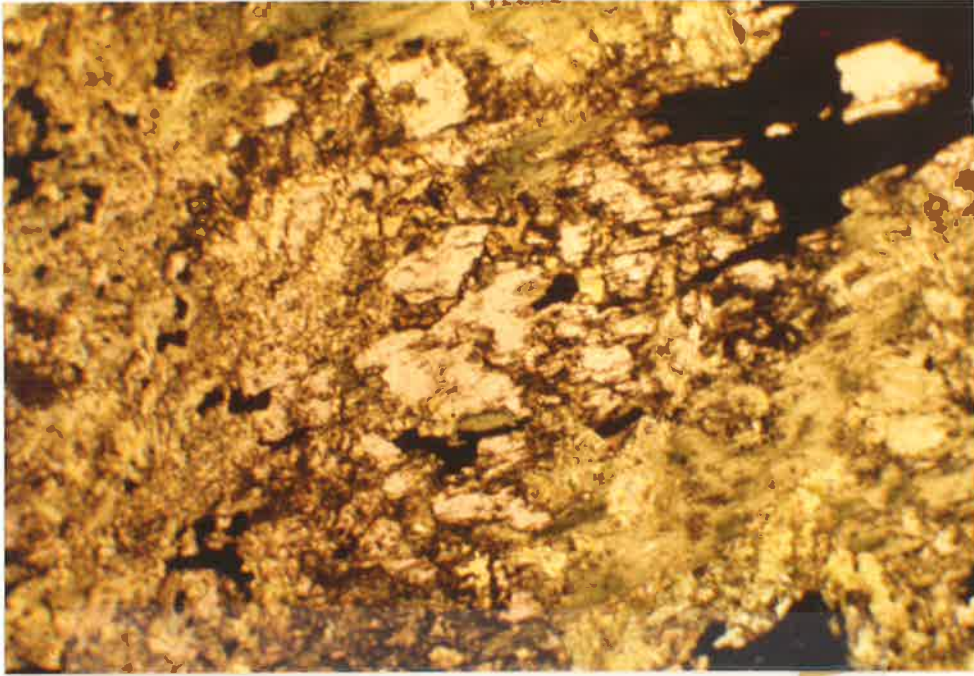
Plate 4.7B

Actinolitic hornblende (dark green) partially replaced by epidote (yellowish). The surrounding white-cream-brown mineral is quartz.
Sample No. 259/99.22, transmitted light.

Plate 4.7C

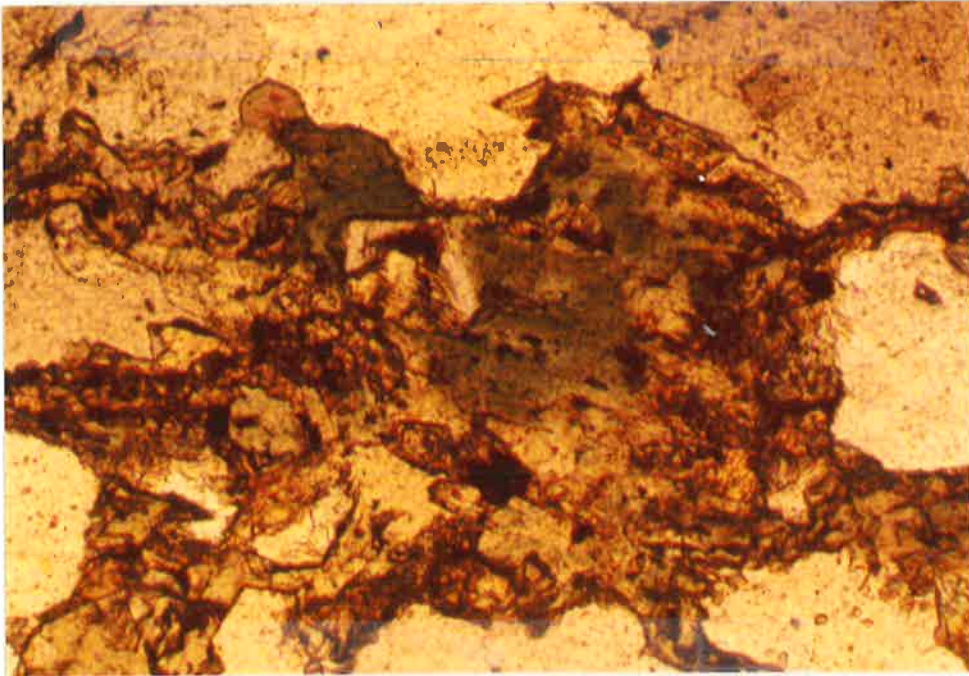
Stilbite crystals partly filling and projecting into a vug or cavity within an actinolite-biotite-epidote schist. The associated pink mineral is ankerite.
Sample No. 268/100.2.

PLATE 4.7



A

0.5 mm



B

0.25mm



C

Plate 4.8A

A field of view dominated by carbonates with a granular texture. The white vein that crosses the bottom right hand corner of the photomicrograph is also composed of carbonate.

Sample No. 276/106.60. Transmitted light, crossed polars.

Plate 4.8B

Folded biotite flakes partly chloritized especially along cleavage planes and also partly sericitized along the flakes' edges.

Sample No. 268/35.84. Transmitted light, crossed polars.

Plate 4.8C

Pyrrhotite(Po) with an angular appearance and magnetite(Mt) grains with "toothed" edges because the two minerals are associated with fibrous chrysotile and chlorite.

Sample No. 22/65.15, reflected light.

Plate 4.8D

Euhedral porphyroblasts of tremolite and pyrite (opaque) in a groundmass of fine talc crystals. Note that the tremolite has been partially replaced by talc along the margins and also in the interior of the crystals.

Sample No. 259/123.32. Transmitted light, partly crossed polars.

PLATE 4.8

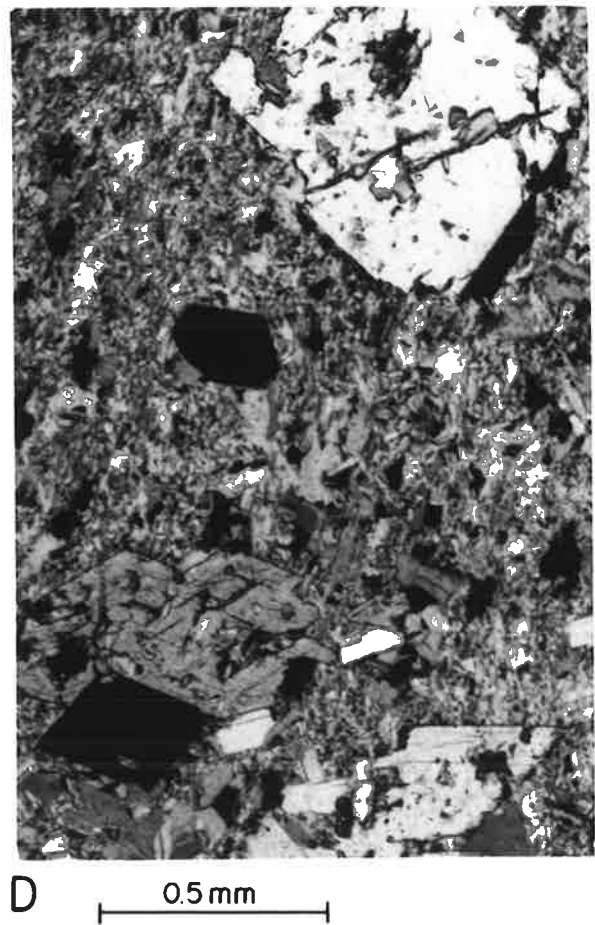
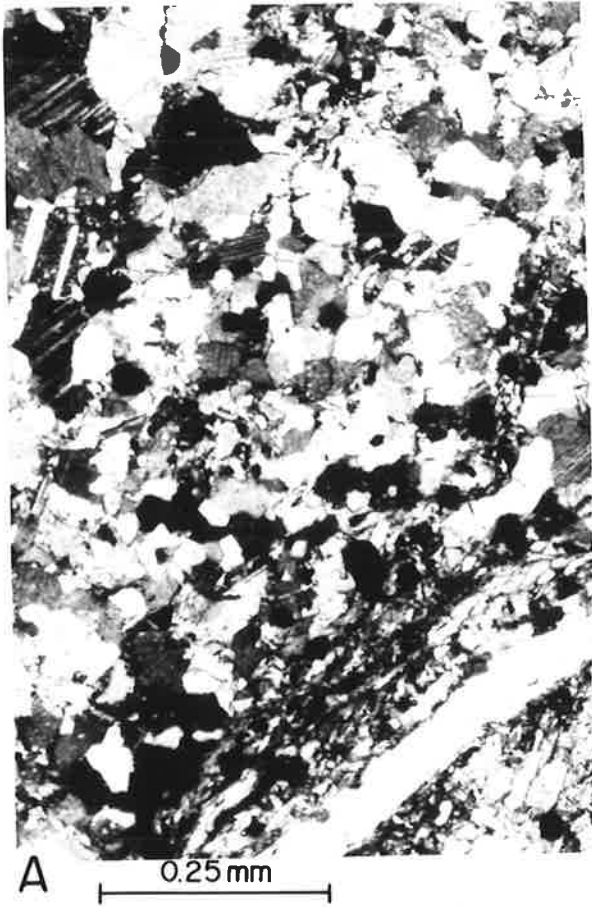


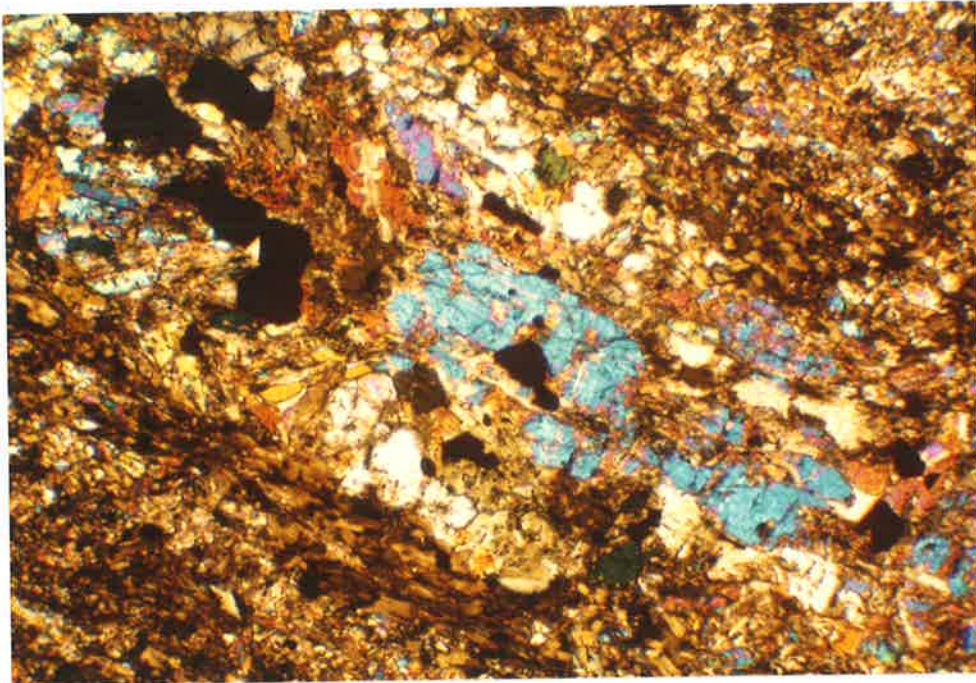
Plate 4.9A

A vein of coarse pyroxene (mainly blue and white) crystals bordered by a mass of fine chlorite crystals (dirty green).
Sample No. 276/116.05. Transmitted light, crossed polars.

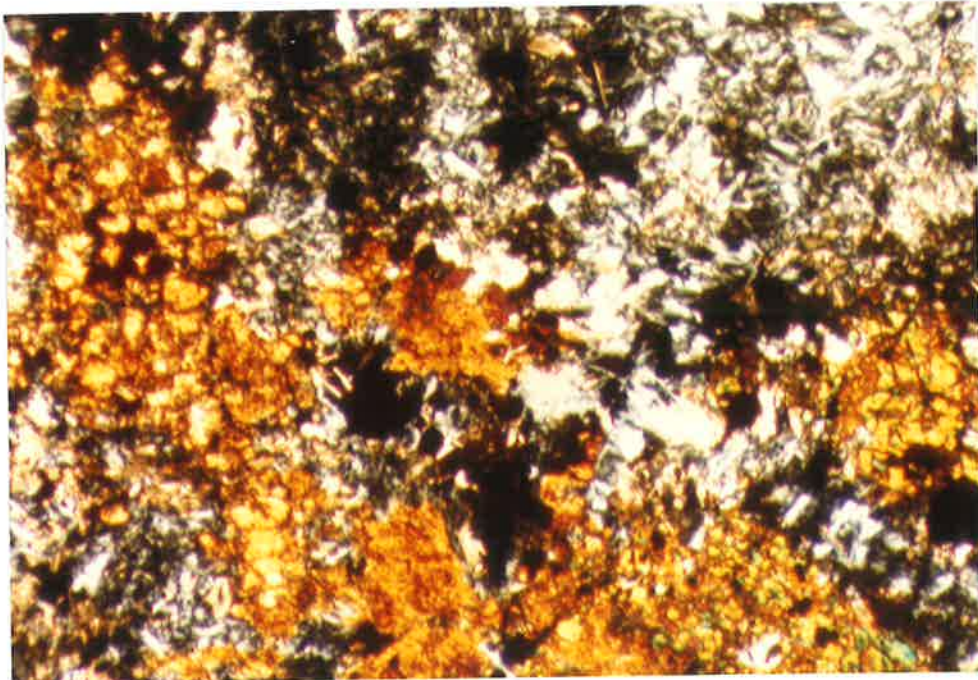
Plate 4.9B

Altered olivine (yellow) partly replaced by chrysotile and chlorite (white) and magnetite (black).
Sample No. 22/65.15. Transmitted light, crossed polars.

PLATE 4.9



A | 0.5mm



B | 0.5mm

tint. For some grains, there is a gradation from the "normal" brown colour at the edges to a core with a distinct purple tinge. In other samples still, the purple tinge is found only in grains in direct contact with pyrite. The variation in colour must be due to one or more foreign elements incorporated in the magnetite lattice; Ti is a possibility. The magnetite that has replaced chromite was analysed (while analysing the chromite) and found to contain as much as 5% Cr_2O_5 . This strengthens the view that it may be a replacement of chromite.

Evidence that the rocks were at one time under stress is also provided by magnetite grains which are sometimes heavily fractured. Gangue minerals have filled in the fractures.

Chromite, ilmenite and hematite

Chromite was identified in only two samples, where it occurs as round grains of about 0.3 mm diameter, surrounded by magnetite. At the margins of the round grains, where they are in contact with magnetite, there are features that appear as dark spots in reflected light. These dark spots form a discontinuous ring between the chromite and the magnetite (Plate 4.6A). The dark spots or "haloes" are due to radioactive inclusions (Uytenbogaardt and Burke, 1971). According to Ramdohr (1980), there may be no replacement between chromite and magnetite "in the strict sense", the magnetite may be an overgrowth over the chromite. However, on the inside of the dark "halo", "tongues" of magnetite can be seen to extend into the chromite in Plate 4.6A and so, it appears there was at least some replacement of the chromite by the magnetite.

Chromite was analysed to confirm its identity. The results are in Appendix 4. Against magnetite, chromite is distinctly darker in reflected light but on its own, confusion with magnetite is possible.

One of the difficult minerals that were identified is ilmenite. This mineral does not only resemble rutile in reflected light but it also has the same type of occurrence and grain size characteristics. It is also often found within sphene. Skaarup (1974) found ilmenite "extensively replaced by sphene" in scheelite skarns in N. Norway. Sphene replacing ilmenite was also observed in amphibolites from the Harts Range (Bowyer, 1982).

Rutile and ilmenite could be distinguished fairly confidently only when they were observed in the same field of view. Then ilmenite is seen to be duller and more strongly anisotropic. The "strong and abundant" internal reflections normally displayed by rutile (Uytenbogaardt and Burke, 1971) were not always observed, even in oil. A few of the ilmenite identifications were done qualitatively using the electron microprobe. Because of the dominance of rutile over ilmenite in the rocks studied, any grains of these minerals that

could not be more positively identified were invariably called rutile. Hence, rutile may be less than "very common" while magnetite may be more than "fairly common."

Martitization has already been briefly referred to. Apparently, all the hematite formed through this process (Plate 4.6B) which implies an increase in oxygen fugacity. Hematite was analysed qualitatively to ascertain its identity; its close association with magnetite helps in its determination. Some magnetite grains had fine inclusions of hematite which resemble exsolution bodies but are believed to be due to supergene alteration of the magnetite.

4.11 Copper minerals

Chalcopyrite is abundant in the rocks at Mount Mulgine but in most cases, it is volumetrically insignificant. In one sample of a quartz-muscovite/sericite rock, (22/71.70), chalcopyrite is the dominant opaque but even in this sample it constitutes less than 2 volume percent of the rock.

It occurs mostly as very fine grains (sometimes so fine that they can barely be recognized under the optical microscope) in all rock types. Where it occurs in association with coarse pyrrhotite and pyrite, the chalcopyrite is also relatively much coarser and grains may be several hundred micrometres across.

Because of its abundance, chalcopyrite is associated with virtually all minerals and has been observed in contact with many of them, especially pyrrhotite, tetrahedrite-tennantite, pyrite and sphalerite; to mention only a few opaques. Perhaps because of its small volume, chalcopyrite does not contain inclusions of many minerals. Magnetite is the only opaque mineral that was observed completely surrounded by chalcopyrite. However, chalcopyrite occurs as inclusions in many minerals including sphalerite, tetrahedrite, pyrrhotite, pyrite, sphene, epidote and fluorite.

Like rutile, chalcopyrite grains are sometimes in groups suggestive of a former associated mineral which has since been replaced. The mineral is, most likely, epidote because chalcopyrite grains were observed in epidote which looked weathered or leached (see page 64).

In many rocks, the distribution of chalcopyrite grains suggests that the mineral is an original accessory component. The association of fluorite and chalcopyrite, however, implies that the latter mineral was also late in the paragenesis (see Figure 4.1). Hence, there are at least two generations of the Cu-Fe sulphide.

Apart from tetrahedrite, which was described earlier (see page 46) and chalcopyrite, the other copper minerals observed are covellite and chalcocite which are believed to be supergene alteration products. Chrysocolla has

also been reported (Maitland, 1917). Covellite is found replacing chalcopyrite, and in most cases, it is being replaced by chalcocite. With its deep blue colour, strong anisotropism and association with chalcopyrite, covellite can hardly be mistaken for another mineral. The identity of chalcocite which, in places, has completely replaced covellite, is not as certain. The mineral was analysed but only qualitatively to confirm the identity. The so-called chalcocite may well be digenite or indeed some other low temperature Cu sulphide.

Chalcopyrite is sometimes found in fractures in more brittle minerals such as pyrite and pyrrhotite. This suggests that chalcopyrite may be later than these minerals. But inclusions of chalcopyrite in these same minerals show that it is at least as old as these minerals. The occurrence of chalcopyrite in fractures in syngenetic or later minerals is interpreted to be due to ductile flow and/or recrystallization during or after deformation. Softer minerals such as chalcopyrite may respond to stress by ductile flow while harder ones such as pyrite respond by brittle fracture (Craig and Vaughan, 1981). Also, the softer minerals recrystallize most readily after deformation; so that evidence for deformation is quickly obliterated.

4.12 Molybdenite

Molybdenite has continued to attract attention at Mount Mulgine since the early part of this century. It is the only Mo mineral that was recognized in this study but "a little ferrimolybdenite" has been observed in the more weathered greisens (Middleton, 1979). Molybdenite is a common mineral at Mount Mulgine and usually occurs along quartz vein edges (Plate 4.6D) or as thin foliae parallel to the schistosity of the host rocks, thus giving them a more fissile character. It has also been observed in fractures in quartz and even in scheelite. As discussed above for chalcopyrite, this need not imply that molybdenite is younger than the fractured minerals.

The mineral is generally fine although aggregates of its foliated crystals are often large enough to be identified megascopically. In reflected light, stibnite is the only mineral, among the minerals identified, that could possibly be confused with molybdenite; their colours are distinct enough to tell them apart - molybdenite being pinkish while stibnite is grey-white. It is also possible for the two minerals to be mistaken for each other in hand specimen. Their crystal forms and modes of occurrence can help in proper diagnosis.

According to Collins (1975) molybdenite at Mount Mulgine is the hexagonal -2H polymorph* and has a Re content of 11-16 ppm. The mineral was

*The molybdenite polymorphs 2H (hexagonal) and 3R (rhombohedral) cannot be distinguished under the optical microscope (Uytenbogaardt and Burke, 1971).

not analysed in this study.

Molybdenite is most commonly associated with the micas; notably muscovite. They are often interleaved and, in some samples, molybdenite has replaced muscovite. This replacement was also reported by Blatchford (1919). Molybdenite was also observed in close association with tremolite and may have replaced some of it. Although generally among the lesser opaques, molybdenite may be the dominant opaque as in sample 252/119.30, of a quartz-chlorite-sericite schist. In this sample, molybdenite "mimicks" the fibrous structure of chlorite.

4.13 Brannerite(?)

A dark grey U-Ti-Ca-minor Si oxide was found in sample 232/51.0 and it is believed to be brannerite $((U, Th, Ca)[(Ti, Fe)_2O_6])$. Unfortunately the electron microprobe analyses gave rather low totals which may be partly due to the presence of other elements (e.g., Th, Pb) which were not included in the analytical programme (see Appendix 4).

The appearance of the mineral and its close association with rutile supports the possibility that it is brannerite. It occurs in a quartz-muscovite rock and has, apparently, partially replaced rutile (Plate 4.5D). Brannerite(?) is rare at Mount Mulgine. In Plate 4.5D, some cloudy exsolved aggregates, which are too fine to be determined, can just be seen in the brannerite. They are assumed to be anatase since brannerite "practically always contains very small laths of pyrrhotite and exsolution or alteration bodies of anatase" (Uytenbogaardt and Burke, 1971, p.197).

4.14 Amphiboles

As a group, amphiboles are very common and they are the most important rock-forming minerals at Mount Mulgine. They constitute over 90 volume % of some of the rocks.

Only the Ca-bearing amphiboles, actinolite, hornblende and tremolite have been recognized in this study but the non-calcic amphiboles, anthophyllite and cummingtonite, which cannot be distinguished from each other under the optical microscope (Hurlbut and Klein, 1977) have been reported by Collins (1975) and Whittle (1977, 1978) respectively.

The amphiboles are best described as a group because they grade into each other both optically and chemically so that quite often, there is no unequivocal way of distinguishing between them. Strongly pleochroic blue or blue-green crystals were called hornblende while the name actinolite was used when the crystals were green or light green and not as strongly pleochroic. Tremolite is colourless or very light green. Clearly, this rather subjective way of distinguishing between amphiboles leaves much to be desired especially

Table 4.6 : Average hornblende analyses, sample No. 276/73.4

(concentrations in wt.%, n.d. means not detected).

Mean for analyses* 1, 2, and 3		Mean for analyses* 4, 5, 6 and 7	
SiO ₂	47.90		45.75
TiO ₂	0.41		0.43
Al ₂ O ₃	7.21		8.15
Cr ₂ O ₃	n.d.		n.d.
FeO**	14.94		16.03
MnO	0.52		0.51
MgO	12.86		11.82
CaO	12.31		12.38
Na ₂ O	0.82		0.88
K ₂ O	0.79		0.97
F	0.42		n.d.
Cl	0.02		0.06
P ₂ O ₅	n.d.		n.d.
NiO	n.d.		n.d.
Total	98.20		97.27
Number of ions***			
Si	7.069)		6.839)
Al	0.931) 8.000		1.161) 8.000
Al	0.324)		0.285)
Ti	0.046)		0.049)
Fe ³⁺	0.675) 5.000		0.730) 5.000
Mg ₂₊	2.830)		2.652)
Fe ²⁺	1.125)		1.284)
Fe ²⁺	0.044)		0.006)
Mn	0.065) 2.100		0.065) 2.074
Ca	1.890)		2.000)
Na	0.234) 0.382		0.256) 0.442
K	0.148)		0.186)

*The individual analyses are in Appendix 4.

**Total iron as FeO. See text for calculation of Fe³⁺ and Fe²⁺.

***Number of ions on the basis of 23 oxygens.

when the colours vary from blue, through green to colourless, which is the case at Mount Mulgine.

More definite amphibole identifications were made using their electron microprobe data, following the IMA system of nomenclature (Leake, 1978). Table 4.6 shows averages of hornblende analyses together with their calculated structural formulae. Fe^{2+} and Fe^{3+} contents were calculated by setting the total number of cations (excluding Na, Ca and K) equal to 13 and then adjusting the $\text{Fe}^{2+}/\text{Fe}^{3+}$ ratio until the total number of cations equalled 13. This method was recommended by Leake (1978) and gives the maximum possible Fe^{3+} (Stout, 1972). According to Figure 3 of Leake (1978), part of which is reproduced here as Figure 4.3, the hornblendes represented in Table 4.6 are both magnesio-hornblendes.

In hand specimen, amphibole crystals, especially tremolite crystals, have a shiny silky or fibrous appearance and a needle-like or tabular habit. The crystals are usually fine but they can be very coarse exceeding 1 cm in length and 2 mm in width. Coarse amphibole crystals or their relicts are sometimes found in a groundmass of very fine mica or talc and (usually) quartz, thus forming blastoporphyratic texture. More often, however, the coarse amphiboles, mostly tremolites, are clearly later and they should be called porphyroblasts. The tremolite porphyroblasts are almost always euhedral, displaying typical amphibole sections (Plate 4.8D) and are usually associated with pyrite megacrysts in the quartz-mica/talc groundmass.

The amphibole crystals commonly have rugged or irregular terminations where they appear to have broken down to microcrystalline talc or sericite. This replacement took place within the crystals as well. Epidote and carbonates have generally replaced the amphiboles and tremolite has replaced pyroxenes (Plate 4.7A). In some samples, biotite and phlogopite have also replaced the amphiboles.

Evidence that was interpreted to mean that there had been two amphibole generations was found in some samples; the earlier amphibole crystals are usually coarser and have obviously broken down while the later crystals are relatively unaltered and more euhedral. Fresh-looking amphiboles are usually found within veins or along the margins of quartz veins. This is especially so for actinolite (see Plate 2.1A) and it may have crystallized out of the solutions that formed the veins. Fluid inclusion leach analysis results indicate that the elements necessary for the formation of minerals such as actinolite and tremolite were available in the solutions. In sample 268/101, euhedral tremolite was observed in a fluorite vein, which strengthens the possibility that some amphiboles also crystallized from late solutions.

$\frac{\text{Mg}}{\text{Mg}+\text{Fe}^{2+}}$		$(\text{Na}+\text{K})_A < 0.50, \text{Ti} < 0.5$								
8.00	7.75	7.5	7.25	7.00	Si	6.75	6.50	6.25	6.00	5.75
tremolite	Tr.Hb				Tsch.	Tschermakite				
Actinolite	Ac.Hb	Magnesio-hornblende			Hb	(Alumino-Tsch.)				
Ferro-Actinolite	Ferro-Ac.Hb	Ferro-hornblende			Ferro-Tsch hb.	Ferro-Tschermakite				

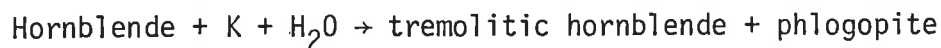
Figure 4.3. Classification of calcic amphiboles, in which $(\text{Ca}+\text{Na})_B \geq 1.34, \text{Na}_B < 0.67$.
(After Leake, 1978).

Abbreviations:

- Tr - Tremolitic
- Ac - Actinolitic
- Hb - Hornblende
- Tsch - Tschermakite or Tschermakitic.

The strongly schistose nature of some of the rocks is due to the alignment of amphibole crystals during dynamic metamorphism. In other rocks, however, the amphiboles are apparently randomly oriented, indicating that static recrystallization (metamorphism) also occurred.

Compositional zoning between actinolite and hornblende, which has long been recognized and is commonly reported in the literature (e.g., Cooper and Lovering, 1970; Brady, 1974; Laird and Albee, 1981) was not observed in this study. However, there is a general tendency for actinolite (or hornblende) to have lighter coloured (tremolitic?) rims or marginal patches which may be due to metasomatism represented by the following schematic reaction suggested by Thomson et al. (1981).



Lack of any obvious actinolite-hornblende zoning may mean that the pressure was low (Hynes, 1982).

4.15 Epidote

One of the easier minerals to tell under the microscope, among those identified, is epidote, mainly because it is usually yellow or yellowish in colour and shows uneven spectral colours between crossed polars (Plate 4.1B). It may also be colourless or greenish.

Epidote is a very common mineral at Mount Mulgine and in some samples has replaced plagioclase, thus providing evidence for retrograde metamorphism. It also appears to have replaced amphiboles (actinolite) - Plate 4.7B. In many samples, epidote looks corroded and all that remains is a dark-brown sponge-like material. The characteristic bright colours of epidote under crossed polars can sometimes still be seen in this material.

Epidote is usually closely associated with opaque minerals, notably pyrite, chalcopyrite and pyrrhotite. It often rims pyrite grains (see Plate 4.3A) and chalcopyrite grains have been observed in relicts of the mineral. Carbonates, phlogopite and scheelite have replaced (or appear to have replaced) epidote.

In quartz veins or along/near their margins, epidote looks relatively fresh and may have been recrystallized or even deposited from the solutions that passed through the fissures now occupied by the veins. Some small veins, entirely filled with epidote have been observed. Some rocks owe their banding partly to epidote because it sometimes forms bands with or without other transparent minerals but usually with opaques.

4.16 Silica minerals

With the possible exception of pyrite, quartz is the most frequently observed mineral at Mount Mulgine. It is abundant.

One thing which is immediately noticeable about quartz is its mode of occurrence. It may occur as microcrystalline grains, more or less homogeneously mixed with similar-sized crystals of mica or micaceous minerals, forming part of the groundmass in porphyroblastic- (or blastoporphyratic-) textured rocks or it may occur as relatively coarser grains, randomly mixed with other rock constituents. The bulk of the quartz, however, occurs in veins, veinlets, pockets or lenses in which it is usually the main constituent if not the only one. Quartz is, therefore, usually identifiable in hand specimen but, on the other extreme, it may be cryptocrystalline.

Where quartz occurs in veins, pockets or lenses, it is, almost without exception, much coarser than that elsewhere in the same rock. Also, other minerals which occur associated with the coarse quartz, occurring either within the above structures or at their margins, are coarser (see Plate 2.1A). Quartz veining is considered to be an important petrographic feature and is covered in

a little more detail in Chapter 2.

There is not much doubt that vein quartz is epigenetic. Even the pockets of quartz grains (called "centres of silicification" by Whittle, 1977, 1978) are considered to have the same origin; although they may be removed from quartz veins. Most of the greenstones would have had little or no quartz originally.

Quartz is closely associated with mineralization and other minerals like fluorite or carbonates which often occur in veins and may be considered as part of the mineralization. The occurrence of mineralized and barren quartz veins, of folded or boudinaged and unstructured (straight) veins, and of concordant and cross-cutting veins, all imply that there were several quartz generations and this is supported by fluid inclusion studies.

In sample 251/139.4 a folded quartz vein has been fractured and mica minerals have been forced into the fractures (see Plate 2.1B). The fracturing indicates that the "meandering-type" veins are so because they have been compressed and not because of some other reason, like being formed in a sinuous fracture. In another sample (22/71.7) quartz shows twinning and the twin crystals show biaxial interference figures. The twinning may also be due to stress.

Quartz is mostly colourless with a lot of relatively large fluid inclusions. Milky quartz, with much smaller and more numerous fluid inclusions is also present.

Another form of silica, which has been called cherty silica, is also present but it is sparse. It has been observed in association with molybdenite and also in colloform textures. It is dark under crossed polars and has a fibrous radiating structure. Where associated with molybdenite, cherty silica is found in interfolia spaces and in the colloform textures it occurs as bands and as very thin parallel laminations (see Plate 2.3B). Each of these laminations or bands would probably represent a depositional episode or a temporary break in deposition.

4.17 Carbonates

Carbonates are common in the rocks at Mount Mulgine. They are usually found in the obviously hydrothermally altered rocks, often having replaced other minerals. Pyroxenes, amphiboles (especially tremolite) and epidote have been replaced by the carbonates.

Qualitative electron microprobe analyses of the carbonates indicate that the varieties present are calcite, ankerite and a Mn-Ca carbonate (kutnohorite?). Carbonates are late minerals and they have been observed as cavity fillings, associated with stilbite (Plate 4.7C) and also in veins.

Sometimes, the mode of occurrence of the carbonates is the same as that which is typical of quartz grains in these rocks - i.e. the carbonates may occur in veins, veinlets or pockets and even with a granular-type texture (Plate 4.8A). They have also been observed as fracture fillings.

Carbonates occur in almost all rock types and have been observed even in the BIF. However, they seem to be more associated with the less Ca-rich lithologies, at least in the greenstones studied. Fluid inclusion studies show that the fluids were carbon-dioxide-rich. This would explain the formation of the carbonates but the source of the carbon dioxide remains a problem. De-gassing of the mantle (Professor P. Ypma, pers. comm.) is a possibility.

4.18 Feldspars

The most commonly observed feldspars in the rocks at Mount Mulgine are K-feldspars. Plagioclase feldspars also occur but they have largely been epidotized, sericitized or saussuritized. The type of plagioclase was not determined because no unaltered crystals suitable for analysis were observed. However, Collins (1975) reports that the anorthite content of the plagioclase is more than 20%. Plagioclase feldspars is fairly common.

The low temperature polymorphs of KAlSi_3O_8 , microcline and adularia, are more frequently observed in these rocks. Adularia was observed in only two samples and is therefore rare. Veins of adularia (associated with carbonates or fluorite) form "tributaries" to larger quartz veins and there is not much doubt that the quartz and adularia veins had the same origin. Microcline, which is also fairly common, looks fresh and it is commonly associated with quartz. Some may be a result of K-feldspathization during hydrothermal metasomatism.

Some feldspar electron microprobe analyses are included in Appendix 4.

4.19 Micas

Like amphiboles, the mica minerals grade into each other and the distinction between the various members of the group, mainly based on colour, is not always unambiguous, so they are better treated as a group. Biotite, phlogopite, muscovite (sericite), damourite and zinnwaldite all occur in the rocks at Mount Mulgine. The latter two micas have been reported by Whittle (1977, 1978) and were not identified in this study.

As a group, micas are abundant and they are generally fine and found in all rocks. Muscovite is more common in the acidic rocks, biotite usually occurs in the relatively Fe-rich rocks while phlogopite is generally found in the rocks high in both Ca and Mg.

Biotite has, in most cases, been partially replaced by chlorite. In one sample, it also appeared to have been replaced by muscovite. The biotite

varies in colour from dirty green, through brown to almost red. Biotite flakes may be clustered together in a groundmass of sericite. Biotite imparts a dark brown colour to the rocks and, when its flakes are clustered together, the rocks have a spotted appearance.

Folded or crumpled biotite flakes (Plate 4.8B) provide more evidence that the rocks were under stress. Biotite may be confined to quartz veins or their environs; when in quartz veins, its crystals are usually aligned along the vein margin. Biotite flakes are sometimes found wrapped around pockets of quartz grains or around large quartz grains, giving the impression that the quartz was intruded into the biotite. However, this is more likely to be a result of deformation of a biotite-quartz assemblage. Some biotite flakes have clearly been fragmented or disintegrated into some cryptocrystalline sericite-like aggregates (see Plate 4.8B).

Phlogopite seems to be a generally late or secondary mineral. In some samples, it had, or appeared to have, replaced epidote, feldspar and tremolite or actinolite. Phlogopitization is believed to be part of the hydrothermal alteration caused by K-rich fluids.

Muscovite flakes are sometimes found as inclusions within the coarse pyrrhotite and pyrite grains and molybdenite has been observed replacing muscovite (e.g., Collins, 1975). Hence, muscovite was, generally, earlier than mineralization. The Si^{+4} contents of muscovites (phengites) were used to estimate the pressure of formation (see page 94). During the microprobe analysis of muscovites, it was found that some are interlayered with chlorite. The mica (muscovite and biotite) analyses are in Appendix 4.

Veins of muscovite were observed but sericite veins are more common. Sericite is common in the rocks at Mount Mulgine but its distinction from other fine mica or micaceous minerals is not always certain. It is usually found in the groundmass mixed with very fine quartz grains.

4.20 Talc, chlorite and serpentine

Talc is fairly common in the rocks at Mount Mulgine. It is possible that it occurs more frequently than apparent in this study because its distinction from muscovite was mainly based on the occurrence of other Mg-rich minerals in the same sample. It is commonly microcrystalline and often forms the groundmass (together with very fine-grained quartz) for tremolite and other porphyroblasts. Tremolite porphyroblasts are often found breaking down to talc in their cores or along the edges (Plate 4.8D).

Chlorite is common at Mount Mulgine and occurs as fine scaly or flake-like crystals which are usually clustered together. It has not been observed in the Ca-Mg-rich (Fe-poor) rocks. Chlorite is often found having replaced

Table 4.7 : Chlorite and Serpentine analyses

concentrations in wt.%, n.d. means not detected.

Sample No.	CHLORITES		SERPENTINE(CHRYSOTILE)	
	276/73.4	268/149.90	22/65.15	
Analysis No.	3	1	1	3
SiO ₂	24.38	29.07	41.23	43.15
TiO ₂	n.d.	n.d.	2.77	n.d.
Al ₂ O ₃	19.32	17.17	1.01	0.90
Cr ₂ O ₃	0.23	n.d.	n.d.	n.d.
FeO	33.51	16.25	5.42	3.15
MnO	0.52	0.42	0.52	0.12
MgO	7.95	21.78	36.22	37.92
CaO	n.d.	n.d.	n.d.	n.d.
Na ₂ O	0.03	0.03	0.02	0.02
K ₂ O	n.d.	n.d.	n.d.	n.d.
F	n.d.	0.41	0.71	0.62
Cl	n.d.	0.06	0.03	0.01
P ₂ O ₅	n.d.	0.15	n.d.	n.d.
NiO	n.d.	n.d.	n.d.	n.d.
Total	85.94	85.34	87.93	85.89
O ≡ F*			0.30	0.26
			87.63	85.63

*See 1 under "explanation of notations in the table of analytical data", Appendix 4.

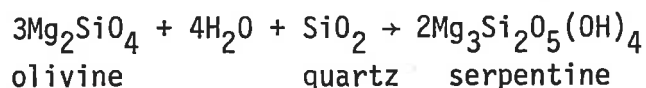
biotite or phlogopite but it is not always clear whether this replacement is a retrograde effect or is due to hydrothermal alteration. Chlorite appears to have been sericitised in some samples.

Small veins of chlorite have been observed but, more often, chlorite flakes occur as a lining along quartz or pyroxene vein margins (Plate 4.9A). Muscovite, chrysolite and sphene are, in some samples, closely associated with chlorite and appear intergrown with it.

Some analyses of chlorite are included in Table 4.7; more analyses are in Appendix 4. Table 4.7 shows that chlorites at Mount Mulgine may vary widely in their compositions, especially in their Mg and Fe contents. In this case, the differences in their compositions are mainly due to the fact that the chlorite in sample 268/149.90 is a hydrothermal alteration product of phlogopite. This sample contains other late minerals such as carbonates, fluorite and adularia and so, there is no doubt that the rock was hydrothermally altered. The chlorite in sample 276/73.4 appears to have formed before hydrothermal alteration. Biotite is present in the same sample but it was not observed in contact with the chlorite. The assemblage quartz + chlorite (and the absence of cordierite) implies that the temperature never exceeded about 550°C, assuming a pressure (P_{H_2O}) of up to 5kb. Otherwise, the following reaction would have taken place: chlorite + quartz → talc + cordierite + vapour (Fawcett and Yoder, 1966).

Serpentine (variety chrysotile) was identified only in samples 22/65.15 and 71/35.5 and is therefore rare. It occurs associated with altered olivine, talc, chlorite, tremolite, pyrrhotite and magnetite. It has clearly replaced the altered olivine and, in places, it also appears to have replaced chlorite and tremolite. The pyrrhotite associated with chrysotile has an angular appearance because of the asbestiform nature of the latter mineral (Plate 4.8C). The magnetite grains have jagged outlines where they have partly followed the fibrous form of the chrysotile. The form of these opaques implies that they formed later or at the same time as the chrysotile.

The reaction that could have taken place to produce serpentine and magnetite from olivine has already been given (page 57). Since no quartz was observed in the samples containing chrysotile, it is possible that the following reaction also took place.



Chrysotile analyses are included in Table 4.19.

4.21 Pyroxenes

From the chemical composition (Table 4.8) and properties, the pyroxene analysed is diopside. However, since other pyroxenes are known to occur at Mount Mulgine (e.g., the orthopyroxene enstatite has been reported - Whittle, 1977, 1978) the general name "pyroxenes" is preferable.

Table 4.8: Pyroxene (Diopside) analyses

Sample No.	concentrations in wt.%		
	268/149.90		268/123.66
Analysis No.	1	2	2
SiO ₂	53.85	54.68	54.09
Al ₂ O ₃	1.17	0.24	0.65
Cr ₂ O ₃	-	-	0.37
FeO	3.78	2.98	5.46
MnO	1.16	0.96	0.25
MgO	14.81	16.34	14.47
CaO	25.27	25.67	25.55
Total	100.04	100.87	100.84

Pyroxenes are fairly common and they usually occur segregated in one part of the rock samples. Only in sample 268/38.05 were pyroxene crystals observed interwoven with sheaths of biotite flakes. In some banded rocks, pyroxenes have been observed forming entire bands bordered by biotite flakes. The pyroxene crystals are usually relatively coarse, sometimes exceeding 1 mm in length. As Plate 4.9A shows, pyroxenes may form veins with clusters of chlorite crystals all along the vein margins.

Pyroxenes have clearly been replaced by actinolite and/or hornblende (see Plate 4.7A). This replacement is a retrograde reaction but this should not be interpreted to mean that the pyroxenes formed during prograde metamorphism. Most of the pyroxenes are believed to be original constituents of the rocks in which they occur (see page 21). Pyroxenes have also been carbonatised and in some samples, phlogopite seems to have replaced them.

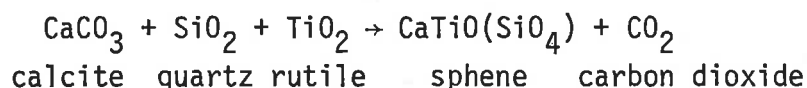
Because of the common occurrence of tremolite in the rocks at Mount Mulgine, some pyroxenes may be easily overlooked as tremolite if extinction angles and optic signs are not determined.

4.22 Sphene

After pyrite, quartz and chalcopyrite, sphene is the fourth most frequently observed mineral at Mount Mulgine. It is very common and occurs in all rock types. Although grains of sphene exceeding 1 mm have been observed, the mineral usually occurs as fine grains, generally less than 0.25 mm.

The sphene grains occur disseminated, sometimes in clusters, throughout the rocks. Veinlets of sphene were also observed. The grains are brown in colour and often have fine pisolitic-type texture. In some rocks, sphene grains have been weathered or leached leaving a dark brown sponge-like mass very similar to and often indistinguishable from that left after the destruction of epidote. The sometimes striking resemblance between epidote, scheelite and sphene has already been mentioned (page 45).

More often than not, sphene has inclusions of rutile or ilmenite or magnetite grains. Of these inclusions, rutile is the most common. Pyrite and chalcopyrite grains were also observed in sphene but this association is not common. Rutile and magnetite may occur in the same grain of sphene (Plate 4.6C). Laird and Albee (1981a) also observed rutile and sometimes ilmenite as cores within sphene. These authors proposed that the following reaction might have taken place.



This is most likely to be the type of reaction that occurred at Mount Mulgine. Excess rutile would remain within the sphene. If ilmenite instead of rutile took part in the above reaction, the Fe and "excess" oxygen from the ilmenite would perhaps combine to form magnetite. Since carbonates are late minerals in the rocks at Mount Mulgine and they (carbonates) are not so common, it is unlikely that the simple reaction represented by the above equation took place. The Ca and Si may have come from a silicate mineral instead of calcite and quartz.

Sphene is also closely associated with chlorite and sometimes assumes the fibrous structure of chlorite, where it grew following or along cleavage planes of chlorite. A few analyses of sphene are included in Appendix 4.

4.23 Other minerals (apatite, fluorite, stilbite, altered olivine, garnets).

Apatite

As would be expected, apatite is found only in those rocks which are relatively rich in P. It is a fairly common mineral at Mount Mulgine.

Usually, two or three fine grains of the mineral will be found in each of those samples where it occurs. The apatite grains may be several mm across and they can be easily seen fluorescing a clear yellow colour in short wavelength UV light. In a muscovite schist sample taken from the Hill deposit, apatite constitutes about 10% of the rock. In the Trench samples, it constitutes less than 1 volume % of the rocks.

Apatite does not appear to be closely associated with any particular minerals but in samples 51/122.8 and 259/108.92 it is associated with molybdenite. This, and the fact that apatite was also observed in an actinolite-carbonate vein implies that apatite might also have formed as one of the later minerals.

Two analyses of apatite are included in Appendix 4 and, from its composition, the mineral is the common variety fluor-apatite.

Fluorite

One of the last minerals to crystallize at Mount Mulgine, possibly the very last, was fluorite. This is indicated by its mode of occurrence, its close association with late minerals and the low salinity and homogenization temperatures of fluid inclusions found in it (see Chapter 5).

Fluorite is common and is usually found in veins. It is also intersititial and was observed along cleavage planes of muscovite. Its closest associates are other vein minerals such as quartz and carbonates. Opaques are usually found within the fluorite and it is believed that they were deposited at about the same time. Pyrite and chalcopyrite are the opaques commonly found in fluorite. The fluorite is colourless to purple and it does not fluoresce in UV light. In sample 268/101, fluorite is not truly isotropic but shows a biaxial negative figure. This is thought to be another indicator of strain.

Stilbite

Crystals of stilbite (Plate 4.7C) were observed growing out into a vug in sample 268/100.2. In this sample, they are associated with pink ankerite. The crystals are a few mm long and some are twinned (interpenetrant twinning). The composition of the stilbite is in Appendix 4 and as it stands, it is closer to that of heulandite ($\text{CaAl}_2\text{Si}_7\text{O}_{18} \cdot 6\text{H}_2\text{O}$) which has one molecule of water less than stilbite ($\text{CaAl}_2\text{Si}_7\text{O}_{18} \cdot 7\text{H}_2\text{O}$). However, the crystal form of stilbite is distinctive.

Stilbite was observed only in the above-mentioned sample and is therefore rare. Its occurrence clearly implies that the solutions from which

it was deposited must have contained Al, although this element was not detected in the fluid inclusion leach analyses (Chapter 5). These analyses showed that Ca and Fe were abundant in the mineralizing solutions and so the occurrence of ankerite is explainable.

Altered olivine (Bowlingite?)

A Mg-Fe-Ti-silicate was found in sample 22/65.15 and it is suspected to be bowlingite. There is not much doubt that it was originally olivine because of the composition (Appendix 4) and also because the irregular fractures, common in olivine, are still retained. However, the mineral cannot be olivine because it is strongly coloured and pleochroic. The colours vary from cream-yellow to deep golden yellow. Also, olivine does not usually contain so much Ti (over 2 wt.% TiO_2 in some analyses). Hence it is best described as altered olivine. The composition of bowlingite shows considerable variation and its detailed constitution is not known (Deer et al, 1980).

Its strong yellow colour may be due to its high content of Ti. The original olivine crystals were quite coarse, some exceeding 3 mm. The crystals have now been partly replaced by serpentine (chrysotile) and magnetite (Plate 4.9B) and this is yet another indication that they were originally olivine crystals. If it is assumed that the original olivine crystals did not contain as much Ti as indicated by the analyses, then Ti must have been mobile, at least locally.

Altered olivine is rare but in some places it may have been completely altered to serpentine and iron oxides. Its high Mg content (over 50 wt.% on average) indicates that it was the variety forsterite in the original ultramafic rocks.

4.22 Garnets

The garnet group minerals are rare at Mount Mulgine. They were observed in samples 22/33.9 and 259/115.77 and from their analyses, shown in Table 4.9, they are largely andradite and spessartite respectively.

Spessartite is colourless and occurs as roundish grains of about 1 mm diameter on average. It is associated with quartz and muscovite and contains many inclusions of small quartz grains but not of muscovite. The spessartite was, therefore, earlier than muscovite. Small pyrite grains are sometimes found within the spessartite, together with the quartz grains. Apart from minor fluorite, which is a late mineral, the sample (259/115.77) containing spessartite is devoid of Ca-bearing minerals.

Andradite is brown and finely granular. The grains vary from about 0.05 mm to generally less than 1 mm but, in some parts of the sample, frac-

Table 4.9 : Garnet compositions

concentrations in wt.%, n.d. means not detected.

	ANDRADITE	SPESSARTITE	
Sample No.	22/33.9	259/115.77	
Analysis No.	1	1	2
SiO ₂	34.06	37.83	47.22
TiO ₂	n.d.	0.08	0.14
Al ₂ O ₃	5.90	19.86	17.05
Cr ₂ O ₃	n.d.	n.d.	0.07
FeO	23.10	7.45	6.68
MnO	0.57	29.76	24.83
MgO	0.05	1.40	1.14
CaO	32.31	2.14	1.97
Na ₂ O	0.03	n.d.	0.02
K ₂ O	n.d.	n.d.	n.d.
F	n.d.	n.d.	n.d.
Cl	0.01	0.01	0.04
P ₂ O ₅	n.d.	n.d.	n.d.
NiO	n.d.	n.d.	n.d.
Total	96.03	98.53	99.16

tured patches of the mineral of up to 2.5 mm in length were observed. This mineral is associated with carbonate, quartz and pyrite. The andradite obviously formed before the pyrite because many small grains of it are found as inclusions within the pyrite. Andradite constitutes about 40 volume percent of sample 22/33.9.

CHAPTER 5 : FLUID INCLUSION STUDIES

5.1 Introduction

Fluid inclusion research has now gained general acceptance as one of the more reliable methods for determining the nature of mineralizing solutions and some of the conditions of formation of ore deposits; so much so that it is now routinely applied during the investigation of most mineral deposits.

Initial reluctance to use fluid inclusion methods or accept fluid inclusion data was mainly based on the possibility of leakage of fluids into or out of inclusions* after entrapment and on the lack of clear distinctions between primary, pseudosecondary and secondary inclusions. Continued research, mainly by E. Roedder and many other workers has greatly improved our understanding of fluid inclusions and dispelled most of these earlier fears. It has been shown that fluid inclusions generally do not leak (Roedder and Skinner, 1968) and criteria are now available (Roedder, 1979a) for distinguishing between the three main types of inclusions mentioned above. This, plus improved instrumentation and advances in studies of phase relations in hydrothermal systems that approximate natural ore fluids, has led to a proliferation of fluid inclusion studies, especially in the last two decades.

In this chapter, the sampling methods, the techniques employed, the inclusions themselves and the experiments are first described before presenting the data and interpreting them. This is considered essential for a proper appreciation or evaluation of the data interpretation.

A knowledge of fluid inclusion terminology is assumed in the following paragraphs. Those unfamiliar with this branch of study should refer to Roedder (1972) for definitions, a summary of fluid inclusion techniques and references.

5.2 Aims of the study

Although fluid inclusion studies can also give information about post-depositional history of mineral deposits, the fundamental reason for embarking on most such studies is to get direct information on the temperature and chemical composition of the solutions when they were trapped in the host mineral. This was the primary aim of this study. Often, it is also possible to estimate the pressure of formation of a deposit from fluid inclusion studies. Furthermore, it was hoped that the fluid inclusion data would indicate the most probable source of mineralizing solutions.

* In this chapter, fluid inclusions are sometimes simply referred to as inclusions.

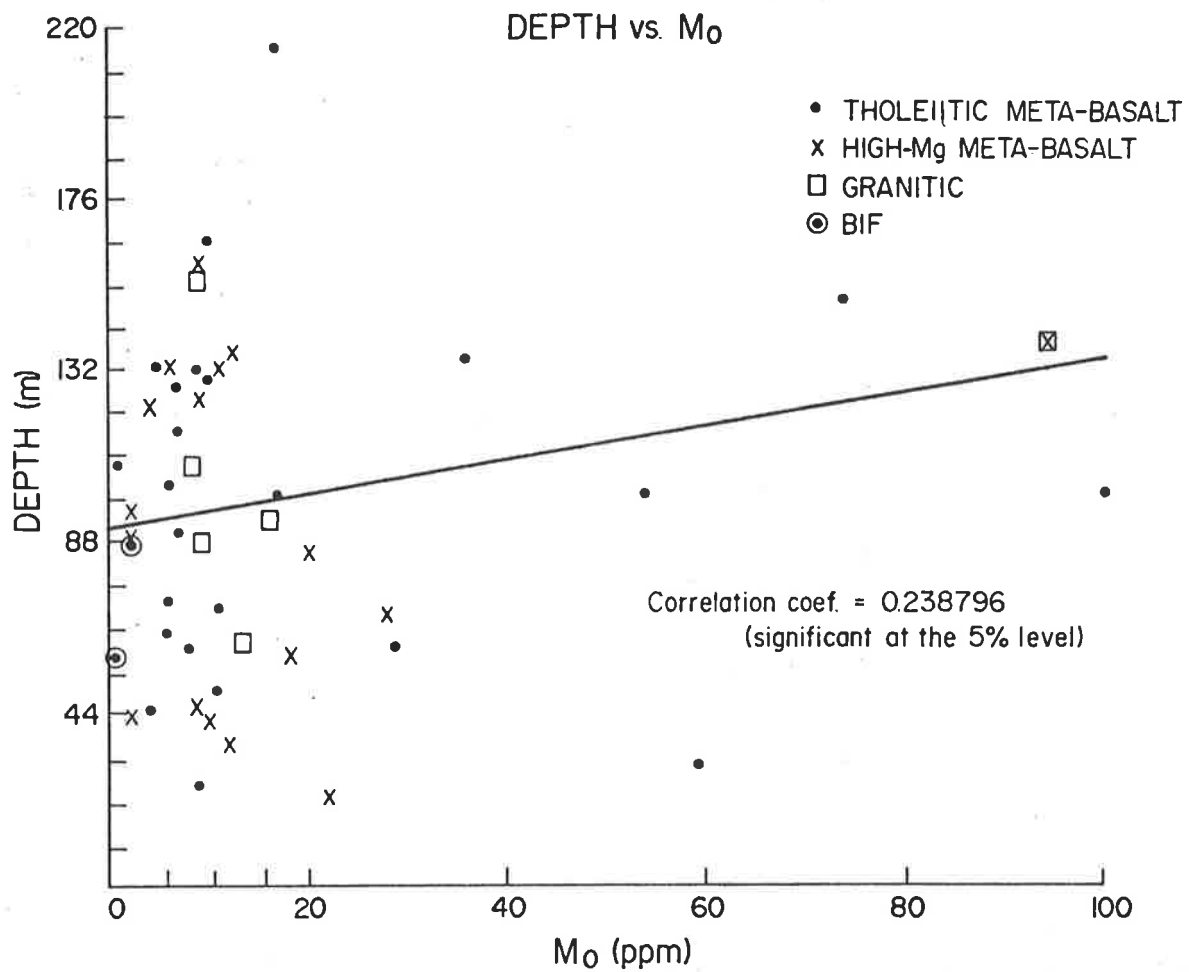


Figure 5.1

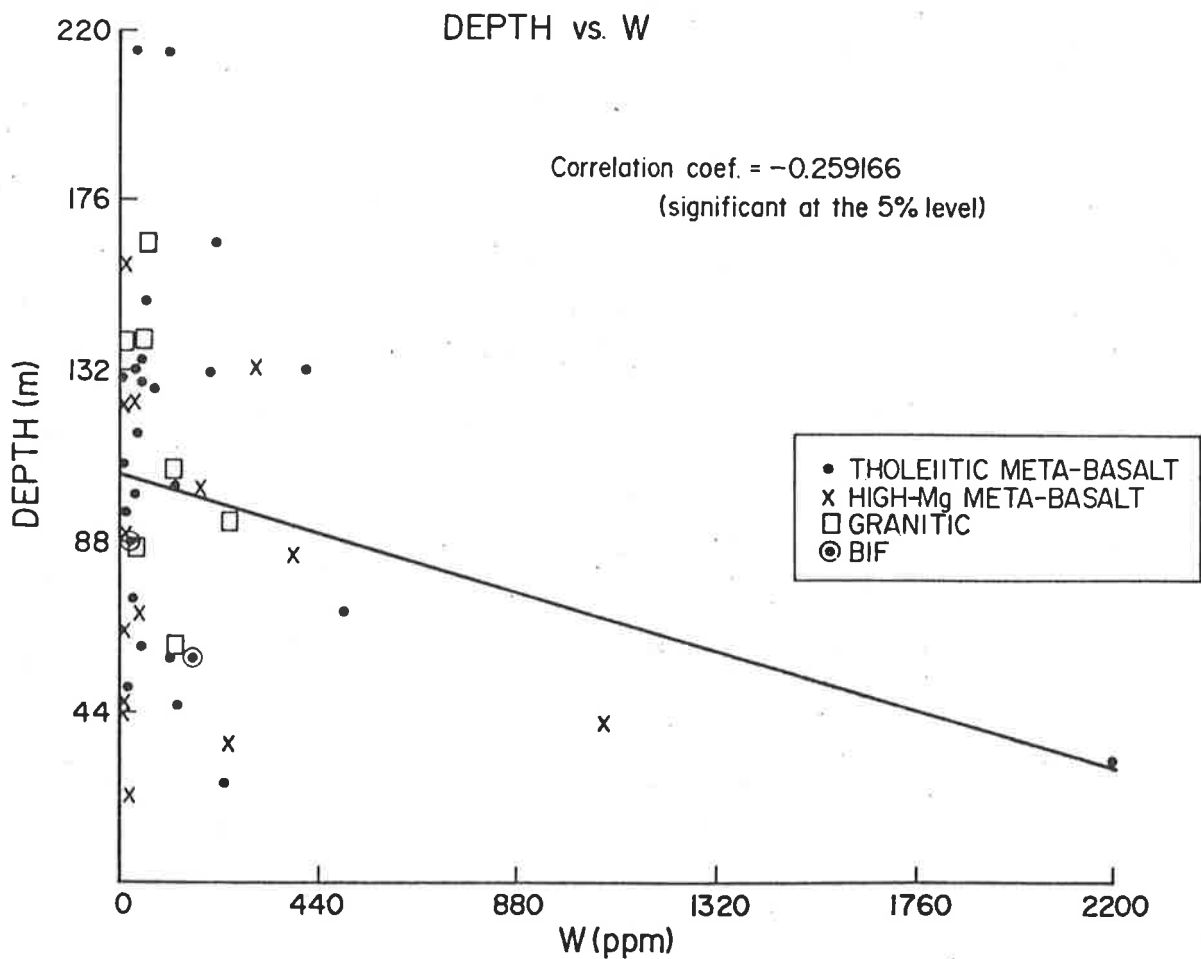


Figure 5.2

Company geologists who worked on this deposit (for example T.W. Middleton of former ANZECO) made the important observation that scheelite mineralization and molybdenite mineralization in the Trench area show a tendency to be spatially separate: scheelite occurs in or is associated with small veins generally close to the surface, whereas molybdenite occurs associated with relatively larger veins and at lower levels from the surface. This observation seems to be supported by a small positive correlation between Mo and depth and a small negative correlation between W and depth (Figures 5.1 and 5.2 respectively). The correlation coefficients, although small, and dependent on a few points, are significant at the 5% level. However, the correlation between W and Mo in the Trench deposit (Figure 5.3) is not significant. It was hoped that fluid inclusion studies would throw some light on some possible explanations for this mineral zoning.

After preliminary studies, when it was clear that not all quartz veins were mineralized, it was decided to examine inclusions in quartz from W-rich areas and also those in quartz from W-poor areas and thus test the possibility of using fluid inclusions as a pathfinder to tungsten mineralization in the Trench.

The extent to which each of the above objectives were realised will be evaluated towards the end of the chapter.

5.3 Sample selection

Initially, inclusions were sought only in quartz but later after realising that there were several quartz generations and that not all the quartz veins were mineralized, it was decided to look for inclusions in fluorite and in scheelite itself. The selection of suitable samples was dictated by the above listed aims of the study.

As the Mount Mulgine Granite was considered a possible source of the mineralizing solutions, suitable samples were selected at increasing distances from the exposed granite and down dip from the granite. The idea being that if the granite was the source of the mineralizing solutions, then the ore fluid temperature might be a function of distance from the granite. However it became clear during the course of the investigations that there is a real possibility that the Mount Mulgine Granite continues underneath the Trench deposit which makes this concept of distances from the granite meaningless.

For the scheelite and molybdenite zoning described above, samples were selected from small and large veins respectively; small veins being arbitrarily defined as those with widths of less than 2 cm and large veins as

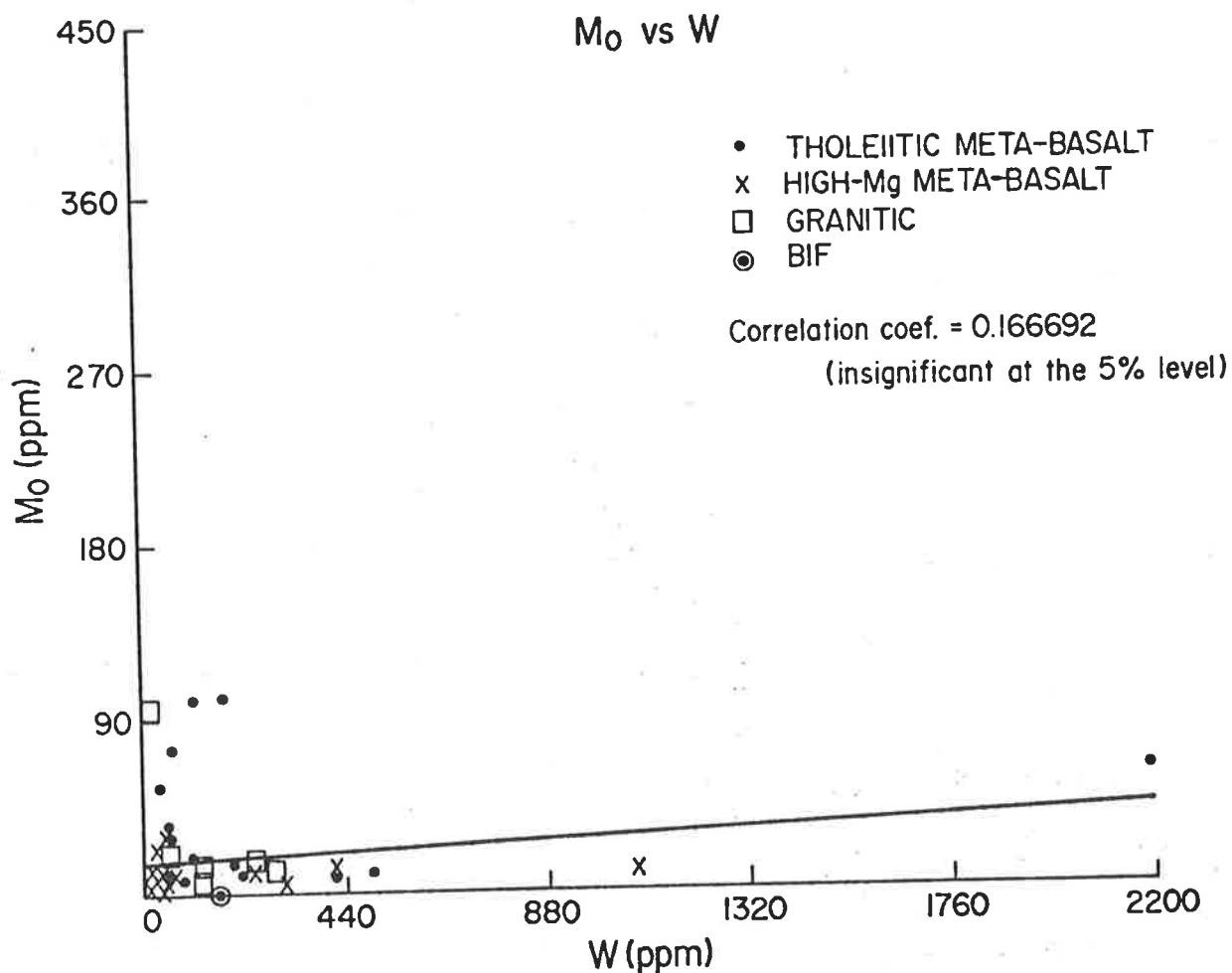


Figure 5.3

those with widths exceeding 6 cm. Some of the samples were selected from shaft 4 bulk sample heaps (Figure A-1, Appendix 1). Molybdenite and scheelite were not physically observed in the shaft samples selected but the large vein samples were picked from the drive bulk sample (DBS) heaps numbers 16, 17 and 21. These were from the lowest level reached by the shaft and also showed the highest Mo assay values. Similarly, the small vein quartz samples were selected from bulk sample (BS) heaps 19, 20 and 21 that were not only from very close to the surface but also showed the highest W values according to the assays. Veins with widths of 2-6 cm were also sampled but they were not classified as "large" or "small".

The last batch of samples were selected from W-rich and W-poor areas, as shown by the geochemical soil anomalies and assays. The W-rich samples were chosen from drill cores that had been recovered from areas showing high W soil anomalies. Further, the samples were picked only from those core sections that assayed at least 0.1% WO_3 and also contained visible scheelite. On the other

extreme, samples were taken as representative of W-poor areas if they did not fulfil any of the above conditions for W-rich samples - that is, the samples had to be from sections of cores that assayed very low or no W and the drill cores themselves had to be from areas of low W according to the soil geochemical map. And, of course, the samples had to be devoid of any W mineralization, preferably lacking mineralization of any kind.

The few scheelite and fluorite samples were picked at random. Based on the assumption that these two minerals formed from the same solutions as vein quartz, the initial idea was to get a few readings and then compare them with the data that were being accumulated on inclusions in quartz. The fluid inclusion sample locations can be found in Appendix 1 (Figure A-1).

5.4 Techniques

Roedder (1972) described a variety of methods, both destructive and non-destructive that can be used to obtain information from inclusions which may be used to unravel the often complex history of mineral deposits. Only a few of these methods could be applied in this study. The chemical composition of the fluids was determined by freezing experiments and also by crushing the samples and leaching out the solutions which were then analysed directly by atomic absorption. These methods are described in detail in later sections.

The temperature of formation was determined by heating the non-homogeneous inclusions until they homogenised. Homogenization temperatures (T_H) thus obtained usually need a pressure-temperature correction to convert to temperatures of formation; unless it can be shown that the inclusions formed from boiling solutions or that they formed in large vugs in open connection to the surface in which case no pressure-temperature correction is necessary (Roedder, 1971).

Fluid inclusions were studied in thin (0.15 to 0.30 mm-thick) flat plates which were thin enough to readily transmit light and reduce thermal lag but thick enough to contain the larger inclusions. For good optics, the plates were polished on both sides; this minimizes the interferences of surface imperfections and excessive diffuse light scattering (Craig & Vaughan, 1981). Thus the actual sample plate thickness varied from sample to sample, depending on the transparency of the host mineral and the size of the inclusions.

Experiments were done on the dual-purpose freezing and heating stage, built by Chaix-Meca in Nancy, France. Briefly, cooling of the stage is effected by circulating pre-cooled nitrogen gas through the stage while

heating is by means of an electric coil within the stage. Sensors attached to the stage are connected to a temperature controller which continuously displays the temperature of the stage. The behaviour of the inclusions is monitored during freezing and heating by viewing in transmitted light on a petrological microscope.

5.5 The fluid inclusions

Distinguishing between primary, pseudo-secondary and secondary inclusions may well be the most difficult part during fluid inclusion studies. It is very important to be able to do this for any meaningful interpretation of fluid inclusion data but even in well crystallized euhedral crystals, this distinction is difficult (Kim, 1981). Although Roedder (1979a, p.689-691) has listed criteria for their identification, it still remains a problem because many inclusions do not permit application of any of the criteria and, besides, any given sample often contains inclusions of more than one generation (Roedder, 1979a).

By far, the vast majority of inclusions found are secondary. Some have clearly necked down (Plate 5.1A), some have shapes suggestive of having necked down while others are obviously fracture controlled. As primary origin could not be proven for any of the inclusions in quartz, it was, initially, decided to take measurements on any optically suitable inclusion in the first few samples designated by a double star (**) in Appendix 5 and then compare the data with that obtained later for inclusions that were selected as most likely to be of primary origin. No difference was observed between the two groups of data, indicating that either there are no primary inclusions surviving, or the fluids in the primary inclusions are not noticeably different from those in secondary inclusions.

Criteria that were often used as evidence for primary origin are:

- a) relative isolation;
- b) lack of healed fracture control and necking or features indicative of necking;
- c) uniformity of phases and phase ratios.

The only inclusions that were classified as primary fairly confidently were found in fluorite (Plate 5.1:B,C,D & E). Although not many readings on inclusions in fluorite were taken, because of the lack of samples and lack of inclusions in those samples, the few readings that were obtained are not very different from those obtained for inclusions in quartz. This

suggests that some of the inclusions in quartz may indeed be primary, or that quartz and fluorite were deposited from the same solutions.

Poor visibility precluded the use of most inclusions in scheelite for freezing and heating experiments. The few readings that were made are very similar to those obtained on inclusions in quartz and fluorite (see Appendix 5).

Apart from the one fluorite sample (268/50.5) which apparently had no inclusions at all, the rest of the samples selected for fluid inclusion studies had abundant inclusions, some of which were suitable for experiments. Inclusions in quartz ranged in size from about 0.06 mm down to the lower limit (about 0.002 mm) of optical resolution (400X magnification). Inclusions in fluorite were generally larger, varying in size from about 0.003 mm up to approximately 0.16 mm (Plate 5.1D). For freezing and heating runs, the inclusions used were usually in the 0.005-0.05 mm range.

The ratio of the liquid volume to the total volume of the inclusion (termed the degree of fill) varies greatly. At one extreme, it is virtually 100% in inclusions that are filled with liquid only and at the other end, it is practically 0%, in inclusions filled with either vapour or solids, in which the liquid cannot be seen. Between these two extremes, it is generally true that the degree of fill is high in most inclusions. Hence, most inclusions homogenize in the liquid phase.

5.6 Types of inclusions

Many types of inclusions were observed and this made a classification scheme necessary. Because many of the inclusions contain CO_2 , it was decided to group the inclusions on the basis of the number of phases observable just above 31°C (the critical temperature of CO_2). In most cases, it has not been possible to ascertain the identity of the solid phases (mostly daughter minerals) in the inclusions and the term "phase" is, in this case, used to mean a physically observable (rather than distinct) entity or kind of substance.

All inclusions were classified prior to freezing and heating (to well above 31°C). This avoids problems that would arise with some inclusions which form new phases (vapour bubbles and/or daughter minerals) on cooling or freezing. The temperature of 31°C ensures that there is one homogeneous CO_2 fluid phase. Inclusions containing CO_2 usually develop a CO_2 -rich vapour phase at some temperature below 31°C . All such inclusions are designated by the letter B in the following classification scheme. Generally, the letters C, A and D mean no vapour bubble, one vapour bubble and two vapour bubbles respectively just above 31°C . The other letters used are explained in the text. The Roman number refers to the number of phases in the inclusion just above 31°C . This scheme has been used because it is easy to apply and is not subjective.

Type I inclusions

These are the simplest and contain only one fluid phase above 31°C. Two varieties were commonly observed: type IC inclusions containing a clear saline fluid (Plate 5.2A) and type IB inclusions which contain CO₂-rich fluid which appears dark because of refractive index contrasts (Plate 5.2C). The latter inclusions are easy to identify because they readily nucleate vapour bubbles on cooling. The vapour bubbles disappear and yield to an expanding liquid at temperatures ranging from below -12°C to a maximum of 30.6°C.

Some very dark-rimmed inclusions presumably contain just vapour but as these did not respond to freezing tests, there was no way of telling their nature. Such inclusions were few and practically useless; they are not included in this classification but if it became necessary to include them, they would be type IA.

Some type IC inclusions nucleated vapour bubbles (one nucleated two vapour bubbles, (see Plate 5.5A & B) and some crystallized daughter minerals on cooling. Others just froze without forming new phases while quite a few of them did not freeze (see later, under Freezing Experiments).

Type II inclusions.

Type II inclusions have two phases at just above 31°C. They comprise the largest and most important group. The following types of inclusions are all varieties in this group which have been observed: type IIA inclusions have a vapour and a liquid. Because type IIA inclusions are the ones most frequently seen, they are sometimes referred to as ordinary inclusions. Type IIB inclusions contain two fluids; a solution enclosing a CO₂-rich fluid. As in type IB inclusions, the CO₂-rich liquid develops a CO₂-rich vapour phase at some temperature below 31°C. Plate 5.2B shows a field of type IIB inclusions. Type IIC inclusions are rare and comprise a solid (daughter mineral) bathed by a liquid but with no vapour phase (Plate 5.2F). Most inclusions of this type are believed to have formed as a result of necking down of inclusions with daughter minerals (see below).

Type III inclusions

Three-phase inclusions belong to this group. A number of varieties have been noted: type IIIA inclusions are similar to type IIA inclusions described above but each contains a daughter mineral as the third phase. Type IIIB inclusions have two fluids and a daughter mineral. The inner liquid is, invariably, a CO₂-rich fluid which may shrink to form a CO₂-rich vapour phase when cooled below 31°C. Type IIIC inclusions, an example of which is shown as Plate 5.2G, have two solids in a fluid, but no vapour phase. Type IIIC inclusions are rare.

Plate 5.1 Primary and Secondary Inclusions.

- A. Necked down inclusions.
Sample No. 262/149; in quartz.

- B. A field of primary inclusions. Note uniformity of phases and phase ratios. The edges of the fluid inclusions are faintly visible against the host which means that the fluids have about the same refractive index as the host.
Sample No. 314/86; in fluorite.

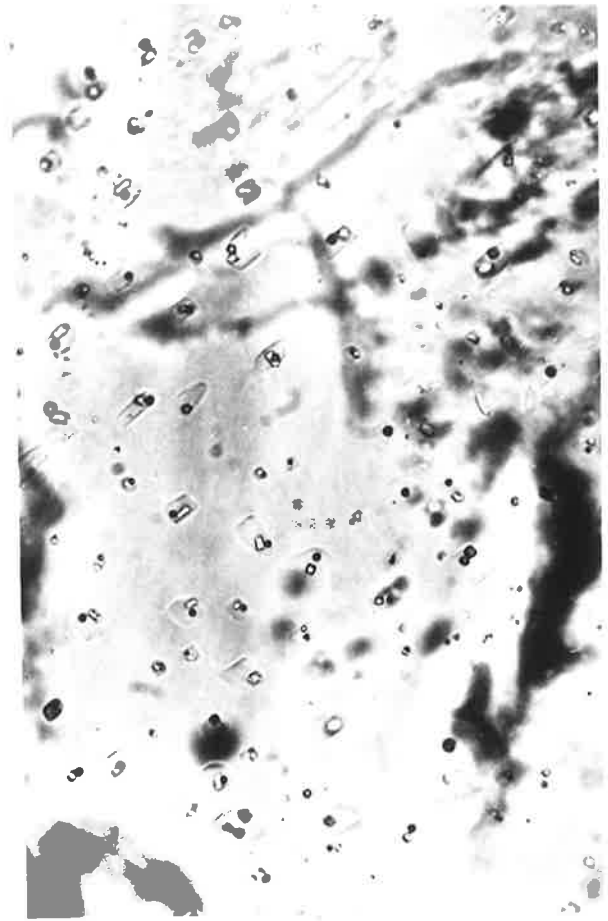
- C. Parallel rows of small inclusions thought to have been trapped along growth planes. If so, they would be primary.
Sample No. 314/86; in fluorite.

- D. The largest fluid inclusion found in this study. The most widely separated points on this inclusion are about 0.168 mm apart. The inclusion is assumed to be primary.
Sample No. 314/86; in fluorite.

- E. Another relatively large fluid inclusion in fluorite, also assumed to be primary because of its size and relative isolation.
Sample No. 42/109.1; in fluorite.

PLATE 5.1 (Primary and secondary inclusions)

A | 0.03mm



B | 0.05mm

C | 0.05mm



E | 0.04 mm



D | 0.05mm

Plate 5.2 Types of Inclusions.

- A. Type IC inclusions, containing aqueous solutions, but no other phases.
Sample No. 42/109.1; in fluorite.
- B. Type IIB inclusions (below 31°C) comprising an aqueous solution (1a) liquid carbon dioxide (1c) and a CO₂-rich vapour phase (g). What appears as a solid inclusion or daughter mineral in the labelled inclusion is not part of the inclusion.
Sample No. 276/158; in quartz.
- C. A type IB inclusion. Liquid carbon dioxide with a large CO₂-rich vapour phase below 31°C.
Sample No. 42/109.1; in fluorite.
- D. A type IIA inclusion with an unusually large vapour phase. Such inclusions are rare, at Mount Mulgine.
Sample No. 314/86; in fluorite.
- E. A type IIC inclusion with an elongate, faintly visible daughter mineral in an aqueous fluid. No vapour phase.
Sample No. 276/158; in quartz.
- F. A type IIIC inclusion with two daughter minerals in a fluid. No vapour phase. (The smaller daughter mineral, labelled d.m., looks like a vapour bubble).
Sample No. 276/158; in quartz.

PLATE 5.2 (Types of inclusions)

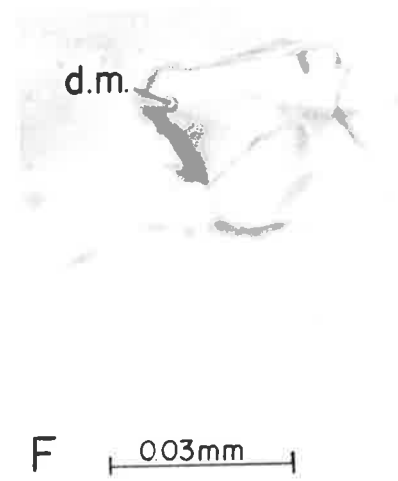
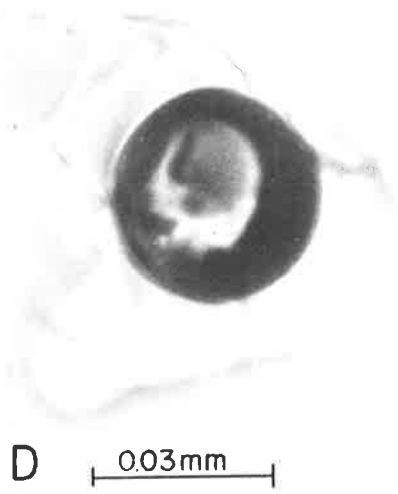
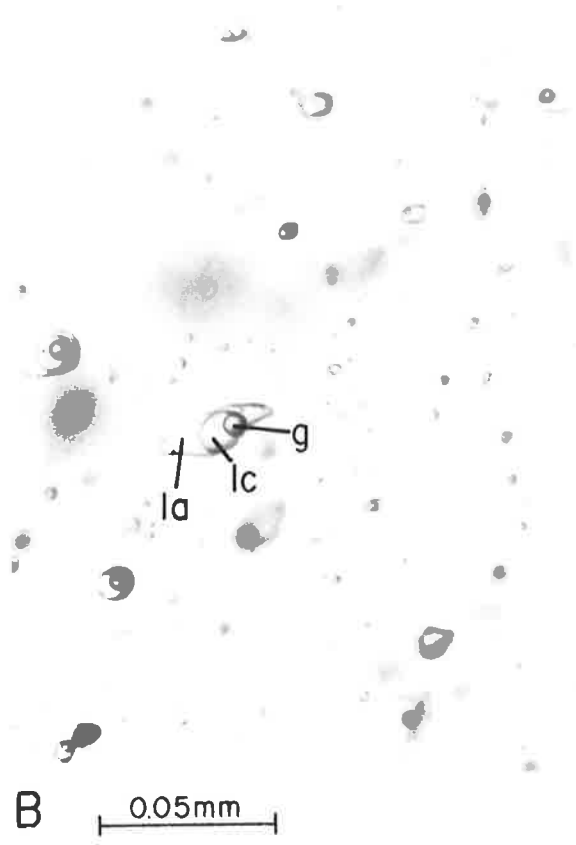
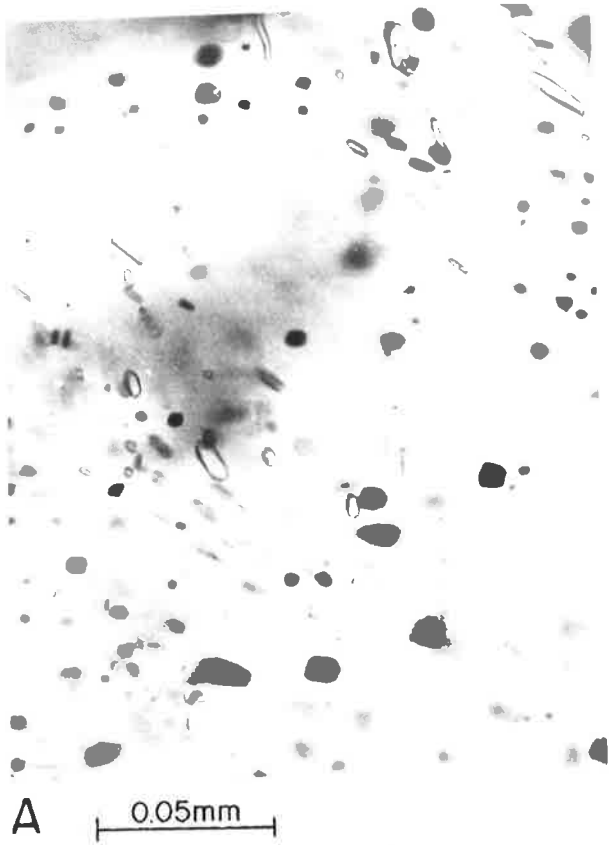


Plate 5.3 Types of Inclusions.

- A. A type IVA inclusion in which one of the daughter minerals is opaque.
Sample No. 274/33; in quartz.
- B. A type IVC inclusion (three daughter minerals in a liquid, but with no vapour phase).
Sample No. 276/158; in quartz.
- C. Two ordinary (type IIA) inclusions with a smaller type IVD inclusion. The type IVD inclusion has two vapour phases, a liquid and one small daughter mineral, labelled d.m.
Sample No. 252/116.0; in quartz.
- D. A type IVE inclusion with an unusually large vapour bubble (g) surrounded by a thin film of liquid carbon dioxide (lc) which is itself surrounded by an aqueous fluid (la). The fourth phase is a daughter mineral which is clearly visible.
Sample No. 314/86; in fluorite.
- E. A stranded crystal (c) believed to have originally been a daughter mineral. It is very similar to the daughter mineral (d.m.) in the inclusion nearby.
See text for explanation.
Sample No. 42/109.1; in fluorite.
- F & G. Inclusions (type IIIA) in which the solid phases, labelled d.m., occupy more than 50 volume % of the inclusion cavity. Such inclusions are believed to be products of necking down. F is from sample No. 276/158, and G is from sample No. 274/33; both in quartz.

PLATE 5.3 (Types of inclusions)



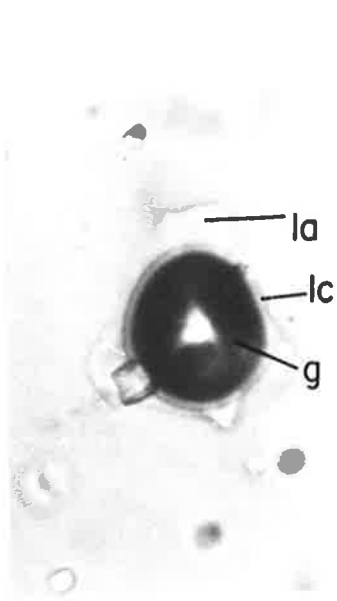
A 0.015mm



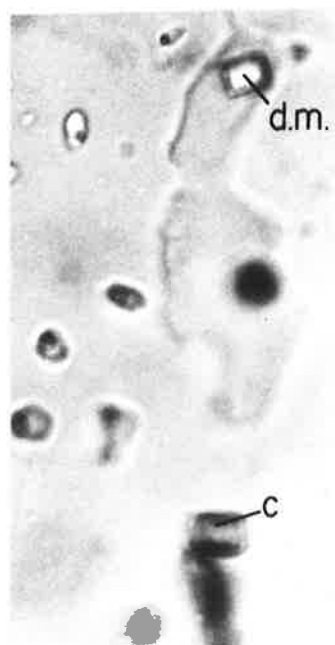
B 0.015mm



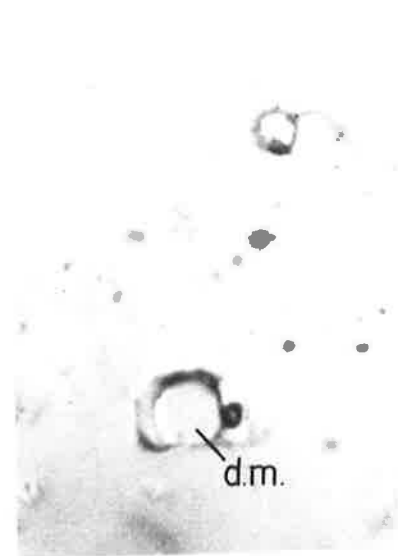
C 0.015mm



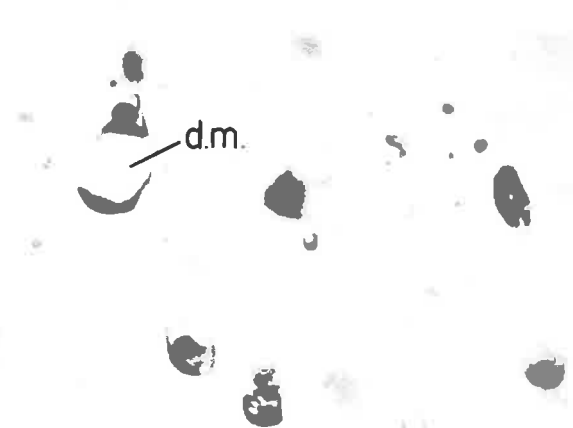
D 0.02mm



E 0.01mm



F 0.015mm



G 0.015mm

Plate 5.4 Complex Inclusions.

- A. A complex inclusion type VD with 2 large daughter minerals, one of which has blocked off a vapour bubble (g) and some of the solution (l_a) in a nook of the inclusion cavity. A second (smaller) vapour bubble developed in the rest of the aqueous solution. Note another complex inclusion, type VIA, with four daughter minerals, the smallest of which looks like a vapour bubble (labelled d.m.).
Sample No. 274/33.0; in quartz.
- B. A type VB complex inclusion. All the phases (except the daughter mineral (d.m.) in the liquid carbon dioxide (lc)) are clearly visible.
Sample No. 276/158; in quartz.
- C. A type VID inclusion with three daughter minerals (d.m.), an aqueous solution (la) and two vapour bubbles (g).
Sample No. 263/137.7; in quartz.
- D. The most complex inclusion found in this study, with two aqueous liquids, two vapour phases and two solid phases. See illustration below the photomicrograph and explanation in text (page 82). Note the other CO_2 -rich inclusions.
Sample No. 252/116.0; in quartz.
a and f - aqueous fluids
b and e - vapour bubbles
c and d - solid phases
- E. A type IVB inclusion with two fluids and two daughter minerals (plus a vapour bubble below $31^{\circ}C$).
Sample No. 252/170.0; in quartz.

PLATE 5.4 (Complex inclusions)

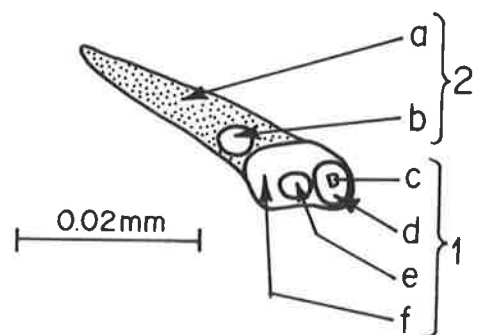
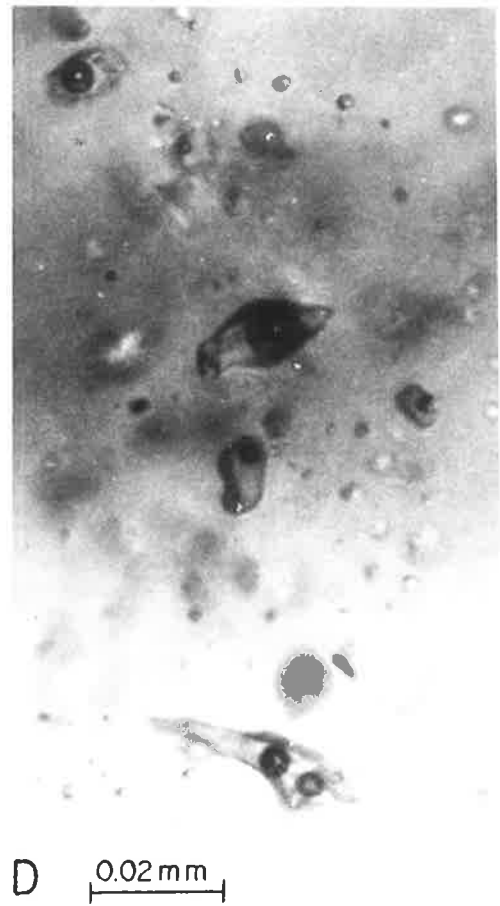
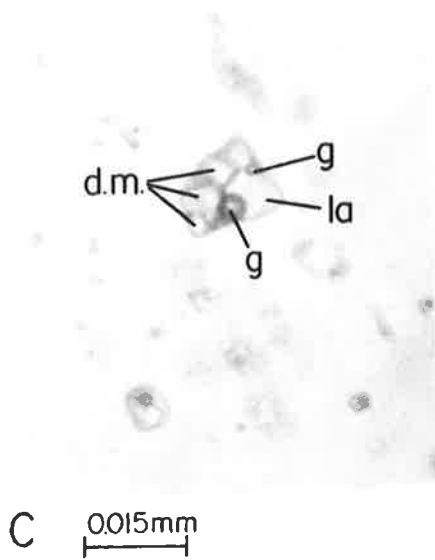
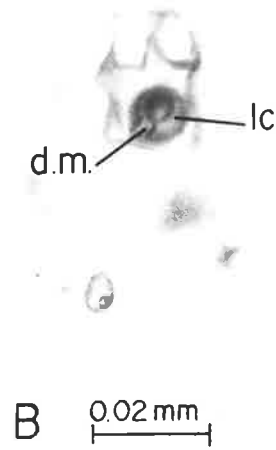
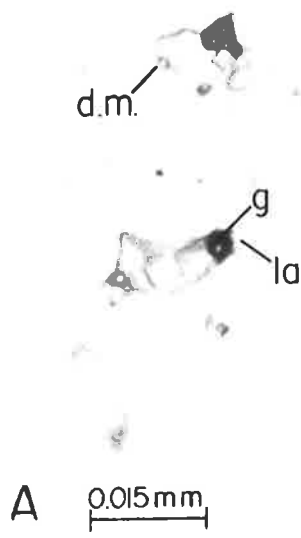


Plate 5.5 Behaviour on Cooling.

- A. An inclusion with two vapour phases, both of which developed on cooling. Before cooling, the inclusion had no vapour phase (type IC).
Sample No. 274/33.0; in quartz.
- B. The same inclusion as in A. On further cooling, the smaller vapour bubble proved very unstable and by -30.1°C it had disappeared.
- C. Melting ice has split the vapour bubble into two parts.
Sample No. 314/~86; in fluorite.
- D. The same inclusion as in C. All the ice has melted and the two vapour bubbles have re-united.
- E. Melting ice has split the vapour bubble into three parts.
Sample No. 314/~86; in fluorite.
- F. The same inclusion as in E, but with the three vapour bubbles re-united. Melting of the ice is still in progress.

PLATE 5.5 (Behavior on cooling or freezing)

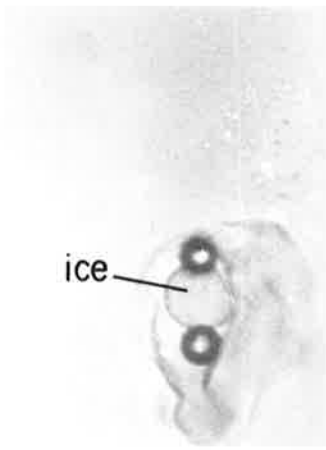


A



B

0.002mm

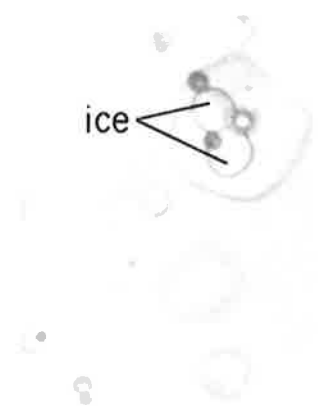


C



D

0.02mm



E



F

0.015mm

Type IV inclusions

Any inclusion with four phases at just above 31°C belongs to this group. With four phases, more combinations (variations) would be expected and the following have indeed been observed:

Type IVA inclusions have two daughter minerals, an aqueous solution and a vapour bubble (Plate 5.3A). A type IVB inclusion comprises two fluids and two daughter minerals. An example of such an inclusion is shown as Plate 5.4E. Type IVC inclusions are so rare that the inclusion shown as Plate 5.3B is the only one of this type that was observed in this study. With no vapour phase, it comprises a fluid phase and three daughter minerals. Type IVD inclusions are rare inclusions comprising a daughter mineral, an aqueous phase and two vapour phases. Although other types of inclusions with two vapour phases were observed several times (see below) the inclusion shown as Plate 5.3C is the only type IVD observed.

Before going further with the classification, it is proper to speculate on how inclusions with two vapour phases could have formed. The presence of at least one daughter mineral was noted in each inclusion with two vapour phases. The crucial factor in the development of two vapour phases seems to be that the solutions must be saturated or oversaturated so that on cooling, a daughter mineral is formed. In this regard, it is important to note that equivalent type IIID inclusions, with a liquid and two vapour bubbles have not been observed.

It is suggested that through nucleation of a daughter mineral, the inclusion is divided into two parts. If this happens before the formation of a vapour phase, then nucleation of a vapour phase would start in each of the two parts of the inclusion. Alternatively, if a vapour phase already exists during the crystallization of the daughter mineral, it would be trapped in one part of the inclusion and the second vapour phase would form in the other part of the inclusion on further cooling. In both cases, continued cooling would result in an increase in size of both vapour phases.

The fifth and last variety of four phase inclusions has been called type IVE and consists of a vapour phase, surrounded by a thin film of fluid (presumably liquid CO₂) which persists above 31°C. The latter in turn is surrounded by an aqueous solution. The fourth phase is a daughter mineral. Plate 5.3D shows a type IVE inclusion and although it was the only one of its kind observed, it is believed that other such inclusions could be present. Such a thin film of liquid around the dark vapour bubble could be easily missed, especially in smaller inclusions.

Complex inclusions

Inclusions with more than four phases will be collectively referred to as complex inclusions. Although no attempt was made to freeze such inclusions and only a few unsuccessful attempts were made to homogenize them, the occurrence of such solid-packed inclusions implies the original solutions must have been highly saline. Their "failure" to homogenize will be discussed later.

The complex inclusions are listed below in a manner which conforms to the above classification scheme for the rest of the inclusions, in which the number refers to the actual number of phases in the inclusion just above 31°C. Type VB inclusions, an example of which is shown as Plate 5.4B consist of two fluids and three daughter minerals. Type VD inclusions have two daughter minerals, an aqueous solution and two vapour phases (Plate 5.4A). No type VA, VC or VE inclusions were observed. Type VIA inclusions (Plate 5.4A) contain four daughter minerals, a fluid and a vapour. Type VID inclusions have three daughter minerals, a fluid and two vapour phases (Plate 5.4C). A type VIF inclusion, the last of the complex inclusions, with two daughter minerals, two fluids and two vapour phases is shown as Plate 5.4D. It is a rather unusual inclusion because both fluids appear to be saline solutions (i.e., there is no CO₂-rich solution). Also, the arrangement of the phases is unusual; the larger daughter mineral appears to be completely enclosing the smaller "daughter mineral" and one of the fluids does not completely enclose the other as usually happens when two fluids occur in the same inclusion. Because the phases and their arrangement may not be clear from the photomicrograph, the inclusion has been sketched below Plate 5.4D.

Unless the slight difference in the colours of the liquids is an optical illusion, such an inclusion is not likely to have formed in the manner suggested for other inclusions with two vapour phases (see page 81). If the two liquids are really different, then a more plausible explanation for the way in which the inclusion formed is that there are, in fact, two inclusions (labelled 1 and 2 in the sketch) which give the impression of being one. The tapering shape of inclusion 2 favours this explanation. Inclusion 1 would have formed first. Then, later, as the host mineral resumed growth over the inclusion a conical cavity would be created (as the host mineral grew to close the space "above" the inclusion). Inclusion 2 would most probably have formed at the same time as its "cage was being built" and so it would be primary or (at least) pseudosecondary.

Several explanations are possible for the apparent arrangement of the solid phases: The smaller solid inclusion may not be a daughter mineral at all. It could be a solid that was trapped as the inclusion was forming and,

later, served as a nucleus for the crystallization of the larger daughter mineral. Alternatively, the smaller solid may also be a daughter mineral which formed first and later served as a nucleus for the crystallization of the larger daughter mineral. Finally, it is also possible that the smaller solid is, in fact, separate and just lies underneath the large daughter mineral.

5.7 Freezing experiments

Most freezing experiments involved type IIA and type IC inclusions whenever the latter were found. A good number of experiments were done on type IB inclusions and only a few were done using type IIIA and type IIB inclusions.

Most of type III and all inclusions with more than three phases were excluded from freezing experiments because of the very small volume of solution in many of them and also because the daughter minerals would facilitate the formation of hydrates and their very presence interferes with the critical observation of first and last stages of melting.

With a few exceptions, all inclusions selected (for freezing) froze between -25°C and -80°C (between -90°C and -107°C for CO_2 inclusions). The few exceptions are inclusions which would not freeze even when kept below -125°C for at least half an hour and then warmed slowly to -80°C and kept at this temperature for five minutes. Supercooling is not uncommon in inclusions. Roedder (1962) suggested that failure to freeze may be due to the lack of nucleation material, implying very slow flow rates of the fluids at the time of trapping, thus avoiding the transport of fine debris in suspension. Apart from not freezing under the stated conditions, these few inclusions did not display any unusual features and those that were heated homogenized as expected.

Nucleation of vapour bubbles (in type IC, IB and IIB inclusions) and formation of daughter minerals (especially in type IIA inclusions) were expected and they were commonly observed. A phenomenon occasionally observed was the splitting of vapour phases by ice during melting (Plate 5.5C, D and E, F); this was repeatable in the inclusion shown as Plate 5.5C & D. An expected but rare phenomenon was the formation of 2 vapour phases in the type IC inclusion shown as Plate 5.5A & B on cooling. One of the vapour bubbles however, proved very unstable and shrunk in the solution as cooling progressed, finally disappearing at -28°C . Fuzikawa (1982) made a similar observation on cooling an inclusion after homogenization. These observations support the suggestion made earlier (page 81) that two gases cannot coexist stably in a solution unless there is a solid partitioning the inclusion.

The CO_2 -rich phases in two type IIB inclusions found in sample

264/81.4 seemed to homogenize on cooling. When the temperature was dropped below 31°C , the two inclusions developed vapour phases as expected. But the vapour phases continued to grow (at the expense of the liquids enclosing them) as cooling progressed until finally, all the CO_2 -rich liquids seemed to have disappeared, leaving only the CO_2 -rich vapour phases. The liquid phases were no longer visible at -7.4°C and -27.4°C . On warming, the liquid reappeared and expanded as the vapour shrank until homogenization (in the liquid phase) at 30.6°C and 28.8°C respectively. Unfortunately, both these two interesting inclusions decrepitated (one below 212°C and the other at 236°C) during a meticulous attempt to homogenise them.

Theoretically, it is impossible for inclusions to have two homogenization temperatures as just described (P. Ypma, pers. comm.) and so it must mean that the observations were incomplete. There are three possible explanations: (1) During cooling, the volume of liquid CO_2 around the CO_2 -rich vapour became so small that it could not be noticed. Roedder (1963b) stated that as much as 10% liquid CO_2 can easily be missed as it clings to the interface of the vapour bubble and water solution and is thus hidden by total reflection. (2) The liquid CO_2 dissolved in water. (3) During cooling, gas hydrates (e.g., $\text{CO}_2 \cdot 5\frac{3}{4} \text{H}_2\text{O}$) formed but were not noticed. Such gas hydrates are notorious for being difficult to observe because their refractive indices are similar to those of most aqueous solutions and they are isotropic (Roedder, 1972). Similar observations were made by Collins (1979). He states (p. 1437) "During cooling, the CO_2 -rich liquid phase was observed to diminish slowly in volume, and in some inclusions disappear completely, without detectable reduction in area of the gas bubble".

Since the actual homogenization temperatures are close to the critical temperatures of CO_2 it seems likely that inclusions with this particular behaviour have CO_2 densities which are close to the critical densities.

The freezing data are in Appendix 5, together with all the other fluid inclusion data. Their interpretation will be attempted below after reporting on other experiments.

5.8 Heating experiments

In general, homogenization experiments were less successful than freezing experiments. The main problem, especially with type IIB inclusions, was decrepitation. Also, heating tends to make the inclusion borders very dark which makes it difficult, sometimes impossible, to observe phases (vapour bubbles or daughter minerals) as they shrink, becoming smaller and smaller and finally disappearing at the homogenization temperature. To make matters worse, those vapour bubbles that are not already touching the inclusion walls usually

migrate to the inclusion border as they move about under the thermal gradients set up during heating.

Ideally, homogenization experiments should be done on the same inclusions that were previously used in freezing experiments. In practice, this cannot always be done. Freezing and heating were done using different objective lenses (25X or 40X and 32X respectively) in different optical arrangements so that inclusions that appeared large and clear enough for freezing looked smaller and often not as clear with the heating lens. But even more serious than this was the fact that heating proved destructive to many inclusions. So, the routine was to do as many freezing experiments as possible before heating started. In any case, for reasons given, many inclusions could not be used in freezing experiments; but many such "rejected" inclusions were quite suitable for heating experiments.

Unlike the freezing experiments, heating experiments were not restricted to any particular types of inclusions. Any non-homogenous inclusion with clearly visible phases and clear borders was suitable for homogenization provided it also fulfilled the previously stated conditions indicative of primary origin.

Many homogenization experiments were unsuccessful because of decrepitation or because the vapour bubbles were lost along the dark inclusion borders or because, for some reason(s), the inclusions simply would not (perhaps could not) homogenize.

Decrepitation was a nuisance especially with CO₂-rich inclusions, despite the fact that it was not unexpected since, according to Burruss (1981), it commonly occurs in CO₂-rich inclusions. Only a few type IIB inclusions were homogenized but only after preparing unusually thick sample plates and making sure that the inclusions were near the centres of these plates, i.e., not near the surface. In all such inclusions which homogenized, it was always the inner CO₂-rich phase expanding and apparently dissolving the outer aqueous solution surrounding it.

For inclusions that did not homogenize, there are two possible explanations. Either the dissolution rates of the phases involved are very slow or the inclusions are products of necking although no evidence of this was found in their immediate vicinity. The longest heating experiment was abandoned after 5½ hours but in the majority of cases, if an inclusion did not homogenize after about 4 hours' heating, the experiment was aborted. This time may not have been enough for the inclusions to homogenize. Roedder (1972) reported an experiment in which an inclusion kept at 410°C took four days to homogenize and heating runs lasting a day or longer are common in the literature. Such endurance would homogenize at least some of the complex inclusions, none of

which would homogenize in these short experiments.

Evidence of necking is ubiquitous in the samples studied and has already been cited (page 78, Plate 5.1A). It is believed that inclusions of the type shown as Plate 5.3F & G, in which the daughter minerals apparently occupy more than 50% of the inclusion cavity, with no consistent daughter to brine volume ratios are also products of necking down, evidence of which has since been obliterated. Such inclusions did not homogenize because they could not. Recrystallization caused necking down and most of the solutions were sealed off in other inclusions that resulted from the same necking process. Those inclusions that ended up with the daughter minerals now have apparently over-size daughter minerals and cannot homogenize because there is not enough liquid to dissolve the solids.

Necking down is also believed to be responsible for solitary crystals of the type shown as Plate 5.3E. These crystals, as far as could be ascertained using the microscope, are in every way similar to the daughter minerals in the inclusions nearby. It is believed that they were also daughter minerals at one time, in inclusions that no longer exist, having been victims of necking down. Necking down channelled away all the liquid that originally bathed them, leaving them stranded. Such stranded crystals have also been reported by Kelly and Turneaure (1970). Of course fracturing could have been responsible for channelling the fluids away but no healed fractures were observed close by.

Heating also caused unexpected (unusual) phenomena. In one sample, BS21, boiling of the inclusion fluids was invariably observed at temperatures above 318°C. Above this temperature, the sample chips would suddenly crack in several places. Drop after drop of inclusion fluids would then be seen welling up from some sort of vent and moving rapidly along the cracks (rather like water drops oozing out of a leaking tap). On cooling to room temperature, the upper surfaces of the sample chips had black tar-like spots where the fractures and, later, fluids had penetrated to the surface. This spectacular phenomenon was observed in only one sample and is thought to be a result of the host quartz being unusually brittle, perhaps due to weathering.

Another unusual phenomenon during heating was the development of "new" vapour phases at higher-than homogenization temperatures, in previously homogenized inclusions. This was relatively common and was observed in several samples. It should not be confused with decrepitation which sometimes manifests itself in a similar manner. The two are distinguishable because a genuine "new" vapour bubble behaves like most other vapour bubbles. On continued heating, it shrinks and may move about the inclusion rapidly before it disappears. Some decrepitated inclusions may appear as if they have new vapour phases but, in those cases, the apparent new vapour phase either expands

quickly to cover the whole inclusion, making it permanently dark or it just stays as it is - neither moving nor shrinking - as the temperature is increased.

Some data were collected on some of the inclusions that developed "new" vapour bubbles at higher temperatures and they are included in Table 5G at the end of Appendix 5. However, the data are not enough for the inclusions to be characterized and so it is not possible to tell which inclusions are most likely to develop "new" vapour bubbles and when. Three attempts to find out if the phenomenon is reproducible failed and so it is concluded that the phenomenon is not reproducible.

Wahler (1956, quoted in Roedder, 1972) made a similar observation, with a new vapour bubble developing at 150°C and vanishing again at 220°C. He believed it was CO₂, resulting from the reversal in the solubility of CO₂ with temperature. This reversal is possible according to the data of Takenouchi and Kennedy (1964), which shows that immiscibility of CO₂ would occur on heating a CO₂-H₂O system. In view of the abundance of CO₂ in the inclusions studied, this is most likely to be the explanation for the development of "new" vapour phases at high temperatures.

5.9 Fluid inclusion leaching

Rather than relying on indirect interpretation of the composition of the inclusion fluids from the freezing data, it was decided to open up the inclusions, extract the solutions and analyse them on the AA. From the daughter mineral content of the solutions and the freezing data, it was becoming more than probable that the solutions in the inclusions represent at least two distinct mineralising solutions. It was hoped that extraction and analysis of the inclusion fluids would clarify this matter.

The procedure is simple crushing of the host mineral followed by leaching with distilled water. The crushing opens up the inclusions (at least some of them) and the solutions are washed out of the debris by distilled water. The details of the technique are at the beginning of Appendix 5.

This method is neither as complicated nor as accurate as some of the methods described in the literature (e.g., Roedder et al, 1963) that require relatively complex and expensive apparatus. The apparatus required for the method is very cheap and will be found in any modern geochemical laboratory. This plus the fact that the method is very quick to apply partly compensates for its lack of precision.

The main limitations and sources of error are:

1) Contamination. The method is beset with serious contamination problems. Contamination can be from the host mineral, from the apparatus or

from the person doing the experiment. The latter two sources of contamination can be eliminated or minimized as described in Appendix 5. In any case, contamination from these two sources is not a serious problem as it would be known and quantified from blank readings. Contamination from the host mineral, however, cannot be avoided and is not easy to determine. To minimize this, the samples were doubly polished like ordinary fluid inclusion sections and then examined under the microscope to make sure that they contained no other solid inclusions other than daughter minerals within the fluid inclusions. Polishing the sample is also necessary because one can check that inclusions are actually present and note their type(s) before crushing.

2) Sample size and multiple generations of inclusions. This is the main limiting factor with this method. Ideally, fluids should be extracted from one inclusion or from inclusions of the same generation. Even if the problem of opening up a single inclusion and extracting the fluids was overcome, the problem of not having enough solution for measurements would still exist. Large enough inclusions that would singly provide enough solution for analysis are very rare and in most such work groups of inclusions, hopefully of the same generation, have to be used in order to get enough solution for measurements. This is where the problem lies, because there is no way of making sure that inclusions in a sample chip are of the same generation. In fact, as Roedder (1979a) pointed out, inclusions in any given sample are seldom of one generation. In this particular case, it was found by trial and error that a minimum of about 0.2g of sample was required to give concentrations of ions easily detectable on the AA. This amount of sample could contain a variety of inclusions of different generations.

3) Adsorption of ions. The last major problem, pointed out by Roedder et al, (1963) is that crushing results in many host mineral grains with many "active" sites for adsorbing ions. Using element or atomic ratios partly overcomes this problem but the problem persists because of differential adsorption for the different ions.

Despite the problems listed above, it is felt that the results, listed in Table 5.1 provide useful information. The dominance of Ca^{++} over Na^+ in the inclusion fluids is demonstrated and the presence of Mg^{++} , suspected from freezing data, is confirmed. The elements Al, Li and Rb are below detection limit in the inclusion leach samples analysed.

Sample 22/143 was selected for crushing and leaching because it had inclusions with daughter minerals. The solutions from this sample would be representative of the more concentrated ore fluids. Sample 51/112 on the

Table 5.1 : Fluid inclusion leach analyses in quartz

Sample No. and weight	Successive crushings and leaches	Element abundances in inclusion fluids (in ppm)						Relative atomic abundance of the elements**						Total*** cations	Atomic ratios			
		Na	K	Ca	Mg	Fe	Cl	Na	K	Ca	Mg	Fe	Cl		K/Na	Ca/Na	Mg/Na	Fe/Na
22/143 sample weight = 0.2422g	first	0.32	0.22	0.78	0.20	0	4.4	1.4	0.6	2.0	0.8	0	12.4	3.4	0.43	1.43	0.57	0
	second	1.29	0.37	5.94	1.02	0.33	6.25	5.6	0.9	14.9	4.3	0.59	17.6	16.44	0.16	2.61	0.77	0.10
	third	1.62	0.47	7.59	1.07	0.22	7.50	7.0	1.2	19.0	4.5	0.39	21.1	20.15	0.17	2.71	0.64	0.06
	fourth	1.68	0.86	6.49	1.22	0.17	7.65	7.3	2.2	16.2	5.1	0.30	21.5	20.3	0.30	2.22	0.70	0.04
51/112 sample weight = 0.2109g	first	0.47	0.06	1.47	0.35	0	5.05	2.0	0.1	3.7	1.5	0	14.2	4.7	0.05	1.85	0.75	0
	second	0.58	0.12	2.13	0.33	0	5.60	2.5	0.3	5.3	1.4	0	15.8	6.15	0.12	2.12	0.56	0
	third	0.50	0.22	1.82	0.35	0	4.02	2.2	0.6	4.6	1.5	0	11.3	5.85	0.27	2.09	0.68	0
	fourth	0.63	0.47	2.04	0.57	0.60	4.25	2.7	1.2	5.1	2.4	1.07	11.9	8.19	0.44	1.89	0.89	0.40
	fifth	0.42	0.46	1.94	0.72	0.65	5.75	1.8	1.2	4.9	3.0	1.16	16.2	7.53	0.67	2.72	1.67	0.64
70/183 sample weight = 0.2814g	first	0.18	0.08	0.72	0.03	n.d.*	n.d.	0.78	0.21	1.79	0.13	-	-		0.27	2.29	0.17	-
	second	0.47	0.51	0.49	0.09	n.d.	n.d.	2.02	1.31	12.35	0.38	-	-		0.65	6.11	0.19	-
	third	0.61	0.78	5.73	0.12	n.d.	n.d.	2.63	2.00	14.34	0.50	-	-		0.76	5.45	0.19	-
	fourth	0.55	0.78	5.68	0.09	n.d.	n.d.	2.37	2.00	12.95	0.38	-	-		0.84	5.34	0.16	-

Notes:

*n.d. = not determined.

**relative atomic abundance = $\frac{\text{element abundance} \times 100}{\text{atomic weight of element}}$

***total cations = sum of relative atomic abundances of the metals. In this summation, the relative atomic abundances of Ca, Mg and Fe were halved since each of these carries two positive charges when ionised.

other hand, was chosen because inclusions in it had very few daughter minerals and so, the solutions from it would most probably be relatively dilute. The last sample, 70/183, was crushed because it was different from the other two in that the host quartz was milky and contained relatively fewer and much smaller inclusions.

Since the ratio of sample weight to leach volume varies and there is no possible control on the amount of fluid released on crushing (Roedder, et al, 1963) the only valid comparisons between the leach analyses are the atomic ratios. These are included in Table 5.1.

From the Table, solutions from sample 22/143 are much more concentrated than those from 51/112, as suspected (compare, for example, total cations). On the basis of atomic ratios alone, it is difficult to be sure whether the two solutions can be called different, implying that they are of different generations. Not much meaning can be attached to the differences in the mean atomic ratios of the two samples because such differences also occur between successive leaches of the same sample.

The only exceptions to this are the Fe/Na ratios. The average Fe/Na ratio for 51/112 is more than seven times that for 22/143. Also, the fact that there is more Fe in the relatively dilute solutions from sample 51/112 than there is in the more concentrated ones from sample 22/143 is unusual and should be noted. Before attempting to seek possible explanations for this, the following difference between the two solutions should also be noted.

It is not unreasonable to assume that solutions in inclusions are neutral. That chlorine ions are the only negative ions is also a fair assumption. Therefore, one would expect the number of chlorine ions to be equal to the total cations. Ignoring the first leach of sample 22/143 for the time being, it can be generally stated that this expectation has been realised for this same sample. The total cations are slightly less than the chlorine atoms in each case and this must surely be due to the presence of other cations whose concentrations are below detection by the AA or which were not analysed for. The story is similar but greatly exaggerated for the other sample, 51/112. For this sample, the total number of cations is far less than the number of chlorine ions, implying the presence of large amounts of undetected cations. As in the case of Fe mentioned above, the relatively dilute solutions (51/112) must be richer in the undetected metals than the more concentrated solutions (22/143). This is the basis for concluding that solutions from samples 22/143 and 51/112 are of at least two different generations. This inference is not possible from the atomic ratios of the dominant cations such as Ca^{++} , K^+ , Mg^{++} and Na^+ . From the ratios alone, the solutions from sample 51/112 might well be just a dilute form of those from sample 22/143. Perhaps the ratios of these elements should

not be taken too seriously because these are the very elements that are always found (in varying amounts) in fluid inclusions from any deposit regardless of its type, age or origin. The solutions from samples 22/143 and 51/112 would represent what have been called "concentrated" and "dilute" solutions respectively (see page 92).

Incidentally, the atomic ratios imply that the solutions from the third sample 80/183 are also different. But as the inclusions in this sample were too small, no more can be said about them.

The fact that the total cations are much less than the chlorine ions in the first leach of sample 22/143 was ignored in the above discussion. It seems this is generally true of all first leaches. A possible explanation for this is differential adsorption of the ions onto quartz fragments after crushing. Perhaps the positive ions are adsorbed more in preference to chlorine ions. Such differential adsorption would not be expected to be as effective in subsequent leaches.

5.10 Melting and homogenization data

Over 290 freezing and about 230 homogenization readings were taken and are listed in Tables 5A-5F in Appendix 5. The data are summarised and displayed graphically in Figures 5.4-5.8.

5.11 Accuracy of the readings

Some inclusions were frozen again or re-heated to check on the reproducibility of the experiments and hence assess the precision of the readings and the possibility of leakage. Generally, melting temperatures were reproducible to within $\pm 0.1^{\circ}\text{C}$. Repeat homogenization readings were almost always lower by about 2 degrees on average. No leakage was detected in the inclusions concerned.

The apparatus was calibrated by Mr. Evert Bleys, Technical Officer of the department of Economic Geology, University of Adelaide; using compounds of known melting points. The resultant calibration graph is included as Figure 5.9. In most cases, the instrument temperature correction does not significantly affect the conclusions drawn from the data because either the correction necessary is small or because it is relatively insignificant in relation to the absolute values and the uncertainties involved in the readings.

Most observed final melting and homogenization temperatures are likely to be on the low side of the true temperatures since it is more likely to assume that a diminishing phase has disappeared (i.e., completely melted or dissolved) when it actually has not, than the contrary (i.e., to assume the

Figure 5.4

General histograms of all the fluid inclusion data.
Shading represents CO₂ inclusions.

- a) Final melting temperatures.
- b) Homogenization temperatures of CO₂ phases only
mostly in type IB and type IIB inclusions.
See also Figure 5.8.
- c) Homogenization temperatures for all the inclusions
that homogenized. Only about 7% of the inclusions
had homogenization temperatures above 300⁰C, and
these were ignored in the discussion in the text.

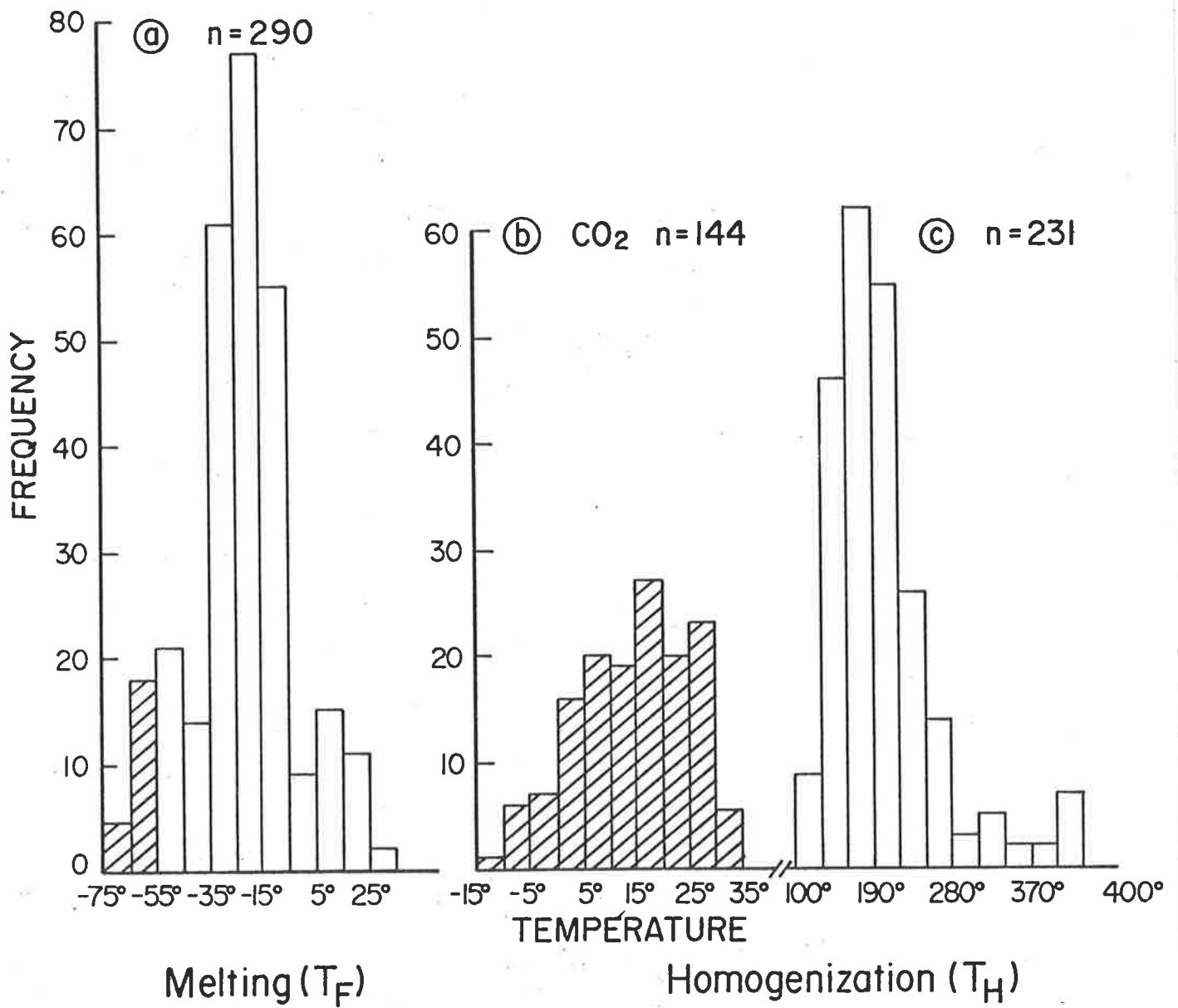


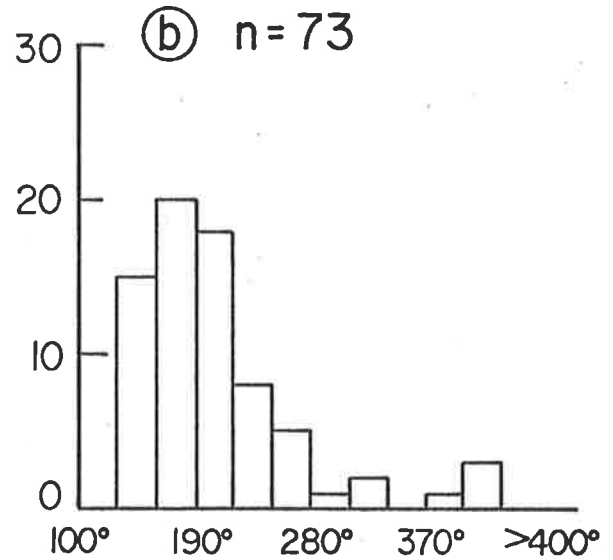
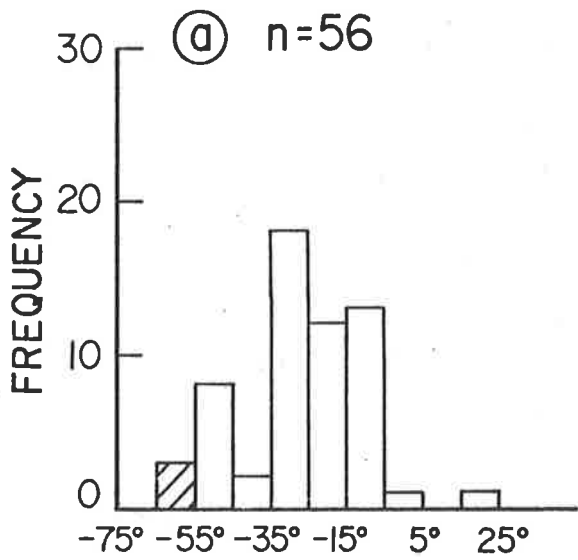
Figure 5.4

Figure 5.5

Melting and homogenization data for inclusions in small (width < 2 cm) and large (width > 6 cm) quartz veins.

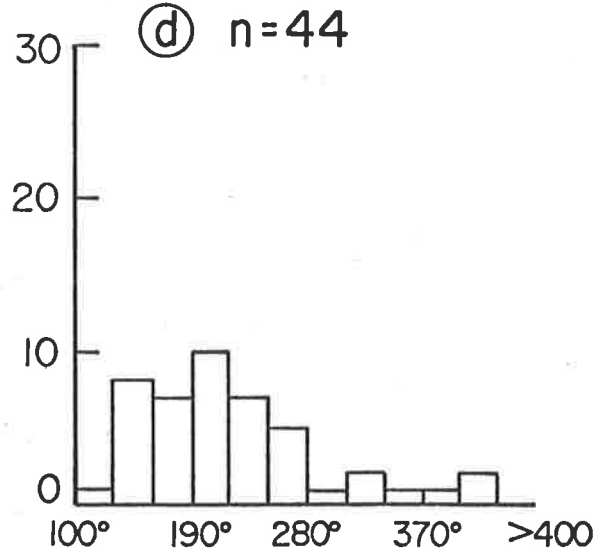
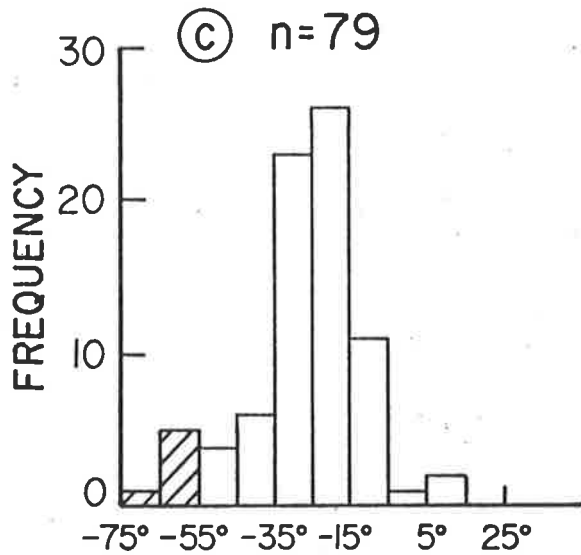
- a) Melting temperatures for inclusions in small veins.
- b) Homogenization temperatures for inclusions found in small veins.
- c) Melting temperatures for inclusions found in large veins.
- d) Homogenization data for inclusions found in large veins.

SMALL VEINS



TEMPERATURE °C

LARGE VEINS



TEMPERATURE °C

Melting (T_F)

Homogenization (T_H)

Figure 5.5

Figure 5.6

Data for inclusions from low and high tungsten areas
(see text, section 5.3).

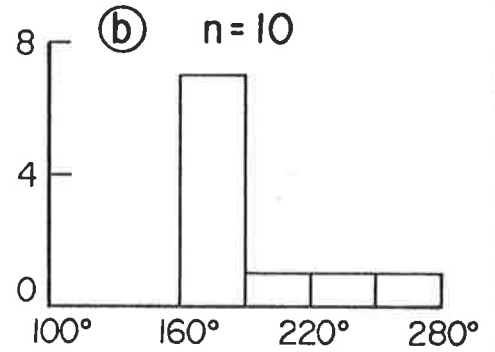
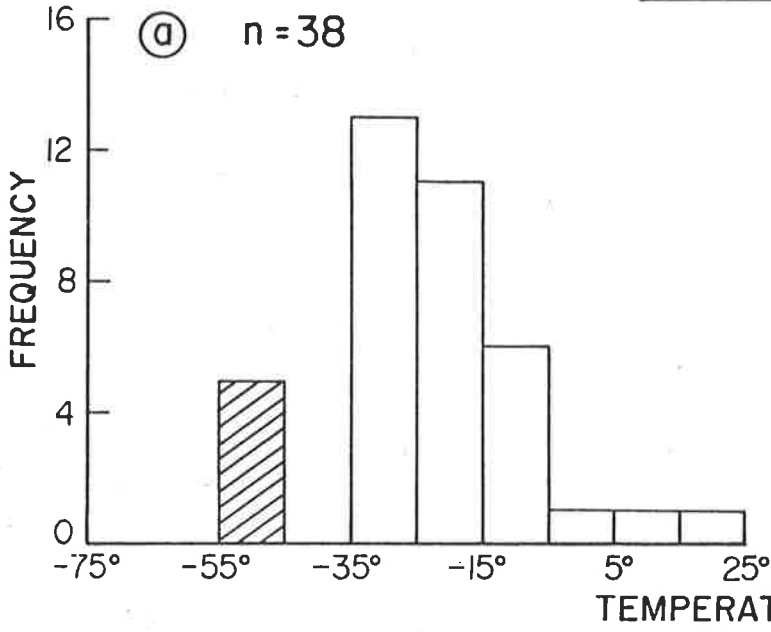
- a) Final melting temperatures for inclusions from tungsten poor zones.

- b) Homogenization temperatures for inclusions from low tungsten areas.

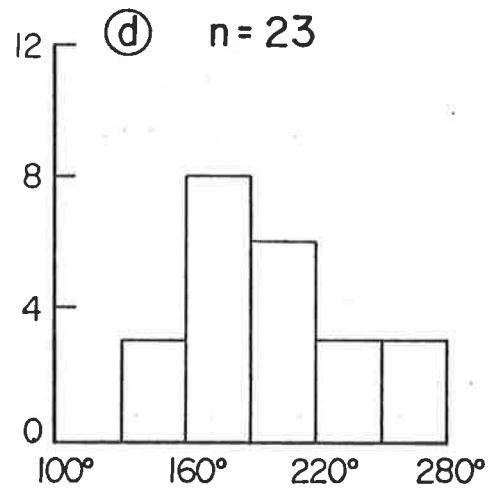
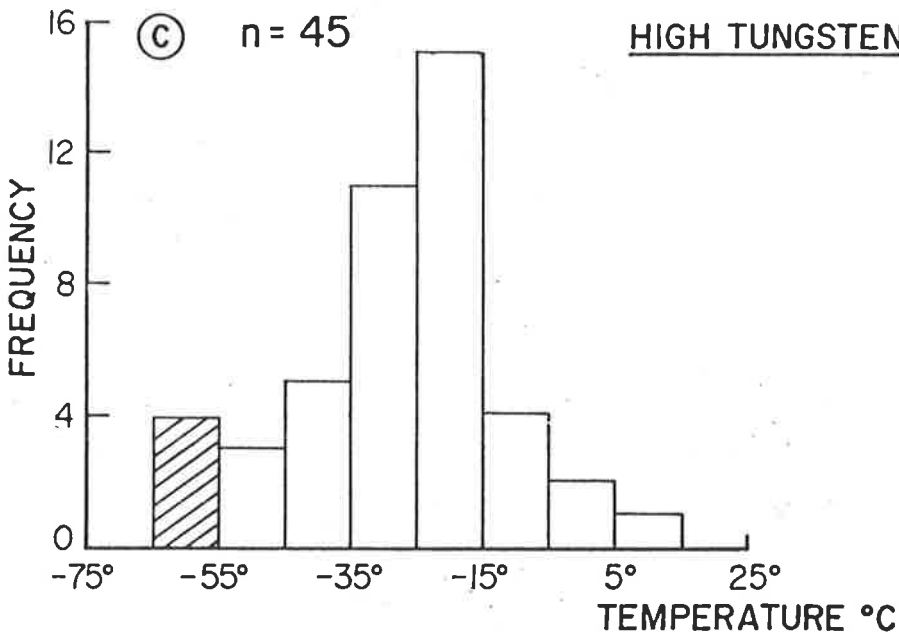
- c) Final melting temperatures for inclusions in samples from high W zones with visible scheelite.

- d) Homogenization temperatures for inclusions in samples from high W areas with visible scheelite.

LOW TUNGSTEN



HIGH TUNGSTEN



Melting (T_F)

Homogenization (T_H)

Figure 5.6

Figure 5.7

Histograms of data for inclusions containing dilute and concentrated solutions (see text, section 5.12.1). It is argued that these represent at least 2 original solutions.

- a) Final melting temperatures for inclusions containing concentrated solutions.
- b) Homogenization temperatures for inclusions with concentrated solutions.
- c) Final melting temperatures for inclusions containing dilute solutions.
- d) Homogenization temperatures for inclusions with dilute solutions.

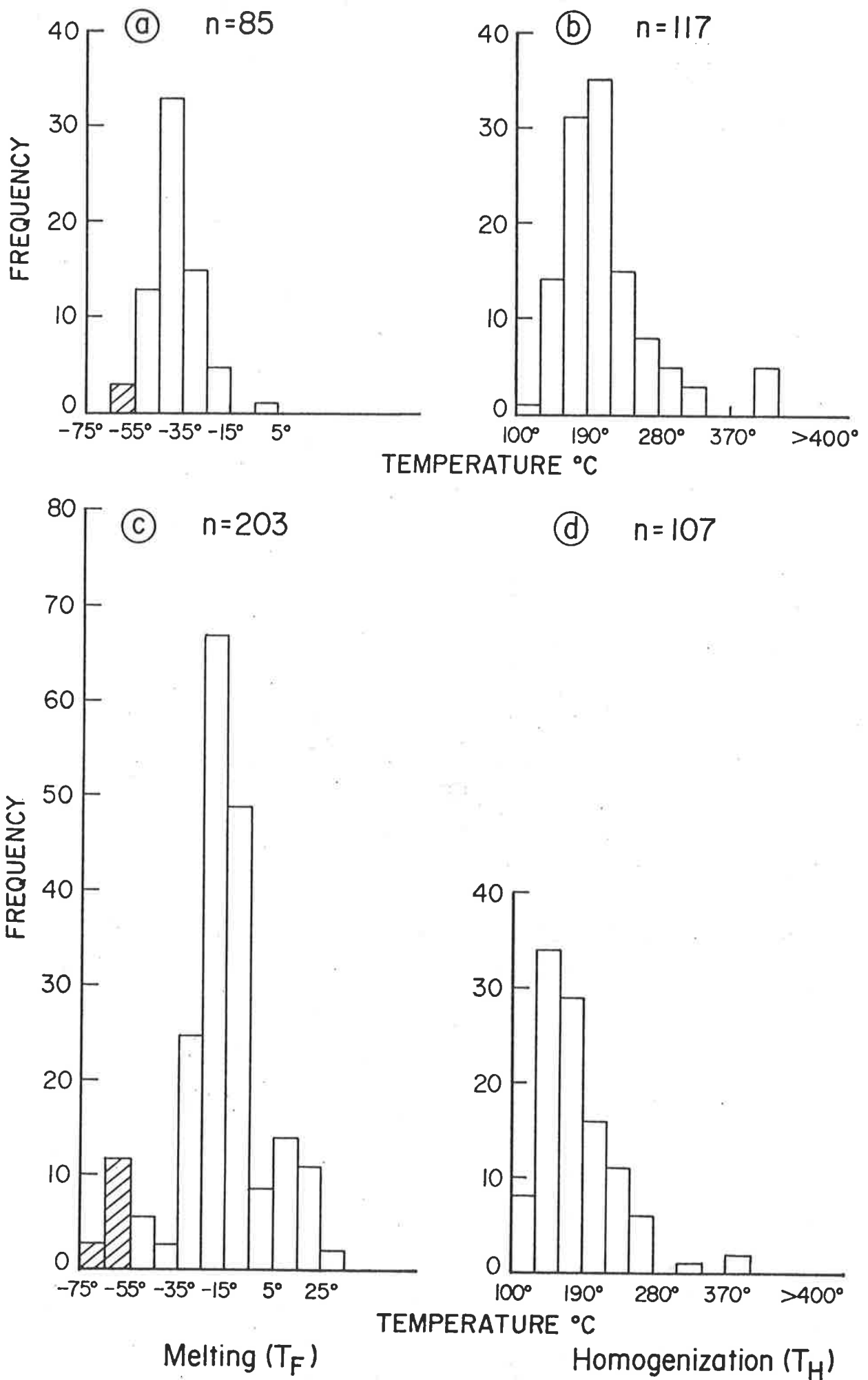


Figure 5.7

Figure 5.8

Homogenization data for carbon dioxide phases only, in carbon dioxide inclusions. This data also implies that there may have been more than one mineralizing solution (see text).

a) Histogram for the homogenization of type IB inclusions.

b) Histogram for the homogenization of CO₂ phases in type IIB inclusions.

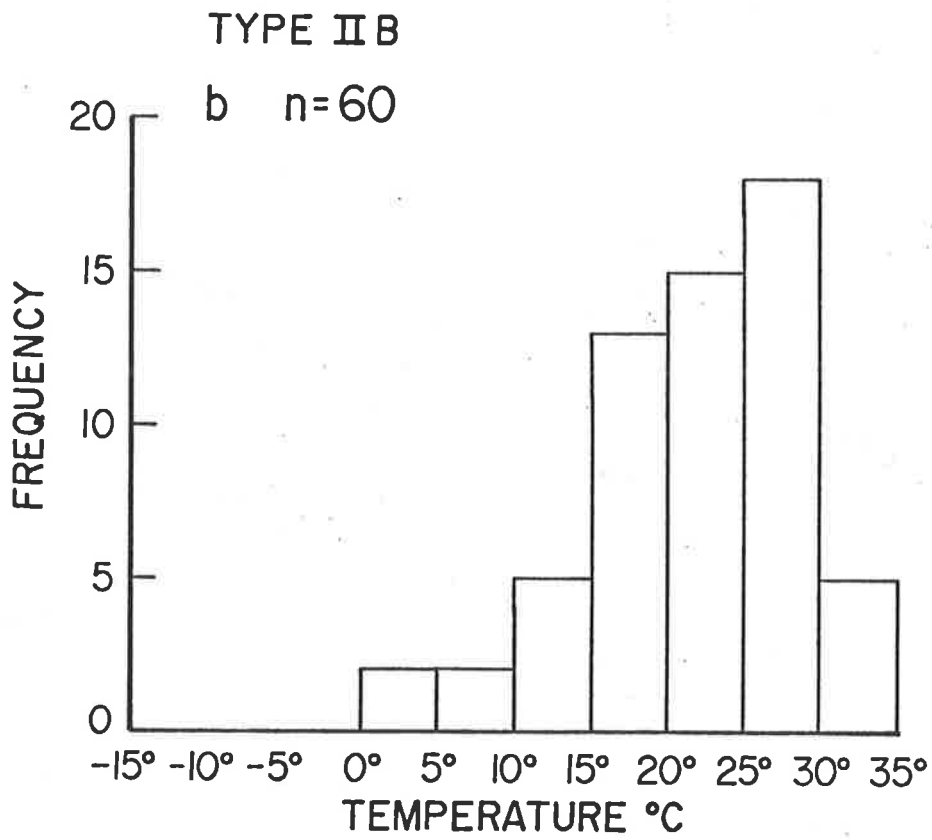
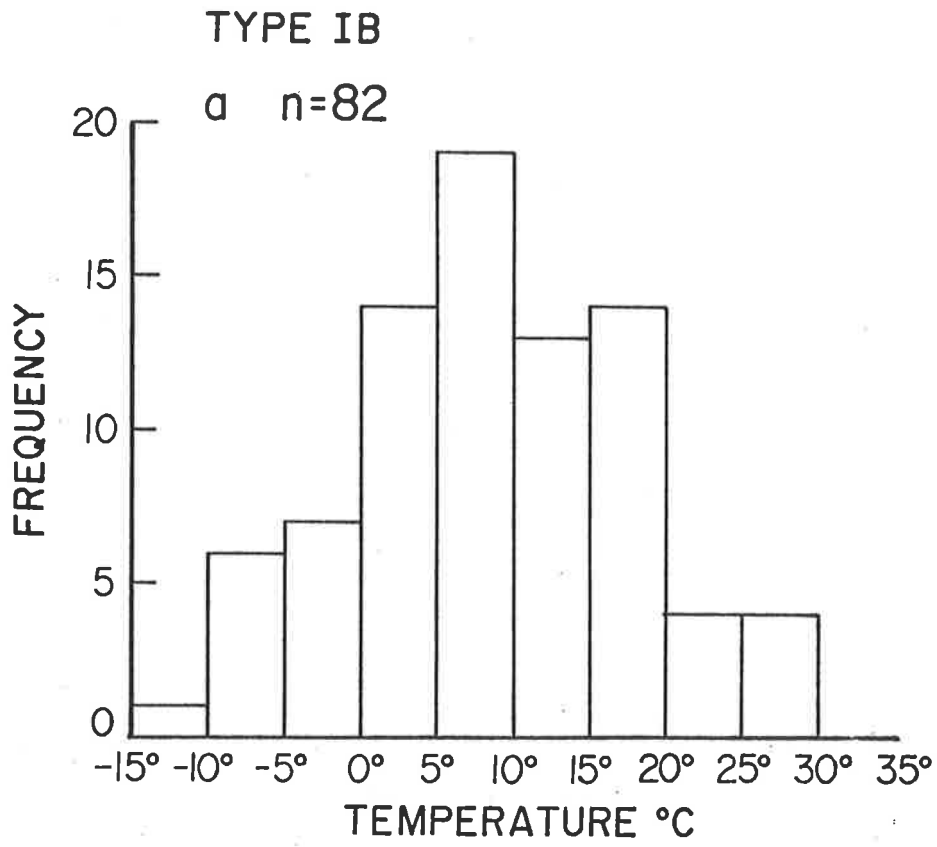


Figure 5.8

phase is still there when it has in fact disappeared). For the first melting temperature, however, the readings are certainly on the high side since the exact temperature of incipient melting could be missed (Appendix 5). The first melting temperature, where recorded, is that temperature at which it was obvious that the inclusion(s) had started melting.

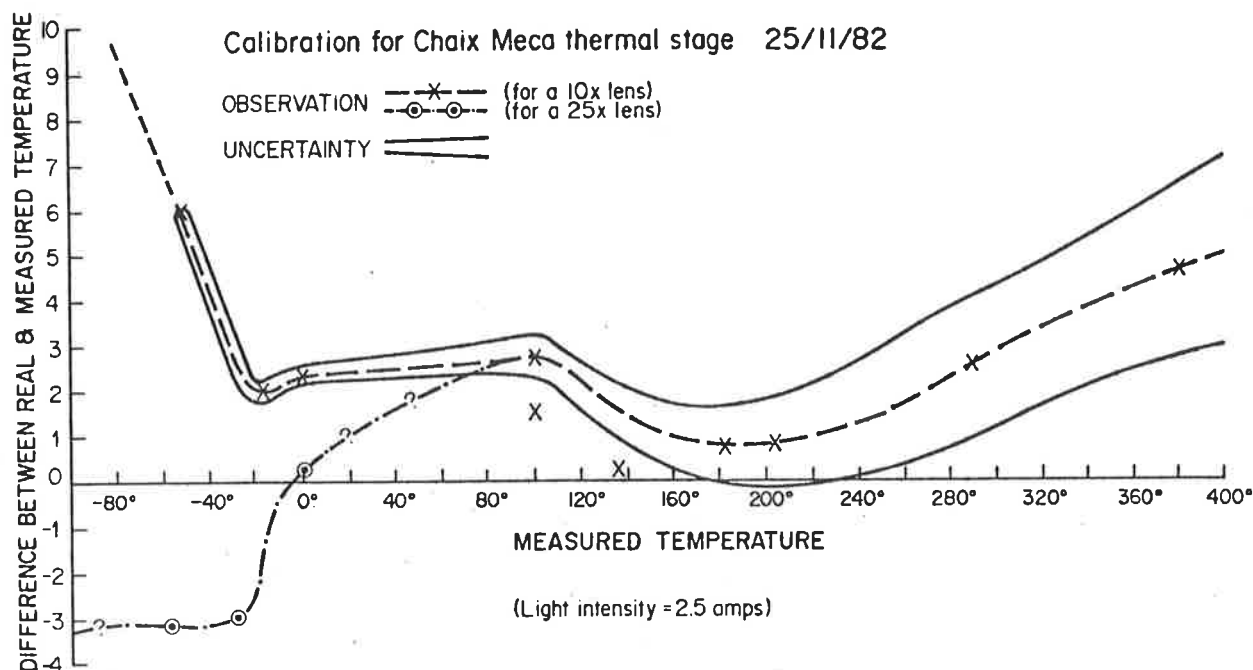


Figure 5.9 (by Evert Bleys)

5.12 Interpretation of the data

5.12.1 Melting data

The first melting temperatures (Appendix 5) indicate the types of cations present while the final melting temperatures give an indication of the amounts of ions present (the salinity) usually stated as NaCl equivalent because NaCl is the most common salt found in fluid inclusions and because the system NaCl-H₂O is the best known.

However, as data are available on several other systems, it is no longer necessary to quote salinities in terms of NaCl equivalents even when it is obvious that Na⁺ is not the dominant cation. In this study, salinities are quoted in terms of CaCl₂ wt.% equivalent since it was established (by fluid inclusion leaching) that CaCl₂ is the dominant salt in the solutions.

Very low first melting points, as low as -76^oC, were recorded and the lowest final melting temperature recorded for a non CO₂-bearing inclusion was -49.4^oC. These figures are indicative of highly saline solutions; -49.4^oC implies salinities of slightly more than 30 wt.% CaCl₂ equivalent

(Figure 5.10). The high salinity of the solutions is also indicated by the final melting temperatures of unidentified hydrates (suspected to be CaCl_2 hydrates). The highest recorded melting temperature of the hydrates is $+28^\circ\text{C}$ and there are several readings of about $+19^\circ\text{C}$. The average final melting temperature for the hydrates is $+12.2^\circ\text{C}$. These three figures correspond to salinities of about 51 wt.% CaCl_2 equivalent, 45 wt.% CaCl_2 equivalent and 40 wt.% CaCl_2 equivalent respectively (Figure 5.10). Thus there can be no doubt that some of the solutions were very concentrated.

On the other extreme, the highest non-hydrate final melting temperature recorded was 0.6°C , which corresponds to almost 0% salts. Thus the inclusion fluids vary in their salinities from practically zero to slightly over 50 wt.% CaCl_2 equivalent. Such a wide range of salinities is believed to be mainly due to several mineralising solutions.

The very low first and final melting points (see Appendix 5) cannot be adequately explained in terms of the system Na-Ca-Mg-Fe-Cl and so, some other cation is indicated. The possible presence of Li salts was suggested (P. Ypma, pers. comm.). Although Li was not detected in the leach samples, the fact that the Mount Mulgine whole rock analyses (Appendix 3) show that the rocks are enriched in Li (Chapter 3, page 36) implies that Li salts may indeed be present.

From the phases present in the inclusions and the way the inclusions behaved during cooling, it was obvious, even without taking readings, that at least two mineralising solutions were present, and this was later confirmed by freezing data and fluid inclusion leach analyses (see Table 5.1). The two have been called the "dilute" and "concentrated" solutions.

Inclusions containing concentrated solutions had abundant daughter minerals and were more difficult to freeze. During cooling their vapour bubbles would sometimes not shrink noticeably. Indeed, there were cases when vapour bubbles actually increased in size on cooling. On freezing, some inclusions did not change much in their appearance so that it was difficult to determine if they were frozen.

On the other hand, inclusions containing dilute solutions were easy to freeze and they contained relatively few or no daughter minerals. Generally, type IV and complex inclusions were not observed in inclusions with dilute solutions. When they froze, they looked earthy-brown and the vapour bubbles were either completely "eliminated" or they were apparently shrunk considerably by the ice due to the small increase in volume of the latter. Also, inclusions with dilute solutions were, more often than not, associated with CO_2 inclusions (see below).

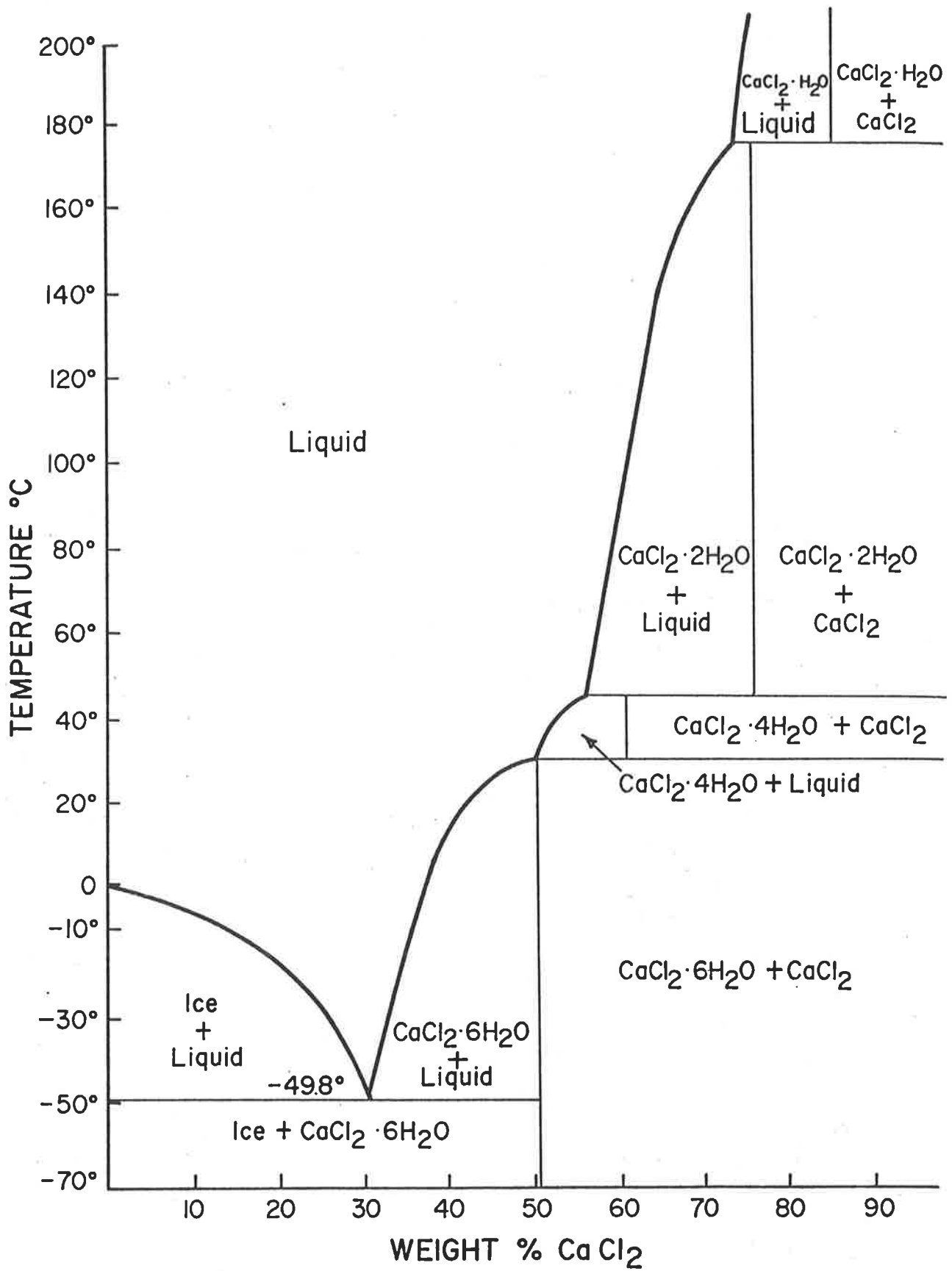


Figure 5.10. Phase diagram of the system CaCl₂-H₂O, below 200°C. (After Fuzikawa, 1982).

The main point here is that there were two demonstrably different liquids represented by inclusions that look different and behave differently on cooling/freezing as described in the preceding two paragraphs. There is no suggestion whatsoever that the so-called dilute and concentrated solutions were the only two solutions. In fact, mineralogical evidence suggests there were more than two mineralizing episodes and thus solutions, but there is no easy way of telling exactly how many.

In any one sample, inclusions with either dilute or concentrated solutions usually dominated and so it was possible to divide the samples into two groups. As Figure 5.7 shows, their data partly overlap.

Most of the final melting temperatures of CO_2 (mainly type IB) inclusions are below -56.6°C (the melting point of pure CO_2) which means that the CO_2 phase must contain some other substance with a lower melting temperature with which it forms solid solution products. Methane is one such substance and its common occurrence in fluid inclusions makes it highly probable that it is present in the inclusions studied. If some of the hydrates observed with melting temperatures above 10°C are CO_2 clathrates, this could further imply the presence of methane (Burruss, 1981). However, the hydrates were thought to be salt hydrates (rather than clathrates) because they were easy to observe and they appeared birefringent. Carbon dioxide clathrates are reported to be difficult to observe and they are also isotropic (Roedder, 1972; Collins, 1979).

5.12.2 Homogenization data

Homogenization temperatures (T_H) are displayed in Figures 5.4 to 5.8 (inclusive). To obtain the temperatures of formation (temperatures of trapping) a pressure-temperature correction must be applied to the homogenization temperatures (Roedder, 1972). The amount of the correction factor necessary depends on the composition of the fluids and on the actual pressure at the time of entrapment. Both must be known to determine the correction factor. Unfortunately, neither the composition nor the pressure were known and so errors of unknown magnitudes are unavoidable in interpreting homogenization data as entrapment temperatures.

Roedder and Bodnar (1980) describe a number of cases when the pressure of entrapment may be obtained from the fluid inclusions themselves. Each of these special cases has some limitations, not the least of which is the fact that the pressure-volume-temperature-composition relationships of the phases involved must be known. But P-V-T-X data are generally incomplete or even lacking for components usually found in fluid inclusions. The system $\text{NaCl-H}_2\text{O}$ is well known because of extensive experimental data (Roedder and

Bodnar, 1980). Since fluids in natural inclusions are hardly ever simple NaCl-H₂O solutions, it becomes all too apparent that the study of fluid inclusions using the available data must involve considerable approximation and extrapolation.

The determination of a pressure-temperature correction was taken seriously because such corrections can be several hundreds of degrees and the amount of correction necessary may be greater than the homogenization temperature itself (Potter, 1977; Roedder and Bodnar, 1980).

5.12.3 Determination of pressure

The problem of determining the pressure of formation and hence the temperature correction, was approached in several ways. Sphalerite geobarometry initially held the greatest promise, but for reasons discussed later, the pressures determined by this method were inconclusive. Pressures obtained were within the wide range of 8.1 ± 0.3 kb to 2.0 ± 0.3 kb. These estimates are probably useful as limiting values, but clearly they are not good enough for the determination of a temperature correction.

Metamorphic minerals and mineral assemblages were then examined. From the minerals it was already known that the metamorphic grade reached was "medium" as defined by Winkler (1979), which is the equivalent of amphibolite facies. From the mineral assemblages in the host rocks the peak temperature of metamorphism would not have exceeded 550°C and it could not have been much less than 500°C. It was then estimated from pressure-temperature information on metamorphic mineral assemblages (Turner, 1980; Winkler, 1979) that the pressure would have been less than about 4 kb. None of the so-called pressure indicator minerals are present.

It was then decided to try the Si⁺⁴ content of muscovite (phengite) in order to estimate the pressure. Velde (1967) has shown that the Si⁺⁴ content of muscovite is mainly dependent on pressure and temperature. The pressure obtained from this method depends, of course, on how accurately the Si⁺⁴ content can be determined and, even more important, on how accurately the temperature can be estimated.

Muscovites, selected from samples which also contain chlorite and/or biotite, were analysed on the electron microprobe. The presence of chlorite and/or biotite means that Mg was available at the time of formation of these minerals and so, the white mica is most likely phengite (or phengitic) rather than pure muscovite. Many analyses were done (see Appendix 4) but those shown in Table 5.2 were the only ones used for pressure estimation.

As discussed above a peak metamorphic temperature of 500°C was estimated to be most reasonable for the mineral assemblages found in these

rocks. There is no evidence to suggest that the temperature during mineralization exceeded this figure. The Si^{+4} contents of the analysed muscovites (phengites) are in Table 5.2. The mean Si^{+4} content is 3.16 and this gives a minimum pressure of 2 kb from Figure 1 of Velde (1967), reproduced here as Figure 5.11. The 2 kb pressure thus obtained is, of course, an estimate, more so because the conditions ($P_{\text{H}_2\text{O}} = P_{\text{total}}$) under which Figure 5.12 was constructed are unlikely to have been realised at Mount Mulgine.

Table 5.2 : Si^{+4} content of phengitic muscovites

Sample number	Analysis point No.	Si^{+4} (atomic wt.%)
251/139.4	(1	3.15
	(2	3.15
	(3	3.16
	(4	3.15
	(5	3.15
	(6	3.15
259/135.1	(1	3.23
	(2	3.21
	(3	3.20
	(4	3.22
22/136.7	(1	3.10
	(2	3.07
	(3	3.08
	(4	3.10
	(5	3.09
	(6	3.48
	(7	3.11
	(8	3.14
	(9	3.11
	(10	3.10

overall mean = 3.16

5.12.4 The pressure-temperature correction

All the methods used to estimate the pressure agree on one point - that the pressure during metamorphism and mineralization was at least 2 kb. This figure was used to calculate a minimum temperature correction necessary for the homogenization temperatures, as follows.

Ignoring the inclusions that had final melting points above zero, the overall average final melting point for all inclusions studied (excluding CO_2 inclusions) is -24°C , which indicates a salinity of 24 wt.% CaCl_2 equivalent (or about 25 wt.% NaCl equivalent, from Figure 4 of Roedder (1962)).

The average homogenization temperature for all the inclusions studied is 187°C (excluding all temperatures above 300°C).

Referring the above data to Figure 6 of Potter (1977), reproduced here as Figure 5.12, shows that a pressure-temperature correction of 180°C should be added to the homogenization temperatures. It must be remembered that this is only an average figure, for strictly, each fluid inclusion would have a unique temperature correction. Ignoring all inclusions with homogenization temperatures above 300°C and still assuming a minimum pressure of formation of 2 kb, then from Potter's (1977) diagrams, all inclusions with up to 25 wt.% salts need temperature corrections in the range of 160°C to about 200°C , depending on their salinities and homogenization temperatures. These are minimum correction figures, obtained using very low (1% NaCl equivalent) to moderate (25% NaCl-equivalent) salinities in the homogenization temperature range obtained; and they can be less only if the pressure was less than 2 kb.

The lowest homogenization temperature recorded was 103°C for an inclusion in fluorite. Assuming a pressure of 2 kb at the time of formation (although unlikely for fluorite - see below), then using the above correction figures, the minimum temperature of formation would have been 263°C . For inclusions in quartz with minimum homogenization temperature of about 135°C , the minimum formation temperature would have been about 295°C , making the same assumptions. For inclusions in scheelite with a mean homogenization temperature of 213°C , the minimum temperature of formation was 373°C , again assuming a 2 kb pressure prevailed and 1% NaCl equivalent salinity.

The maximum temperatures of formation are not as easy to determine because correction curves, similar to those of Potter (1977) for salt concentrations in excess of 25 wt.% and pressures higher than 2 kb, are not available. But if a 2 kb pressure is again assumed and homogenization temperatures above 300°C are excluded, then the maximum formation temperatures (also assuming a 25% NaCl equivalent salinity) would have been around 500°C .

5.13 Homogenization of CO_2 phases

Carbon dioxide inclusions (that is, any inclusion either wholly or partly filled with a CO_2 or CO_2 -rich fluid) were found in most of the samples selected. All such inclusions have a CO_2 -rich vapour phase at some temperature below 31°C . The temperatures at which the CO_2 phases became homogeneous were recorded. The abundance of CO_2 inclusions made this a relatively significant exercise. The readings are in Appendix 5 (Table 5A₍₂₎) and they are summarised graphically in Figure 5.8. All the CO_2 inclusions homogenize in the liquid phase.

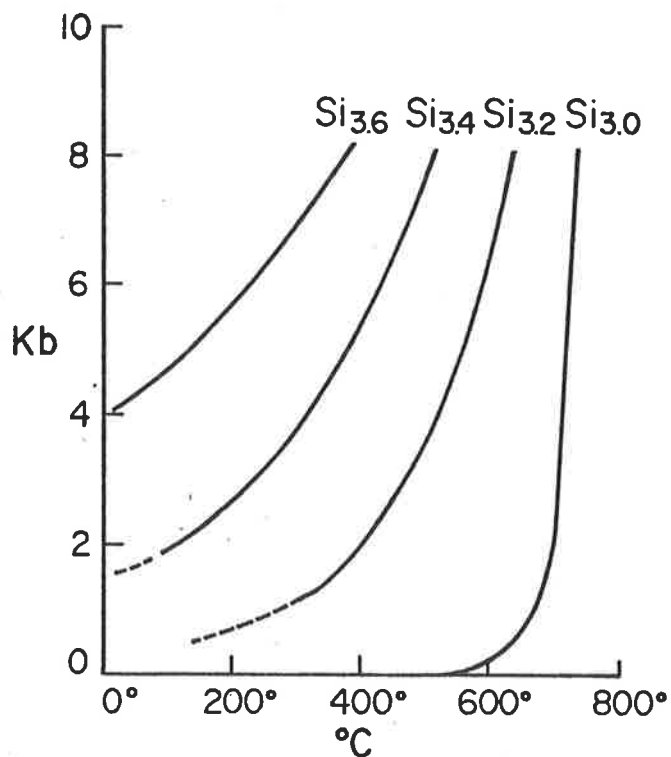


Figure 5.11. Stability curves for various phengite micas of the series $K[Al_2Si_3AlO_{10}(OH)_3] - K[MgAlSi_4O_{10}(OH)_2]$ under conditions of $P_{H_2O} = P_{total}$. The compositions of each mica are represented by the number of Si^{+4} ions present, thus $Si_{3,2} = K[(Mg_{0.2}Al_{1.8})(Si_{3.2}Al_{0.8})O_{10}(OH)_2]$. (After Velde, 1967).

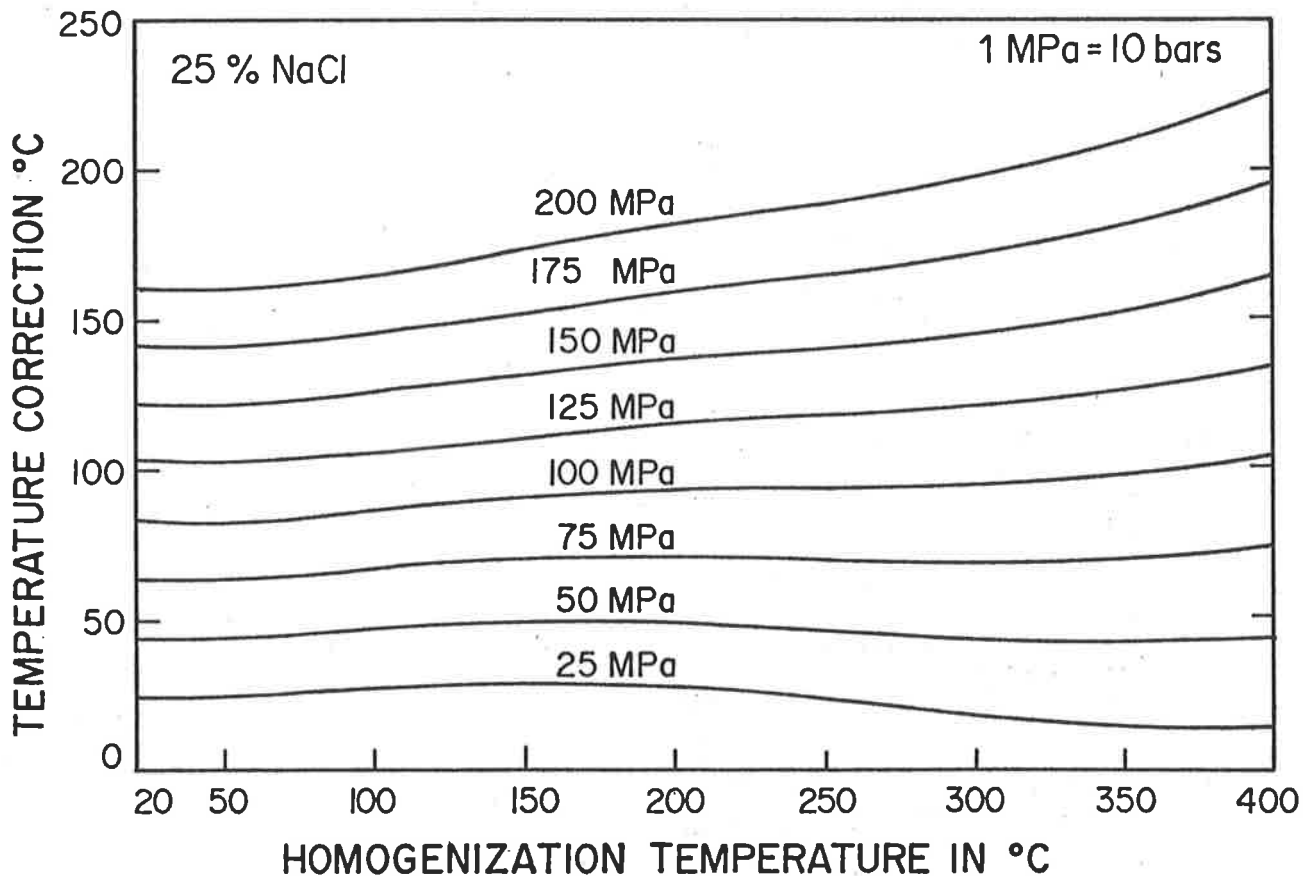


Figure 5.12. Temperature correction for a 25-percent NaCl solution as a function of homogenization temperature and pressure. (After Potter, 1977).

One immediately noticeable feature of these inclusions is their variability. There is a complete range from inclusions wholly filled with CO_2 to inclusions with only about 5 volume % CO_2 . The homogenization temperatures of the CO_2 -rich phases are as variable as the inclusions themselves. Those recorded range from -12.1°C to $+30.6^\circ\text{C}$. The homogenization temperature of CO_2 is dependent on density and pressure. These two variables can be assumed to have been constant for inclusions trapped at about the same time from one homogeneous solution. Pressure is unlikely to have changed much during the formation of any one generation of inclusions and, in any case, from Figure 5.13, it is obvious that pressure changes alone cannot account for the observed variation in homogenization temperatures. Thus the variation in homogenization temperatures appears to be mainly due to different densities of the trapped fluids. But if it is true that there were several generations of fluids, as indicated by various factors discussed earlier in this chapter, then the pressure may have changed between the different generations of fluids. It is, therefore, reasonable to conclude that the variations in homogenization

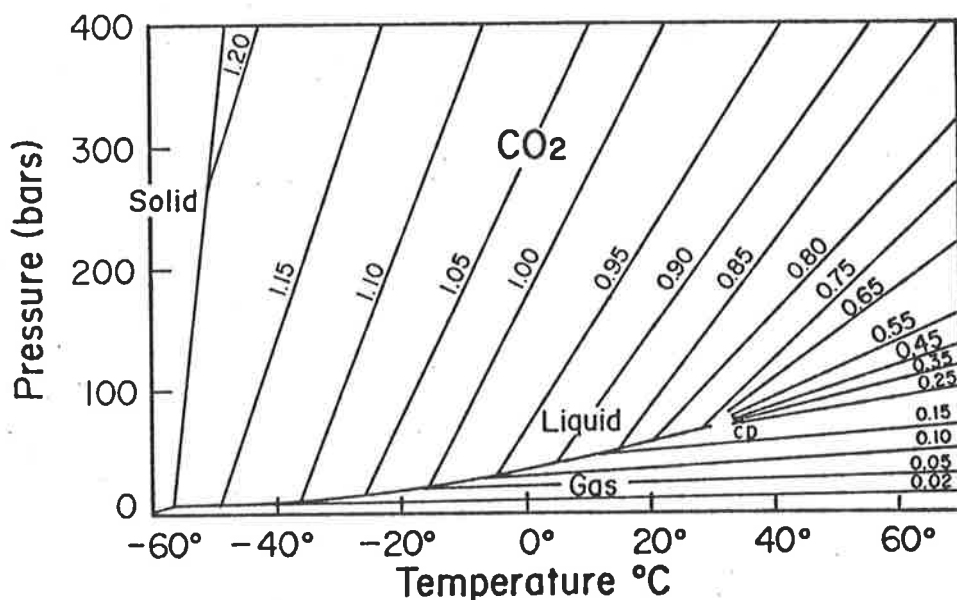


Figure 5.13. Phase diagram for CO_2 , showing densities (g/cc) of several isochores. CP, critical point at 31°C . (After Hollister 1981).

temperature are due to both pressure and density changes.

With very few exceptions, homogenization temperatures of CO_2 -bearing inclusions were determined only for type IB and type IIB inclusions. It was observed that generally type IB inclusions homogenized at lower temperatures than type IIB inclusions (compare Figures 5.8a and 5.8b).

The mean of homogenization temperatures for type IB is 11.4°C^*

* This figure is for positive temperatures only. If the negative figures are included the mean is 8.6°C (see Appendix 5, Table 5A(2)).

and that for type IIB (CO_2 phases only) is 22.4°C . These figures correspond to densities of 0.87g/cc and 0.78g/cc respectively (from Figure 5.13). This range is within the limits possible for different fluid composition, without having to invoke different pressures (P. Ypma, pers. comm). Thus the CO_2 fluid inclusion data also imply that there were at least 2 mineralizing fluids.

As already said, a few type IIB inclusions were completely homogenized. The highest complete homogenization temperature for such inclusions was 274°C and the lowest was 178°C . The average is 227°C . With such low homogenization temperatures, the salinity of the aqueous solutions in these inclusions cannot be high (see Figure 1.3 in Hollister, 1982). The limited data obtained on type IIB inclusions indicate that this is indeed the case. The data are limited because the melting in type IIB inclusions, especially the last melting, proved very difficult to observe. In most cases, information as to whether melting was still going on or had probably ended was obtained from the liquid CO_2 -aqueous solution interface; if it was irregular, then melting was still in progress, and if it was smooth, then melting had probably ended. Thus a range of temperature was recorded rather than a specific reading. In only a few cases was melting ice actually observed, enabling a specific temperature reading to be noted. From the few readings and the temperature ranges recorded (Appendix 5), the salinity of these (type IIB) inclusions is less than 8 wt.% CaCl_2 equivalent; probably much less since it is possible that the ice was still melting when it was assumed to have finished.

5.14 Discussion

A more general discussion will appear in the final chapter, but at this point a brief discussion of the results of the fluid inclusion study, with the aims of the study in mind, is warranted.

After such a report, the following are some of the more serious questions one might ask.

1. It is possible that most, or even all, of the inclusions studied were secondary. How seriously can one take the results obtained?
2. It has been assumed in the pressure estimations that most of the veins formed during metamorphism; what if they formed after metamorphism?

The first question has already been partly answered in the text. No significant differences were observed between data that were obtained randomly, the data that were obtained from inclusions strongly suspected as being primary and the data for inclusions in fluorite which were considered convincingly primary. In the (unlikely?) event that all the inclusions were

secondary, the data are still useful even if only as limiting values (maxima or minima). It is not unreasonable to assume that some of the necked down inclusions were originally primary. The mean of a lot of readings taken on such inclusions would be close to the actual mean reading that would have been obtained from the primary inclusions themselves, assuming no leakage occurred.

For the second question, if many of the veins formed after metamorphism, then the pressure estimates (and therefore the pressure-temperature correction) could be in error. Some of the mineral textures indicate that the "intermediate" minerals (see Figure 4.1), which comprise the bulk of the mineralization were subject to the metamorphism that affected the host rocks. Collins (1975) states that much of the scheelite in the nearby Hill deposit formed during the regional metamorphism of the rocks. Finally, although this might be a coincidence, the estimated maximum temperatures of formation (assuming a pressure of 2 kb during metamorphism) are in reasonable agreement with the estimated peak metamorphic temperature.

The above statements should not be taken to mean that all veins were syn-metamorphism. It has already been hinted that it is unlikely that the pressure during fluorite formation was as high as 2 kb. This is mainly because fluorite is a late mineral and inclusions in it have the lowest homogenization temperatures and some of the lowest salinities (see Appendix 5). If fluorite had formed before or during peak metamorphism, the inclusions in it would never have survived the peak metamorphic heat - they would have decrepitated; unless, of course, the pressure was much higher than has been estimated. It is believed that the fluorite and quartz-fluorite veins formed much later after metamorphism, when the pressure and temperature were lower. It is difficult to estimate the temperature of formation of fluorite and inclusions in it without information about the pressure that prevailed, but it is unlikely to have exceeded about 250°C. The vapour bubbles in some of the type IIA inclusions in fluorite were observed in rapid brownian movement at room temperatures (20-30°C) and this is an indicator of low entrapment temperatures (Mayer, 1976).

Although the variations in inclusion types and data have been mainly attributed to different generations of fluids and necking down, it is also possible that the variations are partly due to phase separation resulting in a CO₂-rich fluid phase and a concentrated brine (P. Ypma, pers. comm.). The phase separations, caused by a drop in temperature and pressure, may be repetitive, resulting in a variety of inclusion types.

While concluding, it is appropriate to recapitulate the aims of the study (see page 74) and relate them to the findings.

Scheelite and related mineralization at Mount Mulgine formed from moderately to highly saline solutions at moderately low pressures and fairly high temperatures. There is evidence that several mineralising solutions were involved, with salinities ranging from less than 5 wt.% CaCl_2 equivalent to as much as 50 wt.% CaCl_2 equivalent. The important homogenization temperature range is 160°C to about 280°C (Figure 5.4) which corresponds to formation temperatures of 340°C to 460°C . A pressure-temperature correction of 180°C , deduced from a minimum indicated pressure of 2 kb during metamorphism has been generally applied. This pressure-temperature correction is probably too large for the later fluorite and quartz veins. From mineral assemblages, it was deduced that peak metamorphic temperatures are unlikely to have exceeded 500°C .

The observed molybdenite-scheelite zoning does not necessarily mean that the two minerals were deposited from chemically different solutions. Figure 5.5 shows that the smaller veins (more associated with scheelite) have inclusions with slightly more saline solutions (and correspondingly slightly higher homogenization temperatures) than inclusions from the larger veins (compare the mean final melting points -28.3°C and -25.2°C) which are more associated with molybdenite. A t-test applied to these means indicated that they are from the same population, at the 5% significance level. The t-test was also applied to the mean homogenization temperatures and gave the same result.

If molybdenite and scheelite were deposited from one solution at about the same time, then some other explanation for their distribution must be sought. However, the above conclusion does not preclude the possibility that scheelite and molybdenite could have been deposited from separate but chemically similar solutions at different times. The facts that powellite (CaMoO_4) has not been observed, that scheelite does not contain Mo which usually proxies for W (see Table 4.2) and that there is no significant correlation between Mo and W (Figure 5.3) all indicate that molybdenite and scheelite may have been deposited from different (i.e., separate) solutions. But as just shown, the solutions were generally similar, chemically.

Data for inclusions in quartz from tungsten-rich and tungsten-poor areas are shown in Figure 5.6. Inclusions from tungsten-poor areas are less saline and their homogenization temperatures are correspondingly lower than those of inclusions from W-rich areas (22 wt.% CaCl_2 equivalent and 176°C compared to 26 wt.% CaCl_2 equivalent and 216°C). The difference in mean salinities (only 4 wt.% CaCl_2 equivalent on the average) is not great and so the t-test was again applied to the mean final melting temperatures and the mean homogenization temperatures. In both cases the test showed that there

is a less than 5% chance that the means come from the same population (i.e., the hypothesis that the means are the same was rejected at a 5% significance level).

Although this difference may be real as suggested by the t-tests, it is unlikely to be of immediate exploratory value since one cannot tell from looking at the inclusions or even taking a few measurements. One positive result from the above exercise is that the conditions of formation of scheelite are more closely defined. The solutions associated with scheelite mineralization averaged about 26 wt.% CaCl_2 equivalent and the temperature of formation of the scheelite was 396°C , on the average, assuming a pressure of 2 kb.

It is not possible, from the fluid inclusion data alone, to say what part the Mount Mulgine Granite played during mineralization. This question is examined further in the final chapter.

CHAPTER 6 : SULPHIDE GEOCHEMISTRY:
SULPHUR ISOTOPE STUDY AND SPHALERITE GEOBAROMETRY

6.1 Introduction

Sulphur isotope work was undertaken for the following reasons: The first and most important is that the results would indicate the most likely source of sulphur and this would put constraints on the source of mineralization in general, and the second is that the temperature of formation might be estimated from the sulphur isotope fractionation between co-existing sulphides and this would serve as a check on the temperatures of formation obtained by other means e.g., fluid inclusion studies (Chapter 5). Thirty pyrite and pyrrhotite samples were selected and analysed as described below.

Since there was no single reliable method based on silicate mineralogy/geochemistry that could be used to determine the pressures that prevailed during metamorphism and mineral deposition, an attempt was made to apply the sphalerite geobarometer to the Mount Mulgine mineralization. This attempt is reported in a later section.

6.2 Sulphur isotope study

6.2.1 Sample selection, preparation and analytical techniques

Because of the modest aims of this study mentioned above, sample selection was not a problem. Any sample with relatively abundant and preferably coarse sulphides was suitable. Samples were selected such that as much of the Trench deposit (volume) as possible was covered. The most abundant sulphide is pyrite and this is reflected in the number of samples of the mineral collected. Pyrrhotite samples were also selected wherever possible.

Coarse sulphides were preferable because the coarser they are the easier it is to separate them from the "gangue". For most of the samples, the sulphides were coarse enough to be extracted with a dental drill. The drilling was done on polished surfaces of the sulphides under a low power microscope so that impurities (inclusions) could be avoided. In about one third of the samples, the sulphides were too small for drilling. These samples were crushed to -150, +200 mesh, washed and dried and the sulphides separated on a Frantz Isodynamic Magnetic Separator. The separated sulphide concentrates were checked for impurities by preparation of polished grain mounts. Except for sample 313/98.8, which had about 5% impurities (mostly molybdenite and silicates), the rest of the samples were estimated (visually) to have less than about 1% impurities.

The "pure" sulphides thus obtained were oxidised to produce SO_2 gas by cuprous oxide. For each sample, an intimate mixture, prepared by grinding a weighed amount of the sulphide with excess cuprous oxide (about three times as much cuprous oxide as the theoretical amount required for complete oxidation) was roasted in a previously evacuated tube for 15 minutes at 900 - 1000°C. Impurities, mainly CO_2 and water vapour, were separated from the SO_2 by fractional distillation. The pressure of the SO_2 gas was then measured using a manometer before collecting and sealing the gas in a sample tube. The gas was later released and analysed on a Micromass 602E mass spectrometer. Repeat analyses indicate a precision of $\pm 0.1\%$ for the analyses.

6.2.2 Theoretical background

Before presenting and attempting to interpret the results of the sulphur isotope study, it is appropriate to briefly cover the theoretical basis for such studies.

Stable isotope geochemistry in general is concerned with measurement of changes in isotope ratios. For comparison purposes, the isotope ratio changes, which are usually small, must be measured relative to an arbitrary international standard. The accepted unit of sulphur isotope ratio measurement is the delta-value $\delta^{34}\text{S}$ given in per mil (‰). The $\delta^{34}\text{S}$ -value is defined as

$$\delta^{34}\text{S}(\text{‰}) = \frac{{}^{34}\text{S}/{}^{32}\text{S}(\text{sample}) - {}^{34}\text{S}/{}^{32}\text{S}(\text{standard})}{{}^{34}\text{S}/{}^{32}\text{S}(\text{standard})} \times 1000$$

The standard for sulphur isotope ratios is troilite (FeS) from the Cañon Diablo iron meteorite whose ${}^{32}\text{S}/{}^{34}\text{S} = 22.220$ (Kajiwara and Krouse, 1971).

Until the late nineteen sixties, sulphur isotope studies essentially involved the determination of the variability in $\delta^{34}\text{S}$ values from "magmatic" values (about 0 ‰). Because many igneous rocks have $\delta^{34}\text{S}$ values around 0 ‰, any mineral that had $\delta^{34}\text{S} \approx 0$ was interpreted to have formed by crystallization from a magma or precipitation from a magmatic hydrothermal fluid. Similarly, if the $\delta^{34}\text{S}$ values deviated considerably (e.g., more than 10 ‰, Ohmoto and Rye, 1979) the deposits were interpreted as biogenic. This interpretation was based on a few assumptions, the most important of which is that the isotopic composition of the minerals was solely dependent on, and accurately reflected the isotopic composition of the mineralizing fluids. It was Sakai (1968) who first showed that this assumption was not always correct - that the isotopic composition of minerals was also dependent on temperature and pH of the hydrothermal fluids. Since then, several authors have continued to refine and expand Sakai's (1968) work (e.g., Kajiwara et al, 1969; Kajiwara and Krouse, 1971; Ohmoto, 1972).

It is now known that the sulphur isotopic composition of the minerals depends on a number of factors, the most important being temperature, pH, oxygen fugacity (fO_2) and total sulphur isotopic composition ($\delta^{34}S_{\Sigma S}$) of the fluid and that the $\delta^{34}S$ values of individual minerals can be very different from $\delta^{34}S_{\Sigma S}$. In short, interpretation of sulphur isotope data is not as simple as it was originally thought and for meaningful interpretations, sulphur isotope studies must be coupled with detailed geologic, mineralogic and other geochemical studies (Rye and Ohmoto, 1974).

6.2.3 Sulphur isotope data and their interpretation

All the sulphur isotope data are in Table 6.1. The data are presented in terms of the conventional per mil deviations ($\delta^{34}S$) relative to the Canon Diablo meteoric standard.

6.2.3.1 Geothermometry

The sulphur isotope fractionations between sulphur-bearing species are a function of temperature and hence sulphur isotope geothermometry is based on the equilibrium sulphur isotope fractionations between co-existing species (Rye and Ohmoto, 1974). The temperature (T) in degrees Kelvin is given by

$$T(K) = \sqrt{\frac{A}{1000 \ln \alpha}} \approx \sqrt{\frac{A}{\Delta^{34}S}}$$

where α is the isotopic fractionation factor between the pair of sulphur-bearing phases and $\Delta^{34}S$ is the isotopic enrichment factor (which is the difference between the $\delta^{34}S$ values for the pair of minerals under consideration) and A is a constant for that pair. In this study, pyrite (py) - pyrrhotite (po) pairs were used and so,

$$\Delta^{34}S_{py-po} = \delta^{34}S_{py} - \delta^{34}S_{po} \quad (\text{see Table 6.1}).$$

The equation used for pyrite-pyrrhotite fractionation is that given by Ohmoto and Rye(1979), viz.

$$T(K) = \frac{0.55 \times 10^3}{(\Delta^{34}S)^{\frac{1}{2}}}$$

Only three pyrite-pyrrhotite pairs suitable for geothermometry were obtained from the samples collected. In these pairs the sulphides were in physical contact and, there being no evidence to suggest the contrary, equilibrium was assumed to have been attained. Both and Smith (1975) found that $\Delta^{34}S$ measurements on isolated mineral pairs may not be meaningful in terms of geothermometry. This is, presumably, due to disequilibrium between the sulphides, an explanation which is consistent with the findings of Scott et al (1977) who showed that equilibrium domains may be very small, "perhaps not much

larger than a polished section".

Of the three pyrite-pyrrhotite pairs, one had a negative $\Delta^{34}\text{S}_{\text{py-po}}$ value (a physical impossibility under equilibrium conditions) and was therefore eliminated. The other two samples, 276/131.05 and 289/123.2, gave temperatures of 505°C and 730°C respectively. The $\delta^{34}\text{S}$ values have an uncertainty of 0.1‰ which means $\pm 0.2\%$ in the $\Delta^{34}\text{S}$ values. This gives a range of 385-730°C for sample 276/131.05 and 505°-1465°C for sample 289/123.2. The upper limits of these temperature ranges, especially that of the latter, are unlikely. Pyrite from sample 289/123.2 gave a low SO_2 yield (79%) and this may be related to the wide temperature range obtained.

In view of the limited data and the sensitivity of the pyrite-pyrrhotite sulphur isotope temperature estimates to very small errors in measurement of $\Delta^{34}\text{S}$ values, it is not possible to arrive at a specific temperature for pyrite-pyrrhotite equilibrium. The temperature ranges indicated by the sulphur isotope data are, however, generally in accord with the range of temperatures estimated from fluid inclusion studies in quartz, viz. 300-500°C (see section 5.12.4).

6.2.3.2 Source of the sulphur

The sulphur isotopic composition of minerals can be used to determine the $\delta^{34}\text{S}_{\Sigma\text{S}}$ value and the source of the sulphur only when the temperature, $f\text{O}_2$, and pH conditions of the ore-forming fluids are known (Ohmoto, 1972). In this case, the temperature may be considered as known but $f\text{O}_2$ and pH are not and so, $\delta^{34}\text{S}_{\Sigma\text{S}}$ cannot be determined. However, in the following two paragraphs it is suggested that the $\delta^{34}\text{S}_{\Sigma\text{S}}$ value may be close to the $\delta^{34}\text{S}$ values of the individual minerals at Mount Mulgine.

At temperatures $\geq 400^\circ\text{C}$, sulphur species are dominated by H_2S and SO_2 (Ohmoto and Rye, 1979). All indications are that these are the temperatures that prevailed during mineralization at Mount Mulgine. In view of the fact that sulphates were neither observed in this study nor have they been reported, it seems reasonable to assume that H_2S was the dominant sulphur species. Conditions cannot have been very oxidising since there is no primary hematite. Figure 6.1 shows that the relative order of ^{34}S enrichment (among the sulphur species) is sulphate $\gg \text{H}_2\text{S} \approx$ sulphide minerals $> \text{S}^{2-}$ and therefore, if H_2S predominates, sulphide minerals precipitating from solutions would exhibit $\delta^{34}\text{S}$ values similar to the $\delta^{34}\text{S}_{\Sigma\text{S}}$ value (Ohmoto, 1972, p. 563). At temperatures much higher than 400°C, the relative enrichment factor between H_2S and the

Table 6.1 : Sulphur isotope data

Sample No.	Mineral	$\delta^{34}\text{S}(\text{‰})$	$\Delta^{34}\text{S}_{\text{py-po}}(\text{‰})$	Temp. ($^{\circ}\text{C}$)
276/131.05	(pyrite (pyrrhotite	0.5) 0.0)	0.5	505
259/108.92	(pyrite (pyrrhotite	0.5) 0.6)	-0.1	-
259/108.50	pyrrhotite	0.9		
71/123	pyrite	0.5		
264/82.6	pyrite	0.5		
315/112.4	pyrite	0.6		
289/123.2	(pyrite (pyrrhotite	0.3) 0.0)	0.3	730
70/126.4	pyrite.c	1.1		
71/144	pyrite	-0.4		
273/109	pyrite.c	0.5		
276/126.75	pyrite.c	0.3		
313/98.8	pyrite.c	-0.4		
314/218.5	pyrite.c	1.5		
252/185.5	pyrite	1.4		
264/54.05	pyrite	0.3		
255/145.3	pyrite	-0.3		
276/129.93	pyrite	0.3		
252/126.1	pyrite	-0.3		
301/142	pyrite.c	0.0		
259/99.35	pyrite	0.1		
274/67.7	pyrite	-0.2		
51/125.0	pyrite	-0.8		
268/67.3	pyrite(repeat)	0.6		
252/158.5	pyrite(repeat)	0.7		
313/61.3	pyrite	-1.2		
51/108	pyrite	1.8		
268/35.84	pyrite(repeat).c	0.9		
70/150	pyrite	0.8		

c = concentrate (mineral separated magnetically after crushing the sample). The other samples were separated with a dental drill.

The $\delta^{34}\text{S}$ values for the samples marked "repeat" are means for 2 separate analyses of the same sample.

sulphide minerals is even smaller (Figure 6.1) and so, $\delta^{34}\text{S}$ values would be closer to $\delta^{34}\text{S}_{\text{H}_2\text{S}} \approx \delta^{34}\text{S}_{\Sigma\text{S}}$.

The assemblage pyrite-pyrrhotite-magnetite is rare at Mount Mulgine and only in samples 71/67.4 and 22/61.08 were the minerals observed in the same polished thin section. Although the three minerals were not all observed in contact in these two samples, it can be assumed that they formed at or near their (pyrite-pyrrhotite-magnetite) triple point as shown in Figure 6.2. The $\delta^{34}\text{S}_{\text{H}_2\text{S}}$ values near the triple point are very close to the $\delta^{34}\text{S}_{\Sigma\text{S}}$ value (0 per mil in the diagram). This further implies that $\delta^{34}\text{S}$ values of the individual minerals at Mount Mulgine are close to $\delta^{34}\text{S}_{\Sigma\text{S}}$.

As can be seen in Table 6.1, $\delta^{34}\text{S}$ values for the sulphides measured are zero or close to zero (the overall mean is 0.4‰ and the maximum deviation is 1.8‰). From the previous paragraphs, these values are approximately the

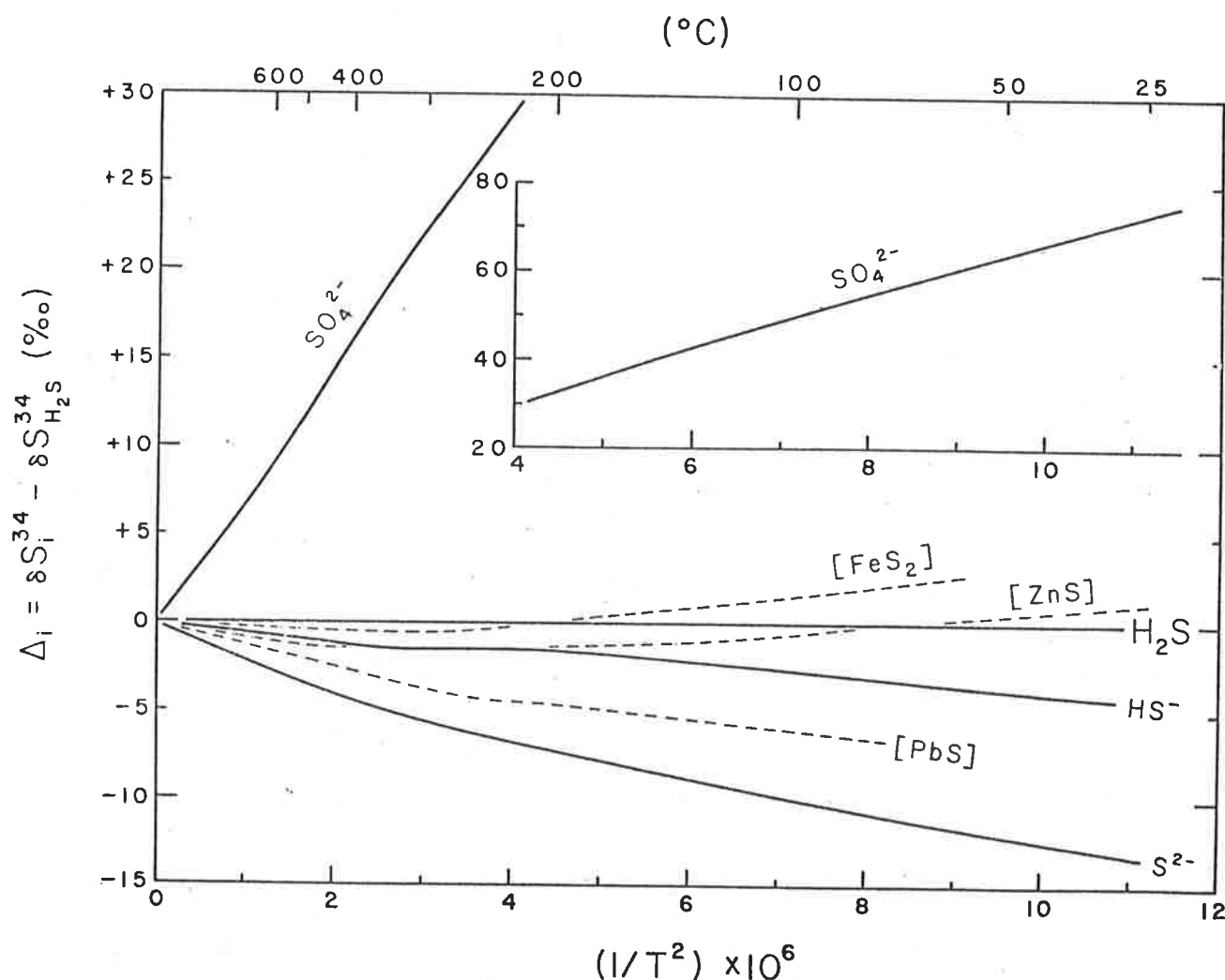


Figure 6.1. Isotopic enrichment factors for important sulphur species. (After Ohmoto, 1972).

same as $\delta^{34}\text{S}_{\Sigma\text{S}}$ for the source. Therefore a magmatic source for the sulphur is indicated (Ohmoto and Rye, 1979, So et al, 1983) which is consistent with the mineralization having been derived from the associated granites/granitoids, or their source.

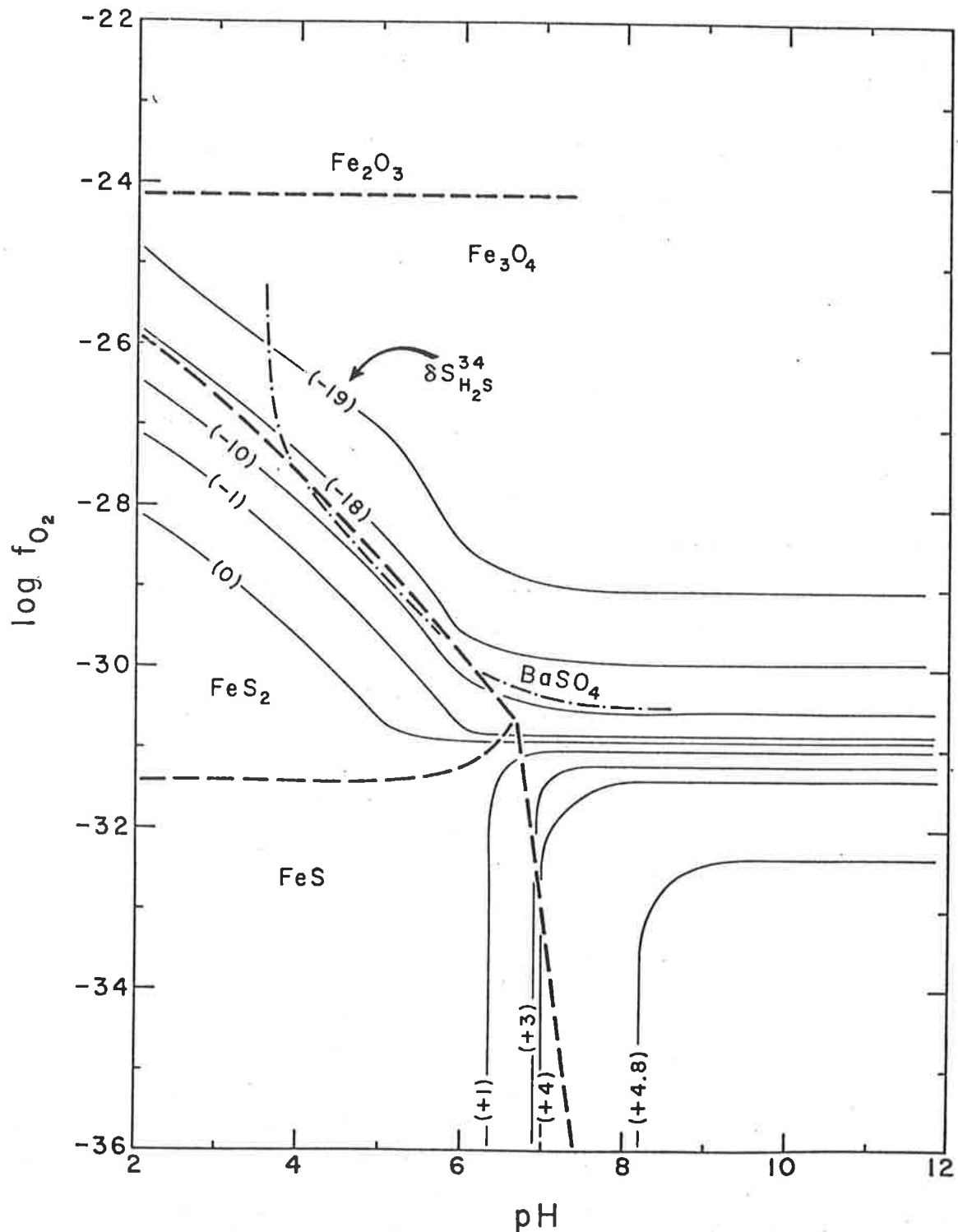


Figure 6.2. Comparison of the positions of δS^{34} contours with the stability fields of Fe-S-O minerals and barite. $T = 350^\circ\text{C}$ and $I = 1.0$.

—: δS^{34} contours. Values in () are for H_2S at $\delta\text{S}^{34}_{\text{R}} = 0\text{‰}$.
 - - - : Fe-S-O mineral boundaries at $\Sigma\text{S} = 0.01$ moles/kg H_2O .
 - · - · : barite soluble/insoluble boundary at $m_{\text{Ba}^{2+}} \cdot m_{\text{S}^{2-}} = 10^{-3}$.
 (After Ohmoto, 1972).

6.3 Sphalerite geobarometry

6.3.1 General remarks

Sphalerite geobarometry has been applied in the investigation of many sulphide deposits and continues to be applied despite the fact that it does not always give reasonable pressure estimates. Most of the problems encountered with sphalerite geobarometry have been attributed to low temperature equilibration or re-equilibration in the Zn-Fe-S system (Groves et al, 1975; Bristol, 1979; Sangameshwar and Marshall, 1980).

The theory behind sphalerite geobarometry is straightforward and was first evolved by Barton and Toulmin (1966). Later work, mainly by Scott and Barnes (1971), Scott (1973, 1976), Lusk and Ford (1978), Hutchison and Scott (1981) and Kissin and Scott (1982) has established the theoretical and experimental basis for this geobarometer. Briefly, the FeS content of sphalerite is a function of temperature, pressure and the FeS activity (a_{FeS}). When sphalerite forms in equilibrium with pyrite and hexagonal pyrrhotite, the a_{FeS} is effectively buffered by the iron sulphides and the FeS content of sphalerite is then dependent on pressure and temperature. It has been shown that the FeS content of sphalerite (in equilibrium with pyrite and hexagonal pyrrhotite) is independent of temperature (thus discrediting the mineral as a geothermometer) in the 300°C to 600°C temperature range for pressures up to 10 kb (Lusk and Ford, 1978; Hutchison and Scott, 1981). Thus within this temperature interval, the FeS content of sphalerite growing in an a_{FeS} buffered system is solely dependent on confining pressure.

For the above temperature range, Hutchison and Scott (1981) have found that the pressure dependence of FeS in sphalerite in equilibrium with pyrite and hexagonal pyrrhotite is best described by the equation

$$P = 42.30 - 32.10 \log N_{\text{FeS}}^{\text{SP}} \quad \text{--- (1)}$$

where P = pressure in kilobars and $N_{\text{FeS}}^{\text{SP}}$ is the FeS mole percent in sphalerite. The above equation is the least squares linear regression line for temperature-independent data compiled by the authors and has a correlation coefficient of 0.99 and a standard error of ± 0.30 kb.

Application of the sphalerite geobarometer requires that sphalerite, pyrite and hexagonal pyrrhotite must have been in equilibrium during deposition or metamorphism (Scott, 1973). At the time when Scott made this statement, it was generally believed that sphalerite, because of its refractory nature, would not re-equilibrate at lower temperatures. More recent work (Groves et al, 1975; Ethier et al, 1976; Bristol, 1979; Sangameshwar and Marshall, 1980) has shown that sphalerite can, in fact, re-equilibrate at lower temperatures.

Accordingly, Scott's (1973) statement needs to be modified. For successful application of sphalerite geobarometry, the sphalerite must have been in equilibrium with pyrite and hexagonal pyrrhotite and it must not have re-equilibrated since formation.

In many cases, equilibrium is difficult to prove and can only be inferred. If the three minerals are in intimate contact, then equilibrium is highly likely and is assumed. Other factors which are used as equilibrium indicators are homogeneity of sphalerite and metamorphic grade. Ores metamorphosed to grades higher than the greenschist facies often contain homogeneous sphalerites, indicating equilibrium (Scott, 1973). The existence of sphalerite in equilibrium with pyrite and pyrrhotite in one polished section does not necessarily mean that all the other sphalerite, pyrite and pyrrhotite grains in the same section are also in equilibrium. This is because equilibrium domains (areas of constant a_{FeS}) can be very small (Scott et al, 1977). Thus it is important that sphalerite and the iron sulphides be in contact before equilibrium can be assumed.

Re-equilibration of sphalerites may be even harder to prove. If other phases in the same section are re-equilibrating or have re-equilibrated (for example, hexagonal pyrrhotite altered to monoclinic pyrrhotite) then it is an indication that the sphalerite composition may have also changed since its formation.

Finally, there are still uncertainties about the effect of Cu dissolved in sphalerite (Hutchison and Scott, 1981). One easy way out of this problem is to avoid sphalerite containing (exsolved?) Cu phases. Other minor elements common in sphalerite (Cd and Mn) have no effect on the sphalerite geobarometer (Scott, 1973).

6.3.2 Geobarometry

The metamorphic grade at Mount Mulgine is medium (amphibolite facies) and, as just mentioned, this is an indicator that equilibrium between sphalerite and the iron sulphides may have been attained. The temperature of metamorphism (Chapter 2) is not likely to have exceeded 550°C and so equation 1 (page 109) is applicable. Despite the problems below, problems that are often encountered in sphalerite geobarometry, it was decided to try this method of estimating pressure because it was important to know the pressure of formation (see Chapter 5) of the minerals.

The biggest uncertainty was the possibility that the sphalerites used may have re-equilibrated at lower temperatures. Low temperature re-equilibration of non refractory pyrrhotite is often found and has been noted by several workers (e.g., Desborough and Carpenter, 1965; Kelly and Turneaure, 1970; Genkin, 1971). Rims of monoclinic pyrrhotite were observed around some

hexagonal pyrrhotite grains (Plates 4.3B and D) and this was interpreted to mean that hexagonal pyrrhotite had been partially replaced by monoclinic pyrrhotite (detected by a magnetic colloid). Such alteration could have affected sphalerite as well.

Because of a general lack of samples containing sphalerite, pyrite and hexagonal pyrrhotite in mutual contact, all the four samples analysed were not exactly ideal. Samples 259/90.70 and 259/118 had all the three minerals in mutual contact but the hexagonal pyrrhotite was rimmed by monoclinic pyrrhotite. Sample 259/115.77 was analysed although some of the pyrrhotite grains in contact with sphalerite were completely altered to monoclinic pyrrhotite. All the above three samples were analysed in the hope that the alteration had not affected sphalerite. The last sample, 259/100.90, had all the three minerals but they were not all in mutual contact. The sphalerite was in contact with hexagonal pyrrhotite and the latter mineral did not show any signs of alteration. Pyrite was present in the same polished section but it was not in contact with the other two minerals. Ethier et al (1976) found that in samples from the Sullivan (British Columbia) Pb-Zn deposit there is "no significant variation in the iron content of sphalerite between sphalerite grains in direct contact with pyrite and pyrrhotite grains and others not in direct contact with both but which are in the same sample". The small number of samples, even if they were all ideal, is also discouraging, especially since they are all from one drill hole.

The full sphalerite analytical results are in Appendix 4, but the important data are summarised in Table 6.2, together with the calculated pressures using equation 1 of Hutchison and Scott (1981, p.144). The results are almost as one would have suspected. Only sample 259/100.90 gave consistent analyses, resulting in consistent pressure estimates. The mean pressure from this sample is 4.59 ± 0.30 kb which is in reasonable agreement with a 3.7 kb figure obtained from muscovite (phengite) analyses (Chapter 5) if the temperature is assumed to have been 550°C .

Pressure estimates from the other three samples (in which pyrrhotite re-equilibration was obvious) are very variable, indicating that the sphalerite has also possibly re-equilibrated. Alternatively, the variability may indicate that the minerals had never attained equilibrium. It is, perhaps, significant that sample 259/115.77, in which most of the hexagonal pyrrhotite had inverted to monoclinic pyrrhotite, gave the highest

Table 6.2 : Sphalerite Geobarometry

Sample No.	Analysis point	Total (%)	FeS mole% in sphalerite	Pressure (kb)
259/90.70	1	92.91	13.31	6.21
	2	93.09	16.46	3.25
	3	97.38	15.17	4.39
259/100.90	1	97.88	14.91	4.63
	2	98.06	14.90	4.64
	3	97.32	15.05	4.50
259/115.77	1	100.33	11.59	8.14
	2	98.67	12.90	6.65
	3	100.42	12.20	7.43
259/118	1	98.63	12.56	7.02
	2	98.72	12.74	6.82
	3	99.03	17.98	2.02
	4	99.13	12.17	7.46
	5	100.22	12.74	6.82
	6	99.62	17.49	2.41

pressure estimates. Several workers have noted that pressure estimates from sphalerite that has possibly re-equilibrated are frequently high (Groves et al, 1976; Sangameshwar and Marshall, 1980). It seems the anomalously high pressures are due to equilibration between monoclinic, rather than hexagonal, pyrrhotite and sphalerite. Monoclinic pyrrhotite is stable at low temperatures (below 254°C), but sphalerite geobarometry has not been extended to temperatures below about 300°C. This is mainly because the a_{FeS} (which determines the FeS content of sphalerite at a given temperature) is inversely related to the sulphur activity of the co-existing iron sulphide assemblage (Scott and Kissin, 1973) and although the Fe-S system has been the subject of many theses and papers in recent years (see Kissin and Scott, 1982), low temperature relations in this system are not yet fully understood. The above pressure indicated by sample 259/100.9, coupled with mineralogical studies and estimates of thickness of the volcanic/sedimentary pile at Mount Mulgine, were the basis for inferring that the pressure at the time of formation of the minerals must have been at least 2 kb. This is also consistent with a maximum pressure of 3.9 kb estimated from hornblende composition (see section 2.5.1).

CHAPTER 7 : ORE GENESIS, DISCUSSION AND CONCLUSIONS

7.1 Genesis

Like fashion, theories on ore genesis change with time. Until recently, the genesis of most W deposits was related to granitic intrusions with which the deposits are almost always associated. Where no such intrusion could be seen even in the immediate vicinity, its presence at depth would be inferred (e.g., John, 1963). In most interpretations of ore genesis, it was generally agreed or implied that W deposition is related to the aftermath rather than the earlier stages of magmatic invasion (Kerr, 1946).

In the last two decades, mainly as a result of research by Maucher, Höll and co-workers, theories about the genesis of many W (especially scheelite) deposits have changed. The idea that such deposits form as a direct result of sedimentary processes (i.e, the deposits are syngenetic or syn-sedimentary) has gained general acceptance; so much so that the genetic theories of some deposits (e.g., the King Island Scheelite deposit, Tasmania, long regarded as a classic example of a contact-metasomatic deposit) have been revised by some workers (Burchard, 1977) in favour of the syn-sedimentary model. Some deposits, the best examples being the strata-bound Kleinarlital and Felbertal deposits in the Eastern European Alps, have been convincingly shown to be sedimentary in origin (Höll et al, 1972). According to Maucher (1972, p.85) "scheelite is a primary rock mineral in volcanics and sediments, changing its mineralogical behaviour according to the grade of metamorphism, thus forming very small grains in the greenschist facies, but porphyroblasts of 10- to 20-mm size in rocks of the amphibolite facies".

In the light of the above statements, it was not enough to merely keep on the lookout for evidence of sedimentary origin of the Mount Mulgine Trench deposit. One of the aims of the second visit to the study area was to specifically look for such evidence. This was done using a UV lamp on all core samples that were known to contain detectable W. It was thought that syn-sedimentary ore fabrics similar to those found by Höll et al (1972) might be found. They were not. However, there were two positive results of the UV light search. The first is that it was realised that the scheelite must be Mo-free since its blue-white fluorescent colour did not contain any hint of yellow (which usually indicates the presence of Mo). This was later confirmed by electron microprobe work (see Table 4.2). The second and more important result is the dependence of scheelite mineralization on quartz veins was highlighted. As Plate 4.1C shows, the scheelite occurs generally as coarse

porphyroblasts within the quartz veins or as fine disseminations in the immediate vicinity of the veins. It is felt that this quartz vein-scheelite association is the key to the genesis of the Trench deposit.

In the discussion of the genesis of a deposit such as the Trench, there are four important factors which must be considered (White, 1968):

- a) The source of the ore constituents.
- b) The solution of ore and other constituents in the hydrous phase.
- c) The migration of the mineralizing fluid.
- d) The selective precipitation of the ore constituents in favourable environments.

Before considering each of the above factors, there are two important assumptions that had to be made which should be emphasized. The first major assumption was that the sulphide minerals (pyrite, sphalerite, pyrrhotite, arsenopyrite) are coeval with W and other mineralization at Mount Mulgine. This assumption seems reasonable in view of the facts that the temperatures of formation indicated for the sulphides and scheelite (see pages 54, 96 & 105) are about the same and that the sulphides are also often found in quartz veins, sometimes associated with scheelite. As shown in Chapter 4, there were other (mostly later) generations of pyrite, pyrrhotite and perhaps other sulphides, but this does not affect this discussion. The second assumption is that the early sulphides and the W minerals were subjected to the regional metamorphism that affected the enclosing rocks. As noted in Chapter 4 (page 42) some of the mineralization has undergone metamorphism but the actual timing of mineralization with respect to the peak metamorphism is not certain. Again, this is not a serious assumption because many minerals show evidence of deformation and it is known that regional metamorphism in the Warriedar Fold Belt was partly syntectonic and outlasted deformation (Baxter and Lipple, 1979).

Having made the above comments, the genesis of the Trench deposit seems straightforward and familiar. Most evidence in this thesis indicates that the mineralization was largely derived from the Mount Mulgine Granite or a similar granite that has been shown to be underneath or subjacent to the Trench (Whittle, 1977, 1978). From the proximity of the Trench deposit to the Mount Mulgine Granite and the fact that the greisens from the granite and those in the Trench deposit are virtually indistinguishable, it is believed that the Mount Mulgine Granite extends beneath the Trench volcano-sedimentary sequence.

There is no doubt that Mount Mulgine Granite, or rather its source, was enriched in W, Mo and probably other trace elements because the granite is associated with another W deposit (the Hill deposit) and also with molybdenite mineralization which attracted the interest of prospectors in the area in the first place. The Hill deposit is, undoubtedly, a contact metasomatic deposit. This empirical evidence that the Mount Mulgine Granite is the source of the mineralization is supported by fluid inclusion and sulphur isotope data obtained in this study. The salinity of the mineralizing fluids (Chapter 5) was sometimes very high (in excess of 30 wt.% CaCl_2 equivalent, and up to as much as 50 wt.% CaCl_2 equivalent) and such high salinities are usually found in magmatic-derived fluids. The $\delta^{34}\text{S}$ values also indicate that the sulphur had a magmatic source (Chapter 6).

All the elements involved in the mineralization need not have come from the postulated magmatic source. There is evidence that the hydrothermal fluids interacted with the country rocks and there was exchange of elements between them (Chapter 2). As in typical skarn deposits, many previous workers consider that Ca was derived from the host and/or country rocks.

The mean values of rock analyses (see Table 2.1) suggest that higher Ca rocks (meta-basalts) have higher W contents. It should be noted, however, that the highest W value was not included in the calculation of the mean for the relatively Ca-poor rocks (the tholeiitic meta-basalts). If the above-mentioned suggestion is true, it would most likely be due to local deposition of scheelite utilizing Ca from the host rocks. This suggestion is not confirmed by the Ca vs W plot for the meta-basalts and there is no significant correlation between Ca and W (correlation coefficient = 0.019 for 36 samples). Also, the highest and most of the high W values were found in the relatively Ca-poor rocks (see Appendix 3).

If there was a lithological control on W mineralization, then one would expect this to show up on Figures such as 1.4 and 5.2, but it does not. This is consistent with the fact that W mineralization is not strata-bound.

A lot of Ca must have been available because, despite the deposition of scheelite, fluorite and other late Ca-bearing minerals (calcite, stilbite etc.) Ca^{++} is still the dominant cation in all the fluid inclusions. At least some of the Ca would have been leached from the country rocks by the mineralizing solutions. It is also possible that percolating meteoric waters helped in the removal of Ca and other elements (e.g., Na) from the country rocks, especially since Ca is one of the most mobile elements during weathering (Pettijohn, 1949). Whether or not the mineralizing hydrothermal solutions had a meteoric component might be determined by stable isotope studies on solutions in fluid inclusions.

The form in which W is transported in hydrothermal ore-forming systems has not yet been definitely established (Barabanov, 1971; Foster, 1977; Higgins, 1980). Because W-bearing minerals often occur associated with halogen-bearing minerals, and fluid inclusions from many W deposits commonly contain Cl and F (e.g., Ivanova and Khodakovskiy, 1968) transport of W as halide complexes was one of the earliest forms of W transport to be suggested. However, Ivanova (1966) showed from thermodynamic calculations that transport of W in halogen compounds was unlikely in nature because these compounds are unstable in the presence of silica, Na-bearing phases and excess water (relative to HF or HCl). Barabanov (1961, cited in Barabanov, 1971) and Kalinicheva and Barabanov (1980) suggested that W may be transported as K tungstate. Higgins (1980) noted that CO₂ is often an important constituent of W-associated fluids evolved from granitic melts under high fluid pressure and suggested that carbonate or bicarbonate complexes may be important in the transport of W at very high fluid pressures.

Recent opinion, however, favours the transport of W in mineralizing fluids, chiefly as the tungstate ion, tungstic acid, Na tungstate or in heteropoly acids (Maucher, 1976; Horsnail, 1979). The existence in solution of particular W ions is primarily determined by the pH, temperature and the silica content of the aqueous medium (Hobbs and Elliot, 1973).

Heteropoly compounds of the type H₈[Si(W₂O₇)₆].3H₂O may be important in the transport of W at low temperatures but they are unlikely to have been important at Mount Mulgine where the indicated temperatures of scheelite formation are well above 300°C.*

Ivanova and Khodakovskiy (1968) suggested that the most probable form in which W is transported in hydrothermal solutions is as tungstic acid. It is believed that the bulk of W at Mount Mulgine was transported in this form.

Which tungsten mineral is precipitated depends not only on the pH and temperature of the mineralizing solution, but also on the activities of Ca⁺⁺, Fe⁺⁺ and Mn⁺⁺ and the oxygen and sulphur fugacities (Foster et al, 1978). According to Hobbs and Elliot (1973) CO₂ and F also play a part in determining which W phase is precipitated. At Mount Mulgine, conditions must have been right for the precipitation of scheelite since it is almost the only W mineral found. As already noted, there must have been abundant Ca and, from the work of Maucher (1976) and Foster et al (1978), the solutions would have been near neutral (but slightly alkaline) at the time of deposition of the scheelite.

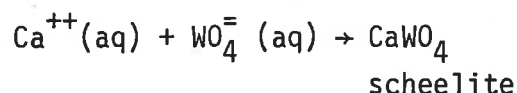
* The heteropoly compounds are stable up to 250-300°C (Maucher, 1976).

It is known that W is transported in alkaline solutions but that precipitation of scheelite takes place at pHs near neutral (Barabanov, 1971; Maucher, 1976). Since there is no evidence that there was extensive host rock - hydrothermal solution interaction which could have resulted in large pH changes before the deposition of scheelite, it can be assumed that the pH of the mineralizing solutions was always close to neutral but slightly alkaline. This would explain why the Fe tungstate (ferberite) was not deposited and why huebnerite ($MnWO_4$) is rare. According to Foster et al (1978) and the experiment work of Gundlach and Thormann (quoted in Horsnail, 1979), ferberite, huebnerite and scheelite are precipitated, in this order, as the pH increases, with ferberite forming from acid solutions, huebnerite from approximately neutral solutions and scheelite from alkaline solutions. At Mount Mulgine, the pH must have been low, locally, to allow the precipitation of huebnerite, but not low enough to allow the formation of ferberite. The huebnerite was later partly replaced by scheelite as the pH of the solutions rose again.

Since the pH seems not to have varied much, it is suggested that the precipitation of scheelite was triggered by the fall in temperature away from the cooling granite. Foster (1977) showed that the solubility of scheelite is, among other things, strongly temperature-dependent. The above interpretation is consistent with the increase in W with increasing distance from the granite (W decreases with increasing depth, see Figure 5.2). This increase in W with distance from the source of the mineralizing solutions might also be partly due to increase in the concentration of Ca^{++} . Solutions further away from the granitic source would have had more "contact" with the host/country rocks and would therefore have had more opportunity to become enriched in Ca^{++} .

Channelways for the mineralizing solutions were the fractures that were created in the supracrustal rocks mainly by the forceful intrusion of the Mount Mulgine Granite, prior to the separation of a W-rich siliceous fluid as the granite crystallized. Thermal energy from the cooling pluton initiated convection and this was responsible for the migration of the fluids.

As the fluids migrated, the concentration of Ca^{++} was increased as more Ca was leached from the country rocks; at the same time the temperature of the fluids dropped. The falling temperature caused dissociation of tungstic acid, thus releasing WO_4^- (Ivanova and Khodakovskiy, 1968). Scheelite was then precipitated in the fractures and also in the host rocks immediately adjacent to the fractures according to the simple reaction



Kalinicheva and Barabanov (1980) proposed the following reaction for the formation of scheelite during skarn formation:



This sort of reaction may have taken place at Mount Mulgine and would explain the presence of scheelite in the host rocks immediately adjacent to the former fractures (now quartz veins).

In summary, then, while the "when" of the scheelite deposition was largely determined by temperature (and perhaps aCa^{++}) the "where" (i.e., localization of the mineral) was dependent on the presence of fractures as well as temperature gradient.

As shown in Chapter 4, the scheelite from Mount Mulgine is Mo-free and, in this respect, it differs from that found in many skarn-type scheelite deposits (Hobbs and Elliot, 1973). Mo is the closest chemical relative of W and it is known that it readily enters the structure of scheelite because it has a smaller atomic radius than that of W (Kiseleva et al, 1980). It is, therefore, natural to wonder why the scheelite is Mo-free despite the presence of Mo mineralization at Mount Mulgine. This is thought to be because W and Mo belonged to different mineralizing episodes. Fluid inclusion studies (Chapter 5) indicate that there were several mineralizing fluids but the fluids did not differ much chemically. The absence of powellite (CaMoO_4) is believed to be due to unfavourable chemical environment. The formation and stability of powellite require low $f\text{S}_2$ and much higher $f\text{O}_2$ than that required for scheelite - at least above the value at which magnetite, hematite and pyrite coexist in equilibrium (Hsu, 1977). No primary hematite was observed and so it is reasonable to conclude that the oxygen fugacity was never high enough.

7.2 Discussion

A survey of the literature on W deposits was conducted in order to find out if there are any other deposits that might be described as "Mount Mulgine-type". As pointed out in the introduction, no such deposit was found, when all the factors are taken into consideration. It is the age and size which make the Mount Mulgine tungsten deposits truly unique.

Generally, W deposits are rare in the Archaean, so much so that Watson (1976) suggested that W (together with Sn and Ta) were not concentrated on a large scale until about 1000 m.y. ago. Archaean W mineralization is known in a few other areas. W occurs as wolframite in quartz veins associated with Archaean pegmatites in S.W. Uganda (von Knorring, 1970). In this part of Uganda, wolframite also occurs associated with graphitic phyllites of possible

Archaean age (Jeffery, 1959; Cahen and Snelling, 1966). W mineralization, mainly in the form of scheelite, occurs widespread through Southern Africa greenstone terrains, but it is invariably a by-product of Au mining (Anhaeusser, 1976).

In several respects the Mount Mulgine W mineralization is as would be expected. The world-wide common association of W and granitic rocks is well known (e.g., Kerr, 1946; Li and Wang, 1946; Dekate, 1967; Hobbs and Elliot, 1973). In Chapter 2, it was shown that the Mount Mulgine Granite is more likely to be I-type according to the granite classification scheme of Chappell and White (1974) and White and Chappell (1977), arguing that those samples that appear to be S-type do so because they have been greisenized. This is consistent with Collins (1975) suggestion that the Mount Mulgine Granite formed from "pre-existing granitoid or gneissic rocks". It is also consistent with the fact that W-Mo mineralization is associated with the granite (Chappell and White, 1974). Tin mineralization, which was not and has not been found at Mount Mulgine, is usually associated with S-type (sedimentary derived) granites.

The meta-volcanic-sedimentary host rocks (Chapter 2) of the Trench deposit at Mount Mulgine are very similar to those of the strata- and time-bound (Early Paleozoic) Felbertal W deposits in Eastern European Alps (Maucher, 1972; Höll et al, 1972). But as already discussed, the syn-sedimentary origin model proposed for the younger deposit by the above authors is not considered applicable to the Mount Mulgine Trench W deposit. From our present knowledge of the Trench deposit, it cannot be described as strata-bound except in the broadest sense of the term. The close association between W mineralization and quartz veins (in fact, the dependence of the mineralization on quartz veins) in the Trench deposit has not been reported in the Felbertal deposit.

The mineralogies of the two deposits, although largely similar, show some important differences: pyrite, the most common and abundant opaque mineral at Mount Mulgine, is rare at Felbertal where pyrrhotite dominates (Holzer and Stumpf, 1980). Scheelite from the Felbertal deposit may occur as isomorphous intergrowths with powellite but as already pointed out, powellite has not been observed at Mount Mulgine. The Felbertal scheelite sometimes has inclusions of members of the molybdenite-tungstenite solid solution series (Höll and Weber-Diefenbach, 1973). Members of this series have not been observed at Mount Mulgine. Tungstenite (WS_2) is a rare mineral which forms under special conditions. Unlike powellite which forms under very high fO_2 /low fS_2 , tungstenite forms under very low fO_2 /high fS_2 (Hsu, 1977). Indeed, according to Hsu (ibid), tungstenite and powellite should not occur together.

Their occurrence at Felbertal may mean that conditions were highly variable during the formation of the deposit. Anyway, the above mineralogical differences imply that the Felbertal and Trench deposits formed under different conditions.

The mineralogy at Mount Mulgine (Chapter 4) is more like that of typical W skarn deposits (e.g., Skaarup, 1974; De Brodtkorb and Brodtkorb, 1977). In fact, since the term "skarn deposit" is free of genetic implications (Einaudi et al, 1981), the Trench deposit qualifies as a skarn deposit. The main difference between the Trench deposit and other W skarn deposits is in their geologic setting: W skarn deposits are usually strata-bound and typically occur in argillaceous carbonate rocks and intercalated carbonate-pelite or carbonate-volcanic sequences. Although carbonate minerals do occur and may be locally abundant at Mount Mulgine, there are no carbonate rocks and, as pointed out above, the term strata-bound (*sensu stricto*) is inapplicable to the Trench deposit. It is known that metamorphism of volcano-sedimentary rock assemblages may yield skarn mineral assemblages (Einaudi et al, 1981, p. 322) and so the skarn mineralogy at Mount Mulgine is not unique.

The fluid inclusion data (Chapter 5) are similar to those for most other W deposits in the literature (e.g., Kwak, 1978; Kelly and Rye, 1979; Sato, 1980; Tanelli, 1982). The S-isotope results (Chapter 6) are almost identical to those obtained by So et al (1983) for the Ssang Jeon W mine, republic of Korea. S-isotope studies of rocks from other parts of the Archaean Yilgarn block of Western Australia were reported by Donnelly et al (1977) and their results are very similar to those obtained for Mount Mulgine. They are also similar to those obtained by Fripp et al (1979) for Archaean banded iron formations in Rhodesia (now Zimbabwe).

Finally, the genetic model proposed for the Trench deposit is neither new nor unexpected. A similar model for the formation of the gold-associated scheelite deposits in the South African greenstone belts was proposed by Foster (1977). It is one of the oldest genetic models and has been proposed for most types of W deposits.

7.3 Conclusions

The main findings of this study have already been stated or implied in the text. They are reiterated and briefly listed below. Details can be found in the relevant chapters.

1. The majority of the volcanic host rocks at Mount Mulgine are tholeiitic and it is inferred that they were derived from a dominantly tholeiitic-basalt magma. Differentiation of this magma produced high-Mg

(ultramafic) rocks, through the early separation of olivine and pyroxene. These rocks are still essentially basaltic and it is proposed that they be referred to as "high-Mg meta-basalts", distinct from the low Mg rocks for which the name "tholeiitic meta-basalts" is appropriate. Differentiation is also thought to have resulted in felsic rocks for which the term-adjective "meta-rhyodacitic" is proposed.

2. The volcanics resemble present-day Mid-Oceanic-Ridge basalts and island arc tholeiites but this resemblance may be fortuitous because there are reasons to believe that such modern environments (deep oceans and deep subduction trenches) did not exist in the Archaean. The rocks appear to have formed in elongate, narrow and initially shallow basins or troughs which subsided with increasing deposition. The deposition environments for greenstones have been likened to present-day intracontinental rifts or back-arc basins.

3. The granitic and mostly greisenized rocks which are concordant with the volcanic rocks do not appear to be volcanic in origin. They are believed to be off-shoots of the Mount Mulgine Granite which is believed to extend down beneath the Trench deposit.

4. Tungsten and most other mineralization at Mount Mulgine were derived primarily from siliceous magmatic differentiates of the Mount Mulgine Granite. Some elements, notably Ca, were also derived from the host/country rocks. It is not clear how elemental exchange between the hydrothermal fluids and the host/country rocks took place. Infiltration and diffusive exchange would have occurred especially in the immediate vicinity of the fluid channelways. It is also possible that some elements were leached from the country rocks and added to the hydrothermal solutions by meteoric waters. D/H isotope studies would help in this matter.

5. The channelways for the mineralizing solutions were the fractures that were largely created by the intrusion of the Mount Mulgine Granite. Some of the fractures were initiated or caused by the forces that were responsible for the folding of the supracrustal rocks in the Warriedar Fold Belt. The fractures later became depositories for the mineral constituents of the hydrothermal fluids and hence the location of the present veins. Thus the locus of the mineralization was mainly determined by the former fractures.

6. All the lithologies were fractured and are now cut by quartz veins. In other words, mineralization is not confined to any one particular rock type, i.e., it is not strata-bound. Minor and local precipitation of scheelite occurred in the rocks along the fracture margins and, as would be expected, this happened more often in the Ca-rich rocks. This type of scheelite deposition appears insignificant and it can be stated that generally

there is no lithological control on the mineralization.

7. Fluid inclusion evidence and consideration of existing experimental data on W solubility suggest that W was carried in moderately to highly saline alkaline solutions mainly as tungstic acid which dissociated with consequent deposition of scheelite as the temperatures dropped to about 400°C.

8. The Mount Mulgine Granite is cut by quartz veins and so there must have been at least another fracturing episode after the crystallization of the granite. This implies there were several mineralizing episodes and this is believed to be the main reason for the wide range of the fluid inclusion data and the complexity of the quartz veining. It is possible that earlier mineralization was remobilized into later fractures. It is felt that quartz veining and its relation to mineralization deserve a more detailed and thorough investigation.

9. Total lack of Mo in scheelite is interpreted to mean that Mo and W were carried in solution at different times, although the solutions were chemically similar. Scheelite was probably deposited before molybdenite.

10. Although it is sometimes never stated explicitly, it is always hoped that such studies as this one will come up with some lead for further exploration. Unfortunately, no definite exploration "tool" was established in this study. But if it is true that the Mount Mulgine Granite or its source was the primary sources of W and the fractures and temperatures were the main controls of scheelite localization and deposition as suggested in this study, then the most promising prospective area is that surrounding (but not far from) the granite. It is possible that what the caretaker at Mount Mulgine (Arthur Moses) told the writer is true. He said that as far as drilling is concerned, the Trench "has not been scratched".

REFERENCES

- AHRENS, L.H., 1970: The composition of stony meteorites (IX). Abundance trends of the refractory elements in chondrites, basaltic achondrites and Apollo 11 fines : *Earth Planet. Sci. Letts.*, 10; p.1-6.
- ANHAEUSSER, C.R., 1976: Archaean metallogeny in southern Africa: *Econ. Geol.*, v.71, p.16-43.
- ARRIENS, P.A., 1971: The Archaean geochronology of Australia : *Geol. Soc. Austral. Spec. Publs.*, 3, p.11-23.
- BAER, A.J., VEIZER, J. and BARAGAR, W.R.A., 1978: Relationships between Archaean granites and greenstones : *Geoscience Canada*, v.5, p.29-32.
- BARABANOV, V.F., 1971: Geochemistry of tungsten : *Internat. Geol. Rev.*, v.13, no. 3, p.332-344.
- BARNES, H.L., (ed.). 1979: *Geochemistry of hydrothermal ore deposits* : New York, Wiley-Interscience, 798p.
- BARTON, P.B., Jr. and TOULMIN, P., III., 1966: Phase relations in the Fe-Zn-S system : *Econ. Geol.*, v.61, p.445-462.
- BAXTER, J.L., 1978: Molybdenum, tungsten, vanadium and chromium in W. Australia : *Geol. Surv. West. Austral. Min. Res. Bull. II*, 150p.
- BAXTER, J.L. and GIBBS, A.D. (in prep.). Mount Mulgine (Yalgoo goldfield). A granite - associated tungsten - molybdenum deposit in the Archaean of the Murchison province, W.A.
- BAXTER, J.L. and LIPPLE, S.L., 1979: Explanatory notes on the Perenjori 1:250,000 geological sheet, Western Australia : *Geol. Surv. West. Austral. Rec.*, 1978/16.
- BENDER, F., 1979: The tungsten situation: supply and demand, present and future, in *Tungsten*, Proceedings of the First International Tungsten Symposium, Stockholm, September 5-7, 1979 : Mining Journal Books Ltd., London, p.2-17.
- BINNS, R.A., 1969: Ferromagnesian minerals in high-grade metamorphic rocks : *Geol. Soc. Aust. Spec. Publ.*, 2, p.323-332.

- BINNS, R.A., GUNTHORPE, R.J. and GROVES, D.I. 1976: Metamorphic patterns and development of greenstone belts in the Eastern Yilgarn Block, Western Australia in B.F. Windley (ed.). The early history of the Earth : New York, John Wiley & Sons, p.303-313.
- BLATCHFORD, T., 1919: On the molybdenite occurrences at Mount Mulgine (Warriedar), Yalgoo Goldfield: Geol. Surv. West Austral. Ann. Rept., 1918, p.16-17.
- BOTH, R.A. and SMITH, J.W., 1975: A sulphur isotope study of base-metal mineralization in the Willyama complex, western New South Wales, Australia : Econ. Geol., v.70, p.308-318.
- BOWYER, D.G., 1982: The geology of part of the Harts Range, Northern Territory, Australia - Petrology, Geochemistry and Structure : [Unpubl.] Hons. thesis, School of Geology, University of Adelaide, 22p.
- BRADY, J.B., 1974: Coexisting actinolite and hornblende from West-Central New Hampshire : Amer. Mineral., v.59, p.529-535.
- BRISTOL, C.C., 1979: Application of sphalerite geobarometry to ores from the Ruttan Mine : Econ. Geol., v.74, p.1496-1502.
- BURCHARD, U., 1977: Genesis of the King Island (Tasmania) Scheelite Mine : in Klemm, D.D. and Schneider, H.J., (eds.) Time - and strata - Bound Ore Deposits : Berlin, Springer Verlag, p.199-204.
- BURRUS, R.C., 1981: Analysis of phase equilibria in C-O-H-S fluid inclusions, in Hollister, L.S., and Crawford, M.L., (eds): Short Course in Fluid Inclusions : Mineralogical Association of Canada, p.39-74.
- CAHEN, L. and SNELLING, N.J., 1966: The geochronology of equatorial Africa, Amsterdam, North-Holland, 195p.
- CANN, J.R., 1970: Rb, Sr, Y, Zr, Nb in some ocean floor basaltic rocks : Earth Planet. Sci. Letts., 10, p.7-11.
- CHAMBERLAIN, J.A., McLEOD, C.R., TRAILL, R.J. and LACHANCE, G.R., 1965: Native metals in the Muskox intrusion : Can. Journ. Earth Sci., v.2, p.188-215.
- CHAPPELL, B.W. and WHITE, A.J.R., 1974: Two contrasting granite types : Pacific Geology 8, p.173-174.
- CLARK, K.F., 1972: Stockwork molybdenum deposits in the Western Cordillera of North America : Econ. Geol., v.67, p.731-758.

- CLIFFORD, T.N., 1966: Tectono-metallogenic units and metallogenic provinces of Africa : *Earth Planet. Sci. Letts.*, 1, p.421-434.
- COLLINS, P.L.F., 1979: Gas hydrates in the CO₂-bearing fluid inclusions and the use of the freezing data for estimation of salinity : *Econ. Geol.*, v.74, p.1435-1444.
- COLLINS, V.P.M., 1975: The lithostructural setting and controls of wolfram-bearing mineralization at Mt. Mulgine, N.W. Yilgarn Craton, W.A.: [unpubl.] Hons. thesis, University of W. Australia.
- CONDIE, K.C., 1976: Trace-element geochemistry of Archean greenstone belts : *Earth-Science Reviews*, 12, p.393-417.
- CONDIE, K.C., 1981: Archean Greenstone Belts; Developments in Precambrian Geology 3 : New York, Elsevier Scientific Publishing Company. 434p.
- COOPER, A.F. and LOVERING, J.F., 1970: Greenschist amphiboles from Haast River, New Zealand : *Contrib. Mineral. Petrol.*, v.27, p.11-24.
- CRAIG, J.R. and VAUGHAN, D.J., 1981: Ore microscopy and ore petrography : New York, John Wiley & Sons, 406p.
- CUNEY, M., 1980: Preliminary results of the petrology and fluid inclusions of the Rössing uraniferous alaskites : *Transactions of the Geological Society of South Africa*, v.83, p.39-45.
- CUNNINGHAM, W.B., HÖLL, R. and TAUPITZ, K.C., 1973: Two new tungsten bearing horizons in the older Precambrium of Rhodesia : *Mineralium Deposita*, v.8, p.200-203.
- DeBRODTKORB, M.K. and BRODTKORB, A., 1977: Stratabound scheelite deposits in the Precambrian basement of the San Luis (Argentina), in Klemm, D.D. & Schneider, H.J. (eds). "Time-and Strata-bound Ore Deposits", Berlin, Springer Verlag, p.141-149.
- DEER, W.A., HOWIE, R.A. and ZUSSMAN, J., 1980: An introduction to rock forming minerals : London, Longman 528p.
- DEKATE, Y.G., 1967: Tungsten occurrences in India and their genesis : *Econ. Geol.*, v.62, p.556-561.
- De La HUNTY, L.E., 1975: Murchison Province, in *Geology of Western Australia* : *Geol. Surv. West. Austral. Mem.*, 2, p.54-64.
- DENINSEKO, V.K. and RUNDKVIST, D.V., 1978: New prospective types of stratiform tungsten mineralization : *International Geology Review*, v.20, no. 5, p.575-586.

- DESBOROUGH, G.A. and CARPENTER, R.H., 1965: Phase relations of pyrrhotite :
Econ. Geol., v.60, p.1431-1450.
- DOCKING, K.S., 1975: A fluid inclusion and sulphur isotope study of the copper mineralization of the Daly-Yudnamutana Mining area, Mt. Painter, S. Australia. [unpubl.] Hons. thesis, Dept. of Econ. Geol., University of Adelaide.
- DONELLY, T.H., LAMBERT, I.D., OEHLER, D.Z., HALLBERG, J.A., HUDSON, D.R., SMITH, J.W., BAVINTON, O.A. and GOLDING, L., 1977: A reconnaissance study of stable isotope ratios in the Archaean rocks from the Yilgarn Block, Western Australia : Geol. Soc. Austral. Jour., v.24, Pt.7, p.409-420.
- EINAUDI, M.T., MEINERT, L.D. and NEWBERRY, R.J., 1981: Skarn deposits : Econ. Geol., 75th Anniversary Volume, 1981, p.317-319.
- ENGEL, A.E.J., ENGEL, C.G. and HAVENS, R.G., 1965: Chemical characteristics of oceanic basalts and the upper mantle : Geol. Soc. Amer. Bull., v.76, p.719-734.
- ERLANK, A.J. and KABLE, E.J.D., 1976: The significance of incompatible elements in Mid-Atlantic Ridge Basalts from 45°N with particular reference to Zr/Nb : Contrib. Mineral. Petrol., v.54, p.281-291.
- ETHIER, V.G., CAMPBELL, F.A., BOTH, R.A. and KROUSE, H.R., 1976: Geologic setting of the Sullivan Orebody and estimates of temperature and pressure of metamorphism : Econ. Geol., v.71, p.1570-1588.
- FARRAR, E., CLARK, A.H. and KIM, O.J., 1978: Age of the Sangdong tungsten deposit, Republic of Korea and its bearing on the metallogeny of the Southern Korean Peninsula : Econ. Geol., v.73, p.547-552.
- FAWCETT, J.J. and YODER, Jr. H.S., 1966: Phase relations of chlorites in the system MgO-Al₂O₃-SiO₂-H₂O: Amer. Mineral., v.51, p.353-380.
- FINLOW-BATES, T. and STUMPFL, E.F., 1981: The behaviour of so-called immobile elements in hydrothermally altered rocks associated with volcanogenic submarine-exhalative ore deposits : Mineralium Deposita, v.16, p.319-328.
- FLEET, M.E., 1970: Structural aspects of marcasite-pyrite transformation: Can. Mineral., v.10, p.225-231.
- FLOYD, P.A. and WINCHESTER, J.A., 1975: Magma type and tectonic setting discrimination using immobile elements : Earth Planet. Sci. Letts., 27, p.211-218.

- FLOYD, P.A. and WINCHESTER, J.A., 1978: Identification and discrimination of altered and metamorphosed volcanic rocks using immobile elements : *Chem. Geol.*, v.21, p.291-306.
- FOSTER, M.D., 1962: Interpretation of the composition and a classification of chlorites : *U.S. Geol. Surv. Proff. Paper* 414-A, 33p.
- FOSTER, R.P., 1977: Solubility of scheelite in hydrothermal chloride solutions : *Chem. Geol.*, v.20, p.27-43.
- FOSTER, R.P., MANN, A.G., ARMIN, T. and BURMEISTER, B., 1978: Richardson's kop wolframite deposit, a geochemical model for the hydrothermal behaviour of tungsten : *in* Verwoerd, W.J., ed., *Mineralization in metamorphic terranes* : *Geol. Soc. S. Afr. Spec. Publ.*, No. 4, p.107-128.
- FOSTER, R.P., MANN, A.G., MILLER, R.G. and SMITH, P.J.R., 1979: Genesis of Archaean gold mineralization with reference to three deposits in the Gatooma area, Rhodesia : *Geol. Soc. S. Afr. Spec. Publ.*, No. 5, p.25-38.
- FRIPP, R.E.P., DONNELLY, T.H. and LAMBERT, I.B., 1979: Sulphur isotope results for Archaean banded iron-formation, Rhodesia : *Geol. Soc. S. Afr. Spec. Publ.*, No. 5, p.205-208.
- FUJIKAWA, K., 1982: Fluid inclusion and oxygen isotope studies of the Nabarlek uranium deposit, N.T., Australia: [unpubl.] Ph.D. thesis, Dept. of Econ. Geol., University of Adelaide.
- GEE, R.D., BAXTER, J.L., WILDE, S.A. and WILLIAMS, I.R., 1981: Crustal development in the Archaean Yilgarn block, Western Australia : *Geol. Soc. Austral. Spec. Pubs.* 7, p.43-56.
- GÉLINAS, L. and BROOKS, C., 1974: Archean quench-texture tholeiites : *Can. Jour. Sci.*, V.11, p.324-340.
- GENKIN, A.D., 1971: Some replacement phenomena in copper-nickel sulphide ores : *Mineralium Deposita*, v.6, p.348-355.
- GIBBS, A.D., 1978: Hill area scheelite prospect, Mount Mulgine, Western Australia: [unpubl.] Minefields Exploration N.L. reports on exploratory shafts 2 and 3, January and March, 1978.
- GILES, C.W. and TEALE, G.S., 1979: The geochemistry of proterozoic acid volcanics from the Frome Basin : *Quarterly Geological Notes*, *Geol. Surv. South Australia*, no. 71, p.13-18.

- GLIKSON, A.Y., 1971: Primitive Archaean element distribution patterns : Chemical evidence and geotectonic significance : Earth Planet. Sci. Letts., 12, p.309-320.
- GLOVER, J.E. and GROVES, D.I., (Eds.), 1981: Archaean Geology : Second International Symposium, Perth, 1980 : Geol. Soc. Aust. Spec. Publs. No. 7, 515p.
- GOLE, M.J. and KLEIN, C., 1981: High grade metamorphic Archaean banded iron-formations, Western Australia; assemblages with coexisting pyroxenes \pm fayalite: Amer. Mineral., v.66, p.87-99.
- GOODWIN, A.M., MONSTER, J. and THODE, H.G., 1976: Carbon and sulphur isotope abundances in Archaean iron-formations and early Precambrian life : Econ. Geol., v.71, p.870-891.
- GROVES, D.I., BINNS, R.A., BARRET, F.M. and McQUEEN, K.G., 1975: Sphalerite compositions from West Australian nickel deposits, a guide to equilibria below 300^oC: Econ. Geol., v.70, p.391-396.
- GROVES, D.I., BINNS, R.A., BARRET, F.M. and McQUEEN, K.G., 1976: Application of sphalerite geobarometry and sulphur isotope geothermometry to ores of Quemont Mine, Noranda, Quebec : Econ. Geol., v.71, p.949-950.
- HALLBERG, J.A., 1972: Geochemistry of Archaean volcanic belts in the Eastern Goldfields region of Western Australia : Jour. Petrol., v.13, p.45-56.
- HALLBERG, J.A., JOHNSTON, C. and BYE, S.M., 1976: The Archean Mardon igneous complex, Western Australia : Precambrian Research, 3, p.111-136.
- HALLBERG, J.A. and WILLIAMS, D.A.C., 1972: Archean mafic and ultramafic rock associations in the Eastern Goldfields region, Western Australia: Earth Planet. Sci. Letts., 15, p.191-200.
- HART, S.R., BROOKS, C., KROGH, T.D., DAVIS, G.L. and NAVA, D., 1970: Ancient and modern volcanic rocks : A trace element model : Earth Planet. Sci. Letts., 10, p.17-28.
- HELSEN, J.N., SHAW, D.M. and CROCKET, J.H., 1978: Tungsten abundances in some volcanic rocks : Geochim. Cosmochim. Acta, v.42, p.1067-1070.

- HIETANEN, A., 1974: Amphibole pairs, epidote minerals, chlorite and plagioclase in metamorphic rocks, northern Sierra Nevada, California : Amer. Mineral., v.59, p.22-40.
- HIGGINS, N.C., 1980: Fluid inclusion evidence for the transport of tungsten by carbonate complexes in hydrothermal solutions: Can. Jour. Earth Sci., v.17, p.823-830.
- HINE, R., WILLIAMS, I.S., CHAPPELL, B.W. and WHITE, A.J.R., 1978: Contrasts between I- and S-type granitoids of the Kosciusko Batholith: Jour. Geol. Soc. Austral., v.25, Pt. 4, p.219-234.
- HING TAN, T. and KWAK, T.A.P., 1979: The measurement of the thermal history around the grassy granodiorite, King Island, Tasmania, by use of fluid inclusion data : Jour. Geol., v.87, p.43-54.
- HOBBS, S.W. and ELLIOTT, J.E., 1973: Tungsten : U.S. Geol. Surv. Proff. Paper 820, p.667-678.
- HOHELLA, Jr. M.F., LIOU, J.G., KESKINEN, M.J. and KIM, S.H., 1982: Synthesis and stability relations of magnesium idocrase : Econ. Geol., v.77, p.798-808.
- HOEFS, J., 1973: Stable isotope geochemistry: New York, Springer-Verlag, 140p.
- HÖLL, R., MAUCHER, A. and WESTENBERGER, H., 1972: Synsedimentary-diagenetic ore fabrics in the strata- and time-bound scheelite deposits of Kleinarlta1 and Felbertal in the Eastern Alps : Mineralium Deposita, v.7, p.217-226.
- HÖLL, R. und WEBER-DIEFENBACH, K., 1973: Tungstenit-Molybdänit-Mischphasen in der scheelitlagerstätte Felbertal (Hohe Tauern, Österreich). [Tungstenite-molybdenite solid solution series from the scheelite deposit of Felbertal (Austria)]: Neues Jahrbuch für Mineralogie Monatshefte, H.1, p.27-34.
- HOLLAND, H.D., 1972: Granites, solutions and base metal deposits : Econ. Geol., v.67, p.281-301.
- HOLLISTER, L.S., 1981: Information intrinsically available from fluid inclusions: in HOLLISTER, L.S., and CRAWFORD, M.L., (eds.) Short Course in Fluid Inclusions : Mineralogical Association of Canada, p.1-12.
- HOLM, P.E., 1982: Non-recognition of continental tholeiites using the Ti-Y-Zr diagram: Contrib. Mineral. Petrol., v.79, p.308-310.
- HOLZER, H.H. and STUMPFL, E.F., 1980: Mineral deposits of the Eastern Alps in Outline of the Geology of Austria: 26th IGC, 1980 excursion guide-book G05, p.171-196.

- HORSNAIL, R.F., 1979: The geology of tungsten in Tungsten, proceedings of the first international tungsten symposium, Stockholm, 1979: London, Mining Journal Books, p.18-31.
- HSU, L.C., 1977: The effects of oxygen and sulphur fugacities on the scheelite-tungstenite and powellite-molybdenite stability relations: *Econ. Geol.*, v.72, p.664-670.
- HSU, L.C., 1981: Phase relations of some tungstate minerals under hydrothermal conditions: *Amer. Mineral.*, v.66, p.298-308.
- HURLBURT, C.S. Jr. and KLEIN, C., 1977: *Manual of Mineralogy* (after J.D. Dana): New York, John Wiley and Sons, 532p.
- HUTCHISON, M.N. and SCOTT, S.D., 1981: Sphalerite geobarometry in the Cu-Fe-Zn-S system: *Econ. Geol.*, v.76, p.143-153.
- HUTCHINSON, R.W., 1979: Evidence of exhalative origin for Tasmanian tin deposits: *Can. Mining Metall. Bull. (CIM)* v.72, no. 808, p.90-103.
- HYNES, A., 1982: A comparison of amphiboles from medium- and low-pressure metabasites: *Contrib. Mineral. Petrol.*, v.81, p.119-125.
- ISHIHARA, S. and TAKENOUCI, S., 1980: (eds.), *Granitic magmatism and related mineralization: Mining Geol. Special Issue, No. 8, 1980; The Society of Mining Geologists of Japan, 247p.*
- IRVINE, T.N. and BARAGAR, W.R.A., 1971: A guide to the chemical classification of the common volcanic rocks: *Can. Jour. Earth Sci.*, v.8, p.523-548.
- IVANOVA, G.F., 1966: Thermodynamic evaluation of the possibility of tungsten transport as halogen compounds: *Geochem. Internat.*, 3, p.964-973.
- IVANOVA, G.F. and KHODAKOVSKIY, I.L., 1968: Transport of tungsten in hydrothermal solutions (abstract). *Geochem. Internat.*, 5, p.779-780.
- JAHN, Bor-Ming, SHIH CHI-YU and V.RAMA MURTHY, 1974: Trace element geochemistry of Archean volcanic rocks: *Geochim. Cosmochim. Acta*, v.38, p.611-627.
- JAKES, P. and GILL, J., 1970: Rare earth elements and the island arc tholeiitic series: *Earth Planet. Sci. Letts.*, 9, p.17-28.
- JAKES, P. and WHITE, A.J.R., 1971: Composition of island arcs and continental growth: *Earth Planet. Sci. Letts.* 12, p.224-230.
- JEFFERY, P.G., 1959: The geochemistry of tungsten, with special reference to the rocks of the Uganda Protectorate: *Geochim. Cosmochim. Acta*, v.16, p.278-295.

- JOHN, Y.W., 1963: Geology and origin of the Sangdong tungsten mine, Republic of Korea: *Econ. Geol.*, v.58, p.1285-1300.
- JOPLIN, G.A., 1968: A petrography of Australian metamorphic rocks: Sydney, Angus and Robertson, 261p.
- KAJIWARA, Y. and KROUSE, H.R., 1971: Sulphur isotope partitioning in metallic sulphide systems: *Can. Jour. Earth Sci.*, v.8, p.1397-1408.
- KAJIWARA, Y., KROUSE, H.R. and SAKAI, A., 1969: Experimental study of sulphur isotope fractionation between co-existing sulphide minerals: *Earth Planet. Sci. Letts.*, 7, p.271-277.
- KALINICHEVA, G.I. and BARABANOV, V.F., 1980: Composition variation in pyroxenes during skarn formation in scheelite shows in the North-west Ladoga area: *Geochem. Internat.* v.17, No. 3, p.48-57.
- KELLY, W.C. and RYE, R.O., 1979: Geologic, fluid inclusion, and stable isotope studies of the tin-tungsten deposits of Panasqueira, Portugal: *Econ. Geol.*, v.74, p.1721-1823.
- KELLY, W.C. and TURNEAURE, F.S., 1970: Mineralogy, paragenesis and geothermometry of the tin and tungsten deposits of the Eastern Andes, Bolivia: *Econ. Geol.*, v.65, p.609-680.
- KERR, P.F., 1946: Tungsten mineralization in the United States: *Geol. Soc. Amer. Memoir* 15. 241p.
- KERR, P.F., 1959: *Optical Mineralogy*: New York, McGraw-Hill, 441p.
- KIM, M.Y., 1981: Fluid inclusion studies relating to tungsten-tin-copper mineralization at the Ohtani Mine, Japan: *Jour. Geosci. Osaka City University*, v.24, p.109-162.
- KISELEVA, I.A., OGORODOVA, L.P. and TOPOR, N.D., 1980: High-temperature micro-calorimetry of scheelite-powellite solid solutions: *Geochem. Internat.*, v.17, No. 3, p.91-94.
- KISSIN, S.A. and SCOTT, S.D., 1982: Phase relations involving pyrrhotite below 350°C: *Econ. Geol.*, v.77, p.1739-1754.
- KRAUSKOPF, K.B., 1971: The source of ore metals: *Geochim. Cosmochim. Acta*, v.35, p.643-659.
- KRETSCHMAR, U. and SCOTT, S.D., 1976: Phase relations involving arsenopyrites in the system Fe-As-S and their application : *Can. Mineral.*, v.14, p.364-386.
- KWAK, A.P.T., 1978: Mass balance relationships and skarn-forming processes at the King Island scheelite deposit, King Island, Tasmania, Australia: *Amer. Jour. Sci.*, v.278, p.943-968.

- KWAK, A.P.T., 1978: The conditions of formation of the King Island scheelite contact skarn, King Island, Tasmania, Australia: *Amer. Jour. Sci.*, v.278, p.968-999.
- LAIRD, J. and ALBEE, A.L., 1981a: Pressure, temperature and time indicators in mafic schist: Their application to reconstructing the poly-metamorphic history of Vermont: *Amer. Journ. Sci.*, v.281, p.127-175.
- LAIRD, J. and ALBEE, A.L., 1981b: High pressure metamorphism in mafic schist from Northern Vermont. *Amer. Jour. Sci.*, v.281, p.97-126.
- LEAKE, B.E., 1965: The relationship between composition of califerous amphibole and grade of metamorphism, *in* Pitcher, W.S. and Flinn, G.W. (eds.). *Controls of metamorphism*, London. Oliver and Boyd, p.279-318.
- LEAKE, B.E., 1978: Nomenclature of amphiboles: *Can. Mineral.*, v.16, p.501-520.
- Le MAITRE, R.W., 1976: The chemical variability of some common igneous rocks: *Jour. Petrol.*, v.17, p.589-637.
- Li, K.C., and WANG, C.Y., 1947: *Tungsten*: New York, Reinhold, 430p.
- LITTLE, H.W., 1956: *Tungsten deposits of Canada*: *Geol. Surv. Can. Econ. Geol. Series*, No. 17, 251p.
- LOWELL, G.R., and GASPARRINI, C., 1982: Composition of arsenopyrite from topaz greisen veins in Southeastern Missouri: *Mineralium Deposita*, v.17, 229-238.
- LUSK, J. and FORD, C.E., 1978: Experimental extension of the sphalerite geobarometer to 10 kbar: *Amer. Mineral.*, v.63, p.516-519.
- MAITLAND, A.G., 1917: Notes on the southern portion of the Yalgoo goldfield. *Geol. Surv. West. Aust. Ann. Rept.*, 1916, p.9-10.
- MASON, B. (ed.), 1971: *Handbook of elemental abundances in meteorites*: New York, Gordon and Breach Scientific Publishers, 555p.
- MASON, R., 1978: *Petrology of the metamorphic rocks* : London, George Allen & Unwin/Thomas Murby, 253p.
- MATHESON, R.S., 1944a: The molybdenite deposits on P.A's 2323, and 2324, Mt. Mulgine, Yalgoo Goldfield: *Geol. Surv. West. Aust. Ann. Rept.* 1943, p.22-24.

- MAUCHER, A., 1972: Time- and strata-bound ore deposits and the evolution of the earth: 24th IGC, 1972, Section 4, p.83-87.
- MAUCHER, A., 1976: The strata-bound cinnabar-stibnite-scheelite deposits, in Wolf, K.H., (ed.), Handbook of strata-bound and stratiform ore deposits: New York, Elsevier Sci. Publ. Company, p.477-503.
- MAYER, T.E., 1976: A fluid inclusion study of six mineral deposits in Adelaidean sediments, N.W. and S. of the Mount Painter Block, S.Australia: [unpubl.] Honours thesis, Department of Economic Geology, University of Adelaide.
- McCALL, G.J.H., 1981: Progress of research into the early history of the Earth: a review, 1970-1980: Geol. Soc. Aust. Spec. Publs., 7, p.3-18.
- MELSON, W.G. and THOMSON, G., 1971: Petrology of a transform fault zone and adjacent ridge segments: Phil. Trans. Roy. Soc. Lond. Ser.A, v.268, p.423-441.
- METZGER, F.W., KELLY, W.C., NESBITT, B.E. and ESSENE, E.J., 1977: Scanning electron microscopy of daughter minerals in fluid inclusions: Econ. Geol., v.72, p.141-152.
- MIDDLETON, T.W., 1979: The geology and resource evaluation of the Trench deposit, Mount Mulgine tungsten project, Western Australia: [unpubl.] Australia and New Zealand Exploration Company report, August 1979.
- MIYASHIRO, A., 1974: Volcanic rock series in island arcs and active continental margins: Amer. Jour. Sci., v.274, p.321-355.
- MURDOCH, J. and BARNES, J.A., 1977: Statistical tables, 2nd edition: New York, John Wiley and Sons., 46p.
- NAQVI, S.M., GOVIL, P.K. and ROGERS, J.J.W., 1981: Chemical sedimentation in Archaean - early Proterozoic greenschist belts of the Dharwar craton, India: Geol. Soc. Aust. Spec. Publs., 7, p.245-254.
- NESBITT, R.W. and SUN SHEN-SU, 1976: Geochemistry of Archaean spinifex-textured peridotites and magnesian and low-magnesian tholeiites: Earth. Planet. Sci. Letts., 31, p.433-453.
- NICHOLLS, G.D. and ISLAM, M.R., 1971: Geochemical investigations of basalts and associated rocks from the ocean floor and their implications: Phil. Trans. Roy. Soc. Lond. ser. A, v.268, p.469-486.

- NORRISH, K. and CHAPPELL, B., 1967: X-ray fluorescence spectrography, in Zussman, J., (ed.), Physical methods in determinative mineralogy: New York, Academic Press, p.161-215.
- OHMOTO, H., 1972: Systematics of sulphur and carbon isotopes in hydrothermal ore deposits : Econ. Geol., v.67, p.551-578.
- OHMOTO, H. and RYE, R.O., 1979: Isotopes of sulphur and carbon in Barnes, H.L., ed., Geochemistry of hydrothermal ore deposits: New York, Wiley Interscience, p.509-567.
- ORVILLE, P.M., 1963: Alkali ion exchange between vapour and feldspar phases: Amer. Jour. Sci., v.261, p.201-237.
- PEARCE, J.A., 1980: Geochemical evidence for the genesis and eruptive setting of lavas from the Tethyan ophiolites, in Panayiotou, A. (ed.), Ophiolites: Proceedings of the international ophiolite symposium, Cyprus, 1979. p. 261-272.
- PEARCE, J.A. and CANN, J.R., 1971: Ophiolite origin investigated by discriminant analysis using Ti, Zr & Y: Earth Planet. Sci. Letts., 12, p.339-349.
- PEARCE, J.A. and CANN, J.R., 1973: Tectonic setting of basic volcanic rocks determined using trace element analyses: Earth Planet. Sci. Letts., 19, p.290-300.
- PEARCE, T.H., GORMAN, B.E. and BIRKETT, T.C., 1975: The TiO_2 - K_2O - P_2O_5 diagram: A method of discriminating between oceanic and non-oceanic basalts: Earth Planet. Sci. Letts., 24, p.419-426.
- PEARCE, T.H., GORMAN, B.E. and BIRKETT, T.C., 1977: The relationship between major element chemistry and tectonic environment of basic and intermediate volcanic rocks: Earth Planet. Sci. Letts., 36, p. 121-132.
- PETTIJOHN, F.J., 1949: Sedimentary rocks: New York, Harper and Brothers, 526p.
- PLIMER, I.R., 1980: Exhalative Sn and W deposits associated with mafic volcanism as precursors to Sn and W deposits associated with granites: Mineralium Deposita, v.15, p.275-289.
- POTTER, R.W., II, 1977: Pressure corrections for fluid-inclusion homogenization temperatures based on the volumetric properties of the system NaCl - H₂O: U.S. Geol. Surv. Jour. Research, v.5, No. 5, p.603-607.

- PRESTVIK, T., 1982: Basic volcanic rocks and tectonic setting. A discussion of the Zr-Ti-Y discrimination diagram and its suitability for classification purposes: *Lithos.* v.15, p.241-247.
- QUINN, E.L. and JONES, C.L., 1936: Carbon dioxide: American Chemical Society Monograph No. 72, New York, Reinhold Publ. Corp., 294p.
- RAMDOHR, P., 1980: The ore minerals and their intergrowths (2nd ed.): London, Pergamon Press, 1207p.
- REIMANN, C. and STUMPFL, E.F., 1981: Geochemical setting of strata-bound stibnite mineralization in the Kreuzeck Mountains, Austria: *Instn. Mining Metall. Trans.* v.90, Sect. B. p.126-132.
- ROEDDER, E., 1962: Studies of fluid inclusions I: Low temperature application of a dual-purpose freezing and heating stage: *Econ. Geol.*, v.57, p.1045-1061.
- ROEDDER, E., 1963b: Studies of fluid inclusions II: Freezing data and their interpretation: *Econ. Geol.*, v.58, p.167-211.
- ROEDDER, E., 1963c: Metastable "superheated" ice in fluid inclusions under high negative pressure (abstract): *Geol. Soc. Amer. Spec. Paper* 76, p.139-140.
- ROEDDER, E., (ed.) 1965: Research on the nature of mineral-forming solutions, with special reference to data from fluid inclusions, International Series of Monographs in Earth Sciences, v.22, Oxford Pergamon Press, 743p.
- ROEDDER, E., 1967c: Metastable superheated ice in liquid-water inclusions under high negative pressure: *Science*, v.155, p.1413-1417.
- ROEDDER, E., 1971: Fluid inclusion studies on the porphyry-type ore deposits at Bingham, Utah, Butte, Montana and Climax, Colorado: *Econ. Geol.*, v.66, p.98-120.
- ROEDDER, E., 1972: Composition of fluid inclusions. U.S. Geol. Surv. Professional paper 440-JJ, 164p.
- ROEDDER, E., 1979a: Fluid inclusions as samples of ore fluids, *in* Barnes, H.L., (ed.), *Geochemistry of hydrothermal ore deposits*: New York, Wiley-Interscience, p.684-737.
- ROEDDER, E. and BODNAR, R.J., 1980: Geologic pressure determinations from fluid inclusion studies: *Ann. Rev. Earth Planet. Sci.*, v.8, p.263-301.

- ROEDDER, E., INGRAM, B. and HALL, W.E., 1963: Studies of fluid inclusions III: Extraction and quantitative analysis of inclusions in the milligram range: *Econ. Geol.*, v.58, p.353-374.
- ROEDDER, E. and SKINNER, B.J., 1968: Experimental evidence that fluid inclusions do not leak : *Econ. Geol.*, v.63, p.715-730.
- ROSE, A.W. and BURT, D.M., 1979: Hydrothermal alteration in Barnes, H.L., (ed.). *Geochemistry of hydrothermal ore deposits*, New York, Wiley-Interscience, p.173-235.
- RYE, R.O. and OHMOTO, H., 1974: Sulphur and carbon isotopes and ore genesis: A review: *Econ. Geol.*, v.69, p.826-842.
- SAKAI, H., 1968: Isotopic properties of sulphur compounds in hydrothermal processes: *Geochem. Jour.*, v.2, p.29-49.
- SANGAMESHWAR, S.R. and MARSHALL, B., 1980: Sphalerite geobarometry of deformed sulphide ores from the C.S.A. mine, Cobar, Australia : *Mineralium Deposita*, v.15, p.305-314.
- SATO, H., 1977: Nickel content of basaltic magmas: identification of primary magmas and a measure of the degree of olivine fractionation: *Lithos* 10, p.113-120.
- SATO, K., 1980: Tungsten skarn deposit of Fujigatoni Mine, South West Japan: *Econ. Geol.*, v.75, p.1066-1082.
- SCHUTTE, J.G., 1977: Everything you always wanted to know about elementary statistics (but were afraid to ask): New Jersey, Prentice-Hall Inc. 229p.
- SCOTT, R., 1966: Variations within ignimbrite cooling units: *Amer. Jour. Sci.*, v.264, p.273-288.
- SCOTT, S.D., 1973: Experimental calibration of the sphalerite geobarometer: *Econ. Geol.*, v.68, p.466-474.
- SCOTT, S.D., 1976: Application of the sphalerite geobarometer to regionally metamorphosed terrains: *Amer. Mineral.*, v.61, p.661-670.
- SCOTT, S.D. and BARNES, H.L., 1971: Sphalerite geothermometry and geobarometry: *Econ. Geol.*, v.66, p.653-669.
- SCOTT, S.D., BOTH, R.A. and KISSIN, S.A., 1977: Sulphide petrology of the Broken Hill Region, New South Wales: *Econ. Geol.*, v.72, p.1410-1425.
- SCOTT, S.D. and KISSIN, S.A., 1973: Sphalerite composition in the Zn-Fe-S system below 300⁰C: *Econ. Geol.*, v.68, p.475-479.

- SHEPHERD, T.J., BECKINSALE, R.D., RUNDLE, C.C. and DURHAM, J., 1976: Genesis of Carrock Fell tungsten deposits, Cumbria: fluid inclusion and isotopic study: *Inst. Mining Metall. Trans.* v.85, section B, p.663-673.
- SHIMIZU, M. and SHIMAZAKI, H., 1981: Application of the sphalerite geobarometer to some skarn-type ore deposits: *Mineralium Deposita*, v.16, p.45-50
- SIMS, P.K. and PETERMAN, Z.E., 1981: Archaean rocks in the southern part of the Canadian Shield - a review: *Geol. Soc. Aust. Spec. Publs.*, 7, p.85-98.
- SKAARUP, P., 1974: Strata-bound scheelite mineralization in skarns and gneisses from the Bindal area, Northern Norway: *Mineralium Deposita*, v.9, p.299-308.
- SMEWING, J.D., SIMONIAN, K.O. and GASS, I.G., 1975: Meta-basalts from the Troodos Massif, Cyprus: Genetic implications deduced from petrography and trace element geochemistry: *Contr. Mineral. Petrol.*, v.51, p.49-64.
- SO, CHIL-SUP., SHELTON, K.L. and RYE, D.M., 1983: Geologic, sulphur isotopic, and fluid inclusion study of the Ssang Jeon tungsten mine, republic of Korea. *Econ. Geol.*, v.78, p.157-163.
- SÖHNGE, P.G., 1950: The Nababeep Near West Tungsten Mine, South Africa: *Amer. Mineral.*, v.35, p.931-940.
- SPEAR, F.S., 1981: An experimental study of hornblende stability and compositional variability in amphibolite: *Amer. Jour. Sci.*, v.281, p.697-734.
- SPRY, A.H., 1969: *Metamorphic textures*: Oxford Pergamon Press, 350p.
- SPRY, P.G., 1978: The geochemistry of iron-rich lithologies associated with the Broken Hill Orebody, N.S.W., Australia: [unpubl.] M.Sc. thesis, Department of Economic Geology, University of Adelaide.
- STOUT, J.H., 1972: Phase petrology and mineral chemistry of coexisting amphiboles from Telemark, Norway: *Jour. Petrol.* v.13, part 1, p.99-145.
- STRECKEISEN, A., 1976: To each plutonic rock its proper name: *Earth-Science Reviews*, v.12, p.1-33.
- SUN, S-S. and NESBITT, R.W., 1977: Chemical heterogeneity of the Archaean mantle, composition of the earth and mantle evolution: *Earth Planet. Sci. Letts.*, 35, p.429-448.
- SUN, S-S. and NESBITT, R.W., 1978: Petrogenesis of Archaean ultrabasic and basic volcanics: Evidence from rare earth elements: *Contrib. Mineral. Petrol.*, v.65, p.301-325.

- SUN, S-S., NESBITT, R.W. and SHARASKIN, A. Ya., 1979: Geochemical characteristics of Mid-Ocean Ridge Basalts: *Earth Planet. Sci. Letts.*, 44, p.119-138.
- TANELLI, G., 1982: Geologic setting, mineralogy and genesis of tungsten mineralization in Dayu district, Jiangxi (People's Republic of China): *An outline: Mineralium Deposita*, v.17, p.279-294.
- TAKENOUCHI, S. and KENNEDY, G.C., 1964: The binary system H_2O-CO_2 at high temperatures and pressures: *Amer. Jour. Sci.* v.262, p.1055-1074.
- TAKENOUCHI, S. and KENNEDY, G.C., 1965b: The solubility of CO_2 in NaCl solutions at high temperatures and pressures: *Amer. Jour. Sci.*, v.263, p.445-454.
- TAKENOUCHI, S. and KENNEDY, G.C., 1965a: Dissociation pressures of the phase $CO_2 \cdot 5\frac{3}{4}H_2O$: *Jour. Geol.*, v.73, p.383-390.
- THOMSON, M.L., FLEET, M.E. and BARNETT, R.L., 1981: Amphiboles from the Renzy Lake Ultramafic Complex, S.W. Quebec: *Can. Mineral.*, v.19, p.469-477.
- TILL, R., 1974: *Statistical methods for the earth scientist: an introduction*: London, MacMillan, 154p.
- TOMICH, S.A., 1978: A review of jaspilitic iron-ore deposits of the Yilgarn block of Western Australia in relation to possible subdivisions of the Archaean: *Minerals Sci., Engng.*, v.10, No. 4, p.247-257.
- TOULMIN, P., III and BARTON, P.B., Jr., 1964: A thermodynamic study of pyrite and pyrrhotite: *Geochim. Cosmochim. Acta*, v.28, p.641-671.
- TURNBULL, K.R. and McDUIE, P.J., 1980: *in* Nesbitt, R.W. and Stanley, J., 1980: *Compilation of analytical geochemistry reports, Centre for Precambrian Research, research report 3, University of Adelaide [unpubl.]*.
- TURNER, F.J., 1980: *Metamorphic Petrology. Mineralogical, field and tectonic aspects*: New York, McGraw-Hill, 403p.
- TWETO, O., 1960: Scheelite in the precambrian gneisses of Colorado: *Econ. Geol.*, v.55, p.1406-1428.
- URBAN, H., 1971: Zur kenntuis der schichtge bundenen Wolfram-Molybdän-Vererzung in Örsdalen (Rogaland), Norwegen. *Mineralium Deposita*, v.6, p.177-195.

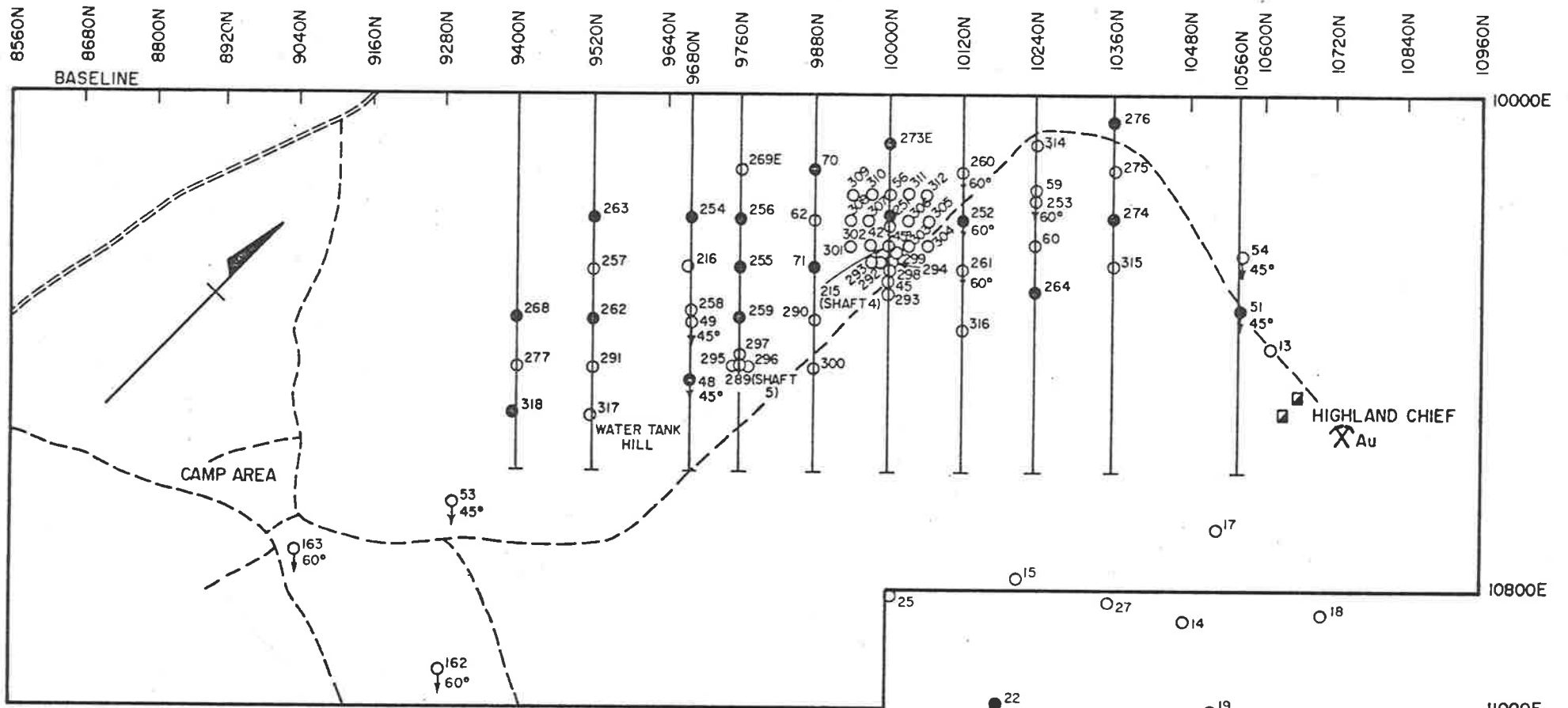
- UYTENBOGAARDT, W. and BURKE, E.A.J., 1971: Tables for microscopic identification of ore minerals: New York, Elsevier Publishing Company, 430p.
- VAUGHAN, D.J. and CRAIG, J.R., 1978: Mineral chemistry of metal sulphides: London, Cambridge University Press, 493p.
- VELDE, B., 1967: Si^{+4} content of natural phengites: Contr. Mineral. Petrol, v.14, p.250-258.
- VERWOERD, W.J. (ed.). Mineralization in metamorphic terranes: Geol. Soc. S. Africa. Spec. Publ. 4, 552p.
- VILJOEN, R.P. and VILJOEN, M.J., 1969: The geological and geochemical significance of the upper formations of the Onverwacht Group: Geol. Soc. S. Africa. Spec. Publ. 2, p.113-51.
- VINOGRADOV, A.P., 1962: Average contents of chemical elements in the principal types of igneous rocks of the earth's crust: Geochemistry 7, p.641-664.
- Von KNORRING, O., 1970: Mineralogical and chemical aspects of pegmatites from orogenic belts of equatorial and Southern Africa; in Clifford, T.N., and Gass, I.G., (eds.), African magmatism and tectonics: Edinburgh, Oliver and Boyd, p.157-184.
- VOYEVODIN, V.N., 1981: The relationship between chemical composition of wolframites and the geological conditions of their formation: International Geology Review, v.23, No. 5, p.561-570.
- WATSON, J., 1976: Mineralization in Archaean Provinces: in Windley, B.F., (ed.). The early history of the earth: New York, John Wiley & Sons, p.443-454.
- WHITE, A.J.R., JAKES, P. and CHRISTIE, D.M., 1971. Composition of greenstones and the hypothesis of sea-floor spreading in the Archaean: Geol. Soc. Aust. Spec. Publs. 3, p.47-56.
- WHITE, A.J.R. and CHAPPELL, B.W., 1977: Ultrametamorphism and granitoid genesis: Tectonophysics 43, p.7-22.
- WHITE, D.E., 1968: Environments of generation of some base-metal ore deposits: Econ. Geol., v.63, p.301-335.

- WHITTLE, A.W.G., 1977: Mount Mulgine tungsten deposit; mineralogical report [unpubl.] Australia and New Zealand Exploration Company report No. 1/77.
- WHITTLE, A.W.G., 1978: DDH71, 70, 62: Trench Area, Mt. Mulgine., mineralogical report: [unpubl.] Australia and New Zealand Exploration Company report No. 1/78.
- WIGGINS, L.B. and CRAIG, J.R., 1980: Reconnaissance of the Cu-Fe-Zn-S system: Sphalerite phase relations: *Econ. Geol.*, v.75, p.742-752.
- WILLIAMS, K.L., 1974: Compositions of sphalerites from the zoned hydrothermal lead-zinc deposits of Zeehan, Tasmania: *Econ. Geol.*, v.74, p.657-672.
- WILSON, H.D.B., ANDREWS, P., MOXHAM, R.L. and RAMLAL, K., 1965: Archean volcanism in the Canadian Shield: *Can. Jour. Earth Sci.* v.2, p.161-175.
- WILSON, A.F., 1970: Some geochemical aspects of sapphirine-bearing pyroxenites and related highly metamorphosed rocks from the Archaean ultramafic belt of South Quairading, Western Australia: *Geol. Soc. Aust. Spec. Publs.* 3, p.401-411.
- WINCHELL, A.N. and WINCHELL, H., 1961: Elements of optical mineralogy, an introduction to microscopic petrography., Part II, Descriptions of Minerals: New York, John Wiley & Sons 551p.
- WINCHESTER, J.A. and FLOYD, P.A., 1977: Geochemical discrimination of different magma series and their differentiation products using immobile elements: *Chem. Geol.*, v.20, p.325-343.
- WINDLEY, B.F. and BRIDGEWATER, D., 1970: The evolution of Archaean low- and high-grade terrains: *Geol. Soc. Aust. Spec. Publs.*, 3, p.33-46.
- WINDLEY, B.F. and NAQVI, S.M., 1978: Archaean geochemistry, developments in preCambrian Geology: New York Elsevier Sci. Publ. Co., 406p.
- WINKLER, H.G.F., 1979: Petrogenesis of metamorphic rocks, New York : Springer-Verlag, 348p.
- WOOD, D.A., JORON, J-L. and TREUIL, M., 1979: A re-appraisal of the use of trace elements to classify and discriminate between magma series erupted in different tectonic settings: *Earth Planet. Sci. Letts.*, 45, p.326-336.

- ZAKRUTKIN, V.V. and GRIGORENKO, M.V., 1967: Titanium and alkalies in amphiboles in metamorphism: Dokl. Acad. Sci. U.S.S.R., Earth Sci. Sect., v.173, p.197-198.
- ZAW, U.K. and CLARK, A.H., 1978: Fluoride-hydroxyl ratios of skarn silicates, Cantung E-zone scheelite orebody, tungsten, Northwest Territories: Can. Mineral., v.16, p.207-221.
- ZHIQING, LIU, 1980: Mechanisms of migration zoning due to concentration difference of mineral particles and of mineralization enrichment in tungsten vein deposits: Scientia sinica: v.XXIII, No.12, p.1559-1569.

APPENDIX 1

Names, location and types of samples collected.



- SECTIONS
 - DIAMOND DRILL HOLE
 - DIAMOND DRILL HOLE (from which several samples were collected)
 - ▭ OUTLINE OF GRID AREA
 - ══ MAIN/ACCESS ROAD
 - - - INTERNAL TRACK
- Metres
0 200 400

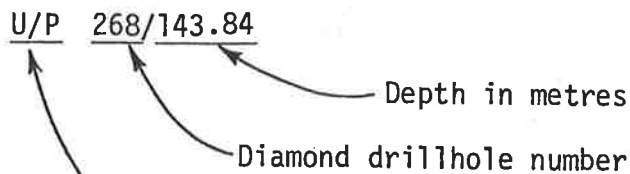
MOUNT MULGINE TRENCH AREA
 Location of diamond drill holes and sections

Figure A-1

Notes and explanations for Appendix 1

1. Sample field number

The sample field number is explained in the example below:



Code letter(s). The code letters refer to field names which were obtained from the cross sections and core logs. The letters are explained in the table below:

[Samples without code letters were collected because they were mineralized].

Code letter(s)	Field name
A	Meta-andesite
B	Meta-basalt
BIF or I	Banded iron formation
D	Meta-dacite
F	Transitional rock
G	Greisen
M, M/G	Microgranite, Quartz porphyry
P	Phlogopite schist
Q	Quartz
R	Meta-rhyolite
Rd	Meta-rhyodacite
T	Meta-olivine(?) pyroxenite (tremolite-talc schist)
U	Meta-pyroxenite (actinolite-chlorite schist)

Other abbreviations used in the first column of Appendix 1 are:

BS	Bulk sample
DBS	Drive bulk sample
F1	Fluorite
Sh	Scheelite
~	Approximately

2. Although the field numbers are informative, they are cumbersome for labelling microscope sections and hard to work with because they are difficult to remember. So each of the samples was assigned a new number, referred to as the section number.

3. The last column in Appendix 1 denotes the nature of the investigations on the samples, using the following symbols:

- F.I. : Fluid inclusion section
- P.S. : Polished section
- P.T.S. : Polished thin section
- T.S. : Thin section
- S.I. : Sulphur isotope analysis
- W.R.A. : Whole rock analysis (including trace elements).

Figure A-1 shows the location of diamond drill holes in the Trench area.

Sample field number ¹ (field name and location)	Section number ²	Type of section ³ cut or data collected
Q DBS16, shaft 4	1	F.I.
Q DBS17 " "	2	F.I.
Q DBS21 " "	3	F.I.
Q BS19 " "	4	F.I.
Q BS20 " "	5	F.I.
Q BS21 " "	6	F.I.
Q BS21 " "	7	F.I.
Q 252/100.30	8	F.I.
Q 252/116.0	9	F.I.
Q 252/~128	10	F.I.
Q 258/148.90	11	F.I.
Q 252/158.30	12	F.I.
Q 252/170.0	13	F.I.
Q 51/59.00	14	F.I.
Q 51/90.60	15	F.I.
Q 51/~103	16	F.I.
Q 51/~112	17	F.I.
Q 51/~122	18	F.I.
A 268/100.2	19	P.T.S., P.S., W.R.A.
A 252/ 61.2	20	P.T.S., W.R.A.
A 276/ 89.9	21	P.T.S., W.R.A.
A 276/ 61.2	22	P.T.S., W.R.A.
A 70/ 56.09	23	P.T.S.
A 51/ 75.00	24	T.S.
A 276/ 58.5	25	-
237/~ 45	26	P.T.S.
51/~122.8	27	P.T.S.
264/116.27	28	P.T.S., P.S.
318/ 54.8	29	P.T.S., P.S.
232/~ 51	30	P.T.S.
259/108.92	31	P.S., S.I.
259/ 65.00	32	P.T.S.
268/~50.5	33	F.I.
259/100.90	34	P.T.S., P.S.
251/ 64.70	35	P.T.S.
22/ 33.5	36	P.T.S.
259/ 97.10	37	P.T.S.
70/188.5	38	F.I.
251/139.4	39	P.T.S.

Sample field number ¹ (field name and location)	Section number ²	Type of section ³ cut or data collected
B 268/44.48	40	P.T.S.
B 268/128.73	41	P.T.S.
B 268/131.95	42	T.S., W.R.A.
B 268/41.46	43	P.T.S., W.R.A.
B 264/67.75	44	P.T.S.
B 268/58.4	45	P.T.S., W.R.A.
B 252/43.30	46	-
B 276/99.70	47	T.S., W.R.A.
A 268/~101	48	T.S., W.R.A.
B 252/50.20	49	P.T.S., W.R.A.
B 276/124.85	50	P.T.S.
B 51/79.90	51	T.S.
B 70/49.90	52	P.T.S.
B 22/48.96	53	P.T.S.
B 268/118.77	54	-
D 259/22.10	55	P.T.S.
D 268/70.87	56	P.T.S., W.R.A.
D 259/30.90	57	P.T.S., W.R.A.
Rd 259/126.87	58	P.T.S.
D 276/73.4	59	P.T.S., W.R.A.
D 51/61.75	60	P.T.S.
U 268/149.90	61	P.T.S., W.R.A.
U(?) 268/38.05	62	P.T.S.
U 268/36.67	63	P.T.S.
U 268/50.34	64	P.T.S.
U 259/52.75	65	P.T.S.
U 259/~69	66	P.T.S., W.R.A.
U 268/137.5	67	P.T.S.
U/P 268/54.62	68	-
U 268/56.68	69	-
U(?) 276/116.05	70	P.T.S., W.R.A.
U 22/51.24	71	P.T.S.
U 70/188.58	72	P.T.S.
U/P 22/143.91	73	P.T.S.
U 51/120.3	74	P.T.S.
U 264/54.05	75	P.T.S., S.I.
P/T 259/123.32	76	P.T.S.
T 259/88.6	77	P.T.S.
Rd 276/126.75	78	P.T.S., S.I.
Rd(?) 259/90.70	79	P.T.S.

Sample field number ¹ (field name and location)	Section number ²	Type of section ³ cut or data collected
Rd 276/47.8	80	P.T.S.
R/G 22/29.55	81	P.T.S.
R 70/214.80	82	P.T.S., W.R.A.
Rd 70/223.03	83	P.T.S.
Rd 22/41.36	84	P.T.S.
Rd 22/136.70	85	P.T.S.
Rd 276/128.00	86	P.T.S., W.R.A.
BIF 276/84.10	87	P.T.S.
BIF 276/88.25	88	P.T.S., S.I., W.R.A.
BIF 259/99.22	89	P.T.S.
BIF 268/58.84	90	P.T.S., W.R.A.
BIF 22/33.9	91	P.T.S.
B/I 264/70.20	92	P.T.S.
BIF 70/77.82	93	P.T.S.
BIF 51/125.58	94	P.T.S.
I/B/R 70/76.20	95	P.T.S.
BIF 51/~124	96	P.T.S.
BIF 70/77.82	97	P.T.S.
B/I 252/119.30	98	P.T.S.
B/I 252/116.60	99	P.T.S.
T(?) 276/106.60	100	P.T.S.
T(?) 276/102.05	101	P.T.S., W.R.A.
T 70/132.15	102	P.T.S.
T 268/35.84	103	P.T.S., S.I.
P/T 51/108.70	104	P.T.S.
T/P 51/~112	105	P.T.S.
T 264/60.50	106	P.T.S.
T 259/84.35	107	P.T.S., W.R.A.
T/P 22/65.15	108	P.T.S.
T 256/54.70	109	P.T.S.
T/P 22/61.08	110	P.T.S.
T/P 51/~112	111	P.T.S.
T(?) 51/89.20	112	P.T.S.
T 256/54.70	113	P.T.S.
T/P 268/140.55	114	P.T.S.
P/T(?) 51/~101	115	P.T.S.
M/G 259/135.10	116	P.T.S., W.R.A.
M/G 276/86.90	117	P.T.S., W.R.A.
M/G 252/75.33	118	P.T.S.

Sample field number ¹ (field name and location)	Section number ²	Type of section ³ cut or data collected
G 252/138.67	119	P.T.S., W.R.A.
G 264/~145	120	P.T.S.
MG 268/106.70	121	P.T.S., W.R.A.
G 264/103.10	122	P.T.S.
M/G 70/210.80	123	P.T.S.
R/G 259/115.77	124	P.T.S.
G 153/47.55	125	P.T.S.
M/G 51/68.57	126	P.T.S.
L/G 22/83.37	127	P.T.S.
G 22/71.70	128	P.T.S.
F 70/214.20	129	P.T.S., W.R.A.
Rd 276/131.05	130	P.T.S., S.I.
L 264/126.35	131	P.T.S.
B 268/22.14	132	P.T.S., W.R.A.
B 268/123.66	133	P.T.S., W.R.A.
D 252/164.90	134	P.T.S., W.R.A.
U 252/45.92	135	P.T.S., W.R.A.
B 259/42.90	136	P.T.S., W.R.A.
Q 22/~143	137	F.I.
Q 70/~183	138	F.I.
Q 153/37.79	139	F.I.
Q 19/32.43	140	F.I.
Q 26/34.10	141	F.I.
Q 263/21.5	142	F.I.
Q 13/57.50	143	F.I.
Q 45/49.90	144	F.I.
Q 48/50.4	145	F.I.
Q 53/46.76	146	F.I.
Q 262/46.4	147	F.I.
Q 262/~149	148	F.I.
Q 274/70.55	149	F.I.
Q 274/~33	150	F.I.
Q 216/190.5	151	F.I.
Q 264/81.4	152	F.I.
Q 253/147.6	153	F.I.
Q 252/115.5	154	F.I.
Q 48/~72	155	F.I.

Sample field number ¹ (field name and location)	Section number ²	Type of section ³ cut or data collected
Q 254/137.9	156	F.I.
Q 254/148.1	157	F.I.
Q 255/62.8	158	F.I.
Q 256/108.4	159	F.I.
Q 259/21.4	160	F.I.
Q 269/~ 127	161	F.I.
Q 259/49.3	162	F.I.
Q 256/~137	163	F.I.
Q 275/89.4	164	F.I.
Q 276/~ 158	165	F.I.
Q 49/~47	166	F.I.
Q 62/~138	167	F.I.
Q 263/137.7	168	F.I.
Sh/F1 42/109.13	169	F.I.
Sh 315/55.7	170	F.I.
D 263/131.8	171	P.T.S., W.R.A.
U 274/~36	172	P.T.S., W.R.A.
D 256/~108	173	P.T.S., W.R.A.
A 262/135.0	174	P.T.S., W.R.A.
A 49/129.4	175	P.T.S., W.R.A.
D 269/130.3	176	P.T.S., W.R.A.
B 254/132.5	177	P.T.S., W.R.A.
D 259/25.6	178	P.T.S., W.R.A.
M/G 62/131.5	179	P.T.S., W.R.A.
B 276/~159	180	P.T.S., W.R.A.
B 275/88.3	181	P.T.S., W.R.A.
B 256/~132	182	P.T.S., W.R.A.
D 255/~ 65	183	P.T.S., W.R.A.
M/G 274/~61	184	W.R.A.
M/G 274/92.6	185	W.R.A.
M/G 274/139.5	186	W.R.A.
M/G 274/154.5	187	W.R.A.
B 255/45.2	188	W.R.A.
B 255/95.2	189	W.R.A.
B 255/122.5	190	W.R.A.
A 71/88.87	191	P.T.S.
T 71/35.5	192	P.T.S.
U 71/40.5	193	P.T.S.
U 71/112.2	194	P.T.S.

Sample field number ¹ (field name and location)	Section number ²	Type of section ³ cut or data collected
D 71/67.4	195	P.T.S.
D 71/67.4	196	P.T.S.
G 88/~64	197	P.T.S.
G 10/~120	198	P.T.S., W.R.A.
G 185/~49	199	P.T.S., W.R.A.
G Mt. Mulgine (peak)	200	P.T.S., W.R.A.
G 167/45.1	201	P.T.S., W.R.A.
G Mt. Mulgine (peak)	202	P.T.S., W.R.A.
275/88.25	203	P.T.S.
71/~123	204	S.I.
71/~144	205	S.I.
315/112.4	206	S.I.
264/82.6	207	S.I.
70/~150	208	S.I.
289/123.2	209	S.I.
276/129.93	210	S.I.
255/145.3	211	S.I.
313/ 61.3	212	S.I.
252/126.1	213	S.I.
51/124.97	214	S.I.
259/108.5	215	S.I.
274/ 67.70	216	S.I.
252/185.5	217	S.I.
259/~118	218	P.S.
301/~142	219	S.I.
273/~109	220	S.I.
70/126.4	221	S.I.
252/158.5	222	S.I.
259/ 99.35	223	S.I.
51/~108	224	S.I.
268/ 67.3	225	S.I.
313/ 98.8	226	S.I.
314/218.5	227	S.I.
F1 314/~86	228	F.I.
301/133.8	229	P.T.S.

APPENDIX 2

Lists of minerals identified in the sections studied.

Notes for Appendix 2

1. In this Appendix, the sample number used is the same as the sample field number in Appendix 1, except that the code letters have been omitted. The microscope section number is shown in the second row. The sections and the remnant samples and sample chips are stored in the School of Geology, University of Adelaide, under the reference number 822.
2. The following abbreviations are used in this Appendix:

Ad	:	Andradite
At	:	Antigorite
Atm	:	Antimony
Ap	:	Apatite
Ars	:	Arsenopyrite
Bi	:	Bismuth
Bl	:	Bowlingite (altered olivine)
Brn	:	Brannerite
Cc	:	Chalcocite
Ch	:	Chert
Chr	:	Chromite
Cht	:	Chrysotile
Cov	:	Covellite
Fd	:	Plagioclase feldspar
Gn	:	Galena
Gb	:	Galenobismutite
Ger	:	Gersdorffite
Hm	:	Hematite
K-t	:	Kobellite-tintinaite
m or (m)	:	minor
Mc	:	Marcasite
Pt	:	Pentlandite
Pr	:	Pyrargyrite
r or (r)	:	relict
Sp	:	Sphalerite
Sps	:	Spessartite
St	:	Stibnite
Stl	:	Stilbite
tr or (tr)	:	trace
T-t	:	Tetrahedrite-tennantite
Ul	:	Ullmannite

Sample number ¹	268/100.2	252/61.2	276/89.9	276/61.2	70/56.09	51/75.00	237/~45
Section number	19	20	21	22	23	24	26
Actinolite or hornblende	✓		✓		✓	✓	
Biotite	✓					✓	
Carbonate	✓		✓				
Chalcopyrite	✓tr		✓tr	✓	✓		✓
Chlorite				✓	✓		
Pyroxene							
Epidote	✓	✓	✓			✓	
Fluorite		✓tr					✓
Ilmenite							
K-feldspar							✓
Magnetite							
Molybdenite	✓	✓					
Muscovite							✓
Phlogopite							
Pyrite	✓	✓	✓	✓	✓		✓
Pyrrhotite					✓		
Quartz	✓	✓	✓	✓	✓	✓	✓
Rutile			✓	✓			
Scheelite	✓	✓		✓	✓		✓
Sericite		✓		✓			
Sphene		✓m				✓	
Talc							
Tetrahedrite	✓	✓					
Tremolite		✓m			✓		
Other ²	St1,T-t	Fd(r)					Fd

Sample number ¹	51/~122.8	264/116.27	318/54.8	232/~51	259/108.92	259/65.00
Section number	27	28	29	30	31	32
Actinolite or hornblende						
Biotite			✓			
Carbonate						
Chalcopyrite	✓		✓	✓tr	✓	
Chlorite						
Pyroxene						✓
Epidote	✓r					✓
Fluorite				✓		
Ilmenite						
K-feldspar						
Magnetite				✓		
Molybdenite	✓	✓				✓
Muscovite				✓		
Phlogopite	✓					✓
Pyrite	✓	✓		✓	✓	✓
Pyrrhotite			✓		✓	
Quartz	✓	✓	✓	✓		✓
Rutile	✓			✓		
Scheelite	✓	✓		✓		
Sericite						
Sphene	✓					✓
Talc						
Tetrahedrite		✓		✓		
Tremolite						
Other ²	Ap	Ars, Sp, K-t	Ars, Sp, St	Ap, Il, Brn	Mc	Ap

Sample number ¹	259/100.90	251/64.7	22/33.5	259/97.1	251/139.4	268/44.48
Section number	34	35	36	37	39	40
Actinolite or hornblende						
Biotite	✓				✓	✓
Carbonate						✓
Chalcopyrite	✓		✓		✓	
Chlorite					✓	
Pyroxene						
Epidote			✓			
Fluorite				✓		✓
Ilmenite						
K-feldspar						✓
Magnetite			✓			
Molybdenite	✓m					
Muscovite	✓	✓			✓	
Phlogopite				✓		
Pyrite	✓m		✓		✓	✓
Pyrrhotite	✓			✓		
Quartz	✓	✓	✓		✓	
Rutile	✓			✓m	✓	
Scheelite		✓	✓	✓		
Sericite						
Sphene	✓			✓		✓m
Talc						
Tetrahedrite						
Tremolite				✓		✓
Other ²		Hbn	Ars, Cc, Hm, Hbn		Mc	St, Ch

Sample number ¹	268/128.73	268/131.95	268/41.46	264/67.75	268/58.4	276/99.7
Section number	41	42	43	44	45	47
Actinolite or hornblende			✓		✓	
Biotite						
Carbonate	✓	✓				
Chalcopyrite			✓tr	✓		
Chlorite	✓					✓
Pyroxene	✓					
Epidote	✓	✓		✓	✓	✓tr
Fluorite						
Ilmenite						
K-feldspar						
Magnetite						
Molybdenite	✓			✓		
Muscovite	✓		✓			
Phlogopite		✓	✓	✓	✓	
Pyrite	✓		✓	✓	✓	✓
Pyrrhotite						
Quartz	✓	✓	✓	✓	✓	✓
Rutile			✓			
Scheelite		✓m				
Sericite	✓					
Sphene	✓	✓	✓	✓	✓	✓
Talc						
Tetrahedrite			✓			
Tremolite	✓	✓	✓	✓		
Other ²						

Sample number ¹	268/~101	252/50.20	276/124.85	51/79.90	70/49.9	22/48.96
Section number	48	49	50	51	52	53
Actinolite or hornblende	✓	✓	✓	✓	✓	✓
Biotite	✓	✓			✓	
Carbonate			✓		✓	
Chalcopyrite		✓	✓		✓	✓
Chlorite						
Pyroxene						
Epidote	✓	✓	✓		√m	✓
Fluorite	✓					
Ilmenite			✓		✓	
K-feldspar						✓
Magnetite						
Molybdenite						
Muscovite						
Phlogopite			✓			
Pyrite		✓	✓		✓	✓
Pyrrhotite					✓	
Quartz	✓	✓	✓	✓	✓	✓
Rutile						✓
Scheelite	✓	√m	✓		✓	
Sericite						
Sphene	✓	✓	✓	✓		✓
Talc						
Tetrahedrite						
Tremolite	✓		√m			√m
Other ²					Pt, T-t	

Sample number ¹	259/22.10	268/70.87	259/30.90	259/126.87	276/73.4	51/61.75
Section number	55	56	57	58	59	60
Actinolite or hornblende	✓	✓	✓		✓	✓
Biotite	✓	✓			✓	✓
Carbonate		✓				
Chalcopyrite	✓	✓tr	✓tr	✓	✓tr	✓
Chlorite	✓				✓	
Pyroxene						
Epidote	✓	✓	✓		✓	✓
Fluorite				✓		
Ilmenite						
K-feldspar				✓tr		
Magnetite	✓	✓			✓	✓
Molybdenite						
Muscovite				✓		
Phlogopite			✓	✓		
Pyrite	✓	✓	✓	✓tr		✓
Pyrrhotite				✓		
Quartz	✓	✓	✓	✓	✓	✓
Rutile			✓	✓		✓
Scheelite	✓		✓			
Sericite				✓	✓	
Sphene	✓	✓	✓		✓	✓
Talc						
Tetrahedrite			✓			✓
Tremolite	✓m		✓			
Other ²	Hm			Ars(m),Sp	Hm	

Sample number ¹	268/149.9	268/38.05	268/36.67	268/50.34	259/52.75	259/~69
Section number	61	62	63	64	65	66
Actinolite or hornblende				✓		
Biotite			✓			
Carbonate	✓		✓			
Chalcopyrite	✓tr		✓tr	✓tr	✓tr	
Chlorite	✓		✓			
Pyroxene	✓	✓				
Epidote	✓			✓m		✓m
Fluorite	✓		✓	✓		
Ilmenite			✓			
K-feldspar	✓					
Magnetite						
Molybdenite						✓
Muscovite			✓			
Phlogopite	✓	✓				
Pyrite	✓	✓	✓	✓	✓	✓
Pyrrhotite						
Quartz	✓	✓	✓	✓	✓	✓
Rutile	✓tr			✓	✓	
Scheelite						
Sericite						
Sphene	✓	✓	✓	✓	✓	
Talc						✓
Tetrahedrite					✓	✓
Tremolite	✓m	✓		✓	✓	✓
Other ²	Ap		St	Ch		Fd(m)

Sample number ¹	268/137.5	276/116.05	22/51.24	70/188.58	22/143.91	51/120.3
Section number	67	70	71	72	73	74
Actinolite or hornblende		✓	✓		✓	✓
Biotite			✓		✓	
Carbonate	✓	✓	✓			
Chalcopyrite	✓tr	✓tr	✓		✓	✓tr
Chlorite		✓				
Pyroxene		✓				✓
Epidote	✓		✓	✓	✓	
Fluorite						
Ilmenite						
K-feldspar						
Magnetite						
Molybdenite			✓			
Muscovite						
Phlogopite	✓	✓				✓
Pyrite	✓	✓	✓	✓	✓	✓
Pyrrhotite						
Quartz	✓		✓			✓
Rutile	✓	✓tr	✓			
Scheelite						
Sericite						
Sphene	✓	✓	✓	✓	✓	✓
Talc					✓	
Tetrahedrite	✓					
Tremolite	✓	✓	✓m	✓	✓	✓
Other ²	St				Ap(tr), Fd(r)	Fd

Sample number ¹	264/54.05	259/123.32	259/88.6	276/126.75	259/90.70	276/47.8
Section number	75	76	77	78	79	80
Actinolite or hornblende						
Biotite				✓	✓m	
Carbonate						
Chalcopyrite	✓	✓	✓	✓	✓	
Chlorite	✓					✓
Pyroxene						
Epidote						
Fluorite		✓	✓			
Ilmenite						
K-feldspar						
Magnetite						
Molybdenite			✓	✓		
Muscovite	✓			✓	✓	
Phlogopite		✓	✓			
Pyrite	✓	✓	✓	✓	✓	✓
Pyrrhotite				✓	✓	
Quartz		✓m	✓	✓	✓	✓
Rutile	✓		✓m	✓	✓	✓
Scheelite						
Sericite	✓		✓	✓		✓
Sphene	✓	✓	✓		✓m	✓tr
Talc						
Tetrahedrite	✓	✓	✓			
Tremolite	✓	✓	✓	✓		
Other ²	Ch	Ars, Sp, T-t	Sp		Mc, Sp	

Sample ₁ number	22/29.55	70/214.80	70/223.03	22/41.36	22/136.70	276/84.10
Section number	81	82	83	84	85	86
Actinolite or hornblende						
Biotite	✓		✓	✓	✓	✓
Carbonate			✓			
Chalcopyrite	✓tr	✓	✓	✓	✓	✓
Chlorite			✓	✓	✓	✓
Pyroxene						
Epidote	✓		✓		✓	✓r
Fluorite						
Ilmenite						✓
K-feldspar			✓		✓	
Magnetite	✓		✓	✓		
Molybdenite						
Muscovite		✓			✓	✓
Phlogopite						
Pyrite	✓	✓		✓	✓	✓
Pyrrhotite		✓			✓	
Quartz	✓	✓	✓	✓	✓	✓
Rutile		✓			✓	✓
Scheelite						
Sericite			✓m			✓
Sphene				✓m		✓tr
Talc						
Tetrahedrite						
Tremolite						
Other ²						

Sample ₁ number	276/84.10	276/88.25	259/99.22	268/58.84	22/33.9	264/70.2
Section number	87	88	89	90	91	92
Actinolite or hornblende		√m	√			
Biotite			√			√
Carbonate	√		√	√	√	
Chalcopyrite	√				√	√
Chlorite	√	√				√
Pyroxene						
Epidote			√			√
Fluorite						√m
Ilmenite	√					
K-feldspar						
Magnetite		√	√	√	√	√
Molybdenite	√					√
Muscovite						
Phlogopite				√		
Pyrite	√	√	√	√	√	√
Pyrrhotite					√tr	
Quartz	√	√	√	√	√	√
Rutile	√tr					
Scheelite						
Sericite						
Sphene	√	√	√m			√m
Talc						
Tetrahedrite			√tr		√	
Tremolite		√m	√			
Other ²	Ars				Cov, Ad	Cc, Cov, Mc(m)

Sample ₁ number	70/77.82	51/125.58	70/76.20	51/~124	70/77.82	252/119.30
Section number	93	94	95	96	97	98
Actinolite or hornblende			✓		✓	
Biotite	✓	✓	✓	✓	✓	
Carbonate	✓	✓	✓m	✓	✓	
Chalcopyrite	✓m	✓	✓tr	✓	✓	✓
Chlorite					✓	✓
Pyroxene	✓		✓			
Epidote	✓	✓	✓		✓	
Fluorite						✓
Ilmenite						
K-feldspar						✓
Magnetite		✓		✓		
Molybdenite	✓		✓m			✓
Muscovite						
Phlogopite						
Pyrite	✓	✓	✓	✓	✓	✓
Pyrrhotite						✓tr
Quartz	✓	✓	✓	✓	✓	✓
Rutile						✓
Scheelite						
Sericite						✓
Sphene	✓		✓	✓	✓	✓
Talc						
Tetrahedrite	✓m	✓tr				✓tr
Tremolite			✓			
Other ²						

Sample number	252/116.60	276/106.60	276/102.05	70/132.15	268/35.84	51/108.70
Section number	99	100	101	102	103	104
Actinolite or hornblende	✓					
Biotite	✓					
Carbonate	✓	✓	✓			
Chalcopyrite		✓	✓tr			✓
Chlorite		✓	✓		✓	
Pyroxene		✓				
Epidote	✓	✓	✓			✓
Fluorite		✓m				
Ilmenite						
K-feldspar						
Magnetite	✓			✓		
Molybdenite					✓	✓
Muscovite						
Phlogopite		✓			✓	✓
Pyrite	✓	✓	✓	✓	✓	✓
Pyrrhotite						
Quartz	✓	✓m	✓			✓
Rutile		✓			✓m	✓
Scheelite			✓		✓	✓
Sericite						
Sphene		✓	✓		✓	✓
Talc		✓	✓	✓	✓	
Tetrahedrite		✓m				✓
Tremolite		✓	✓	✓		✓
Other ²	Ap			Hm	Pt, Ger, Ul, Ch	Cc, Fd, Pr, Bi, Gb

Sample number ¹	51/~112	264/60.50	259/84.35	22/65.15	256/54.70	22/61.08
Section number	105	106	107	108	109	110
Actinolite or hornblende						
Biotite						
Carbonate						√tr
Chalcopyrite	√tr	√	√	√		√
Chlorite						√
Pyroxene			√	√		
Epidote						
Fluorite	√tr		√			
Ilmenite						
K-feldspar						
Magnetite				√		√
Molybdenite						
Muscovite			√			√tr
Phlogopite	√	√			√	
Pyrite	√	√	√		√	√
Pyrrhotite	√tr			√		√tr
Quartz	√					
Rutile	√tr	√	√		√	
Scheelite			√			
Sericite						
Sphene	√	√	√		√m	
Talc			√	√		√m
Tetrahedrite			√		√	
Tremolite	√	√		√	√	√
Other ²			St, Fd(r)	Bl(?) Cht		Cht

Sample ₁ number	51/~112	51/89.20	256/54.7	268/140.55	51/101	259/135.1
Section number	111	112	113	114	115	116
Actinolite or hornblende						
Biotite						
Carbonate		✓		✓		
Chalcopyrite	✓	✓	✓tr		✓	✓
Chlorite			✓			
Pyroxene						
Epidote	✓	✓				
Fluorite	✓	✓m				✓
Ilmenite				✓		
K-feldspar						
Magnetite	✓			✓		
Molybdenite	✓					
Muscovite		✓				✓
Phlogopite	✓		✓		✓	✓
Pyrite	✓	✓	✓	✓	✓	✓
Pyrrhotite						✓
Quartz	✓	✓			✓	✓
Rutile	✓	✓	✓		✓	✓
Scheelite		✓		✓m		
Sericite						
Sphene	✓	✓	✓r		✓	
Talc	✓				✓	
Tetrahedrite	✓			✓	✓	
Tremolite		✓	✓	✓		
Other ²	Ap, Chr	Ap		Chr	Ars	Mc

Sample number ¹	276/86.9	252/75.33	252/138.67	264/~145	268/106.7	264/103.1
Section number	117	118	119	120	121	122
Actinolite or hornblende					√tr	
Biotite						
Carbonate						
Chalcopyrite	√tr	√	√			
Chlorite	√m					
Pyroxene						
Epidote					√tr	
Fluorite		√	√m			
Ilmenite						
K-feldspar					√m	
Magnetite						
Molybdenite		√	√			
Muscovite	√	√	√	√	√	√
Phlogopite						
Pyrite	√	√	√		√	
Pyrrhotite						
Quartz	√	√	√	√	√	√
Rutile	√m		√		√	
Scheelite		√				
Sericite		√			√	
Sphene	√m		√r			
Talc						
Tetrahedrite		√			√	
Tremolite						
Other ²			Sp		Mc	

Sample ₁ number	70/210	259/115.77	153/47.55	51/68.57	22/83.37	22/71.70
Section number	123	124	125	126	127	128
Actinolite or hornblende						
Biotite						
Carbonate						
Chalcopyrite		✓	✓	✓	✓	✓
Chlorite				✓m		
Pyroxene						
Epidote					✓r	
Fluorite		✓				
Ilmenite						
K-feldspar			✓			
Magnetite						
Molybdenite					✓	✓m
Muscovite	✓	✓	✓	✓	✓	✓
Phlogopite		✓				
Pyrite	✓	✓	✓	✓	✓	✓
Pyrrhotite		✓				
Quartz	✓	✓	✓	✓	✓	✓
Rutile	✓	✓		✓		✓
Scheelite						
Sericite	✓	✓			✓	✓
Sphene	✓m			✓tr	✓r	✓
Talc						
Tetrahedrite					✓	✓
Tremolite						
Other ²		Sp, Sps	Cc	Fd(r)	Fd(r)	Sp

Sample number	70/214.20	276/131.05	264/126.35	268/22.14	268/123.66	252/164.90
Section number	129	130	131	132	133	134
Actinolite or hornblende	✓			✓		✓
Biotite		✓		✓		✓
Carbonate	✓				✓	
Chalcopyrite	✓	✓	✓	✓tr		✓
Chlorite		✓		✓		
Pyroxene					✓	
Epidote	✓			✓m	✓	✓m
Fluorite						
Ilmenite						
K-feldspar						
Magnetite						✓
Molybdenite		✓	✓		✓	✓
Muscovite		✓	✓			
Phlogopite	✓				✓	
Pyrite	✓	✓	✓	✓	✓	✓
Pyrrhotite		✓	✓			
Quartz	✓	✓	✓	✓	✓	✓
Rutile		✓	✓	✓	✓	✓
Scheelite						
Sericite		✓				
Sphene	✓		✓	✓m	✓	
Talc						
Tetrahedrite	✓				✓	✓
Tremolite	✓					
Other ²			Ars(tr), Cc,Fd			

Sample ₁ number	252/45.92	259/42.90	263/131.8	274/~36	256/~108	262/135
Section number	135	136	171	172	173	174
Actinolite or hornblende	✓	✓	✓		✓	
Biotite	✓					✓
Carbonate			✓		✓	✓
Chalcopyrite	✓	✓	✓	✓tr		✓
Chlorite			✓			✓
Pyroxene	✓					✓
Epidote	✓	✓m	✓		✓	✓
Fluorite						
Ilmenite					✓	
K-feldspar						
Magnetite					✓	✓
Molybdenite						
Muscovite						
Phlogopite				✓		
Pyrite	✓	✓	✓	✓	✓	✓
Pyrrhotite				✓tr		
Quartz	✓		✓	✓	✓	✓
Rutile	✓	✓		✓m		✓tr
Scheelite	✓					
Sericite	✓					
Sphene	✓	✓		✓	✓	✓m
Talc			✓			
Tetrahedrite			✓	✓tr		
Tremolite			✓	✓		
Other ²						

Sample number	49/129.4	269/130.3	254/132.5	259/25.6	62/131.5	276/~159
Section number	175	176	177	178	179	180
Actinolite or hornblende		✓	✓	✓		✓
Biotite	✓					
Carbonate		✓m	✓			✓m
Chalcopyrite	✓	✓	✓	✓		✓tr
Chlorite	✓					
Pyroxene						✓
Epidote	✓	✓	✓	✓	✓	✓
Fluorite				✓tr		
Ilmenite						
K-feldspar						
Magnetite		✓				
Molybdenite					✓	
Muscovite						
Phlogopite			✓		✓	✓
Pyrite	✓	✓	✓	✓	✓	✓
Pyrrhotite						
Quartz	✓	✓	✓	✓	✓	
Rutile	✓		✓m			✓m
Scheelite						
Sericite	✓					
Sphene	✓	✓	✓	✓	✓	✓m
Talc				✓		
Tetrahedrite						
Tremolite					✓r	
Other ²			Fd(r)			Ap(m)

Sample number ¹	275/88.3	256/~32	255/~65	71/88.87	71/35.5	71/40.5	71/112.2
Section number	181	182	183	191	192	193	194
Actinolite or hornblende	✓	✓	✓	✓		✓	
Biotite				✓		✓	
Carbonate			✓				
Chalcopyrite			✓	✓	✓m	✓tr	✓tr
Chlorite			✓		✓		
Pyroxene	✓						
Epidote	✓m	✓	✓tr	✓		✓	
Fluorite							
Ilmenite			✓				
K-feldspar							
Magnetite			✓		✓		
Molybdenite							✓
Muscovite							✓
Phlogopite		✓					✓
Pyrite	✓	✓	✓	✓	✓	✓	✓
Pyrrhotite							
Quartz		✓m	✓	✓			✓
Rutile		✓tr				✓m	✓
Scheelite							
Sericite			✓	✓		✓	✓
Sphene	✓	✓		✓			
Talc					✓		
Tetrahedrite	✓	✓					
Tremolite		✓			✓		
Other ²					Cht		Mc

Sample number ¹	71/67.4	71/67.4	88/~64	10/~120	185/~49	Mt. Mulgine (peak)	167/45.1
Section number	195	196	197	198	199	200	201
Actinolite or hornblende	✓						
Biotite	✓	✓		✓			
Carbonate	✓	✓					
Chalcopyrite	✓	✓		✓m	✓		✓
Chlorite	✓tr	✓				✓	
Pyroxene							
Epidote	✓	✓				✓	
Fluorite			✓tr		✓m		✓
Ilmenite	✓					✓	
K-feldspar				✓		✓	✓
Magnetite	✓	✓					
Molybdenite							
Muscovite			✓	✓	✓	✓m	✓
Phlogopite							
Pyrite	✓	✓		✓	✓	✓	✓
Pyrrhotite	✓						✓
Quartz	✓	✓		✓	✓	✓	✓
Rutile				✓			
Scheelite							
Sericite	✓	✓		✓			✓
Sphene	✓	✓					✓m
Talc							
Tetrahedrite							
Tremolite							
Other ²			Ap				Cov

Sample number ¹	Mt. Mulgine (peak)	275/88.25	301/133.8
Section number	202	203	229
Actinolite or hornblende		✓	
Biotite			
Carbonate			✓
Chalcopyrite			✓
Chlorite			
Pyroxene			
Epidote		✓	✓
Fluorite			
Ilmenite			
K-feldspar	✓		
Magnetite			
Molybdenite			
Muscovite	✓		
Phlogopite			
Pyrite	✓	✓	✓
Pyrrhotite			
Quartz	✓	✓	✓
Rutile	✓		
Scheelite		✓m	✓
Sericite			
Sphene	✓m	✓	
Talc			
Tetrahedrite		✓m	✓
Tremolite		✓	✓
Other ²			Atm, Gn

APPENDIX 3

Whole rock and trace element analyses

APPENDIX 3

WHOLE ROCK AND TRACE ELEMENT ANALYSES

Preparation of the samples for analysis

Each of the selected samples was first crushed using a small jaw crusher and then ground to about 200-mesh in a chrome steel vessel on a Siebtechnik mill.

For the whole rock analysis, about 6 cm³ of each sample was pre-heated in an oven at 110°C for 2-3 hours before being weighed and heated in a furnace at 960°C for at least 12 hours. After ignition, the samples were cooled in a dessicator and re-weighed.

Except for sample 268/58.84 which gained 0.25% of its weight, all the other samples lost weight on ignition, as much as 9.5 wt.% in sample 276/61.2. Sample 268/58.84 is of a BIF and the gain in weight is thought to be mainly due to oxidation of Fe²⁺ to Fe³⁺.

The XRF whole rock analyses were done on fused buttons, each made from the following mixture:

0.280g rock powder
0.020g sodium nitrate
1.500g flux.

The flux is a mixture of lithium tetraborate, lithium carbonate and lanthanum oxide.

XRF trace element measurements were done on pressed pellets. The sample pellets, which have boric acid powder bases and sides, were made using the method described by Norrish and Chappell (1967).

Na₂O values were obtained by flame photometry: About 0.03g of each sample powder was digested in 2 cm³ sulphuric acid and 10 cm³ hydrofluoric acid, in a teflon beaker. The solutions were made up to 100 cm³.

Other trace elements (Ag, Be, Co, Cu, Li and Pb) were determined on the Techtron AA-6 spectrophotometer: Approximately 1g of each sample powder was digested in 2 cm³ perchloric acid and 10 cm³ hydrofluoric acid. For some samples nitric acid and/or hydrochloric acid had to be added to effect complete digestion. The final solutions were made up to 100 cm³ containing 2,000 ppm K as an ionization suppressor.

Detection limits

The following table shows the detection limits obtained by the XRF and the AA techniques used for the trace element analyses.

DETECTION LIMITS (in parts per million)

XRF		AA	
Element	Detection limit (3 σ confidence)	Element	Detection limit (approximate)
Sr	1.2	Cu	2.7
Rb	1.3	Li	1.8
Y	1.4	Pb	5.4
Ga	2.6	Ag	1.5
Ba	4.1	Be	0.6
Sc	1.0	Co	3.0
Zr	2.4		
Nb	1.6		
Ni	3.4		
Mo	2.3		
W	5.8		
Sn	4.2		
Cr	4.9		
V	2.4		
As	2.0		
Zn	1.5		
Sb	6.6		
Ce	8.0		
Nd	4.6		

Explanation of symbols in table of analytical data

- a) For explanation of the sample numbers, refer to Appendix 1.
- b) Total iron is given as Fe₂O₃.
- c) Totals are expressed as loss (on ignition)-free.
- d) Rb interferes with Y in XRF analyses and in the case of sample 259/84.35, the very high Rb (the highest obtained in this study) produced an unsatisfactory Y value.
- e) Samples with an unsatisfactory value for Ce. Some of these samples have very high As values and it is known that high As and/or Cs can cause problems with Ce analyses.
- f) The Cr values may be high because of contamination from the chrome steel grinding vessel that was used in preparation of the samples.

- g) Sample 268/58.84 which is a BIF gained weight on ignition. All the other samples lost weight on ignition.
- h) G. M.M. peak - Granite samples collected from the Mount Mulgine peak.

WHOLE ROCK ANALYSIS AND TRACE ELEMENT DATA

Sample group (this study)	THOLEIITIC META-BASALTS				
Sample field number ^a	A268/100.2	A252/61.2	A276/89.9	B276/99.70	A268/~101
Section number	19	20	21	47	48
<u>oxides (wt.%)</u>					
SiO ₂	51.98	49.63	53.17	56.27	51.76
TiO ₂	0.76	1.19	1.00	1.12	0.75
Al ₂ O ₃	14.58	14.70	11.89	14.62	15.10
Fe ₂ O ₃ ^b	10.52	13.29	11.51	12.07	9.94
MnO	0.20	0.18	0.24	0.16	0.18
MgO	7.78	7.22	8.70	9.76	7.34
CaO	7.73	7.69	8.32	1.51	10.38
Na ₂ O	1.42	0.11	0.79	1.61	2.30
K ₂ O	4.31	5.15	4.19	2.52	2.27
P ₂ O ₅	0.07	0.10	0.09	0.09	0.10
Total ^c	99.35	99.26	99.91	99.71	100.12
Loss on ignition	3.05	4.51	2.27	4.79	3.70
<u>Elements (ppm)</u>					
Ag	10	6	4	3	12
As	193	61	145	49	156
Ba (XRF)	332	168	366	85	80
Ba (AA)	330	190	380	70	60
Be	10	14	9	4	26
Ce	13	14	8	16	7
Co ^f	44	34	42	33	39
Cr	189	184	695	729	173
Cu	315	242	56	154	245
Ga	18	28	15	18	23
Li	368	392	42	140	168
Mo	54	29	7	17	100
Nb	3	8	3	3	6
Nd	8	8	8	11	9
Ni (XRF)	110	53	145	169	93
Ni (AA)	122	61	161	180	102
Pb	49	6	30	4	247
Rb (XRF)	808	917	494	312	453
Rb (AA)	830	1050	530	350	480
Sb	235	130	45	20	295
Sc	38	39	48	46	41
Sn	10	25	<5	5	20
Sr	176	177	122	37	273
V	233	269	293	351	216
W	30	50	20	30	170
Y	8	16	16	19	11
Zn (XRF)	141	104	110	114	152
Zn (AA)	140	98	107	116	150
Zr	38	50	60	65	32

WHOLE ROCK ANALYSIS AND TRACE ELEMENT DATA

Sample group (this study)	THOLEIITIC META-BASALTS				
Sample field number ^a	B252/50.20	D268/70.87	D259/30.90	D276/73.4	U268/149.90
Section number	49	56	57	59	61
<u>oxides(wt.%)</u>					
SiO ₂	55.99	50.08	51.00	51.00	48.57
TiO ₂	0.97	1.53	0.83	1.80	1.32
Al ₂ O ₃	12.93	14.01	13.88	13.27	14.74
Fe ₂ O ₃ ^b	10.07	15.32	12.45	18.41	13.06
MnO	0.17	0.22	0.21	0.31	0.22
MgO	9.11	6.36	5.67	4.82	6.76
CaO	5.11	7.87	9.76	5.92	8.42
Na ₂ O	0.35	0.45	0.61	0.75	0.14
K ₂ O	4.98	3.73	4.04	3.62	5.60
P ₂ O ₅	0.10	0.08	0.08	0.21	0.29
Total ^c	99.78	99.65	98.53	100.10	99.12
Loss on ignition	3.12	3.87	6.05	3.09	5.56
<u>Elements(ppm)</u>					
Ag	4	6	24	4	17
As	50	172	72	126	167
Ba (XRF)	80	126	144	261	393
(AA)	60	90	80	150	250
Be	8	12	59	7	9
Ce	5	12	14	24	13
Co	41	46	36	46	45
Cr ^f	608	134	251	165	286
Cu	150	201	448	96	444
Ga	15	18	28	18	23
Li	275	192	323	79	326
Mo	11	11	59	6	74
Nb	2	5	3	5	22
Nd	10	18	8	18	10
Ni (XRF)	164	42	58	63	61
(AA)	167	45	64	60	72
Pb	40	34	460	13	9
Rb (XRF)	1050	739	805	496	758
(AA)	1100	730	790	490	870
Sb	25	85	115	40	400
Sc	43	36	29	42	41
Sn	10	10	15	5	20
Sr	85	102	136	98	413
V	297	378	185	389	308
W	20	500	2190	30	60
Y	25	29	29	36	18
Zn (XRF)	166	144	101	156	80
(AA)	160	137	104	150	79
Zr	51	85	38	109	67

WHOLE ROCK ANALYSIS AND TRACE ELEMENT DATA

Sample group (this study)	THOLEIITIC META-BASALTS				
Sample field number ^a	U(?)276/116.05	B268/22.14	D252/164.90	B254/132.5	D263/131.8
Section number	70	132	134	177	171
<u>oxides(wt.%)</u>					
SiO ₂	52.88	53.06	50.99	52.70	52.24
TiO ₂	0.89	0.98	1.56	0.77	1.08
Al ₂ O ₃ ^b	11.78	12.1	14.54	15.52	15.07
Fe ₂ O ₃ ^b	11.41	12.53	14.78	7.55	12.72
MnO	0.24	0.23	0.23	0.17	0.19
MgO	9.40	10.62	6.42	6.65	5.63
CaO	9.53	8.19	5.98	10.64	8.00
Na ₂ O	0.26	1.48	1.00	1.92	0.19
K ₂ O	3.75	0.92	4.05	3.55	4.44
P ₂ O ₅	0.09	0.09	0.16	0.08	0.10
Total ^c	100.23	100.20	99.71	99.53	99.65
Loss on ignition	2.95	2.34	2.71	3.00	3.47
<u>Elements(ppm)</u>					
Ag	5	3	4	6	3
As	114	16	38	51	70
Ba ^(XRF AA)	75 170	22 20	106 50	226 -	95 -
Be	6	4	21	9	10
Ce	18	9	15	2	12
Co ^f	41	51	37	22	36
Cr ^f	742	700	179	209	135
Cu	115	113	741	114	22
Ga	15	14	33	16	20
Li	116	134	232	107	179
Mo	7	22	10	5	16
Nb	2	2	15	3	3
Nd	5	13	10	6	11
Ni ^(XRF AA)	140 141	164 156	58 51	97 -	43 -
Pb	30	9	13	77	6
Rb ^(XRF AA)	508 540	169 190	675 680	527 -	791 -
Sb	85	25	80	100	70
Sc	44	47	54	43	40
Sn	<5	5	30	<5	<5
Sr	117	45	99	235	233
V	297	303	311	231	291
W	40	20	210	300	200
Y	14	21	24	9	15
Zn ^(XRF AA)	85 85	133 132	232 223	85 -	110 -
Zr	50	57	93	39	64

WHOLE ROCK ANALYSIS AND TRACE ELEMENT DATA

Sample group (this study)	THOLEIITIC META-BASALTS				
Sample field number ^a	D256/~108	A262/135.0	A49/129.4	D269/130.3	D259/25.6
Section number	173	174	175	176	178
<u>oxides (wt.%)</u>					
SiO ₂	56.68	51.42	51.36	51.15	51.78
TiO ₂	1.91	1.25	1.56	1.65	0.99
Al ₂ O ₃	10.89	14.33	14.53	12.65	14.57
Fe ₂ O ₃ ^b	12.50	13.57	14.39	14.01	11.89
MnO	0.18	0.21	0.18	0.20	0.16
MgO	2.53	5.69	6.70	2.89	6.08
CaO	14.47	9.05	3.03	16.81	7.97
Na ₂ O	0.12	0.12	0.13	0.14	1.44
K ₂ O	0.13	3.30	6.60	0.02	4.23
P ₂ O ₅	0.18	0.12	0.17	0.16	0.10
Total ^c	99.58	99.06	98.65	99.67	99.21
Loss on ignition	4.48	2.53	2.73	1.62	3.75
<u>Elements (ppm)</u>					
Ag	3	3	3	3	6
As	31	240	75	17	55
Ba (XRF AA)	3	244	333	0	131
Be	3	6	7	3	13
Ce	16	4	10	25	-e
Co	19	42	18	35	26
Cr ^f	165	212	124	155	126
Cu	96	165	393	84	685
Ga	20	20	23	30	18
Li	39	160	292	8	188
Mo	1	36	10	0	9
Nb	5	6	5	5	3
Nd	18	10	20	25	10
Ni (XRF AA)	16	75	38	25	55
Pb	5	0	2	17	58
Rb (XRF AA)	15	556	1286	2	791
Sb	50	90	60	20	70
Sc	29	38	43	40	35
Sn	<5	5	<5	<5	5
Sr	255	250	96	234	129
V	359	348	407	418	263
W	10	50	50	<10	230
Y	32	19	34	29	14
Zn (XRF AA)	72	105	193	68	138
Zr	107	66	119	89	53

WHOLE ROCK ANALYSIS AND TRACE ELEMENT DATA

Sample group (this study)	THOLEIITIC META-BASALTS			HIGH Mg META-BASALT
Sample field number ^a	M/G62/131.5	D255/~65	B255/45.2	B255/122.5
Section number	179	183	188	190
<u>oxides(wt.%)</u>				
SiO ₂	54.05	51.62	51.62	50.14
TiO ₂	0.85	1.96	1.00	0.85
Al ₂ O ₃	14.68	14.41	11.21	9.43
Fe ₂ O ₃ ^b	7.88	17.63	12.84	14.29
MnO	0.20	0.30	0.21	0.22
MgO	6.37	6.51	10.82	13.60
CaO	9.88	3.76	8.94	9.44
Na ₂ O	0.48	0.88	0.54	1.35
K ₂ O	5.11	2.77	2.55	0.67
P ₂ O ₅	0.11	0.12	0.13	0.10
Total ^c	99.60	99.46	99.74	100.10
Loss on ignition	4.87	4.34	2.40	1.52
<u>Elements(ppm)</u>				
Ag	4	3	1	2
As	108	9	13	69
Ba (XRF (AA	248	61	97	20
Be	16	9	5	2
Ce	4	9	7	5
Co	27	19	41	68
Cr ^f	159	69	608	1450
Cu	106	141	81	64
Ga	17	22	14	14
Li	218	153	80	63
Mo	9	6	4	4
Nb	3	3	3	2
Nd	8	14	14	14
Ni (XRF (AA	72	37	122	331
Pb	15	0	2	7
Rb (XRF (AA	797	490	361	101
Sb	100	15	20	45
Sc	37	41	46	44
Sn	5	<5	<5	<5
Sr	142	41	79	68
V	192	544	294	269
W	410	10	10	<10
Y	12	23	19	17
Zn (XRF (AA	100	174	147	94
Zr	55	86	72	51

WHOLE ROCK ANALYSIS AND TRACE ELEMENT DATA

Sample group (this study)	HIGH Mg META-BASALTS				
Sample field number ^a	B268/131.95	B268/41.46	B268/58.4	U259/~69	B268/123.66
Section number	42	43	45	66	133
<u>oxides (wt.%)</u>					
SiO ₂	52.17	53.84	47.33	49.58	51.56
TiO ₂	0.87	0.54	0.92	0.48	0.61
Al ₂ O ₃	6.53	6.03	10.40	4.76	5.48
Fe ₂ O ₃ ^b	10.04	10.91	14.49	10.03	9.04
MnO	0.24	0.27	0.21	0.38	0.23
MgO	15.06	14.46	12.69	16.57	15.77
CaO	12.72	11.03	8.30	13.56	12.82
Na ₂ O	0.32	0.28	0.70	0.12	0.15
K ₂ O	1.74	2.16	4.63	3.31	3.64
P ₂ O ₅	0.09	0.06	0.09	0.04	0.06
Total ^c	99.77	99.58	99.77	98.83	99.36
Loss on ignition	2.33	3.33	3.90	3.02	2.11
<u>Elements(ppm)</u>					
Ag	9	6	6	22	8
As	194	164	593	1820	449
Ba (XRF (AA	52 90	122 130	299 310	63 40	101 80
Be	15	40	42	9	13
Ce	15	8	10	14	5
Co	52	49	37	77	60
Cr ^f	1620	2450	1020	2770	2210
Cu	215	115	220	297	153
Ga	15	13	16	11	9
Li	123	178	487	405	624
Mo	5	10	18	28	9
Nb	4	7	4	3	2
Nd	11	6	9	9	8
Ni (XRF (AA	257 262	248 280	89 123	274 296	270 280
Pb	9	9	2	245	11
Rb (XRF (AA	341 370	419 480	1140 1140	700 670	887 860
Sb	250	205	155	655	210
Sc	60	55	33	53	50
Sn	10	15	15	20	10
Sr	81	57	251	49	40
V	274	234	269	191	231
W	40	1070	110	40	30
Y	16	11	8	4	6
Zn (XRF (AA	146 141	141 134	210 198	247 223	127 124
Zr	49	22	26	14	26

WHOLE ROCK ANALYSIS AND TRACE ELEMENT DATA

Sample group (this study)	HIGH Mg META-BASALTS				
Sample field number ^a	B259/42.90	U274/~36	U252/45.92	B276/~159	B275/88.3
Section number	136	172	135	180	181
<u>oxides (wt.%)</u>					
SiO ₂	51.33	53.87	51.82	51.03	52.37
TiO ₂	0.68	0.58	0.91	0.61	0.58
Al ₂ O ₃	6.96	5.96	12.7	6.11	6.05
Fe ₂ O ₃ ^b	12.01	9.41	11.55	8.79	11.10
MnO	0.26	0.25	0.23	0.21	0.26
MgO	15.53	16.85	12.33	15.92	15.22
CaO	11.91	9.83	6.48	12.22	13.34
Na ₂ O	0.96	0.24	0.55	0.21	0.46
K ₂ O	0.39	2.17	3.96	3.74	0.72
P ₂ O ₅	0.06	0.07	0.09	0.06	0.06
Total ^c	100.09	99.23	100.62	98.90	100.16
Loss on ignition	2.30	2.38	3.07	1.52	2.19
<u>Elements (ppm)</u>					
Ag	3	3	3	11	4
As	78	156	25	451	243
Ba (XRF AA)	18 30	62 -	66 50	81 -	37 -
Be	7	12	9	10	3
Ce	12	- ^e	11	- ^e	7
Co	66	64	71	48	53
Cr ^f	999	5140	1890	2430	1400
Cu	199	85	140	206	70
Ga	9	14	15	8	9
Li	60	147	94	382	17
Mo	2	12	9	9	2
Nb	2	4	3	1	1
Nd	9	13	15	6	8
Ni (XRF AA)	259 259	476 -	475 437	255 -	227 -
Pb	4	0	19	32	90
Rb (XRF AA)	42 70	468 -	822 810	878 -	108 -
Sb	20	55	20	100	50
Sc	63	61	51	49	62
Sn	<5	5	10	<5	<5
Sr	52	44	55	36	126
V	278	286	311	260	259
W	<10	240	130	10	<10
Y	15	14	31	6	11
Zn (XRF AA)	120 115	247 -	275 258	235 -	112 -
Zr	34	27	47	24	26

WHOLE ROCK ANALYSIS AND TRACE ELEMENT DATA

Sample group (this study)	HIGH Mg META-BASALTS		META-RHYODACITIC ROCKS	
Sample field number ^a	B256/~132	B255/95.2	Rd276/128.00	M/G274/154.5
Section number	182	189	86	187
<u>oxides</u> (wt.%)				
SiO ₂	52.58	52.92	62.02	67.3
TiO ₂	0.57	0.59	1.28	0.37
Al ₂ O ₃	6.29	5.97	15.86	16.65
Fe ₂ O ₃ ^b	9.94	10.12	11.25	5.08
MnO	0.22	0.20	0.13	0.07
MgO	15.56	14.81	4.14	2.30
CaO	11.86	14.07	0.53	0.37
Na ₂ O	0.56	0.39	0.17	0.18
K ₂ O	1.70	0.47	4.48	6.7
P ₂ O ₅	0.06	0.07	0.11	0.20
Total ^c	99.34	99.60	99.95	99.22
Loss on ignition	1.85	1.44	4.02	3.64
<u>Elements</u> (ppm)				
Ag	4	2	4	2
As	46	27	8	12
Ba (XRF AA)	31	23	107	693
Be	-	-	80	-
Ba	6	1	9	13
Ce	-e	6	13	80
Co	45	51	38	8
Cr ^f	2210	1740	137	85
Cu	129	28	250	250
Ga	9	7	24	23
Li	212	28	195	296
Mo	11	2	7	9
Nb	0	1	3	7
Nd	10	11	11	34
Ni (XRF AA)	270	281	88	17
Pb	-	-	94	-
Pb	7	0	9	33
Rb (XRF AA)	399	70	658	896
Rb	-	-	580	-
Sb	125	25	20	10
Sc	62	65	42	10
Sn	<5	<5	10	5
Sr	49	58	14	80
V	268	273	377	92
W	410	<10	80	60
Y	10	12	13	7
Zn (XRF AA)	132	67	85	68
Zn	-	-	87	-
Zr	24	28	67	130

WHOLE ROCK ANALYSIS AND TRACE ELEMENT DATA

Sample group (this study)	ALTERED ROCKS						
	A276/61.2	R70/214.80	T(?)276/102.05		T259/84.35	F70/214.20	
Sample field number ^a							
Section number	22	82	101		107		129
<u>oxides(wt.%)</u>							
SiO ₂	48.54	45.90	45.64	44.85	39.55	39.11	46.50
TiO ₂	2.33	0.82	1.04	1.02	0.47	0.47	0.89
Al ₂ O ₃	12.42	7.43	13.28	13.00	8.50	8.37	10.16
Fe ₂ O ₃ ^b	29.90	26.60	13.85	13.78	13.11	13.03	17.19
MnO	0.14	0.09	0.19	0.19	0.26	0.27	0.25
MgO	4.52	13.05	8.59	8.39	21.11	21.14	10.04
CaO	0.39	0.15	10.23	10.10	3.78	3.77	12.15
Na ₂ O	0.29	0.30	0.20	0.20	0.11	0.11	0.11
K ₂ O	1.29	4.50	3.54	3.47	8.03	7.96	2.21
P ₂ O ₅	0.27	0.10	0.11	0.10	0.04	0.04	0.12
Total ^c	100.09	98.94	96.66	95.10	94.96	94.27	99.62
Loss on ignition	9.53	4.63	5.19	5.19	4.22	4.22	5.85
<u>Elements(ppm)</u>							
Ag	4	3	3		23		4
As	235	110	85		1390		336
Ba (XRF)	57	80	117		83		65
(AA)	60	110	100		40		70
Be	3	3	9		10		24
Ce	26	13	10		4		12
Co	28	9	55		56		40
Cr ^f	175	454	622		3340		954
Cu	34	258	132		348		140
Ga	20	17	19		20		23
Li	190	248	103		897		165
Mo	8	17	6		20		100
Nb	7	4	2		1		12
Nd	17	9	8		9		8
Ni (XRF)	60	171	124		727		118
(AA)	60	213	148		873		134
Pb	15	6	4		40		0
Rb (XRF)	211	826	494		2160		454
(AA)	250	730	490		2120		440
Sb	15	75	35		555		285
Sc	30	22	45		21		40
Sn	<5	5	10		15		15
Sr	6	21	157		38		210
V	379	175	296		128		238
W	110	40	120		380		110
Y	39	7	140		_d		14
Zn (XRF)	107	184	83		316		156
(AA)	104	181	77		198		144
Zr	144	37	57		18		45

WHOLE ROCK ANALYSIS AND TRACE ELEMENT DATA

Sample group (this study)	GRANITITIC ROCKS				
Sample field number ^a	M/G259/135.10	M/G276/86.90	G252/138.67	M/G268/106.70	M/G274/~61
Section number	116	117	119	121	184
<u>oxides (wt.%)</u>					
SiO ₂	72.27	74.32	80.76	70.76	73.68
TiO ₂	0.37	0.29	0.03	0.29	0.31
Al ₂ O ₃	15.23	15.22	13.03	15.38	16.33
Fe ₂ O ₃ ^b	3.86	3.18	1.65	2.75	2.36
MnO	0.06	0.03	0.04	0.05	0.00
MgO	1.22	1.29	0.11	1.18	0.95
CaO	1.20	0.18	0.63	2.16	0.34
Na ₂ O	0.23	0.16	0.56	2.62	0.18
K ₂ O	5.25	5.12	3.17	4.80	5.54
P ₂ O ₅	0.14	0.11	0.01	0.11	0.12
Total ^c	99.84	99.90	99.99	100.10	99.81
Loss on ignition	3.70	2.73	2.27	2.52	2.93
<u>Elements (ppm)</u>					
Ag	3	2	2	9	9
As	209	42	25	129	46
Ba (XRF AA)	556 580	730 550	76 60	1221 1240	663 -
Be	9	7	7	9	8
Ce	58	28	11	72	45
Co ^f	11	8	4	7	0
Cr ^f	200	146	240	244	127
Cu	85	2	168	208	136
Ga	23	21	19	24	27
Li	490	181	23	136	273
Mo	12	9	94	8	13
Nb	8	7	28	8	6
Nd	24	10	8	24	16
Ni (XRF AA)	10 11	10 8	22 23	10 7	9 -
Pb	4	11	41	111	8
Rb (XRF AA)	683 760	678 710	254 290	536 560	639 -
Sb	25	5	40	195	55
Sc	6	3	4	6	5
Sn	10	10	<5	10	5
Sr	<5	12	45	203	19
V	58	37	7	53	63
W	280	30	10	120	120
Y	4	4	11	5	11
Zn (XRF AA)	45 49	19 20	31 32	65 72	42 -
Zr	150	168	50	154	159

WHOLE ROCK ANALYSIS AND TRACE ELEMENT DATA

Sample group (this study)	GRANITIC ROCKS		BIF	
Sample field number ^a	M/G274/92.6	M/G274/139.5	BIF276/88.25	BIF268/58.84
Section number	185	186	88	90
<u>oxides(wt.%)</u>				
SiO ₂	73.02	80.75	40.08	44.97
TiO ₂	0.31	0.13	0.02	0.10
Al ₂ O ₃	16.12	13.10	0.26	0.69
Fe ₂ O ₃ ^b	3.00	1.05	58.49	48.07
MnO	0.01	0.00	0.12	0.19
MgO	1.10	0.41	0.62	2.79
CaO	0.40	0.04	0.49	2.55
Na ₂ O	0.19	0.15	0.08	0.17
K ₂ O	5.51	4.22	0.03	0.25
P ₂ O ₅	0.14	0.02	0.22	0.13
Total ^c	99.80	99.87	100.41	99.91
Loss on ignition	3.31	2.10	0.63	0.25 ^g
<u>Elements(ppm)</u>				
Ag	3	4	3	3
As	17	7	209	12
Ba (XRF (AA	986 -	290 -	2 10	13 30
Be	8	8	2	1
Ce	63	23	11	12
Co	0	0	29	11
Cr ^f	143	147	346	259
Cu	301	247	153	90
Ga	24	18	5	11
Li	222	142	4	30
Mo	16	20	2	0
Nb	7	8	1	2
Nd	21	10	12	4
Ni (XRF (AA	8 -	7 -	161 120	20 10
Pb	7	6	0	0
Rb (XRF (AA	600 -	450 -	11 30	54 30
Sb	15	105	20	25
Sc	4	4	1	9
Sn	5	<5	5	10
Sr	14	15	2	45
V	46	27	71	45
W	240	50	20	160
Y	4	3	8	3
Zn (XRF (AA	38 -	23 -	22 31	276 256
Zr	168	81	1	24

WHOLE ROCK ANALYSIS AND TRACE ELEMENT DATA

Sample group (this study)	MOUNT MULGINE GRANITE				
Sample field number ^a	G10/~120	G185/~49	G.MM peak ^h	G167/45.1	G.MM peak ^h
Section number	198	199	200	201	202
<u>oxides(wt.%)</u>					
SiO ₂	79.00	74.66	81.90	77.64	78.69
TiO ₂	0.14	0.22	0.05	0.07	0.10
Al ₂ O ₃	4.01	13.34	11.36	13.23	12.81
Fe ₂ O ₃ ^b	1.22	1.89	1.30	0.61	0.94
MnO	0.00	0.04	0.01	0.00	0.01
MgO	0.31	0.36	0.04	0.03	0.08
CaO	0.71	1.47	0.40	0.28	0.47
Na ₂ O	0.19	4.00	0.57	2.70	1.68
K ₂ O	4.42	3.60	4.21	5.37	4.86
P ₂ O ₅	0.02	0.08	0.02	0.02	0.02
Total ^c	100.02	99.65	99.84	99.94	99.66
Loss on ignition	2.26	1.22	1.66	0.66	1.88
<u>Elements(ppm)</u>					
Ag	1	0	2	0	2
As	5	8	4	7	3
Ba (XRF AA)	326	875	366	445	719
Be	5	4	6	6	3
Ce	2	47	13	27	26
Co	0	0	0	0	0
Cr ^f	179	213	252	181	180
Cu	129	14	299	13	10
Ga	23	18	17	18	19
Li	68	33	32	52	68
Mo	7	3	6	9	15
Nb	17	8	16	10	7
Nd	6	14	5	9	4
Ni (XRF AA)	4	9	6	7	7
Pb	7	46	90	74	64
Rb (XRF AA)	435	211	355	323	309
Sb	55	<5	25	<5	<5
Sc	4	3	3	2	2
Sn	<5	<5	<5	<5	<5
Sr	16	200	32	57	51
V	25	21	10	7	14
W	40	<10	200	10	30
Y	6	5	7	7	3
Zn (XRF AA)	26	50	45	11	19
Zr	86	133	52	87	82

APPENDIX 4

Electron Microprobe Analyses

APPENDIX 4

Electron Microprobe Analyses

All electron microprobe analyses were performed on the JEOL 733 Superprobe, in the Electron Optical Centre of the University of Adelaide. The machine is equipped with three wavelength-dispersive spectrometers (utilizing LiF, PET, STE and TAP crystals) and an energy-dispersive Si(Li) spectrometer. It is controlled by PDP-11/34 mini-computer. The operating programs are written in FORTRAN IV. Standard procedures were used for full matrix (ZAF) corrections.

Samples (polished blocks or polished thin sections) were carbon-coated and then analysed using an electron beam generally of 10 μm diameter, using accelerating voltages of 15 kV (for oxides and silicates) and 25 kV (for sulphides). The probe current was maintained at about 20 nA.

Primary standards used were a range of pure elements and simple compounds. Secondary mineral standards were usually analysed prior to sample analysis. Detection limits are given in the Table below.

TABLE 4A : ELECTRON PROBE DETECTION LIMITS

	OXIDES		SILICATES		SULPHIDES	
Program file name	DY1:S16Ø.DAT		DY1:S14.DAT		DY1:S13.DAT	
	Oxide	Detection limit(wt.%)	Element as oxide	Detection limit(wt.%)	Element	Detection limit(wt.%)
	P ₂ O ₅	0.02	SiO ₂	0.03	Cu	0.04
	SiO ₂	0.01	TiO ₂	0.04	Pb	0.31
	TiO ₂	0.02	Al ₂ O ₃	0.02	Zn	0.05
	Cr ₂ O ₃	0.04				
	FeO	0.03	Cr ₂ O ₃	0.06	Ni	0.04
	MnO	0.03	FeO	0.07	Sb	0.09
	MgO	0.01	MnO	0.06	As	0.06
	CaO	0.02	MgO	0.02	Ag	0.09
	NiO	0.06	CaO	0.04	S	0.03
	Sc ₂ O ₃	0.03	Na ₂ O	0.02	Cd	0.09
	WO ₃	0.25	K ₂ O	0.03	Bi	0.31
	SnO ₂	0.08	F	0.30	Ti	0.04
	MoO ₃	0.11	Cl	0.01	Sn	0.10
	Nb ₂ O ₅	0.13	P ₂ O ₅	0.10	Fe	0.03
	Ta ₂ O ₅	0.20	NiO	0.11		
	UO ₂	0.11				

Index to Appendix 4

The mineral analyses are arranged in three groups under the classifications oxides, silicates and sulphides. The minerals are arranged in alphabetical order in groups as shown below:

<u>Oxides and tungstates</u>	<u>Silicates and phosphates</u>	<u>Native elements and sulphides</u>
Brannerite(?)	Adularia	Antimony
Chromite	Andradite	Arsenopyrite
Huebnerite	Apatite	Bismuth
Ilmenite	Biotite	Chalcopyrite
Magnetite	Bowlingite(?)	
Rutile	Chlorite	Galenobismutite
Scheelite	Chrysotile	Gersdorffite
	Diopside	Kobellite-Tintinaite
	Epidote	Pentlandite
	Hornblende	Pyrrhotite
	Microcline	Pyrite
	Muscovite	Pyrrhotite
	Phlogopite	Sphalerite
	Spessartite	Tetrahedrite
	Sphene	Tetrahedrite-Tennantite
	Stilbite	Ullmannite
	Tremolite	

Explanation of notations in the table of analytical data

n.d. = not detected., the value obtained was below the detection limit.

1. The presence of F and/or Cl produces high totals because all the cations are assumed to be combined with oxygen although, in reality, some of the cations would be bonded to these halides. This assumption leads to excess oxygen and the high totals. Chlorine, where present, occurs in very small amounts (usually less than 0.1 wt.%) but as much as 6 wt.% F was obtained for some minerals. In those compounds in which the F content exceeds 0.5 wt.%, the oxygen equivalent of F ($O \equiv F$) was calculated as described by Deer et al. (1980, p. 516-517) and subtracted from the high totals to give a more realistic total.
2. The EDS programme used for some minerals does not print out very low concentrations, hence, the blank spaces in the table.
3. Low totals, mostly given by oxides, with no obvious explanation. Some may be due to the presence of additional elements that were not included in the analytical programme or they may be just bad analyses.
4. For epidote, the value shown for FeO is actually that of Fe₂O₃, recalculated

from the FeO value.

In magnetite, Fe is also present as Fe_2O_3 . The former total iron (as FeO) was recalculated and the Fe_2O_3 value is shown below the FeO value.

OXIDES AND TUNGSTATES

Analyses in wt.%

Mineral and sample no.	Brannerite(?) 232/~51		Chromite 268/140.55	Huebnerite 251/64.70		Ilmenite 268/140.55
	1	2	1	1	2	1
P ₂ O ₅	0.08	0.08	n.d.	0.16	0.17	0.02
SiO ₂	2.98	2.67	0.43	n.d.	n.d.	0.03
TiO ₂	34.93	35.73	0.11	n.d.	n.d.	48.96
Cr ₂ O ₃	0.11	n.d.	47.89	n.d.	0.08	0.24
FeO	0.85	0.84	33.83	1.63	1.31	38.89
MnO	0.68	0.68	2.42	21.57	21.80	7.96
MgO	n.d.	0.02	2.48	0.20	0.16	0.20
CaO	6.62	5.21	n.d.	0.04	0.04	n.d.
NiO	n.d.	n.d.	n.d.	n.d.	n.d.	n.d.
Sc ₂ O ₃	n.d.	n.d.	n.d.	n.d.	n.d.	n.d.
WO ₃	0.25	30	0.26	79.52	78.49	n.d.
SnO ₂	n.d.	n.d.	n.d.	n.d.	n.d.	n.d.
MoO ₃	n.d.	n.d.	n.d.	n.d.	n.d.	n.d.
Nb ₂ O ₅	0.53	0.82	n.d.	n.d.	n.d.	n.d.
Ta ₂ O ₅	n.d.	0.30	n.d.	n.d.	n.d.	n.d.
UO ₂	29.27	29.93	n.d.	n.d.	n.d.	n.d.
Total	76.30 ³	76.58 ³	87.42 ³	103.12	102.05	96.30 ³

NUMBER OF ATOMS

	Basis: 6 oxygens		Basis: 4 oxygens	Basis: 4 oxygens		Basis: 4 oxygens
P	-	-	-	-	-	-
Si	0.22	0.20	0.02	-	-	-
Ti	1.94	2.00	-	-	-	0.97
Cr	0.01	-	1.64	-	-	0.01
Fe	0.05	0.05	1.23	0.07	0.05	0.86
Mn	0.04	0.04	0.09	0.89	0.90	0.18
Mg	-	-	0.16	0.01	0.01	0.01
Ca	0.52	0.41	-	-	-	-
Ni	-	-	-	-	-	-
Sc	-	-	-	-	-	-
W	-	0.01	-	1.00	1.00	-
Sn	-	-	-	-	-	-
Mo	-	-	-	-	-	-
Nb	0.20	0.03	-	-	-	-
Ta	-	0.01	-	-	-	-
U	0.48	0.49	-	-	-	-
Total	3.46	3.24	3.14	1.97	1.96	2.03

OXIDES AND TUNGSTATES

Analyses in wt.%

Mineral and sample no.	M a g n e t i t e				Rutile 232/~51	Scheelite 232/~51
	276/73.4	269/130.3	268/140.55			
oxide or element	1	1	1	2	1	1
P ₂ O ₅	n.d.	n.d.	0.02	0.02	n.d.	0.19
SiO ₂	0.06	0.01	0.02	0.03	0.01	n.d.
TiO ₂	0.08	0.02	n.d.	0.02	90.78	0.02
Cr ₂ O ₃	0.11	n.d.	5.10	5.00	0.00	n.d.
Fe ⁴	29.91 66.47	29.61 65.80	28.14 62.5	28.31 62.91	1.07	n.d.
MnO	0.10	n.d.	0.22	0.16	n.d.	0.06
MgO	0.01	0.01	0.03	0.05	n.d.	0.02
CaO	n.d.	n.d.	n.d.	n.d.	0.02	17.88
NiO	n.d.	n.d.	0.28	0.29	n.d.	n.d.
Sc ₂ O ₃	n.d.	n.d.	n.d.	n.d.	n.d.	0.34
WO ₃	n.d.	n.d.	n.d.	n.d.	0.34	81.18
SnO ₂	n.d.	n.d.	n.d.	n.d.	n.d.	n.d.
MoO ₃	n.d.	n.d.	n.d.	n.d.	n.d.	n.d.
Nb ₂ O ₅	n.d.	n.d.	n.d.	n.d.	1.96	n.d.
Ta ₂ O ₅	n.d.	n.d.	n.d.	n.d.	0.64	n.d.
UO ₂	n.d.	n.d.	n.d.	n.d.	n.d.	n.d.
Total	96.74 ³	95.45 ³	95.86 ³	96.79	94.82 ³	99.69

NUMBER OF ATOMS

	Basis : 4 oxygens		Basis: 2 oxygens		Basis: 4 oxygens	
P	-	-	-	-	-	0.01
Si	-	-	-	-	-	-
Ti	-	-	-	-	0.97	-
Cr	-	-	0.16	0.16	-	-
Fe ⁴	1.00 1.99	1.00 2.00	0.94 1.87	0.94 1.88	0.01 -	- -
Mn	-	-	0.01	0.01	-	-
Mg	-	-	-	-	-	-
Ca	-	-	-	-	-	0.92
Ni	-	-	0.01	0.01	-	-
Sc	-	-	-	-	-	-
W	-	-	-	-	-	1.01
Sn	-	-	-	-	-	-
Mo	-	-	-	-	-	-
Nb	-	-	-	-	0.01	-
Ta	-	-	-	-	-	-
U	-	-	-	-	-	-
Total	2.99	3.00	2.99	2.99	0.99	1.94

OXIDES AND TUNGSTATES

Analyses in wt.%

Mineral and sample no.	S c h e e l i t e				Scheelite	
	251/64.70				51/108.7	268/35.84
oxide or element	3	4	5	6	1	2
P ₂ O ₅	0.19	0.18	0.17	0.19	0.22	0.14
SiO ₂	n.d.	n.d.	n.d.	n.d.	n.d.	n.d.
TiO ₂	n.d.	n.d.	n.d.	n.d.	n.d.	n.d.
Cr ₂ O ₃	n.d.	n.d.	n.d.	0.06	0.04	n.d.
FeO	n.d.	n.d.	n.d.	n.d.	n.d.	n.d.
MnO	0.08	0.06	0.11	0.07	n.d.	n.d.
MgO	n.d.	n.d.	n.d.	0.01	0.01	n.d.
CaO	18.82	19.10	18.95	19.04	18.94	19.36
NiO	n.d.	n.d.	n.d.	n.d.	n.d.	n.d.
Sc ₂ O ₃	n.d.	n.d.	0.03	n.d.	n.d.	n.d.
WO ₃	83.68	83.12	82.79	82.21	82.41	83.23
SnO ₂	n.d.	n.d.	0.10	n.d.	n.d.	n.d.
MoO ₃	n.d.	n.d.	n.d.	0.14	n.d.	0.24
Nb ₂ O ₅	n.d.	n.d.	n.d.	n.d.	n.d.	n.d.
Ta ₂ O ₅	n.d.	n.d.	n.d.	n.d.	n.d.	n.d.
UO ₂	0.12	n.d.	n.d.	n.d.	0.19	n.d.
Total	102.89	102.46	102.15	101.72	101.81	102.97

NUMBER OF ATOMS

	Basis : 4 oxygens				Basis : 4 oxygens	
P	0.01	0.01	0.01	0.01	0.01	0.01
Si	-	-	-	-	-	-
Ti	-	-	-	-	-	-
Cr	-	-	-	-	-	-
Fe	-	-	-	-	-	-
Mn	-	-	-	-	-	-
Mg	-	-	-	-	-	-
Ca	0.94	0.96	0.95	0.96	0.95	0.96
Ni	-	-	-	-	-	-
Sc	-	-	-	-	-	-
W	1.01	1.01	1.01	1.00	1.00	1.00
Sn	-	-	-	-	-	-
Mo	-	-	-	-	-	-
Nb	-	-	-	-	-	-
Ta	-	-	-	-	-	-
U	-	-	-	-	-	-
Total	1.96	1.98	1.97	1.97	1.96	1.97

SILICATES AND PHOSPHATES

Analyses in wt.%

Mineral and sample no.	Adularia 268/149.90	Andradite 22/33.9	Apatite 268/149.90		Red biotite 22/136.70	Biotite 276/73.4	
			1	2		2	3
oxide or element	4	1	1	2	2	2	3
SiO ₂	65.37	34.06	n.d.	n.d.	37.03	36.82	37.63
TiO ₂	n.d.	n.d.	n.d.	n.d.	1.93	2.14	2.34
Al ₂ O ₃	17.70	5.90	0.02	0.03	17.31	14.59	14.43
Cr ₂ O ₃	n.d.	n.d.	n.d.	n.d.	0.14	n.d.	0.09
FeO	0.03	23.10	n.d.	n.d.	13.51	20.35	17.68
MnO	n.d.	0.57	n.d.	n.d.	0.24	0.19	0.27
MgO	n.d.	0.05	n.d.	0.02	13.94	11.01	12.45
CaO	n.d.	32.31	56.50	56.84	n.d.	n.d.	n.d.
Na ₂ O	0.20	0.03	n.d.	n.d.	0.08	0.10	0.06
K ₂ O	16.18	n.d.	n.d.	n.d.	10.68	9.57	9.69
F ¹	n.d.	n.d.	6.00	6.19	1.26	1.33	1.22
Cl ¹	0.05	0.01	0.04	0.03	n.d.	0.02	n.d.
P ₂ O ₅	n.d.	n.d.	42.71	42.80	n.d.	n.d.	n.d.
NiO	n.d.	n.d.	n.d.	n.d.	n.d.	n.d.	n.d.
Total	99.53	96.03 ³	105.27	105.91	96.12	96.12	95.86
O ≡ F ¹			-2.53	-2.61	-0.53	-0.56	-0.51
			102.74	103.30	95.59	95.56	95.35

NUMBER OF ATOMS

	Basis: 8 oxygens	Basis: 12 oxygens	Basis: 18 oxygens		Basis: 24 oxygens		
Si	3.03	3.07	-	-	6.05	6.20	6.26
Ti	-	-	-	-	0.24	0.27	0.29
Al	0.97	0.63	-	-	3.33	2.90	2.83
Cr	-	-	-	-	0.02	-	0.01
Fe	-	1.74	-	-	1.85	2.87	2.46
Mn	-	0.04	-	-	0.03	0.03	0.04
Mg	-	0.01	-	-	3.39	2.76	3.09
Ca	-	3.12	7.21	7.23	-	-	-
Na	0.02	-	-	-	0.02	0.03	0.02
K	0.96	-	-	-	2.23	2.06	2.06
F	-	-	2.26	2.33	0.65	0.71	0.64
Cl	-	-	0.01	0.01	-	-	-
P	-	-	4.31	4.30	-	-	-
Ni	-	-	-	-	-	-	-
Total	4.98	8.61	13.79	13.87	17.80	17.83	17.72

SILICATES
Analyses in wt.%

Mineral and sample no.	Bowlingite(?) ² - altered olivine 22/65.15				Chlorite ²	
					251/139.4	259/135.10
oxide or element	1	2	3	4	1	1
SiO ₂	37.85	37.61	37.34	36.75	24.92	30.82
TiO ₂	1.83	1.79	2.41	2.28	0.12	
Al ₂ O ₃					19.91	19.75
Cr ₂ O ₃					0.42	
FeO	7.35	7.40	8.72	8.20	27.11	9.54
MnO	0.19	0.16	0.15	0.18	0.30	1.18
MgO	51.22	51.42	50.15	49.92	13.22	23.94
CaO						
Na ₂ O					0.22	
K ₂ O						1.62
F						
Cl						
P ₂ O ₅						
NiO						
Total	98.44	98.38	98.77	97.33	86.22	86.85
NUMBER OF ATOMS						
	Basis: 4 oxygens				Basis: 28 oxygens	
Si	0.94	0.94	0.93	0.93	5.43	6.07
Ti	0.03	0.03	0.05	0.04	0.02	
Al					5.11	4.58
Cr					0.07	
Fe	0.15	0.15	0.18	0.17	4.94	1.57
Mn	-	-	-	-	0.06	0.20
Mg	1.90	1.91	1.86	1.88	4.29	7.02
Ca						
Na					0.09	
K						0.41
F						
Cl						
P						
Ni						
Total	3.02	3.06	3.04	3.02	20.01	19.85

SILICATES
Analyses in wt.%

Mineral and sample no.	Chlorites					Chrysotile	
	268/149.90	276/73.4				22/65.15	
oxide or element	1	1	2	3	4	1	3
SiO ₂	29.07	27.63	25.36	24.38	25.34	41.23	43.15
TiO ₂	n.d.	n.d.	n.d.	n.d.	0.04	2.77	n.d.
Al ₂ O ₃	17.17	17.19	19.21	19.32	18.83	1.01	0.90
Cr ₂ O ₃	n.d.	n.d.	0.16	0.23	0.15	n.d.	n.d.
FeO	16.25	27.19	31.90	33.51	30.35	5.42	3.15
MnO	0.42	0.47	0.49	0.52	0.40	0.52	0.12
MgO	21.78	14.75	9.67	7.95	10.66	36.22	37.92
CaO	n.d.	n.d.	n.d.	n.d.	n.d.	n.d.	n.d.
Na ₂ O	0.03	0.02	0.05	0.03	0.06	0.02	0.02
K ₂ O	n.d.	0.05	0.03	n.d.	0.08	n.d.	n.d.
F ¹	0.41	0.11	n.d.	n.d.	n.d.	0.71	0.62
Cl ¹	0.06	n.d.	0.03	n.d.	0.01	0.03	0.01
P ₂ O ₅	0.15	n.d.	n.d.	n.d.	n.d.	n.d.	n.d.
NiO	n.d.	n.d.	n.d.	n.d.	n.d.	n.d.	n.d.
Total O≡F ¹	85.34	87.41	86.90	85.94	85.92	87.93 -0.30 87.63	85.89 -0.26 85.63

NUMBER OF ATOMS

	Basis : 28 oxygens					Basis: 9 oxygens	
Si	6.02	5.91	5.61	5.52	5.63	2.52	2.63
Ti	-	-	-	-	0.01	0.13	-
Al	4.19	4.33	5.01	5.16	4.93	0.07	0.07
Cr	-	-	0.03	0.04	0.03	-	-
Fe	2.81	4.86	5.90	6.35	5.64	0.28	0.16
Mn	0.07	0.08	0.09	0.10	0.08	0.03	0.01
Mg	6.72	4.70	3.19	2.68	3.53	3.29	3.45
Ca	-	-	-	-	-	-	-
Na	0.01	0.01	0.02	0.01	0.03	-	-
K	-	0.01	0.01	-	0.02	-	-
F	0.27	0.07	-	-	-	0.14	0.12
Cl	0.02	-	0.01	-	-	-	-
P	0.03	-	-	-	-	-	-
Ni	-	-	-	-	-	-	-
Total	20.14	19.97	19.87	19.86	19.90	6.46	6.44

SILICATES

Analyses in wt.%

Mineral and sample no.	Diopside ²				Epidote 268/149.90	Hornblende 276/73.4	
	268/123.66		268/149.90			1	2
oxide or element	1	2	1	2	1	1	2
SiO ₂	53.47	54.09	53.85	54.68	37.56	46.44	48.93
TiO ₂					n.d.	0.37	0.44
Al ₂ O ₃	0.62	0.65	1.17	0.24	22.04	8.18	6.54
Cr ₂ O ₃	0.22	0.37			n.d.	n.d.	n.d.
FeO	5.49	5.46	3.78	2.98	13.22 ⁴	15.64	14.50
MnO	0.35	0.25	1.16	0.96	0.20	0.48	0.51
MgO	14.26	14.47	14.81	16.34	0.05	12.27	13.34
CaO	25.33	25.55	25.27	25.67	23.98	12.32	12.33
Na ₂ O					0.13	0.93	0.73
K ₂ O					0.03	0.86	0.74
F ¹					n.d.	0.54	0.24
Cl ¹					0.07	n.d.	0.05
P ₂ O ₅					n.d.	n.d.	n.d.
NiO					n.d.	n.d.	n.d.
Total O≡F ¹	99.74	100.84	100.04	100.87	97.28	98.03 - 0.23 97.80	98.35

NUMBER OF ATOMS

	Basis : 6 oxygens				Basis: 13 oxygens	Basis: 23 oxygens	
	1	2	1	2		1	2
Si	1.98	1.98	1.98	1.99	3.25	6.91	7.17
Ti					-	0.04	0.05
Al	0.03	0.03	0.05	0.01	2.25	1.44	1.13
Cr	0.01	0.01			-	-	-
Fe	0.17	0.17	0.12	0.09	0.04	1.95	1.78
Mn	0.01	0.01	0.04	0.03	0.01	0.06	0.06
Mg	0.79	0.79	0.81	0.89	0.01	2.72	2.91
Ca	1.01	1.00	0.99	1.00	2.22	1.97	1.94
Na			0.01		0.02	0.27	0.21
K					-	0.16	0.14
F					0.02	0.25	0.11
Cl			0.01		0.01	-	0.01
P					-	-	-
Ni					-	-	-
Total	4.00	3.99	4.00	4.00	7.83	15.77	15.51

SILICATES
Analyses in wt.%

Mineral and sample no.	(Magnesio) - Hornblende 276/73.4						
	3	4	5	6	7	8	9
SiO ₂	48.32	45.45	45.76	45.61	46.18	47.74	48.55
TiO ₂	0.42	0.40	0.52	0.37	0.43	0.41	0.37
Al ₂ O ₃	6.91	8.30	8.32	8.07	7.92	7.24	7.17
Cr ₂ O ₃	n.d.	n.d.	n.d.	n.d.	n.d.	n.d.	n.d.
FeO	14.67	16.30	16.00	15.67	16.16	14.87	14.97
MnO	0.58	0.53	0.47	0.52	0.53	0.54	0.48
MgO	12.99	11.65	11.96	11.81	11.86	12.43	12.35
CaO	12.27	12.44	12.25	12.38	12.46	11.91	11.92
Na ₂ O	0.79	0.90	0.97	0.84	0.81	0.77	0.79
K ₂ O	0.76	0.99	1.05	0.91	0.92	0.76	0.77
F ¹	0.47	n.d.	0.27	0.38	n.d.	0.53	0.34
Cl ¹	n.d.	0.04	0.09	0.09	0.02	0.02	0.03
P ₂ O ₅	n.d.	n.d.	n.d.	n.d.	n.d.	n.d.	n.d.
NiO	n.d.	n.d.	n.d.	n.d.	n.d.	n.d.	n.d.
Total O ≡ F ¹	98.18	97.00	97.66	96.65	97.29	99.22 <u>-0.22</u> 99.00	97.74

NUMBER OF ATOMS

	Basis : 23 oxygens						
Si	7.12	6.85	6.86	6.90	6.92	7.17	7.17
Ti	0.05	0.05	0.06	0.04	0.05	0.05	0.04
Al	1.20	1.48	1.47	1.44	1.40	1.25	1.25
Cr	-	-	-	-	-	-	-
Fe	1.81	2.06	2.01	1.98	2.03	1.83	2.25
Mn	0.07	0.07	0.06	0.07	0.07	0.07	0.06
Mg	2.85	2.62	2.67	2.67	2.65	2.73	2.72
Ca	1.94	2.01	1.97	2.01	2.00	1.88	1.89
Na	0.22	0.19	0.28	0.25	0.23	0.22	0.23
K	0.14	0.11	0.20	0.18	0.18	0.14	0.14
F	0.22	-	0.13	0.18	-	0.25	0.16
Cl	-	-	0.02	0.02	0.01	-	0.01
P	-	-	-	-	-	-	-
Ni	-	-	-	-	-	-	-
Total	15.72	15.44	15.73	15.74	15.54	15.59	15.92

SILICATES
Analyses in wt.%

Mineral and sample no.	Microcline ² 70/223.03		Muscovite ² 259/135.10				
	1	2	1	2	3	4	5
SiO ₂	65.71	64.55	47.36	47.23	45.61	46.50	46.40
TiO ₂			0.95	0.91	1.03	0.99	0.92
Al ₂ O ₃	17.60	17.54	29.68	29.85	29.73	29.43	29.13
Cr ₂ O ₃							
FeO			1.38	1.47	1.53	1.50	1.32
MnO							
MgO			3.15	3.33	2.95	3.59	3.33
CaO	0.48	0.41					
Na ₂ O	0.25						
K ₂ O	16.58	16.77	10.78	10.80	10.59	10.69	10.53
F							
Cl ¹		0.12					
P ₂ O ₅							
NiO							
Total	100.62	99.39	93.30	93.59	91.44	92.70	91.63
NUMBER OF ATOMS							
	Basis: 32 oxygens		Basis: 22 oxygens				
Si	12.09	12.06	6.46	6.42	6.36	6.40	6.44
Ti			0.10	0.09	0.11	0.10	0.10
Al	3.82	3.86	4.77	4.78	4.89	4.77	4.77
Cr							
Fe			0.16	0.17	0.18	0.17	0.15
Mn							
Mg			0.64	0.67	0.61	0.74	0.69
Ca	0.09	0.08					
Na	0.09						
K	3.89	3.99	1.88	1.87	1.88	1.87	1.83
F							
Cl		0.04					
P							
Ni							
Total	19.98	20.03	14.01	14.00	14.03	14.08	13.98

SILICATES
Analyses in wt.%

Mineral and sample no.	Muscovites ² 22/136.70						
	6	7	8	9	10	11	12
oxide or element							
SiO ₂	45.45	45.12	45.29	45.46	45.84	46.14	47.36
TiO ₂	1.14	1.11	1.14	1.14	1.13	1.34	1.41
Al ₂ O ₃	33.60	32.93	33.92	33.37	33.55	33.73	34.23
Cr ₂ O ₃							0.17
FeO	1.77	1.94	1.69	2.15	2.09	1.88	1.81
MnO							
MgO	1.22	0.98	1.05	1.12	0.99	1.24	1.35
CaO							
Na ₂ O	0.30				0.20	0.29	0.30
K ₂ O	10.63	10.96	10.50	10.63	10.64	10.11	9.15
F							
Cl							
P ₂ O ₅							
NiO							
Total	94.11	92.64	93.59	93.87	94.44	94.73	95.78
	NUMBER OF ATOMS						
	Basis: 22 oxygens						
Si	6.16	6.21	6.14	6.17	6.19	6.19	6.23
Ti	0.12	0.11	0.12	0.12	0.12	0.13	0.14
Al	5.36	5.34	5.42	5.34	5.34	5.33	5.31
Cr							0.02
Fe	0.20	0.22	0.19	0.24	0.24	0.21	0.20
Mn							
Mg	0.25	0.20	0.21	0.23	0.20	0.25	0.27
Ca							
Na	0.08					0.08	0.08
K	1.84	1.85	1.82	1.84	1.83	1.73	1.54
F							
Cl							
P							
Ni							
Total	14.01	13.93	13.90	13.94	13.92	13.92	13.79

SILICATES
Analyses in wt.%

Mineral and sample no.	M u s c o v i t e ²						
	22/136.70		251/139.4				
oxide or element	13	14	15	16	17	18	19
SiO ₂	46.82	46.30	47.52	46.95	46.89	45.70	47.56
TiO ₂	1.17	1.46	0.60	0.85	0.91	0.92	1.15
Al ₂ O ₃	33.67	33.64	32.55	31.98	32.19	31.04	32.21
Cr ₂ O ₃			0.26	0.36	0.31	0.59	0.58
FeO	1.71	1.71	1.01	0.98	0.88	0.94	1.11
MnO							
MgO	1.07	1.39	2.58	2.63	2.38	2.36	2.53
CaO							
Na ₂ O		0.16					
K ₂ O	9.22	8.87	10.80	10.88	10.85	10.79	10.84
F							
Cl							
P ₂ O ₅							
NiO							
Total	93.65	93.53	95.32	94.63	94.41	92.34	95.98
	NUMBER OF ATOMS						
	Basis : 22 oxygens						
Si	6.29	6.22	6.32	6.31	6.30	6.30	6.30
Ti	0.12	0.15	0.06	0.09	0.09	0.09	0.11
Al	5.33	5.33	5.10	5.06	5.10	5.04	5.03
Cr			0.03	0.04	0.03	0.06	0.06
Fe	0.19	0.19	0.11	0.11	0.10	0.11	0.12
Mn							
Mg	0.21	0.28	0.51	0.53	0.48	0.49	0.50
Ca							
Na		0.04					
K	1.58	1.52	1.83	1.86	1.86	1.90	1.83
F							
Cl							
P							
Ni							
Total	13.72	13.73	13.96	14.00	13.96	13.99	13.95

SILICATES
Analyses in wt.%

Mineral and sample no.	Muscovite 251/139.4	M u s c o v i t e ² 268/128.73				
		20	1	2	3	4
SiO ₂	47.28	44.85	42.65	43.98	43.61	44.25
TiO ₂	0.99				0.13	
Al ₂ O ₃	32.27	10.86	10.86	11.35	11.32	11.68
Cr ₂ O ₃	0.23					
FeO	0.88	3.14	3.78	3.58	3.48	4.22
MnO		0.18	0.27	0.20	0.22	
MgO	2.49	23.40	22.46	23.14	23.07	23.32
CaO						
Na ₂ O						
K ₂ O	10.95	10.17	10.12	10.34	10.51	10.19
F						
Cl						
P ₂ O ₅						
NiO						
Total	95.09	92.60	90.14	92.59	92.34	93.66
NUMBER OF ATOMS						
Basis: 22 oxygens						
Si	6.31	6.45	6.35	6.35	6.33	6.32
Ti	0.10				0.01	
Al	5.08	1.84	1.91	1.93	1.94	1.97
Cr	0.02					
Fe	0.10	0.38	0.47	0.43	0.42	0.50
Mn		0.02	0.03	0.02	0.03	
Mg	0.50	5.01	4.98	4.98	4.99	4.97
Ca						
Na						
K	1.86	1.86	1.92	1.91	1.95	1.86
F						
Cl						
P						
Ni						
Total	13.97	15.56	15.66	15.62	15.67	15.62

SILICATES
Analyses in wt.%

Mineral and sample no.	M u s c o v i t e ² 264/54.05					Phlogopite	
	7	8	9	10	11	1	3
SiO ₂	42.25	42.84	41.99	42.76	41.61	41.52	41.73
TiO ₂			0.13			0.74	0.72
Al ₂ O ₃	11.65	11.16	11.83	11.37	10.96	12.76	12.92
Cr ₂ O ₃			0.47		0.21	n.d.	n.d.
FeO	3.91	3.92	4.06	4.07	4.15	8.22	6.58
MnO					0.16	0.31	0.46
MgO	24.27	24.24	24.11	24.25	23.57	20.53	21.68
CaO						n.d.	n.d.
Na ₂ O						0.08	0.10
K ₂ O	10.16	10.24	10.13	10.14	10.00	10.19	10.19
F ¹						3.04	3.12
Cl ¹						n.d.	0.11
P ₂ O ₅						n.d.	n.d.
NiO						n.d.	n.d.
Total	92.24	92.40	92.72	92.59	90.66	97.39	97.61
O=F ¹						1.28	1.31
						96.11	96.30
NUMBER OF ATOMS							
Basis : 22 oxygens						Basis:24 oxygens	
Si	6.15	6.23	6.10	6.20	6.19	6.60	6.58
Ti			0.01			0.09	0.09
Al	2.00	1.91	2.02	1.94	1.92	2.39	2.40
Cr			0.05		0.02	-	-
Fe	0.48	0.48	0.49	0.49	0.51	1.09	0.87
Mn					0.02	0.04	0.06
Mg	5.27	5.25	5.22	5.24	5.22	4.86	5.09
Ca						-	-
Na						0.02	0.03
K	1.89	1.90	1.88	1.88	1.90	2.05	2.05
F						1.53	1.55
Cl						-	0.03
P						-	-
Ni						-	-
Total	15.79	15.77	15.77	15.75	15.78	18.67	18.75

SILICATES

Analyses in wt.%

Mineral and sample no.	Spessartite 259/115.77		Spheue ² 71/67.4		Spheue 268/149.90
	1	2	1	2	1
SiO ₂	37.83	47.22	30.81	30.41	29.02
TiO ₂	0.08	0.14	32.97	33.99	32.52
Al ₂ O ₃	19.86	17.05			3.00
Cr ₂ O ₃	n.d.	0.07			n.d.
FeO	7.45	6.68	1.65	1.45	0.62
MnO	29.76	24.83	0.12	0.12	0.14
MgO	1.40	1.14			0.03
CaO	2.14	1.97	29.24	28.35	29.04
Na ₂ O	n.d.	0.02			0.02
K ₂ O	n.d.	n.d.			n.d.
F ¹	n.d.	n.d.			0.72
Cl ¹	0.01	0.04			0.06
P ₂ O ₅	n.d.	n.d.			n.d.
NiO	n.d.	n.d.			n.d.
Total O≡F ¹	98.53	99.16	94.79 ³	94.32 ³	95.17 ³ -0.30 94.87 ³
NUMBER OF ATOMS					
	Basis: 24 oxygens		Basis : 6 oxygens		
Si	6.19	7.29	1.28	1.27	1.21
Ti	0.01	0.02	1.03	1.07	1.02
Al	3.83	3.10			0.15
Cr	-	0.01			-
Fe	1.02	0.86	0.06	0.05	0.02
Mn	4.12	3.25			-
Mg	0.34	0.26			-
Ca	0.37	0.33	1.30	1.27	1.24
Na	-	0.01			-
K	-	-			-
F	-	-			0.09
Cl	-	0.01			-
P	-	-			-
Ni	-	-			-
Total	15.88	15.14	3.67	3.66	3.73

SILICATES
Analyses in wt.%

Mineral and sample	Stilbite 268/100.2	Tremolite ² 264/54.05		
		1	1	2
oxide or element				
SiO ₂	60.36	54.44	58.06	58.17
TiO ₂	0.04			
Al ₂ O ₃	17.03	0.17	0.22	0.21
Cr ₂ O ₃	n.d.			
FeO	0.05	0.60	0.52	1.11
MnO	n.d.	0.19	0.13	0.21
MgO	0.24	23.92	24.02	23.34
CaO	8.12	13.20	13.59	13.34
Na ₂ O	0.79			
K ₂ O	0.15	0.11	0.16	
F	n.d.			
Cl	0.02			
P ₂ O ₅	n.d.			
NiO	n.d.			
Total	86.80	96.63	96.70	96.38
NUMBER OF ATOMS				
	Basis: 72 oxygens	Basis: 23 oxygens		
Si	27.01	8.02	7.97	8.02
Ti	0.01			
Al	8.98	0.03	0.04	0.03
Cr				
Fe	0.02	0.07	0.06	0.13
Mn	-	0.02	0.01	0.02
Mg	0.16	4.89	4.91	4.79
Ca	3.89	1.94	2.00	1.97
Na	0.68			
K	0.09	0.02	0.03	
F	-			
Cl	0.01			
P	-			
Ni	-			
Total	40.86	14.99	15.02	14.96

NATIVE ELEMENTS AND SULPHIDES

Analyses in wt.%

Mineral and sample no.	Antimony 301/133.8			Arsenopyrite 259/123.32		Bismuth 51/108.70	Chalcopyrite 259/~118
	1	2	3	1	2	1	1
Fe	n.d.	n.d.	n.d.	35.70	35.40	0.10	29.41
Cu	n.d.	n.d.	n.d.	0.07	0.19	0.21	36.67
Pb	n.d.	n.d.	n.d.	n.d.	n.d.	n.d.	n.d.
Zn	n.d.	n.d.	n.d.	n.d.	n.d.	n.d.	0.26
Ni	n.d.	n.d.	n.d.	0.17	0.05	n.d.	n.d.
Sb	99.64	98.64	101.21	n.d.	n.d.	n.d.	n.d.
As	0.70	0.76	0.80	44.67	44.71	n.d.	n.d.
Ag	n.d.	n.d.	0.04	n.d.	n.d.	n.d.	n.d.
S	0.05	n.d.	0.05	20.79	20.58	n.d.	34.26
Cd	n.d.	n.d.	n.d.	n.d.	n.d.	n.d.	n.d.
Bi	0.34	n.d.	n.d.	n.d.	n.d.	102.23	n.d.
Ti	n.d.	n.d.	0.07	n.d.	n.d.	0.07	n.d.
Sn	0.42	0.48	0.43	n.d.	n.d.	n.d.	n.d.
Total	101.15	99.88	102.56	101.40	100.93	102.61	100.60

Mineral and sample no.	Galenobismutite 51/108.70	Gersdorffite 268/35.84		Kobellite-Tintinaite 264/116.27	Pentlandite 268/35.84	Pyrargyrite 51/108.70
	1	1	2	1	1	1
Fe	0.03	8.98	10.67	0.03	25.90	0.08
Cu	0.06	n.d.	n.d.	1.24	0.07	0.09
Pb	65.67	n.d.	n.d.	46.17	0.45	n.d.
Zn	n.d.	n.d.	n.d.	n.d.	n.d.	n.d.
Ni	n.d.	27.05	25.74	n.d.	30.78	n.d.
Sb	n.d.	0.09	n.d.	15.78	0.34	23.80
As	n.d.	44.34	44.72	n.d.	0.07	0.16
Ag	0.22	n.d.	n.d.	1.72	n.d.	59.86
S	9.40	19.85	19.71	17.00	42.19	17.27
Cd	n.d.	n.d.	n.d.	n.d.	n.d.	n.d.
Bi	25.67	n.d.	n.d.	n.d.	n.d.	n.d.
Ti	n.d.	n.d.	n.d.	n.d.	n.d.	n.d.
Sn	n.d.	n.d.	n.d.	n.d.	n.d.	n.d.
Total	101.05	100.31	100.84	100.94	99.80	101.26

SULPHIDES
Analyses in wt.%

Mineral and sample no.	P y r i t e				Pyrrhotite		
	264/116.27	51/108.70	259/~118	259/90.70	259/90.70		
Element	1	1	1	1	1	2	3
Fe	47.52	47.37	46.27	46.23	59.53	59.55	59.67
Cu	n.d.	n.d.	n.d.	n.d.	n.d.	n.d.	n.d.
Pb	n.d.	n.d.	n.d.	n.d.	n.d.	n.d.	n.d.
Zn	n.d.	n.d.	0.05	n.d.	0.54	0.38	0.43
Ni	n.d.	0.12	n.d.	0.09	0.31	0.28	0.28
Sb	n.d.	n.d.	n.d.	n.d.	n.d.	n.d.	n.d.
As	0.06	n.d.	0.13	0.08	n.d.	n.d.	n.d.
Ag	n.d.	n.d.	n.d.	n.d.	n.d.	n.d.	n.d.
S	54.59	54.30	53.21	53.37	38.69	39.08	39.00
Cd	n.d.	n.d.	n.d.	n.d.	n.d.	n.d.	n.d.
Bi	n.d.	n.d.	n.d.	n.d.	n.d.	n.d.	n.d.
Ti	n.d.	n.d.	n.d.	n.d.	n.d.	n.d.	n.d.
Sn	n.d.	n.d.	n.d.	n.d.	n.d.	n.d.	n.d.
Total	102.17	101.79	99.66	99.77	99.07	99.29	99.38

Mineral and sample no.	Pyrrhotite 259/100.90		Pyrrhotite 259/~118		Sphalerite 259/115.77		
	1	2	1	2	1	2	3
Fe	59.47	60.28	60.07	60.04	6.95	7.44	7.11
Cu	n.d.	n.d.	n.d.	n.d.	n.d.	n.d.	n.d.
Pb	n.d.	n.d.	n.d.	n.d.	n.d.	n.d.	n.d.
Zn	n.d.	n.d.	n.d.	n.d.	58.53	57.76	59.28
Ni	n.d.	n.d.	0.06	0.04	n.d.	n.d.	n.d.
Sb	n.d.	n.d.	n.d.	n.d.	n.d.	n.d.	n.d.
As	n.d.	n.d.	n.d.	n.d.	n.d.	n.d.	n.d.
Ag	n.d.	n.d.	n.d.	n.d.	n.d.	n.d.	n.d.
S	38.32	38.67	37.91	38.54	34.44	33.11	33.44
Cd	n.d.	n.d.	n.d.	n.d.	0.27	0.31	0.32
Bi	n.d.	n.d.	n.d.	n.d.	n.d.	n.d.	n.d.
Ti	n.d.	n.d.	n.d.	n.d.	n.d.	n.d.	n.d.
Sn	n.d.	n.d.	n.d.	n.d.	n.d.	n.d.	n.d.
Total	97.79	98.95	98.04	98.62	100.19	98.62	100.15

SULPHIDES
Analyses in wt.%

Mineral and sample no.	S p h a l e r i t e			
	259/100.90			259/90.70
Element	1	2	3	3
Fe	8.62	8.67	8.49	8.22
Cu	n.d.	n.d.	n.d.	n.d.
Pb	n.d.	n.d.	n.d.	n.d.
Zn	54.56	54.18	55.55	57.22
Ni	n.d.	n.d.	n.d.	n.d.
Sb	n.d.	n.d.	n.d.	n.d.
As	n.d.	n.d.	n.d.	n.d.
Ag	n.d.	n.d.	n.d.	n.d.
S	33.21	33.05	32.72	31.10
Cd	1.26	1.23	1.13	0.24
Bi	n.d.	n.d.	n.d.	n.d.
Ti	0.07	0.05	n.d.	n.d.
Sn	n.d.	n.d.	n.d.	n.d.
Total	97.72	97.18	97.89	96.78

Mineral and sample no.	S p h a l e r i t e					
	259/~118					
Element	1	2	3	4	5	6
Fe	7.13	7.25	10.54	7.00	7.40	10.09
Cu	n.d.	n.d.	n.d.	0.04	n.d.	4.35
Pb	n.d.	n.d.	n.d.	n.d.	n.d.	n.d.
Zn	58.39	58.43	54.46	58.58	59.02	51.70
Ni	n.d.	n.d.	n.d.	n.d.	n.d.	n.d.
Sb	n.d.	n.d.	n.d.	n.d.	n.d.	n.d.
As	n.d.	n.d.	n.d.	n.d.	n.d.	n.d.
Ag	n.d.	n.d.	n.d.	n.d.	n.d.	n.d.
S	32.56	32.67	33.66	33.02	33.35	33.13
Cd	0.39	0.33	n.d.	0.22	0.30	0.27
Bi	n.d.	n.d.	n.d.	n.d.	n.d.	n.d.
Ti	n.d.	n.d.	n.d.	n.d.	0.04	n.d.
Sn	n.d.	n.d.	n.d.	n.d.	n.d.	n.d.
Total	98.47	98.68	98.66	98.86	100.11	99.54

SULPHIDES

Analyses in wt.%

Mineral and sample no.	T e t r a h e d r i t e				Tetrahedrite -Tennantite 259/123.32	Ullmannite 268/35.84	
	301/133.8	259/84.35	264/116.27	259/123.32		1	2
Element	1	1	1	1	2	1	2
Fe	2.91	4.13	2.27	5.42	5.43	0.14	0.05
Cu	34.17	35.74	28.68	36.28	31.38	n.d.	n.d.
Pb	n.d.	n.d.	n.d.	n.d.	n.d.	n.d.	n.d.
Zn	3.94	2.69	4.41	1.82	2.03	n.d.	n.d.
Ni	n.d.	n.d.	n.d.	n.d.	3.59	27.63	27.51
Sb	30.15	29.73	23.67	30.58	26.37	56.01	56.90
As	0.50	0.36	3.44	0.33	9.72	2.73	2.87
Ag	4.37	2.95	13.28	1.47	1.05	n.d.	n.d.
S	24.38	24.45	23.79	24.16	24.38	14.31	15.16
Cd	0.64	0.13	0.37	n.d.	n.d.	n.d.	n.d.
Bi	n.d.	n.d.	n.d.	n.d.	n.d.	0.51	0.41
Ti	n.d.	n.d.	n.d.	0.05	n.d.	n.d.	n.d.
Sn	n.d.	n.d.	n.d.	n.d.	n.d.	0.23	0.26
Total	101.06	100.18	99.91	100.11	103.95	101.56	103.16

APPENDIX 5

Fluid inclusion homogenization and melting data and leaching analyses.

APPENDIX 5

Fluid inclusion homogenization and melting data and leaching analyses.

Crushing and leaching of fluid inclusions

The crushing apparatus was an agate mortar and lid and a zirconium ball. These were cleaned thoroughly and rinsed several times with distilled water. They were then soaked in nitric acid (20% HNO_3) for 30 minutes after which they were rinsed again.

The selected samples were weighed individually and also cleaned as described for the apparatus. This was done in a teflon dish.

The usual precautions were taken to prevent Na and any other contamination from the body, i.e., handling the mortar and lid with gloved hands and the samples and the ball with tongs. After cleaning, the ball and the sample were put in the mortar, being careful not to break the sample at this stage.

Using a previously rinsed 10 ml syringe, 5 mls of distilled water were put in the mortar. The water was deliberately passed over the ball, the sample and the sides of the mortar. After allowing it to settle for a few minutes, the 5 mls of water were drawn out of the mortar and kept as a blank sample. This procedure was repeated, thus obtaining a second blank sample.

To get the first leach sample, 5 ml of distilled water were poured into the mortar, the lid was put on and the apparatus was then shaken vigorously by hand for 1 minute. It was then left to settle down for 10 minutes after which 2 mls of solution were drawn off. The 2 mls were then made up to 10 mls and this became the first leach.

For the second leach sample, the 2 mls drawn off were replaced by 2 mls of distilled water and the apparatus was again shaken vigorously for 1 minute after which it was allowed to settle for about 15 minutes before drawing off another 2 mls of solution which was then diluted to 10 mls and labelled "second leach".

The third, fourth and fifth leach samples were obtained in a similar manner, the only variation being in the time allowed for settling of the quartz fragments before drawing off the 2 mls of solution. This time had to be increased for successive crushings because the quartz particles take much longer to settle down as they get finer.

The leach samples were then analysed by atomic absorption in the normal manner. The AA was adjusted for maximum sensitivity and the aspiration rate was reduced because of the small volumes of the samples involved. Chlorine was determined using a specific ion electrode.

Index and notes for the fluid inclusion data tables

There are seven tables, labelled and arranged as shown below:

Table 5A	- Carbon dioxide inclusions
Table 5B	- Inclusions in fluorite
Table 5C	- Inclusions in scheelite
Table 5D	- (Other) inclusions in quartz
Table 5E	- Inclusions in quartz from W-rich areas and samples (see pages 76-77)
Table 5F	- Inclusions in quartz from W-poor areas and samples
Table 5G	- Inclusions that developed new vapour bubbles.

Abbreviations:

C	: Concentrated.
D	: Dilute; depending on the abundance of daughter minerals etc, (see text); it was usually possible to tell whether inclusions in any one sample had concentrated or (relatively) dilute solutions.
L	: Large; this refers to samples from large quartz veins, arbitrarily defined as those veins with widths greater than 6 cm.
S	: Small; this refers to samples from small quartz veins, arbitrarily defined as those veins with widths of less than 2 cm.
1st (melting temperature):	that temperature at which it was clear that the frozen inclusion(s) had started melting. This could only be recorded for a few inclusions.
T_F	: Final melting temperature which, ideally, should be the freezing temperature. T_F is, in practice, different from the freezing temperature because of supercooling and formation of hydrates and clathrates.
$T_{F(CO_2)}$: Final melting temperature of (presumably) solid carbon dioxide.
T_H	: Homogenization temperature of the whole fluid inclusion.
$T_{H(CO_2)}$: Homogenization temperature of the carbon dioxide (or carbon dioxide-rich) phases. This temperature should not exceed 31°C , the critical temperature of carbon dioxide.
*	: Last melting temperature (T_F) of a hydrate. In most cases, such hydrates are believed to have been salt hydrates but some would have been gas hydrates (clathrates) - the distinction is not easy.
**	: Samples in which experiments were done on any suitable fluid inclusion, without considering whether the inclusions are primary or not.

Notes for Appendix 5 (cont'd)

- p : Inclusions in fluorite, thought to be definitely primary.
- d.n.f. : Inclusions that did not freeze (see text p. 83).
- dec : Inclusions that decrepitated at the temperatures indicated.
- > : greater than
- < : less than
- ~ : approximately equal to
- ^ : between
- : In Tables 5B-5G, readings along the same horizontal line were from the same inclusion.

TABLE 5A₍₁₎

CARBON DIOXIDE INCLUSIONS : FREEZING DATA

Sample number	Type of inclusion	$T_F(\text{CO}_2)$	Sample number	Type of inclusion	$T_F(\text{CO}_2)$
274/~33(D,L)	IB	-57	263/137.7(C)	IB	-57
	IB	-57	269/~127(C)	IB	-56
262/~149(D,S)	IB	-54	252/170.0(D)	IB	-60
252/115.5(D,S)	IB	-56	252/130.30(D)	IB	-63
	IB	-64		IB	-62
264/81.4(D,L)	IB	-52	IB	-63	
	IB	-54	IB	-60	
	IB	-54	IB	-63	
259/21.4(D,S)	IB	-55	IB	-66	
	IB	-56	252/116.0(D)	IB	-68
276/~158(D)	IB	-57	IB	-64	
	IB	-55	IB	-65	
48/50.4(C,S)	IB	-56	IB	-60	
274/70.55(C,S)	IB	-56			

TABLE 5A₍₂₎

CARBON DIOXIDE INCLUSIONS : HOMOGENIZATION DATA

Sample number	Type of inclusion	$T_H(\text{CO}_2)$	Sample number	Type of inclusion	$T_H(\text{CO}_2)$
DBS21(C,L)	IIB	27	DBS21(C,L)	IB	6
	IIB	29		IB	14
	IIB	29		IB	18
	IIB	26		IB	-5
	IIB	29		IB	9
	IIB	30		IB	10
	IB	-4		IB	3
	IB	6		IB	9
	IB	8		IB	21
	IB	10		IIB	22
	IB	8		IB	9
	IB	13		IB	17
	BS19(S)	IB		4	BS19(S)
IB		12	252/116.0(D)	IIB	28
IB		12	IB	1	
IB		12	IB	3	
IB		22	DBS16(C,L)	IIB	25
IIB	28		IIB	21	

TABLE 5A₍₂₎(cont'd) CARBON DIOXIDE INCLUSIONS : HOMOGENIZATION DATA

Sample number	Type of inclusion	T _H (CO ₂)	Sample number	Type of inclusion	T _H (CO ₂)	
BS19(S)	IIB	14		IIB	19	
	IB	-5		IIB	23	
	IB	2		IIB	19	
	IB	5		IIB	25	
70/188.5	IB	11		IIB	22	
	IB	16		IIB	21	
	IB	25		IIB	17	
	IIB	30		IIB	21	
252/116.0(D)	IB	7		IB	24	
	IB	14		IB	28	
	IB	7		IB	27	
	IB	11		IB	25	
	IB	11		IB	3	
	IB	6		IB	5	
	IB	0		IIB	30	
	IB	-1		IIB	30	
	IB	9		252/100.30(D)	IB	1
	IIB	23			IB	-3
	IIB	29			IB	10
	IIB	16			IB	-12
	IIB	28			IB	20
	IIB	26			IB	18
	IIB	15			IIB	25
	IIB	17			IIB	28
252/100.30(D)	IIB	25	259/21.4(D,S)	IB	12	
	IIB	20		IB	16	
	IIB	26		IIB	20	
	IIB	24	264/81.4(D.L)	IIB	31	
	IIB	24		IIB	30	
	IIB	26		IIB	18	
	IIB	16		IIB	20	
	IIB	29		IIB	21	
	IIB	12		IIB	17	
	IIB	16		IB	14	

TABLE 5A₍₂₎ (cont'd) CARBON DIOXIDE INCLUSIONS : HOMOGENIZATION DATA

Sample number	Type of inclusion	T _H (CO ₂)	Sample number	Type of inclusion	T _H (CO ₂)
252/170.0(D)	IB	7	252/115.5(D,S)	IB	19
	IB	17		IB	5
	IB	19		IB	10
	IIB	9		IB	12
	IIB	10		IB	15
	IIB	15		IB	16
BS21(C,S)	IB	17		IIB	2
	IB	16		IIB	15
	IB	7		IIB	14
	IB	15		IIB	6
	IB	12		B	4
	IB	8		IB	0
	IIB	23	IB	2	
	IIB	21	IB	3	
259/21.4(D,S)	IB	-9	48/50.4(C,S)	IB	-9
	IB	-3		IB	-4
	IB	-2		IIB	4
	IB	1		IIB	10
	IB	2		IIB	16
	IB	7		IIB	27
48/50.4(C,S)	IIB	29			
262/~149(D,S)	IB	-9			
	IB	-6			

TABLE 5B: INCLUSIONS IN FLUORITE

Sample number	Type of inclusion	Melting temp. °C		Homogenization temp. (T _H) °C
		1st	Final(T _F)	
42/109.13(D)	IIA	-47	-10	
	IIIA		-10	
	II-IA		-14	
	IIA		-15	
	IIIA			147
	IIA			148
	IIIA		-4	
	IIA			
	IIA			121
	IIA			131
	IIA	-49	16*	<157
	IIA		-35	218
	IIA	<-50	-35	233
	IIA		-35	136
	IIA	-57	-14	145
	IIA		-15	178
	IIA			110
	IIIA	-58	0*	164
	IIA		5*	143
	IIIA		14*	152
	IIA			128
	IVA(P)			150
	IIIA(P)		-36	145
	IIIA(P)			145
	IIA(P)		15*	
	IIA(P)		15*	
	IIA(P)		-34	
	IA		-11	
	IIA		-13	
	IIA			121
IVA			175	
314/~86(D)	IIA		-14	
	IIA		-10	
	IIA		-9	

TABLE 5B (cont'd)

INCLUSIONS IN FLUORITE

Sample number	Type of inclusion	Melting temp. °C		Homogenization temp. (T _H) °C
		1st	Final (T _F)	
314/~86(D)	IIA		-1	
	IIA		0*	
	IIA	-48	-14	
	IIA		-15	
	IIA		-15	
	IIA	~-50	-15	
	IC		-12	
	IIA	-50	-23	118
	IIA		-17	
	IC		-17	
	IIA(P)	-50	-18	132
	IIA			103
	IIA			131
	IIA			144
	IIA		-17	105
	IIA		-19	111
	IIIA			-11
	IIA			-12
	IIA			-10
	IIA			-10
	IIA			192
	IIA			199
	IIA			258
	IIA	-47	-23	
	IIA		-21	
	IIIA		-15	
	IIA		-14	
	IIIA		-13	
	IIA(P)		-17	
	IIA(P)	-48	-15	
	IIA(P)		-15	
IIA(P)		-15		
IIA(P)		-15		

TABLE 5C : INCLUSIONS IN SCHEELITE

Sample number	Type of inclusion	Melting temp. °C		Homogenization temp. (T _H) °C
		1st	Final(T _F)	
42/109.13(D)	IIA	-49	-11	
	IIA		-12	
	IIA	-53	-11	
	IC		-14	
	IIA		-15	
	IIA	-67	-40?	
	IIA		-32?	
	IIA	-50	-10	
	IIA		-12	
	IIA		-12	
	IIA		-13	
	IIA			210
	IIA			212
	IIA			220
	IIA			222
	IIA			224
	IIIA			204
	IIA			179
	IIA			230
	IIA			240
	IIA			234
	IIA			214
	IIA			180
	IIA			182
	IIA			246
	IIA			206
IIA			204	

TABLE 5D: OTHER INCLUSIONS IN QUARTZ

Sample number	Type of inclusion	Melting temp. °C		Homogenization temp. (T _H) °C
		1st	Final (T _F)	
252/100.30(D)**	IIA	-49	-18	
	IIA	-57	-25	158
	IIIA	-61	-18	172
	IIA	-66	15*	161
	IIA	-76(?)	17*	164
	IIA	-69	10*	159
	IIA	-37	-19	
	IIA	-37	-27	
	IIIA	-36	-20	
	IIA		-14	
	IIB		-12	
	IIA		-20	170
	IIA		-22	173
	IIA			162
	IIA	-49	-15	166
	IIA	-48	-16	197
	252/116.0(D)**	IIA	-56	-25
IIA		-38	-25	180
IIA		-34	-25	185
IIA		-31	-22	<200
IIA		-30	-15	150
IIA		-51	-15	
IIA		-48	4*	
IIA		-33	-15	
IIA		-42	-26	
IIB		-42	18*	
IIB		-46	-23	
IIA		-43	-23	
IIA		-46	-26	
IIA		-51	-15	
IIA		-43	-21	
IIA		-41	-23	
IIA		-44	-23	
IIA		-73(?)	13*	
IIA		-36	-13	
IIA			6*	
IIA			-21	

TABLE 5D: OTHER INCLUSIONS IN QUARTZ (cont'd)

Sample number	Type of inclusion	Melting temp. °C		Homogenization temp. (T _H) °C
		1st	Final (T _F)	
252/116.0(D)**	IIIA		-27	
	IIA		-27	
	IIA		6*	
	IIA		-16	
	IIA		-16	
	IIA		-12	
	IIA		-14	
	IIB		-10	
	IIA		-24	
	IIB			dec. 193
	IIB			dec. 231
	IIB			dec. 313
	IIB	-25, -27	-10, -5	
	IIB	-28	-9, -4	
	IIB	-29(?)	-5	
252/~128(D)**	IIA	49	15*	
	IIA	-43	3*	
	IIA	-43	4*	
	IIA		12*	
	IIB		27*	
	IIIA		15*	
	IIA		19*	
	IIA		28*	
	IIA			199
	IIA	d.n.f.		152
	IIA		6*	
	IIIA		19*	
	IIIA		23*	
252/170.0(D)**	IIIA		-41	
	IVA			dec. 300
	IVA			dec. 279
	IVA			dec. 258
51/~122(C)**	IIA		-10	
	IIA		-14	
	IIA		-49	
	IIA		-31	
	IIA		-18	152

TABLE 5D:(cont'd) OTHER INCLUSIONS IN QUARTZ

Sample number	Type of inclusion	Melting temp. °C		Homogenization temp. (T _H) °C	
		1st	Final (T _F)		
276/158(D)	IIIA			173	
	IIC			232	
	IVA			249	
	IIB			212	
	IIB			215	
	IIB			<240	
	IIIA			172	
	IIIA			192	
	IIA			<160	
	IIB			203	
	IVB			246	
	IIA			190	
	IIA			196	
	IIIA	-40	16*		
	IC		6*		
	IIA			172	
	IIA			185	
	IIIA			159	
	IIIA			215	
	IIA			<170	
	IIA			166	
	269/~127(C)	IIA	-40	-22	
		IIA		19*	
IIA		-58	11*		
IIA		-57	11*		
IIA		-68	-42		
IIA		<-60	-26		
IIA			-24		
IIA			-17		
IIIA				166	
IIIA				170	
274/~33(D,L)	IIIA			212	
	IIA			147	
	IIA	d.n.f.		158	
	IIA	-53	-20	152	
	IIA		-14		

TABLE 5D (cont'd): OTHER INCLUSIONS IN QUARTZ

Sample number	Type of inclusion	Melting temp. °C		Homogenization temp. (T _H) °C
		1st	Final (T _F)	
274/~33(D,L)	IIIA	d.n.f.		155
	IVC			339
	IIIA			165
	IIIA			207
	IVA			387
	IIA	-42	-15	
	IIA	-40	-12	
	IIA	-52	-14	
	IIA	-49	-13	
	IC		-21	
	IC		24	
	IIA			158
	IIA			162
	IIA			161
	IIA			165
	IIIA			227
	IIIA			252
256/108.4	IIA			158
	IIIA			308
	IIIA			313
	IIIA			381
259/21.4(D,S)	IIA			193
	IIB			274
	IIB			225
	IIB			250
	IIB			263
	IIA			262
	IIA			213
	IIB			187
	IIA	-40, -50	-20	
	IIA		-19	
	IIA	-40, -50	-11	
	IIA	-43	-16	
	IIA	-42	-15	
	IIA	-45	-13	
	IIA	-47	-12	

TABLE 5D: (cont'd) OTHER INCLUSIONS IN QUARTZ

Sample number	Type of inclusion	Melting temp. °C		Homogenization temp. (T _H) °C
		1st	Final (T _F)	
259/21.4(D,S)	IIA	-57	-21	
	IIA		-18	
	IIA		-20	
	IIA		-14	
	IIA		-14	
	IIA		-10	
	IIA	-57	-21	
	IIA		-14	
	IIA		-9	
	IIA		-7	
BS21(C,S)**	IIA	-61	-30	195
	IIA	-76	-33	193
	IIA	-76	-30	174
	IIA	-62	-49	283
	IIA	-67	-37	189
	IIA	-72	-24	148
	IIA	-72	-35	131
	IIA	-74	-42	158
	IIA	-75	-49	160
	IIA	-72	-44	150
	IIA	-68	-46	182
	IIA	-76	-48	153
	IIIA	-76	-28	160
	IIA		-35	194
	IIA		-23	>190
	IIA		-31	192
	IIA		-33	
	IIA			260
	IIA			224
	IIA			262
	IIA			204
	IIA			216
	IIA			240
IIA			226	
IIA			236	
IIA			240	

TABLE 5D:(cont'd) OTHER INCLUSIONS IN QUARTZ

Sample number	Type of inclusion	Melting temp. °C		Homogenization temp. (T _H) °C
		1st	Final(T _F)	
BS21(C,S)**	IIA			191
	IIA			269
	IIIA			259
	IIIA			155
	IIIA			208
	IIA	-75	-48	217
	IIIA	-76	-32	185
	IIA	<-67	-30	183
	IIA	-40	-20	dec. 405
	IIA	-74	-26	
	IIA	-69	-29	
	IVA		-49	
	IIA			175
	IIA			165
	IIA			165
	IVA			>476
	IVA			405
	IIIA			330
	IIA			169
	IIIA			166
BS20(C,S)**	IIA			181
	IIA	-67	-26	215
	IIA	-65	-33	213
	IIIA			192
	IIIA			213
	IIIA			217
	IIIA			178
	IIIA			191
DBS16(C,L)**	IIIA			222
	IIB	-68	-45	168
	IIA	-68	-43	165
	IIA	-69	-46	164
	IIIA			190
	IIIA			230
	IIA			162
	IIA			148
IIA			155	

TABLE 5D: (cont'd)

OTHER INCLUSIONS IN QUARTZ

Sample number	Type of inclusion	Melting temp. °C		Homogenization temp. (T _H) °C	
		1st	Final (T _F)		
DBS16(C,L)**	IIIA			196	
	IIIA			229	
DBS21(C,L)**	IIA	-69	-43	259	
	IIA	-34	-24	180	
	IIA	-60	-18	206	
	IIA	-71	-20	~305	
	IIA	-66	-35	215	
	IIIA	-58	-41	191	
	IIIA	-59	-15	>515	
	IIA		-27	146	
	IIA		-32	130	
	IIA			327	
	IIIA			234	
	IIIA			405	
	DBS17(C,L)**	IIA	-59	-25	209
		IIA	-66	-32	146
IIA		-54	-28	158	
IIA		-70	-27	141	
IIA		-67	-49	152	
IIIA				203	
IIIA				191	
IIIA				192	
IIIA				196	
IIIA				325	

TABLE 5E: INCLUSIONS IN QUARTZ, FROM W-RICH AREAS AND SAMPLES

Sample number	Type of inclusion	Melting temp. °C		Homogenization temp. (T _H) °C
		1st	Final (T _F)	
263/137.7(C)	IIA			173
	IIA			185
	IIA			189
	IIIA			218
	IIIA			279
	IIA	-73	-30	
	IIA	<-70	-42	
	IIIA	<-68	-48	172
	IIIA		-45	
	IIA		-35	186
	IIA	<-68	-32	
	IIA	-63	-33	
	IIA	<-66	-38	197
	IIA	<-66	-24	198
	IIA	<-66	-46	
	IIA	<-66	-25	
	IIIA			186
	IIIA			199
	IIIA			341
	IIA		-44	
	IIIA		-41	
	IIA			189
	IIIA			205
	IIIA			211
	IIIA			263
	IIA			271
252/115.5(D,S)	IIA	<-65	-32	
	IIA	-64(?)	-19	
	IIIA			238
	IIIA	-66	-19	<250
	IIA			169
	IIB			dec. 263
	IIB			240

TABLE 5E:(cont'd)

INCLUSIONS IN QUARTZ, FROM W-RICH AREAS AND SAMPLES

Sample number	Type of inclusion	Melting temp. °C		Homogenization temp. (T _H)°C
		1st	Final(T _F)	
252/115.5(D,S)	IIIA		7*	>350
	IIA	-62	-22	159
	IIA		-17	158
	IIA		-27	
	IIA		-24	156
	IIA		-14	
	IIA		-24	
	IIIB		-9	
48/50.4(C,S)	IIA		-29	
	IIA		-32	
	IIA		-20	
254/148.1(D)	IIA	<-64	-19	
	IIA	<-64	-17	
	IIA	<-64	-7	
	IIA	<-64	-5	

TABLE 5F: INCLUSIONS IN QUARTZ, FROM W-POOR AREAS AND SAMPLES.

Sample number	Type of inclusion	Melting temp. °C		Homogenization temp. (T _H) °C
		1st	Final(T _F)	
264/81.4(D,L)	IIB			dec. 208
	IIB			dec. 247
	IIB			dec. 209
	IIB			dec. 214
	IIB			244
	IIB	-27	1*	
	IIA		-15	
	IIA		-6	
	IIA		-12	
	IIA		-14	
	IIB	-25	-5	
	IIA		-15	
	IIA			143
	IIB			dec. 204
	IIB			215
	IIB			dec. 208
	IIB			178
	IIA	-62	-27	137
	IIA	<-60	-22	140
	IIA		-25	
	IIA		-22	
	IIA		-14	
	IIA	-33	-17	
	IIB		-17	
	IIA		-8	
	IIB	-29(?)	-5	
	IIB	-28	-7	
	IIB		1*	
	IIB	-25	3*	
	IIB	-28(?)	1*	
IIB	-26	0*		

TABLE 5F: (cont'd) INCLUSIONS IN QUARTZ, FROM W-POOR AREAS AND SAMPLES

Sample number	Type of inclusion	Melting temp. °C		Homogenization temp. (T _H) °C
		1st	Final (T _F)	
274/70.55(C,S)	IIA	d.n.f.		178
	IIA	d.n.f.		175
	IIA	d.n.f.		172
	IIA	d.n.f.		171
	IIA	-65	-29	
	IIA	~65	-23	
	IIA	~65	-30	
	IIA	~65	-27	
	IC		-33	
	IIIA		7*	
	IIIA		-32	
	IIA		-19	
	IIA		-23	
	IIA		-19	
	IIA	-67	-21	
	IIA	-66	-26	
	IIA	-65	-33	
	IIA	-64, -69	-30	
	IIA	~69	-25	
	IIA	-66	-24	
262/~149(D,S)	IC		-20	

TABLE 5G : INCLUSIONS THAT DEVELOPED NEW VAPOUR BUBBLES AFTER HOMOGENIZATION

Sample number	First homogenization temp. °C	Temperature at which new vapour formed/ was observed	Second homogenization temp. °C
256/108.4	158	298	338
	?	300	381
269/~127	168	325	>411
274/~ 33	?	313	370
314/228	<160	183	<301
252/115.5	211	242	~259
	?	270	321
	?	273	367